UNIVERSITY OF READING

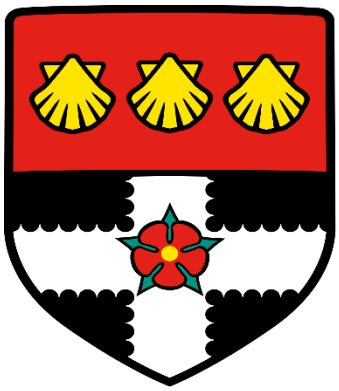

Developing Gene Therapy for Duchenne muscular dystrophy using Adeno Associated virus (AAV) Expressing Estrogen Related Receptor Gamma (ERRγ)

Muzna AL-Siyabi

Thesis submitted for the degree of Doctor of Philosophy

School of Biological Sciences

October 2018

Declaration

I confirm that this is my own work and the use of all materials from other sources has been properly and fully acknowledged. However, the microarray analysis and Principal Components Analysis were was conducted by Dr. Bend Denecke, RWTH Aachen University, Aachen, Germany and Dr. David Chambers, Kings College London. Moreover, the titration of the virus was carried out by Dr. Helen Foster, Reading University.

Acknowledgment:

Completion of this thesis would not have been possible if it was not with the support of many people.

Firstly, I would like to express my sincere gratitude to my supervisor Dr. Keith Foster for helping me to the end of this long, difficult part journey of my life. Your support, encouragement and faith on me has been critical for the completion of this thesis in the presence of many laboratory difficulties throughout. Thank you for inspiring me to pass all of that.

Secondly, the laboratory team; Dr Helen Foster and Dr Wouter Eilers. I will never forget your guidance, support, patience and technical assistance with my studies and I will always feel privileged to have been part of this team. Thank you

I would like to thank my dear friends Aida and Wadha. I knew I have been talking a lot in the last 4 years on how difficult being a PhD student. I thank you for listening, encouraging, inspiring. To my friend (Ahmed) who was a PhD student and passed away just before defending his thesis, rest in peace.

Parents play an important and large role in the development and shaping of their children behaviours, thoughts and life. I was and I am still fortunate to have the best parents that anyone could asked for. Their faith, commitment, patience and support to me have made all my accomplishments today possible. I will always be grateful for all they have done for me. I would like to express my deepest appreciations to my mother (Jokha), my father (Saif). I hope the finished PhD thesis brings you much pride.

To my sisters; Marwa, Waad and Mazoon, My brothers; Mazin, Mohanned, Zahran and Basil, thank you for constant voice messages, joyful holidays in the last four years, Allah bless you all.

Aside from myself, I cannot think of anyone else more excited to see this thesis completed-thank you for your enthusiasm, well done.

Abstract:

Skeletal muscle is the most abundant tissue in the body, exhibiting major metabolic activity by contributing up to 40% of the resting metabolic rate in adults. One of the most remarkable trait of skeletal muscle is its great adaptability to numerous environmental and physiological challenges by changing its phenotype profile in terms of size and composition that are brought about by changes in gene expression, biochemical and metabolic properties. Amongst these adaptations is the increase in oxidative metabolism that is supported by increase in blood flow and capillary density. Estrogen related receptor gamma (ERRγ) belongs to a family of orphan nuclear receptors. It is considered to be a master switch for both oxidative and angiogenic factors. ERRγ is down-regulated in *mdx* along with its target metabolic and angiogenic genes. Transgenic overexpressing ERRγ in *mdx* mice, improve sarcolemmal integrity and muscle perfusion with restoration of metabolic and angiogenic genes.

Duchenne muscular dystrophy (DMD) is an X-linked, recessive neuromuscular disorder caused by the loss of dystrophin that causes progressive loss of muscle fibre leading to cardiac and respiratory failure and ultimately death within the third decade. It is characterized by sarcolemmal fragility, impaired blood perfusion, calcium dysregulation, impaired mitochondrial function and oxidative stress. Following transcriptomic analysis we hypothesize that postnatal over-expression of ERRγ might improve oxidative capacity and angiogenesis in *mdx* mice. We first examined the effect of intramuscular administration of ($5X10^{10}$ vg) AAV8-ERRγ into *tibialis anterior* (TA) muscle of two cohorts of *mdx* male mice, initiating the experiment at either 6 or 12 weeks of age. There was no difference in mass, cross sectional area of muscle fibres nor was there a difference in myosin heavy chain fibre typing in the TAs of either cohort; however, succinate

dehydrogenase analysis (SDH) was significantly increased in both cohorts and H&E analysis demonstrated a 10% reduction of centrally nucleated fibres, but this reduction was restricted to the 6 week-old cohort only. This gave proof of principle data of an improvement in metabolic and pathological parameters in dystrophic muscle following ERRγ over-expression and leading to systemic administration protocols. Surprisingly, systemic administration of ($1x10^{12}$ vg) of AAV8-ERRγ into 6 week-old *mdx* male mice showed no functional improvement of EDL muscle and no difference in any examined markers. Therefore, we carried out an earlier systemic administration of ($2 X10^{12}$ vg) of AAV8-ERRγ into three week-old *mdx* mice for longer time and resulted in improved specific force of EDL muscle while the eccentric contraction-induced force deficit was unaffected. EDL muscles showed improvements in SDH activity, a reduction in centrally nucleated fibres, with no change in IgG positive fibres or CK assay. EDL muscles showed an increase in capillary density, increased transcript levels of PGC-1α, angiogenesis, inflammation markers and a reduction in transcript levels of GADD34 and 4EBP1.

Collectively, this data provides prima facia evidence that ERRγ over-expression at an early time point is a potential therapeutic strategy to overcome metabolic and pathological problems associated with dystrophic skeletal muscles.

Abbreviation:

AAV	Adeno associated virus
Ach	Acetycholine
AchE	Acetycholinestrase
AMPK	AMP-activated protein kinase
AON	Antisense oligonucleotides
ATP	Adenosine triphosphate
BMD	Becker muscular dystrophy
Ca+2	Calcium
cGMP	Cyclic guanosine monophosphate
CK	Creatine Kinase
Cmap	Connectivity map
COXIV	Cytochrome c oxidase subunit IV
DAMP	Damage-associated molecular patterns
DMD	Duchenne muscular dystrophy
EC	Endothelial cells
Enos	Endothelial nitrc oxide synthase
ERRα	Estrogen related receptor alpha
ERRγ	Estrogen related receptor gamma
ER	Endoplasmic reticulum
ETC	Electron transport chain
g	Gram
GABPA	GA binding protein transcription factor, alpha
Gadd34	Growth arrest and DNA damage inducible protein
FOXO	Forkhead box O
GLUT	Glucose transporter
HIF-1α	Hypoxia-inducible factor 1α
H&E	Haematoxylin and Eosin
IGF	Insluin growth factor
IL-1β	Interleukin-1β
IL-6	Interleukin-6
IL-10	Interleukin-10
iNOS	Inducible nitric oxide synthase
IP3	Inositol 1,4,5-trisphosphate
Kg	Kilogram
L	Liter
ml	Milliliter
mM	Millimolar
MPC	Myogenic precursor cells
mtDNA	Mitochondrial DNA
MurF	Muscle RING finger-1
MYH-3	Myosin Heavy Chain 3
ND2	NADH dehydrogenase 2

NK-κB	Nuclear factor of kappa light polypeptide gene enhancer in B cells
Nnos	Neuronal nitric oxide synthase
NRF	Nuclear receptor factor
OXPHOS	Oxidative phosphorylation
PDK	Pyruvate dehydrogenase kinase
Perm-1	PGC-1/ERR-induced regulator in muscle 1
PGC-1α	Peroxisome proliferator-activated receptor gamma coactivator 1-alpha
PI3K	Phosphatidylinositol 3-kinase
PNC	Purine nucleotide cycle
p-p38 MAPK	Phospho-p38 mitogen-activated protein kinase
p38 MAPK	p38 mitogen-activated protein kinase
qRT-pcr	Quantitative real time PCR
RNS	Reactive nitrogen species
ROS	Reactive oxygen species
RYR	Ryanodine receptor
SAC	Stretch activated channel
SC	Stem cell
SDHA	Succinate dehydrogenase complex, subunit A
SERCA	Sarco/Endoplasmic Reticulum Ca^{2+}-ATPase,
SIRT1	Sirtuin 1
SO	Sequence optimization
Sod	Superoxide dismutase
TCA	Tricarboxylic acid cycle
TFAM	Transcription factor A, mitochondrial
TNF-α	Tumour necrosis factor alpha
UPR	Unfold protein response
VEGF	Vascular endothelia growth factor
VSMC	Vascular smooth muscle cells
4EBP1	Eukaryotic translation initiation factor 4E binding protein 1
µl	Micro liter

Table of contents

List of figures:

List of table:

1.Chapter One
Literature Review

1.1. Structure of muscular tissue:

Muscle tissue is one of the four primary types of body tissues, together with epithelial, connective and nervous tissues. Muscle cells are highly specialized for contraction; they produce movement in certain organs and the body as a whole. There are three different types of muscle within the body, each with its own specific functions and different morphological features. These muscle types are smooth, cardiac and skeletal muscles and the structure of each type is adapted to its physiological role.

Smooth muscles are a constituent of internal organs and blood vessels. Their muscle cells are not striated and not under voluntary control because they cannot contract by conscious means. This muscle type is innervated by autonomic nervous system and contracts very slowly. Muscle cells present in smooth muscle are relatively long spindle shape with a single central nucleus. The contraction of smooth muscle is mediated by calcium interacting with calmodulin, which is a calcium binding protein (Koledova and Khalil, 2006).

Smooth muscles play variable roles in different body organs. For example; in cardiovascular system, they regulate blood pressure and control the distribution of blood. In the walls of digestive tract, extensive layers of smooth muscle cells play an essential role in moving materials along the tract. In addition, they can alter the diameter of respiratory passageways when they contract and relax (Martini, 2007).

Cardiac muscles are the specialized type, exclusively found in the heart that have function to provide the force required for circulating blood around the body. They are known as striated muscles and considered involuntary. However, a typical

cardiac cell has one central nuclei (Martini, 2007). There is close association between blood flow and metabolic demand in cariac muscles. For example; in the presence of oxidative or metabolic stress, these muscles are essential to maintain blood flow. However, smooth and cardiac muscles are not the basis of this thesis and the focus will be on skeletal muscles.

1.2. Skeletal Muscle development:

Skeletal muscles are of mesodermal origin and are derived from somites during embryonic development. These mesodermal cells migrate and differentiate forming myoblasts that exists either as a single myoblast cell with mitotic potential or they proliferate and fuse to form multinucleated myotubes (Jones et al., 2004). The majority of skeletal muscle fibres are formed in two phases; 1) Primary (embryonic) myogenesis when myoblasts proliferate and fuse to form primary myotubes, followed by (2) secondary (fetal) myogenesis when myoblasts fuse along the surface of the primary myotubes, giving rise to a population of smaller and more numerous secondary myotubes (Matsakas et al., 2010). 5-10% of myoblast cells remain without fusion, undifferentiated, known as muscle stem cells (satellite cells) in the mature muscle. They lie between the plasma membrane and the basement membrane of muscle fibres. Each satellite cell is composed of a large nucleus with a thin layer of cytoplasm and they activated during damage and diseases to compensate the damaged fibres.

A group of transcription factors regulate the transition from myoblast to myotubes. Of these, four members of the myogenic regulatory factors (MRFs) family are the master regulators of myogenesis; MRF4, myf5, myoD and myogenin (Endo, 2015). Muscle fibres present in skeletal muscle are multinucleated, long

cylindrical cells which are arranged to form bundles. Using electron microscopy, 50-60 myonuclei per millimetre of fibre length were found in slow and fast muscles in the mouse (Bruusgaard et al., 2003). Contractile proteins within the muscle fibre allow for powerful contractions by the muscle and also give the muscle its striated appearance. The contraction of skeletal muscle is voluntary and is controlled by somatic motor innervations. In human body, there are around 600 individual skeletal muscles, representing around 40-50% of body mass, differ significantly in their size, shape and arrangement of myofibril. As a result of these variations, they exhibit different functions (Martini, 2007, MacIntosh et al., 2006). One of the interesting feature of the skeletal muscle, they are highly adaptable tissues, responding to different environmental and physiological stimuli, such as mechanical loading, unloading, inactivity, disuse and nutrient availability (Pette and Staron, 2000). Skeletal muscles are capable of producing various motions in different organs, such as gross movement in large muscles like quadriceps muscle as well as the extraocular muscle of the eye, which has a fine contract motion. Based on these characteristics of skeletal muscles, they have multiple important functions: 1) Support soft tissues such as abdominal wall and floor of pelvic cavity, 2) Maintain posture and body position, 3) Maintain body temperature through heat production, 4) Produce skeletal muscle movement, as the contractions of skeletal muscle moves the bones of the skeleton by pulling the tendons (Martini, 2007) and 5) Store glycogen (Jensen et al., 2011).

1.3. Skeletal muscle structure:

Skeletal muscles are comprised a number of different tissues such as blood vessels, nerve fibres and connective tissues. Each muscle is surrounded by a dense layer of connective tissue called the epimysium acts to give each muscle

its shape by surrounding entire muscle and separates the muscle from the surrounding environment. Muscle fibres within the muscle are held in bundles called (fascicles) by another connective tissue called perimysium, where blood vessels and nerves pass through. Individual muscle myofibre within each fascicle are surrounded by a third connective tissue layer called the endomysium. The three different connective tissues are continuous and come together at both ends of the muscle where they form tendons. The tendons are responsible to attach muscle fibres to bone. Individual striated muscle fibres are long multi nucleated, surrounded by a cell membrane called ‘’sarcolemma’’ and the cytoplasm of a myofibre is referred to as ‘’a sarcoplasm’’. Satellite cells are undifferentiated mononuclear myogenic cells, lying between endomysium and the sarcolemma and represent a reserve of precursor cells to facilitate growth and regeneration (figure 1.2). The sarcolemma has a narrow tubules (T-tubule) that through invaginations penetrates throughout the myofibres. T-Tubule is essential for excitation-contraction coupling by conducting impulses from sarcolemma into the sarcoplasmic reticulum (SR). Each Myofibril is surrounded by the SR which is specialized endoplasmic reticulum and represents the main calcium (Ca^{+2}) reservoir that mediates muscle contraction and relaxation through ionic Ca^{+2} handling. The sarcoplasmic reticulum in contact with the T-tubule forms the terminal cisternae (Martini, 2007, Lieber, 2009, MacIntosh et al., 2006).

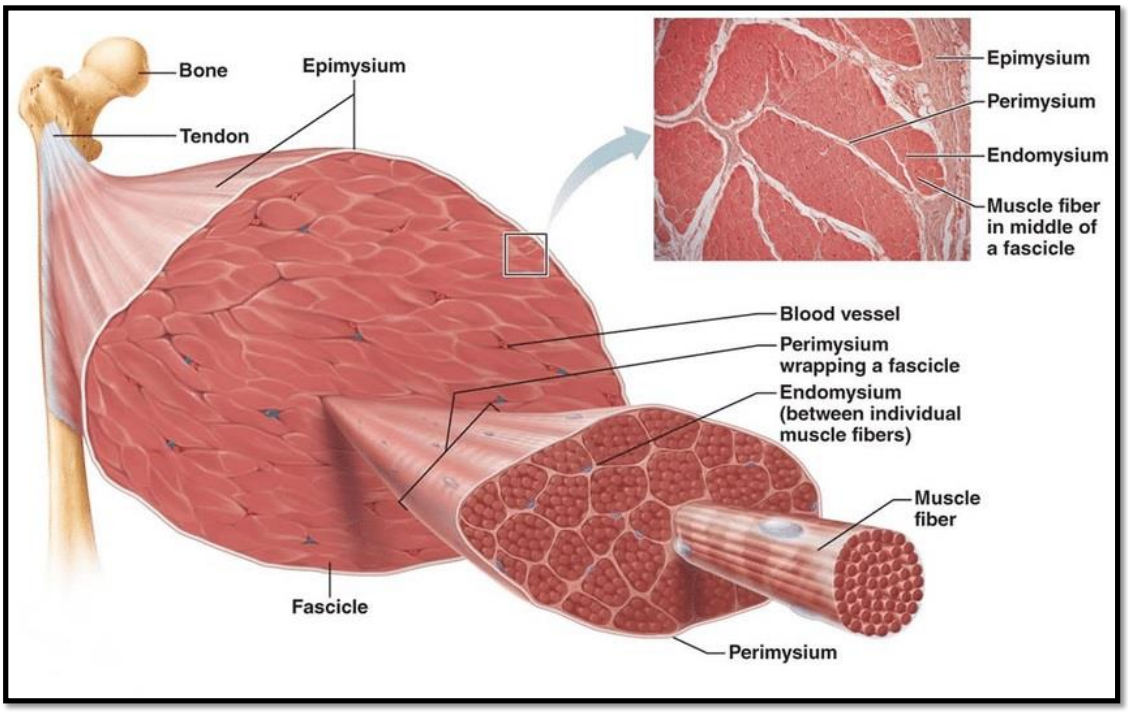

Figure 1.1. Skeletal muscle structure

The diagram illustrates smaller components of skeletal muscle. The muscle consists of fascicles, bundles of muscle fibres surrounded by the epimysium. The fascicles bundles are separated by the perimysium connective tissue. Individual muscle fibres are surrounded by the endomysium. Extension of epimysium forms tough cord of connective tissue, the tendons that anchor muscles to bones. https://www.researchgate.net/publication/313845971_Modeling_of_the_sEMGForce_relationship_by_data_analysis_of_high_resolution_sensor_network/figures?lo=1. (From Pearson Education Company

Skeletal muscle is often referred to as striated muscle as the myofibres appear striped or 'striated' when they viewed longitudinally due to the arrangement of proteins. Muscle fibres range from few millimetres to 10 cm in length and from 5-100 µm in diameter. Each myofibre consists of protein filaments called myofibrils, with a diameter of about one µm. The myofibrils are comprised of contractile elements called sarcomere which is the basic unit for muscular contraction (Aidley and Ashley, 1998, Saladin and Miller, 1998).

A sarcomere of 2 μm in length contains myosin, actin, and other proteins that regulate interactions and proteins which stabilize the positions of the filaments. Each sarcomere has dark bands (A) and light bands (I). The A band contains three subdivisions; M-line which contains proteins, functioning in connecting the central portion of each thick filament to its neighbours, therefore help in stabilizing the position of the myosin. H-zone contains only thin filaments and finally zone of overlap, which is the area where thin and thick filaments are surrounded by each other. (I) band contains thin filaments only and extend from A band of one sarcomere to the A band of the next sarcomere. Z-line marks the boundaries between adjacent sarcomeres and contains actinin proteins, which connect thin filaments of adjacent sarcomeres. Titin proteins extend from the tips of myosin to the site at the Z-line. Titin's function in keeping actin and myosin in a proper alignments and also preventing extreme stretching which may disrupt the contractive properties of muscle (Martini, 2007, MacIntosh et al., 2006) (figure 1.3).

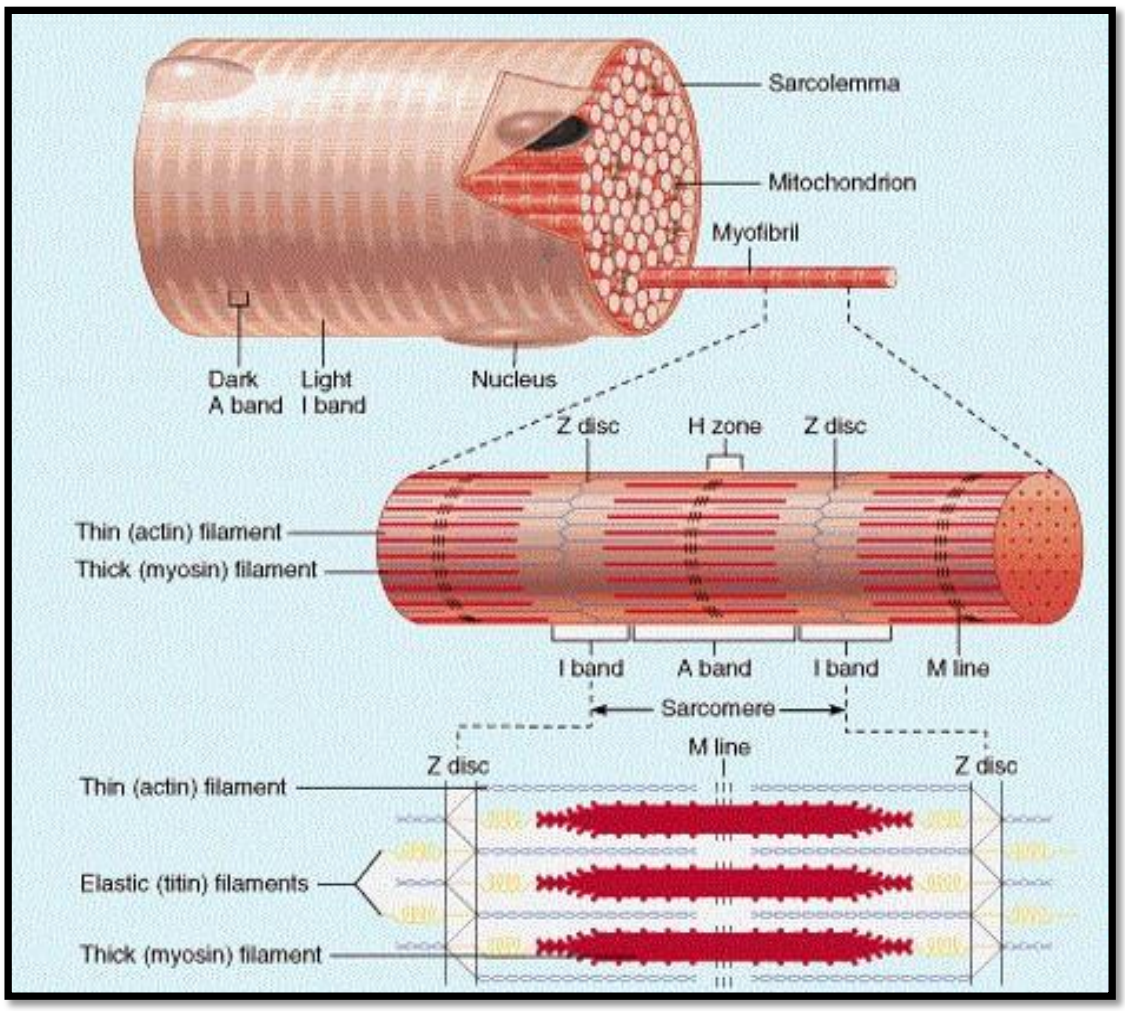

Figure 1.2. Structure of sarcomere

(http://www.easynotecards.com/print_list/51510?fs=1&dis=1&pi=on)

(Benjamin Cummings Company)

Each myosin molecule composed of two-rod like tail woven around each other and ends into two globular heads. The head links thin and thick filaments together forming cross bridges. The heads contain actin binding site and ATPase enzyme that hydrolyse ATP to produce energy for contraction. The actin molecule formed by two rows of globular-actin (G-actin) molecules. Actin contains some regulatory proteins such as troponin, tropomyosin and nebulin. Troponin composed of three polypeptides; Tn-I which acts as myosin binding inhibitory, Tn-T which maintains binding of actin and myosin and Tn-c which binds to calcium ion. Tropomyosin binds to actin filaments and play roles in the activation process that leads to

myofilaments sliding and generation of force, whereas nebulin holds actin strands together (Martini, 2007).

1.4. Skeletal muscle physiology:

1.4.1. Excitation-contraction coupling:

Muscle fibres respond with a rapid depolarization to an excitable signal from their associated alpha motor neuron. The events preceding muscle contraction begin with depolarization of motor neuron and subsequent action potential along the motor nerve. Action potential is generated when a neuron is activated by a large, short-lived increase in the permeability of plasma membrane to sodium ions (Na^{+2}). The increase in (Na^{+2}) permeability leads to membrane depolarization. However, the steps of excitation-contraction coupling are summarized in the following points: (Lamb, 2000)

1. The arrival of an action potential. When the neuronal signal arrives to the presynaptic nerve terminal at the neuromuscular junction, an action potential propagates leading to flow of Ca^{+2} ions from the extracellular fluid, which causes the release of acetylcholine (ACh) into the synaptic cleft because of change in the permeability of the synaptic terminal membrane with the arrival of action potential.

2. ACh binds at the motor end plate. ACh molecules bind to ACh receptors at the motor end plate at the surface of sarcolemma. These binding changes the permeability of motor end plate to (Na^{+2}) ions, which influx and accumulate in the sarcoplasm until acetylcholinesterase (AchE) enzyme removes ACh from its receptors.

3. Action potential in the sarcolemma. The arrival of an action potential at the synaptic terminal lead to the appearance of the action potential in the sarcolemma that becomes depolarized, due to sudden inrush of (Na^{+2}) ions. This depolarization in the sarcolemma spreads along a conducting T-tubule, passes transversely into the muscle cells and surrounds each myofibril forming a membranous network of the sarcoplasmic reticulum and ends at the terminal cisternae which releases the Ca^{+2} at the junction between the (A) and (I) band of each sarcomere (figure 1.4).

From the initial transmission of the action potential across the sarcolemma, the events lead to muscle contraction are collectively called excitation-contraction (E-C) coupling, which is a unique mechanism that gives skeletal muscle its contractile properties (Lamb, 2000).

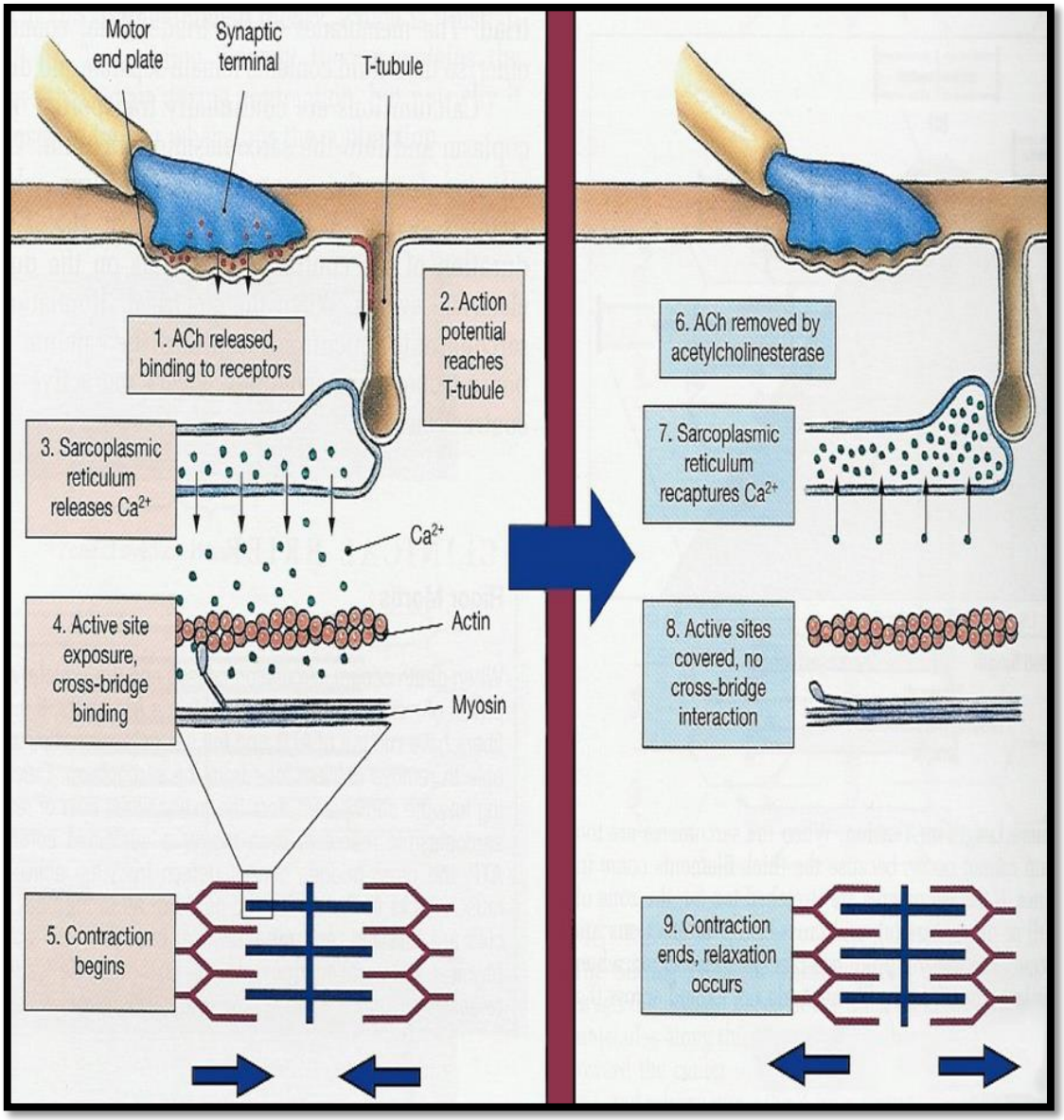

Figure 1.3. Steps involved in skeletal muscle excitation, contraction and relaxation

From Martini, 2006.

In resting state, intracellular Ca^{+2} concentration is maintained at approximately 50 nM which corresponds to inactive state of contractile apparatus in which tropomyosin protein winds a round actin filament and cover the myosin binding site on actin through forming a complex with troponin to prevent actin from binding to myosin (Kress et al., 1986).

Upon the transient release of SR Ca^{+2} and subsequent increase in the intracellular Ca^{+2} to 5 mM, the cytosolic Ca^{+2} ions then bind to troponin binding site results in conformational changes in the troponin complex, causes the tropomyosin to lift from actin and exposing the active site on the actin filament. The exposed myosin binding sites are now able to bind to myosin heads, initiating the energy-dependent cross-bridge cycling mechanism and inducing muscle contraction (Cooke, 1997).

Cross-bridge cycling is an active process requires the hydrolysis of adenosine triphosphate (ATP) by myosin ATPase to adenosine diphosphate (ADP) and inorganic phosphate (P_i) which then provides the energy for muscle contractions. Myosin ATPase enzyme is stored in the globular myosin head region (Cooke, 1997). Effective cross bridge formation requires Ca^{+2} entry into the sarcoplasm which then binds to troponin so that myosin binding site on actin is exposed (MacLennan et al., 1997). Following contraction, the excitation by the action potential terminates as the Ach are removed by AchE in the gap between motor neuron and sarcolemma (neuromuscular junction). Then, Ca^{+2} pumped back into SRs through Ca^{+2} regulatory protein, sarco (endo) plasmic reticulum Ca^{+2} ATPase pump (SERCA), returning Ca^{+2} concentration to normal level and thus troponin-tropomyosin complex returns to its normal position and re-cover the active site of actin preventing any further cross-bridge and hence causing muscular relaxation (Scott et al., 2001).

In fact, the efficient handling of Ca^{+2} requires a regular supply of ATP which are both essential molecules for E-C coupling and cross-bridge formation. However, ATP depletion and increased Ca^{+2} concentration have been involved in a variety

of clinical conditions. For example; Brody's disease, which is caused by defective SR Ca^{+2} ATPase activity and increased Ca^{+2} concentration; central core disease and malignant hyperthermia are both caused by accumulation of intracellular Ca^{+2} due to a mutation in ryanodine receptor (RYR) and dystrophin muscular dystrophy, which is caused by a mutation of dystrophin that leads to increased membrane permeability and increased Ca^{+2} accumulation (Berchtold et al., 2000).

1.5. Skeletal muscle plasticity:

Skeletal muscle plasticity can be defined as '' the ability of a muscle to alter the amount and/or the type of protein (phenotype of isoform) in response to any type of stimulus that disrupts its normal homeostasis'' (Booth and Baldwin, 2010). This is demonstrated more in response to endurance or resistance training, lack of use or disease. Such stimuli results in significant adaptations to induce muscle hypertrophy, muscle fibre type transitions and mitochondrial biogenesis (Matsakas and Patel, 2009).

1.5.1. Plasticity of skeletal muscle mass:

1.5.1.1. Skeletal muscle wasting:

Loss of muscle mass and strength occurs in many clinical conditions and chronic diseases such as muscle disuse, aging, cachexia and muscular dystrophies. They are serious due to their direct effects on loss of individual independence and increased risk of death.

Muscle wasting associated with cachexia can be developed in a variety of acute and chronic conditions, these include infectious diseases, such as HIV/AIDS,

malaria and tuberculosis, as well as many chronic conditions like cancer, chronic heart failure (CHF), chronic kidney disease (CKD), cystic fibrosis, stroke and neurodegenerative disease (von Haehling et al., 2009, Onwuamaegbu et al., 2004, Mak et al., 2011). Cachexia is characterized by a loss of muscle, fat mass and a loss of body weight which is associated with a significant increase in mortality risk in patients with heart failure. Another condition is sarcopenia, which is age-related loss of muscle mass, associated with a reduction in lean body mass with an increase in fat mass. Sarcopenia is also accompanying by mitochondrial dysfunction, inflammation, leading to a decrease in muscle strength, metabolic rate and oxidative capacity (Sakuma and Yamaguchi, 2012). Aetiology of sarcopenia includes decreased physical activity, inflammation, nutritional deficiencies, metabolic homeostasis, oxidative stress and hormonal changes. Decreased physical activity or bedrest lead to a reduction in muscle mass with an increase in fat mass (atrophy accompanying with muscle disuse), (reviewed in (Evans, 2010)).

Simultaneously, the term of muscle atrophy is used when a patient is subjected to extended bed rest and inflammatory myopathies. Generally, muscle is genotypically normal in all of these conditions except dystrophies in which a genetic mutation causes loss of muscle mass. With age, disuse and disease, the muscle fibres decrease in number and/or size, associated with a loss of muscle function. There are distinct differences in the biochemical process and wasting outcomes between these conditions. For example; in sarcopenia, there is a reduction in fibre size and number, with a transition towards fibre type I. There is a firm evidence that with aging, type II fibres are more vulnerable to atrophy than type I fibres (Brooks and Faulkner, 1994), therefore, it is a protective mechanism

against further muscle loss. In contrast, in atrophy resulted from disuse, although, the fibre number is not affected with a decrease in fibre size, it is a companying with a fibre type shift towards type II. Another example of difference between these conditions showed in muscle wasting of cachexia, which affected type II fibres, whereas heart failure results in a degradation of type I or type IIA fibres (Romanick et al., 2013). Although different aetiology causes cancer cachexia and MD; cancer associated muscle degenerative disease vs genetic, respectively. They showed similar features, for example; dysfunction of dystrophin-glycoprotein complex, reduced dystrophin and a compensatory upregulation of utrophin (Acharyya et al., 2005), activation of systemic and muscle inflammatory pathways (Li et al., 2008) and dysfunction of regeneration potential as shown in the upregulation of satellite cells markers (Pax7) (He et al., 2013).These similarities highlight the importance of applying same therapeutic approach to more than one condition associated with muscle loss and weakness. In this thesis, the focus will be on duchenne muscular dystrophy.

1.5.1.2. Plasticity of skeletal muscle mass:

Under selected physiological and environmental stimuli, skeletal muscle cell modifies its size. One of these stimuli is sarcopenia, which is an aging-related decline in skeletal muscle mass that can be opposed by resistance type of exercise to augment muscle mass and strength. Previous studies in older adults have shown that the muscle adapt to resistance exercise by hypertrophy of type II muscle fibre (Verdijk et al., 2009). Muscular hypertrophy is an increase in muscle mass and cross sectional area (Russell et al., 2000).

Skeletal muscle growth is controlled by different factors such as growth hormones. Myostatin and IGF-1 are growth hormones with opposing roles on regulating skeletal muscle growth and size, with myostatin inhibiting regulator of muscle mass and IGF-1 stimulating muscle growth (Garikipati and Rodgers, 2012).

Myostatin is a member of transforming growth factor (TGF-β), essential for proper regulation of skeletal muscle mass by negatively regulating skeletal muscle growth (McPherron et al., 1997). Mice carrying a targeted deletion of myostatin have a dramatic increase in muscle mass, due to generalized hyperplasia (increase in number of fibre) and to lesser extent hypertrophy (increase in the size of muscle fibre). Myostatin mutation has shown massive increase in skeletal muscle tissue in sheep (Clop et al., 2006) and dogs (Mosher et al., 2007). In diseased states, inhibition of myostatin has become an attractive therapeutic strategy to enhance muscle growth. For example; blocking myostatin via systemic administration of monoclonal antibodies in adult mice enhance muscle growth by 30%, suggesting a therapeutic effect to induce muscle mass and whole body metabolism in aged muscle (LeBrasseur et al., 2009, Zhang et al., 2011). Despite the increase in muscle mass in the absence of myostatin, there is a reduction in specific force coupled with a decrease in mitochondrial DNA and mitochondrial number, suggesting a potential negative effect on oxidative characteristics, capillary density of skeletal muscle and fatigue extremely rapidly (Amthor et al., 2007). In aged muscle, inhibiting myostatin resulted in conflicting results in terms to muscle mass such as no change in mice at the protein level (Carlson et al., 2008), a decrease in rats at the mRNA level (Haddad and Adams,

2006) and an increase in humans at the mRNA and protein levels (Leger et al., 2008).

IGF-1 is a circulating polypeptide hormone secreted essentially in liver and regulated by growth hormone (GH). In skeletal muscles, IGF-I plays a major role in growth, differentiation and regulating homeostasis. As shown by Sakowski et al., mice muscles of amyotrophic lateral sclerosis (ALS) model have large fibres and become stronger following over-expression of IGF-I using viral delivery. ALS muscle fibres are characterized with a decrease in the muscle mass (Sakowski et al., 2009). On the opposite side, transgenic mice with IGF-IR deficiency, a receptor that regulate IGF-1 activity, die after short period of birth due to muscle hypoplasia which in turn disable lung inflation (Powell-Braxton et al., 1993). In addition, dozens of studies have been focusing on studying the role of IGF-I in muscle hypertrophy and regeneration after damage. For example; over-expression of IGF-1 using adeno associated virus (AAV) in aged mice showed induced skeletal muscle force, hypertrophy and preventing the loss of muscle fibre type IIB (Barton-Davis et al., 1998), suggesting a role of IGF-1 to maintain the symptoms associated with age.

1.5.2. Plasticity of skeletal muscle fibre type:

Skeletal muscle exhibit a unique features due to its composition of a large number of different types of muscle fibres that contribute to different functions. These muscle fibre types differ in their metabolic, molecular, structural and contractile properties. The progress of fibre type classifications has imply different technologies. Using myosin ATPase and mitochondrial NADH-tetrazolium reductase activities as marker for the oxidative potential, the muscle

fibres can be classified into slow-twitch and fast-twitch fibres with ATP reaction, and the fast-twitch subdivided into fast oxidative glycolytic and fast glycolytic fibres by NADH-TR activities (Barany, 1967, Armstrong and Phelps, 1984). In the beginning, a combination of different pH with ATPase activity revealed four types of fibres; I, IIA, IIX, IIB. Then, the development of MHC antibodies enabled the detection of four types of myosin isoforms (Brooke and Kaiser, 1970). To date, the most accepted method to distinguish between fibre types is based on specific myosin profile (Pette and Staron, 2001). For example; the contractile properties depend on the composition of myosin heavy chain isoform (MHC). MHC encoded by a multigene family, which is the major component of the contractile apparatus combining with actin to form the actomyosin complex, responsible for the elastic and contractile properties of muscle (Kammoun et al., 2014). Collectively, MHC are subdivided based on the expression of (pure) MHC isoform or (hybrid) which is more than one MHCs isoforms. In limb muscles of small mammals, the major isoform in slow twitch muscles is the slow MHC-I, whereas the abundant isoforms are IIA, IIB and IIX. Moreover, skeletal muscles include different fibre types which co-express hybrid isoforms for example; I and IIA, IIA and IIX, IIX and IIB. Distribution of myosin isoforms in muscle varies between animals and depends on the function of that muscle and the diversity of muscle fibres is reflected in part by motor units where motor unit is made up of a motor neuron and the skeletal muscle fibres that neuron innervates (Greising et al., 2012).

Innervation ratio represent the number of muscle fibre innervated by a single motor neuron, which differ between muscle and helps giving a gradual response. For example; a muscle required for fine control, its motor units may have an innervation ratio as (10:1), which makes it more capable of finer and gradual

change in contraction, such as, eyes and fingers. Compared with a muscle required for course contraction such as gastrocnemius, its motor unit will have a high innervation ratio that has been estimated to be (2000:1).

Motor units are classified into smaller (slow) motor units innervate slow-twitch muscle fibres or larger motor units that innervate fast-twitch muscle fibres (Greising et al., 2012). The motor units are the driving force behind fibre type. The slow-twitch fibres are recruited when the input is slow and they generates less force than the fast twitch but they are able to maintain the force for longer time. However, when the largest motor neurons are activated, the fast-twitch are recruited and produce large amount of force, but fatigue rapidly (Floeter, 2010).

However, the metabolic requirement of each muscle fibre differs markedly, aerobic (type I), termed as slow-twitch fibres, exhibit slow contraction due to the ATPase activity associated with the type I myosin, small cross sectional area, large mitochondrial number, have more capillaries surrounding each fibre, exhibit oxidative metabolism, and high resistance to fatigue. In contrast, anaerobic (type II), fast twitch fibres, exhibit quick contractions and fatigue rapidly, have large cross sectional area, few mitochondria and are considered glycolytic (Bassel-Duby and Olson, 2006).

Additionally, fibre types differ in their expression of other proteins such as; tropomyosin, myosin light chain, troponin subunit and (SERCA). Quantitative differences do not lead to precise determination of fibre type but lead to overlap between the different myosin isoforms based on their enzyme activity levels. However, based on metabolic enzyme classification, fibre types are divided into three main types; fast twitch-glycolytic (FG), fast-twitch-oxidative-glycolytic

(FGO) and slow-twitch oxidative (SO). Therefore, MHC-IIB fibres equal to FG and MHC-IIA equal to FGO. Type MHC-I represent the highly correlated fibres between the two classification types where it equal to SO (Pette and Staron, 1997) (Table 1.1).

Table 1.1. Skeletal muscle fibres and physiological performances

	Type I fibres	Type IIA fibres	Type IIX fibres	Type IIB fibres
Contraction time	Slow	Moderately fast	Fast	Very fast
Size of motor neuron	Small	Medium	Large	Very large
Resistance to fatigue	High	Fairly High	Intermediate	Low
Force produced	Low	Medium	High	Very High
Mitochondrial density	High	High	Medium	Low
Capillary density	High	Intermediate	Low	Low
Oxidative capacity	High	High	Intermediate	Low
Glycolytic capacity	Low	High	High	High

Modified from (Pette and Staron, 1997)

The plasticity of skeletal muscle fibres in response to metabolic stress is afforded through induction of slow type oxidative phenotype fibres (Timpani et al., 2015). It is well established that skeletal muscle myofibres undergo phenotypic transition in aging, in response to physical activity and in chronic disease (Schiaffino and Reggiani, 2011, Yan et al., 2011). Remodelling phenotypic profiles of skeletal muscle fibres is of great interest in terms of chronic disease via transforming myofibres into more oxidative, more resistant to damage. The experiment of cross innervation study where slow-twitch muscle fibres were innervated with nerve fibres that supply fast-twitch muscle caused an increase in contractile speed of the muscle and conversely, innervation of fast twitch muscle with nerve normally found on slow-twitch muscles resulted in slow contraction, initiated studies in understanding the underlying mechanisms of muscle fibre type

transition (Buller et al., 1960). Endurance exercise, specifically, is the most studied area in inducing fibre type transformation. Researches have demonstrated that endurance exercise induces transformation of glycolytic fibres into oxidative phenotype within the fast twitch fibre types (IIb to IIx to IIa) in rodents and (IIx to IIa to I) in humans (Andersen and Henriksson, 1977, Green et al., 1979).

Subsequently, studies have established that activation of calcineurin, which activates nuclear factor of activated T cells (NFAT), results in inducing expression of slow twitch muscle genes, through transgenic animal studies as well as studies targeted deletion/ activation of calcineurin (Chin et al., 1998, Yan et al., 2011). Additionally, Ca^{+2}/calmodulin-dependent protein kinase (CaMK) activation of myocyte enhancer factor-2 transcription factors-(MEF2) through de-repression of class II histone deacetylase such as HDAC proteins (4, 5, 9), is also involved in the transformation of myofibres to those more oxidative (Potthoff et al., 2007). Furthermore, AMP-activated protein kinase (AMPK) and peroxisome proliferator activated receptor-γ coactivator-1α (PGC-1α) have been linked to muscle adaptation in response to metabolism and contractile activity. AMPK has been shown as an essential regulator of fibre type transformation in response to exercise, whereas PGC-1α maintains slow twitch-type I fibres independent of exercise and induces mitochondrial biogenesis (Geng et al., 2010, Rockl et al., 2007) (figure 1.5).

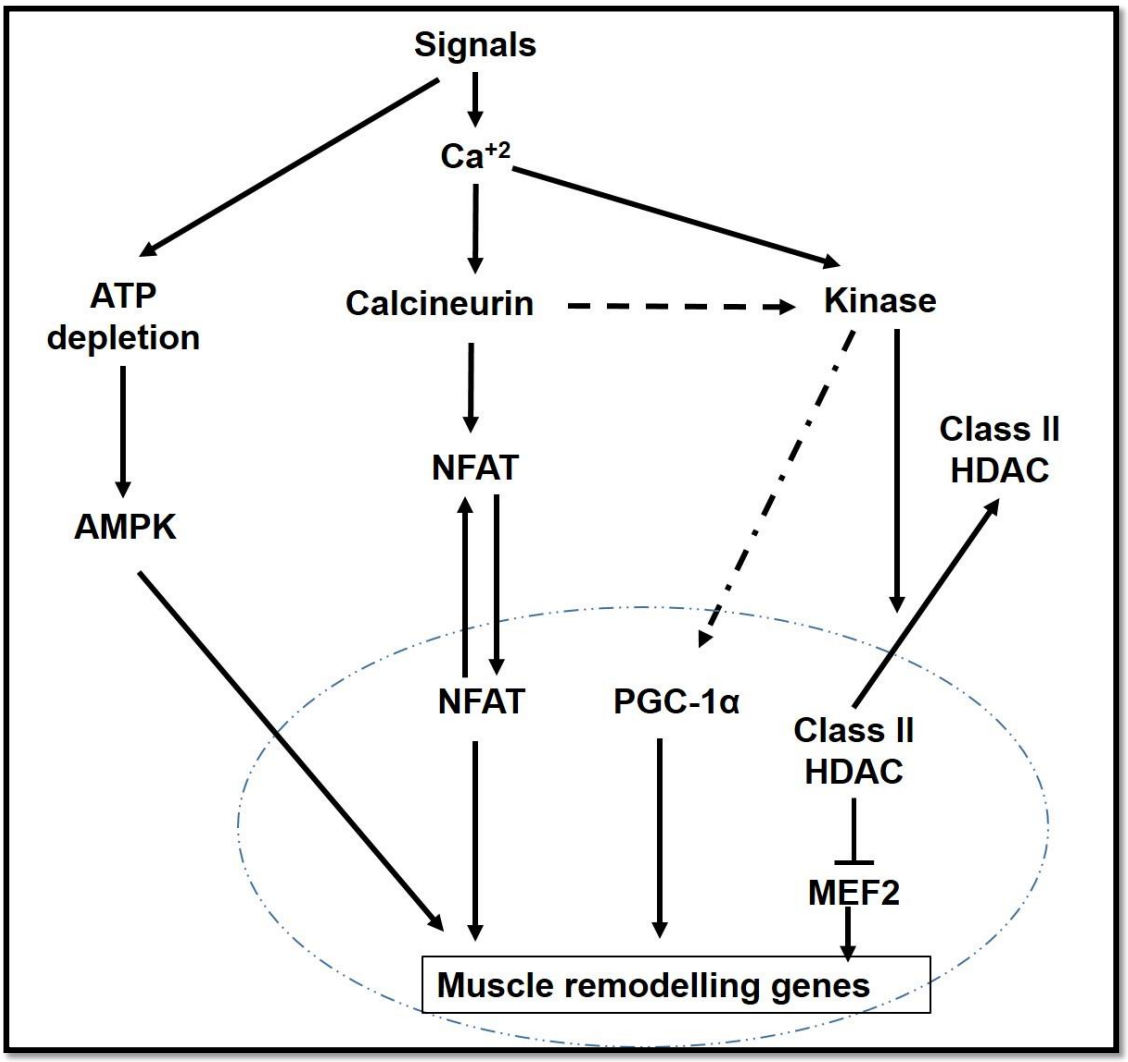

Figure 1.4. Signalling pathways activates skeletal muscle fibre type transformation.

Signalling pathway leading to altered muscle fibre type. These signals include Ca^{+2}, NFAT, PGC-1α, AMPK and MEF2.

1.5.3. Plasticity of skeletal muscle oxidative capacity:

Mitochondria are pivotal for aerobic ATP synthesis and proper cell function. In skeletal muscle, mitochondria quantity and quality is required for performance and health. Mitochondrial biogenesis is growth and division of pre-existing mitochondria in terms of size, number and mass and can be altered in response to environmental stress such as exercise, nutrition and oxidative stress (Baker et

al., 2007). The regulation of mitochondrial biogenesis and function is controlled via different mechanisms including transcriptional regulators that sense metabolic and energetic demands associated with physiological states (Matsakas and Patel, 2009, Hock and Kralli, 2009).

1.5.3.1. Cellular energy metabolism and mitochondrial biogenesis:

DNA-binding transcription factors such as nuclear respiratory factor-1 and 2 (NRF-1 and NRF-2) have been found to activate the expression of oxidative phosphorylation (OxPhos) genes, mitochondrial transporters, mitochondrial ribosomal proteins and mitochondrial transcription factor A (TFAM) (Scarpulla, 2008). In addition, they have been reported as part of energy-sensing pathways in mammalian cells, where their expression is induced in response to increased Ca^{+2} flux in skeletal muscles (Ojuka et al., 2003) and to the activation of AMPK (Bergeron et al., 2001).

Peroxisome proliferator activated receptors (PPARα, PPARγ, PPARδ) control the expression of uncoupling proteins (UCPs), that play roles in oxidative capacity, reactive oxygen species (ROS) production and thermogenesis and enable the mitochondrial adaptation to metabolic demands through interaction with other regulators of mitochondrial biogenesis such as; NRF-1 and 2, peroxisome proliferator activated receptor-γ coactivator-1α (PGC-1α) and PGC-1β (Hock and Kralli, 2009). PPARδ is highly abundant in skeletal muscles and heart, and the role of PPARδ in skeletal muscle mitochondrial biogenesis has been investigated through transgenic mice specifically express PPARδ in muscle and resulted in increased expression of oxidative metabolism genes and a shift towards oxidative fibres (Wang et al., 2004). Moreover, over-expression of PPARδ

promotes mitochondrial biogenesis and expression of UCPs, glucose transporter (GLUT4) and PGC-1α, possibly via induction of PGC-1α expression in muscle (Tanaka et al., 2003).

Another important regulator of mitochondrial biogenesis is PGC-1α. The PGC-1α proteins are important for the mitochondrial biogenesis because of their abilities to bind to NRF-1, NRF-2, PPARs, and estrogen related receptors (ERRs) (Hock and Kralli, 2009). Over-expression of PGC-1α in many cells results in induction of genes related to mitochondrial biogenesis and enhanced respiration for example; TFAM, UCP and ATP synthase (Handschin and Spiegelman, 2006). Transgenic over-expression of PGC-1α in skeletal muscles increases mitochondrial genes expression, mitochondrial content and promotes a shift towards slow oxidative fibres (Lin et al., 2002). Conversely, inactivation of PGC-1α using null mice of PGC-1α results in a decrease in the mitochondrial enzymatic activities, reduces exercise performance and decreases expression of mitochondrial genes (Lin et al., 2004). In response to exercise, PGC-1α expression has increased in null mice and induced the expression of NRF-1 and NRF-2 (Baar et al., 2002).

Energetic demands vary between cell types as well as in different physiological status. For example, in response to a single bout of exercise, the level of PGC-1α, NRF-1, PPARδ, estrogen related receptor α (ERRα) and mitochondrial target genes were increased (Baar et al., 2002). In response to a nutrient restriction such as fasting and caloric restriction, SIRT1 is induced in muscle and promotes the expression of PGC-1α, ERRα, TFAM and genes involved in OxPhos, fatty acid oxidation and tri carboxylic acid cycle (TCA) (Gerhart-Hines et al., 2007).

Moreover, AMPK senses energetic deficiencies in skeletal muscle as in fasting via adiponectin, where the activated AMPK turns off ATP-consuming process such as synthesis of lipids, carbohydrates and proteins and turns on ATP synthesis pathways including mitochondrial biogenesis (de Lange et al., 2006).

Feeding rats with a pharmacological activator of AMPK (β-guanadinopropionic acid) β-GPA for 8 weeks leads to activation of AMPK in skeletal muscle. Therefore, activation of AMPK induced expression of PGC-1α, NRF-1, cytochrome c protein and mitochondrial content and consequently mitochondrial biogenesis through PGC-1α and NRF-1 by sensing energy status of the muscle cell (Bergeron et al., 2001). Also, AMPK has been shown to activate other mitochondrial genes independent of PGC-1α such as (Ucp3) which is a mitochondrial enzyme and pyruvate dehydrogenase kinase isoenzyme 4 (Pdk4), which involves in glucose metabolism (Jäger et al., 2007).

Calcium-regulated signalling pathways also involve in the control of mitochondrial biogenesis. Observations from *in vitro* studies showed that calcium/calmodulin-dependent protein kinase IV (CaMKIV) influences gene expression in oxidative fibres (Wu et al., 2000). Transgenic over-expression of CaMKIV in skeletal muscle showed an increase in mitochondrial DNA (mtDNA) as well as increased mitochondrial number. It is accompanied by increased mRNA level of cytochrome b and carnitine palmitoyltransferase (CPT) (Wu et al., 2002). On the other hand, CaMKIV null mice showed similar protein level of PGC-1α and COX IV compared to wild type, suggesting that CaMKIV may not be required for mitochondrial biogenesis (Akimoto et al., 2004). Similarly, transgenic mice specifically expresses p38 mitogen activated protein kinase (p38 MAPK) in skeletal muscle

showed increased protein expression of cytochrome oxidase IV and PGC-1α. Moreover, exercised mice showed induced expression of p38 MAPK and hence increased PGC-1α activation, this suggest that the latter is working downstream of AMPK (Akimoto et al., 2005).

1.5.4. Plasticity of skeletal muscle angiogenesis:

Vasculature of skeletal muscles can remodel itself to enhance oxygen delivery to the active muscles. Remodelling occurs when the excited vasculature is insufficient to meet the muscle activity or metabolic demand of the tissue. Vascular remodelling can occur in two types; arteriogenesis and angiogenesis. The first refers to an increase in the diameter of exciting arterial vessels, whereas the latter is the increase in the number of capillaries necessary for blood/muscle oxygen exchange (Lloyd et al., 2005).

Angiogenesis is the formation of new capillaries from existing capillaries. It has been shown that endurance exercise induces angiogenesis through two main mechanisms; intussusception and sprouting angiogenesis. The first mechanism defines as the process by which a single capillary splits into two capillaries within the lumen and the second mechanism refers to the branching out of endothelial cells from an existing capillary. The capillary network is responsible for the diffusive exchange of oxygen, carbon dioxide and nutrients between the vascular space and the intracellular space of the muscle fibres. It has been reported that endurance exercise training results in increased capillary density (angiogenesis). In response to exercise, there is an increase in the oxygen and nutrient supply to the muscle by expanding the capillary network (Prior et al., 2004). Additionally, vascular endothelial growth factor (VEGF) has been found as the most important

mitogen of endothelial cells to induce angiogenesis. Muscle specific deletion of VEGF showed a reduction in the endurance exercise capacity and capillary density (Olfert et al., 2009). The literatures has supported a correlation between oxidative capacity of mitochondria and the capillary density in different skeletal muscles (Maxwell et al., 1980).

Hypoxia has been shown as a stimulus of angiogenesis in which a transcription factor, hypoxia inducible factor-1 (HIF-1α) lead to an increase in the activity of VEGF promoter in cell culture (Forsythe et al., 1996). Signalling cascade that emerge to regulate angiogenesis in skeletal muscle involves (PGC-1α) under the condition of hypoxia in HIF-1α-independent manner through co-activation of ERRα (Arany et al., 2008). Further, muscle specific deletion of PGC-1α displayed a reduced angiogenesis and VEGF expression in response to endurance exercise (Geng et al., 2010). Mechanistically, the role of PGC-1α on angiogenesis and exercise induced-VEGF is under the control of the upstream p38γ AMPK, mediated through ERRα (Chinsomboon et al., 2009).

Therefore, the understanding of these muscle plasticity processes are important in the condition where oxidative metabolic and vascular density is compromised, such as in Duchenne muscular dystrophy.

1.6. Duchenne muscular dystrophy:

Muscular dystrophy is a group of more than 30 hereditary disorders which results in progressive loss of skeletal muscle fibres, causes muscle weakness and respiratory failure (Emery, 2002). Duchenne muscular dystrophy (DMD) is caused by out of frame mutation with complete loss of dystrophin protein (Kunkel,

2005). DMD is an X-linked, recessive neuromuscular disorder with an incidence of 1:3500-5000 new born males and it is the most common type of muscular dystrophies in childhood (Mah et al., 2016). DMD is initially characterized by a delay in motor function, calf hypertrophy and a marked elevated serum levels of creatine kinase (CK). The progressive muscle weakness results in a loss of ambulation between 7-12 years leading to a reduced life expectancy due to respiratory and/or cardiac failure (Allen et al., 2016).

Other allelic conditions exists; Becker muscular dystrophy (BMD) is a milder form caused by in frame mutation lead to expression of partially (truncated) but functional dystrophin protein, whereas X-linked dilated cardiomyopathy is a rare disorder related to dystrophinopathy and caused by mutation in the dystrophin gene, presenting with a cardiac pathology only (Nakamura, 2015).

Dystrophin protein is expressed in muscle and connects the γ-actin of the subsarcolemmal cytoskeleton system to proteins in the surface membrane forming dystrophin protein complex (DPC). Function of DPC can be divided into two main categories; mechanical and signalling roles. Mechanical role in which DPC protects the sarcolemma from damage following repeated cycles of contractions and acts as a crucial link between extracellular matrix and intracellular actin cytoskeleton. Dystrophin binds to actin and β-dystroglycan, which is connected to laminin via α-dystroglycan. The second signalling role of DPC initiated with the fact that signalling molecules related to muscle function such as nitric oxide synthase (NOS) is in contact with DPC. Proteins that play roles in the signalling function of DPC are sarcoglycan, α-dystrobrevins, syntrophins, sarcospan, biglycan, integrin and neuronal nitric oxide synthase

(nNOS). Further, DPC is linked to contractile elements via intermediate filaments; desmin, syncoilin and desmuslin. In addition, DPC has been shown to link to Z-disc via filamin-C protein through interaction with δ and γ sarcoglycan (Allen et al., 2016) (figure 1.6).

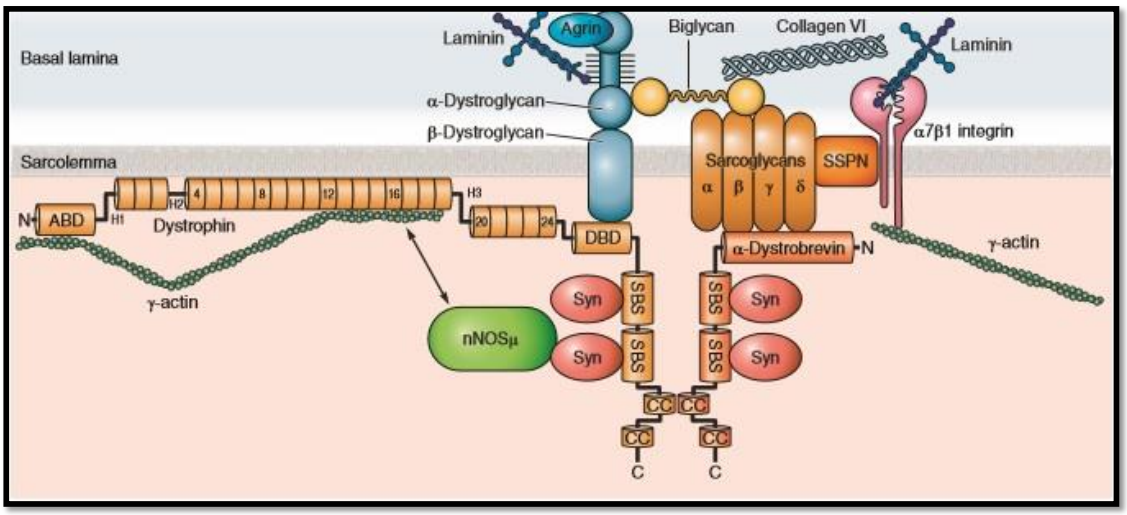

Figure 1.5. Dystrophin glycoprotein complex

Dystrophin-glycoprotein complex composed of dystroglycan α and β subcomplex which connect the basal lamina proteins; agrin, laminin and perlecan to the sarcolemma cytoskeleton F-actin. The sarcolemma proteins composed of dystrophin, syntrophin α, β, and dystrobrevin (DTNA). In addition, nNOSμ is linked to the complex by interacting to both the dystrophin and syntrophin. Sarcoglycan-sarcospan sub-complex stabilizes the DGC to the sarcolemma and comprises of α, β, γ and δ sarcoglycan and sarcospan (SSPN) (Allen et al., 2016).

1.7. Changes in the absence of dystrophin:

Dystrophin has a major role in signalling pathways for example; activation of nitric oxide (NO) production, regulation of Ca^{+2} and production of (ROS) as well as transmission of force laterally across the muscle and helps in maintaining the association between intracellular cytoskeleton and extracellular matrix. Loss of dystrophin leads to complete loss of DPC and disruption of costameres that makes muscle fibre more susceptible to contraction-induced damage and increases loss of calcium homeostasis, which in turn causes on-going

degeneration and regeneration of muscle fibres and eventually necrosis. At early stage of the disease, the regenerative process could compensate the degenerated muscle fibres and fibrotic cells, with time, however, the capacity of this process starts to dissipate and therefore the adipose and connective tissue replace the muscle fibres (Allen and Whitehead, 2011). Multiple factors contribute to muscle damage in DMD; loss of Ca^{+2} homeostasis, increased level of ROS, inflammation and necrosis (Shin et al., 2013).These factors in combination impact on the regenerative capacity of the muscle by compromising satellite cells that become exhausted by the progression of the dystrophy with time (Abou-Khalil et al., 2010).

1.7.1. Oxidative stress:

It has been established that a disruption of redox signalling is a characteristic of dystrophic muscles where the increased susceptibility of dystrophic muscles to oxidative stress is likely occur as a combination between a reduction of the endogenous antioxidant and increased ROS-activated pathways (Shkryl et al., 2009, Whitehead et al., 2010).

Oxidative stress is increased in dystrophic muscle as shown by increased level of lipid peroxidation, glutathione status and superoxide (Whitehead et al., 2008, Burdi et al., 2009, Dudley et al., 2006). In DMD, oxidative stress leads to damage of muscle function, atrophy, reduced regenerative capacity and eventually muscle weakness (Barbieri and Sestili, 2012)

The exact impact of oxidative stress on dystrophic muscle is uncertain. Some researchers suggested the elevation of ROS is the primary occurrence in dystrophic muscle, due to deregulation of NO (Thomas et al., 1998, Wehling et

al., 2001). Others have suggested it is occurring following excessive Ca^{+2} influx and inflammation (Yeung et al., 2005). However, abnormal uptake of calcium by mitochondria in *mdx* mice induce greater production of ROS. Increased level of protein oxidation (measured by carbonyl group) and lipid peroxidation (measured by isoprostanes) has been detected in DMD and *mdx* samples as an evidence of increased ROS (Haycock et al., 1996, Grosso et al., 2008, Hauser et al., 1995, Messina et al., 2006). Mechanical distension of the sarcolemma induced by contraction causes the formation of superoxide radicals by the cation of nicotinamide adenine dinucleotide phosphate oxidases (NADPH-oxidase), NOX, which cannot be processed by NO due to low bioavailability in DMD muscles. NOX is a major source of ROS during muscle contraction with presence of different isoforms (1-5) expressed in a wide range of tissues (Bedard and Krause, 2007). (NOX2) isoform is located in skeletal muscle at the sarcolemma and T-tubules of muscle fibres and more importantly is a dystrophin associated protein (Khairallah et al., 2012). Therefore, loss of dystrophin leads to a highly disorganized microtubule network and induces activation of NOX2, which is a major source of ROS in *mdx* during exercise (Khairallah et al., 2012). Elevated levels of ROS by NOX2 induction may be involved in the opening of stretch activated channels (SACs) and Ca^{+2} entry into myofibres. Consequently, increased Ca^{+2} leads to elevated mitochondrial Ca^{+2} levels, an increase in mitochondrial ROS production and dysfunctional mitochondrial, which perturb muscle function (Whitehead et al., 2010).

NOX2 is up-regulated at early stage of the disease during the oxidative stress period when the inflammatory cells such as macrophages and neutrophils utilize NOX2 to produces superoxides, which increase ROS production (Lawler, 2011).

However, further ROS production contribute to disruption of cell signalling, in particular, through activation of NF-κB that increases activation of pro-inflammation cytokines such as tumour necrosis factor α (TNFα), which are found to be elevated in *mdx* mice (Altamirano et al., 2012, Acharyya et al., 2007, Kumar and Boriek, 2003).

Increased ROS production and down regulation of antioxidants such as glutathione (Renjini et al., 2012) and NRF-2 (Petrillo et al., 2017) in *mdx* mice, make regulation of ROS activity and stimulation of antioxidants response pathway important targets for the modulation of dystrophic pathology. Initial therapies to maintain Ca^{+2} homeostasis included the use of Ca^{+2} blockers such as diltiazem, however this did not demonstrate any benefits in clinical trials (Shin et al., 2013). On the other hand, antioxidants treatments, for example; Pyrollidine dithiocarbamate (PDTC) has been used through minimizing the effect of NF-κB (Carlson et al., 2005).

1.7.2. Calcium influx:

Ca^{+2} is essential to the function, maintenance of skeletal muscle and physiological transduction pathway of excitation-contraction coupling, which effectively regulates skeletal muscle contraction (Berchtold et al., 2000, Goll et al., 2003) and regulation of mitochondrial function (Das and Harris, 1990, Brookes and Darley-Usmar, 2004). As a result of significant roles of Ca^{+2} in all cellular events, its concentration is regulated tightly in skeletal muscle fibres through SR, mitochondria, a number of ion channels such as calcium channel ryanodine receptor 1 (RyR-1) and sarcoplasmic/endoplasmic reticulum calcium-ATPase 1 (SERCA-1) and intermediate binding proteins that move Ca^{+2} between

the SR and the storage reservoirs (Berchtold et al., 2000). In DMD, the fibres are more susceptible to intracellular Ca^{+2} and damage (Culligan and Ohlendieck, 2002). It has been accepted in the literatures that Ca^{+2}-dependent muscle necrosis is responsible for the severe wasting characteristic in *mdx* and DMD. Ca^{+2} is thought to flow into myocytes leading to an increase in intracellular Ca^{+2} level and subsequent down-regulation of various Ca^{+2}-binding proteins that initiate Ca^{+2} dependent proteolysis such as calpains that alters mitochondrial function and apoptosis. However, it is still widely debated on the exact mode of Ca^{+2} entry and primary cause of dystrophic pathology. At the same time it is generally accepted that dystrophin provides a degree of protection to the sarcolemma against mechanical injury and without it the membrane is disposed to tear and subsequent Ca^{+2} leak (Bodensteiner and Engel, 1978, Whitehead et al., 2006).

As shown in Fong et al., both *mdx* mice and cultured biopsies of DMD patients have greater levels of intracellular Ca^{+2} compared to control muscle (Fong et al., 1990). It has been reported that calcium permeability of the sarcolemma is affected through; 1) Mechano-sensitive voltage-independent calcium channel (MSC), which increases leaking channel activity, resulting in calcium overloading and excessive ROS production (Turner et al., 1991). 2) Store-operated calcium channel (SOCE), which is activated by SR Ca^{+2} depletion and calcium leak channels due to hypernitrosylation of ryanodine receptor (RyR-1) (Berg et al., 2002, Davies and Nowak, 2006, Bellinger et al., 2009). 3) SR Ca^{+2} pump (SERCA-1), which functions to return Ca^{+2} from the sarcoplasm to the SR and causes relaxation. Controversial data have been reported in the literatures of SERCA-1 in *mdx*, with decreased function (Kargacin and Kargacin, 1996),

increased function (Robin et al., 2012) and unchanged function (Takagi et al., 1992). However, studies have shown improvement of the dystrophic phenotype such as central nuclei, fibrosis and a reduction in creatine kinase level following over-expression of SERCA-1 in *mdx* (Goonasekera et al., 2011). Goll et al., has proposed that abnormal Ca^{+2} overloading causes activation of calcium-dependent proteases such as calpains which involve in protein degradation, fibre necrosis and eventually cell death at a rate cannot be compensated by progenitor satellite cells and regeneration (Goll et al., 2003).

1.7.3. Metabolic system defect:

Defects in cellular energy system have been reported in skeletal muscles from *mdx* and DMD patients where the capacity of mitochondrial oxidative phosphorylation is impaired (Kuznetsov et al., 1998, Even et al., 1994, Timpani et al., 2015). Adequate ATP production is required to maintain integrity and function of all cells. ATP is generated via the creatine phosphagen system, metabolism of glucose through glycolysis and fatty acid oxidation via β-oxidation. Products of glucose and fat metabolism, pyruvate and acetyl CoA, are transported into tricarboxylicacid (TCA) and electron transport chain (ETC) in the mitochondrial and ATP is generated via oxidative phosphorylation (OXPHOS) process (Rybalka et al., 2015). As a consequence of ATP-dependent Ca^{+2} buffering, satellite cell-mediated muscle repair, dysregulation of redox system and autophagy, there is a huge demand for ATP production in dystrophic muscle, which is an environment with impaired metabolic system. Reduced glucose availability due to loss of NO signalling is another factor that contributes to the reduced ATP producing capacity of mitochondria in dystrophic muscle (Rybalka et al., 2015). Glucose uptake is maintained by Glut4, which is reduced in

dystrophic muscles and therefore affect the ability to bring sufficient glucose into the muscle fibres to maintain energy production (Olichon-Berthe et al., 1993, Timpani et al., 2015). Glucose transport into the cells occurs through translocation of Glut4 from cytoplasm to the sarcolemma/T-tubules, in response to contraction. Due to alteration in Glut4 level or localization within the cells, as shown in *mdx* and DMD, it is likely that reduced substrate availability is a precursor to energy system de-regulation that impact the overall glucose metabolism, contributing to the metabolic stress in dystrophic muscle (Rybalka et al., 2015, Schneider et al., 2018). In addition, various metabolic defects have also been demonstrated in dystrophic muscle; impairments of fatty acid metabolism (Lin et al., 1972), glycolysis (Di Mauro et al., 1967), TCA, ETC (Chi et al.) and purine nucleotide cycle (PNC) (van Bennekom et al., 1984). All of these lead to 50% reduction in resting ATP level within dystrophin-deficient myofibres, which are incapable to meet the huge demand of ATP (Austin et al., 1992).

Reduced ATP in dystrophic muscle has been accompanied by reduced regeneration capacity, exacerbated muscle degeneration and promoted muscle wasting (Rybalka et al., 2015). Impaired ATP production capacity by mitochondria is thought to be linked to deficiency in complex I function whereby ATP production rely on NADH-mediated shuttling of H^+ into the (ETC) through complex I. It was shown the complete inhibition of complex I with rotenone and activation of complex II with succinate at the same time results in partial recovery of mitochondrial-ATP production (Rybalka et al., 2015) (figure 1.7).

(A)

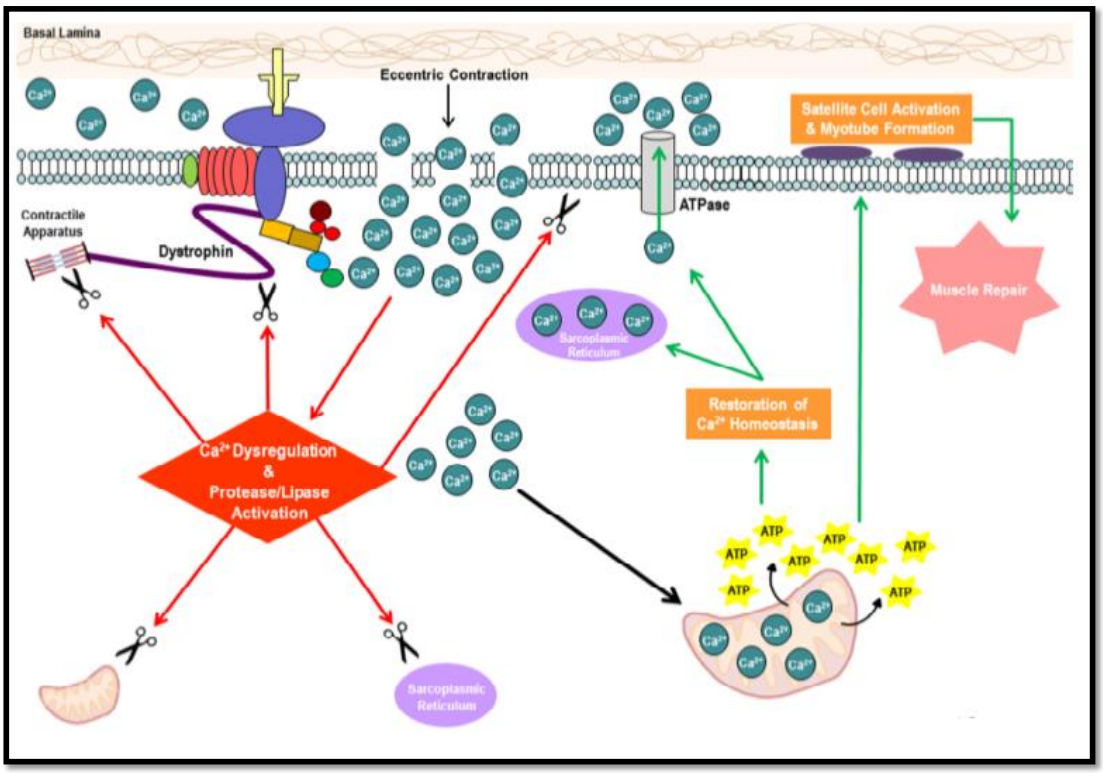

(B)

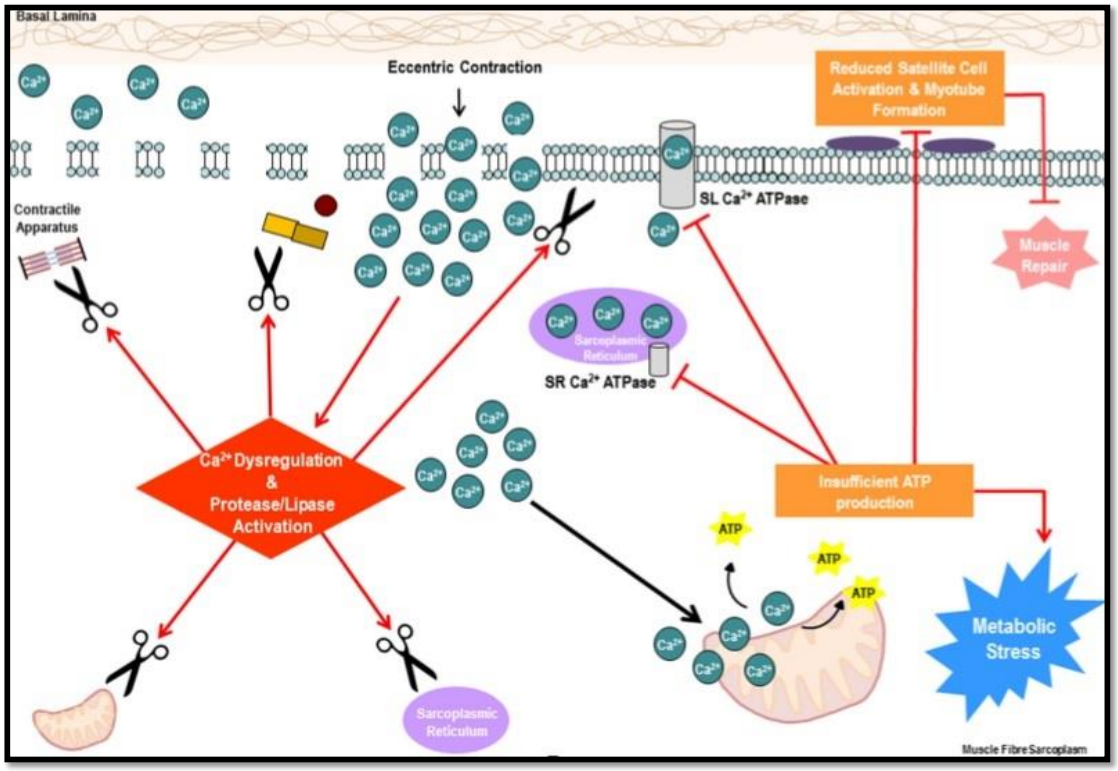

Figure 1.6. Role of ATP in healthy and dystrophic skeletal muscle

A) Eccentric contraction in healthy muscle potentiate Ca^{+2} influx into the intracellular matrix which in turn increased in concentration and then activate protease that rupture mitochondria, SR and sarcolemma. Ca^{+2} uptake into the mitochondrial activates OXPHOS and ATP production to support ATP-fuelled Ca^{+2} pumps thus restoring Ca^{+2} homeostasis and mitigate the severity of damage. ATP also fuels satellite cell replication and skeletal muscle repair. B) The increased propensity for membrane rupture following eccentric contraction causes the same degenerative events. Mitochondrial dysfunction coupled with insufficient ATP production lead to failure in ATP-dependent Ca^{+2} buffering to alleviate damage, therefore, degenerative capacity is amplified (Rybalka et al., 2015).

1.7.4. Blood flow dysregulation:

In healthy muscles, NO acts as a paracrine signal to regulate blood flow through diminishing sympathetic (α-adrenergic) vasoconstriction. The mechanism by which NO attenuate α-adrenergic possibly involves cyclic guanosine monophosphate (cGMP) (Francis et al., 2010). However, the ability of skeletal muscles of *mdx* mice to reduce α-adrenergic vasoconstriction is defective due to the miss localization of nNOSμ, leading to muscle ischemia. NO has been suggested as antagonism of α-adrenergic vasoconstriction since NO diffuses to arterioles and results in vasodilation that increases blood flow (Thomas et al., 1998). Evidence showed that *mdx* has impaired vascular density and angiogenesis. Immunostaining of arterioles in *mdx* has revealed a reduction in vascular density of heart and gracilis muscles (Loufrani et al., 2004). Matasakas et al., have used microfil-perfusion for *tibialis anterior* (TA) in *mdx* and showed reduced vasculature in *mdx* compared to wild type (Matsakas et al., 2013). Moreover, images of hind limb muscles with Laser Doppler perfusion showed compromised blood flow in *mdx* (Palladino et al., 2013). Therefore, in the context of DMD, which is suffered from oxidative stress, this lack of vascularisation, will increase the stress, leading to overt pathology. However, it is believed that loss

of dystrophin causes translocation of nNOSμ from sarcolemma to accumulate in the cytosol (Brenman et al., 1995).

Skeletal muscles expressed three different types of nitric oxide synthase (NOS); NOS1 (nNOS), NOS2 (iNOS), NOS3 (eNOS). Splicing of nNOS results in four different isoforms; nNOSα, nNOSβ, nNOSγ and nNOSμ, the latter is the most predominant isoform in skeletal muscles. Association of nNOSμ with DPC requires α-syntrophin and dystrophin where nNOSμ converts L-arginine to nitric oxide (NO), which functions in regulating glucose uptake, vascular perfusion during muscle contraction, maintaining mitochondrial function and regulation of (RYR) function (Allen et al., 2016). These physiological functions result from the ability of NO to stimulate guanylate cyclase, therefore enhances the production of cGMP (Francis et al., 2010).

Understanding the factors involve in the regulation of angiogenesis has been of a significant value for the DMD therapy. Vascular endothelial growth factors exist in several isoforms; VEGF121, VEGF145, VEGF-165, VEGF-183, VEGF-189 and VEGF-206 (Tammela et al., 2005a). Specific blockade of VEGF in skeletal muscles resulted in reduced capillary density compared to wild type (Olfert et al., 2009). In normal skeletal muscle, VEGF is expressed in vascular structure but not in muscle fibre. Following muscle damage, VEGF expression was detectable in regenerating muscle fibre and satellite cells which highlights the pro-myogenic effect of VEGF in skeletal muscles in promoting muscle regeneration through neovascularisation of necrotic area (Arsic et al., 2004). Over-expression of VEGF via adeno associated virus (AAV) gene transfer in *mdx* mice resulted in increasing capillary density, regenerative fibre areas and reducing necrosis in 4

weeks treated *mdx*. In the same study, over-expression of VEGF was shown to increase strength of forelimb muscles which highlighted the importance of VEGF as a pro-regenerative factor in skeletal muscles (Messina et al., 2007).

To stimulate nNOS, administering L-arginine (NO precursor) in combination with metformin (pharmacological activator of AMPK) into DMD patients resulted in an increase in cGMP and mitochondrial proteins in skeletal muscles as a result of increasing level of NO (Hafner et al., 2016).

1.7.5. Inflammation:

Inflammation process is divided into two main classifications, acute or chronic. Acute inflammation is an immediate non-specific response that is considered the first line defence against injury by removing the dead and damaged myofibres and promote activation of resident satellite cells, which mediate replacement of injured muscle. Skeletal muscle of DMD is characterized by chronic inflammation (Tidball, 2005). However, the newly formed myofibres contain the defective gene and are subjected to further degeneration. As a result, the satellite cells population becomes exhausted or unable to mediate repair, resulting in continued cycles of regeneration and degeneration followed by a chronic inflammatory response due to abnormal presence of inflammatory cells. All of these events lead to replacement of muscle tissue by adipose and fibrotic tissue (Serrano et al., 2011).

As described earlier, dystrophin deficient muscles are more susceptible to mechanical injury as the plasma membrane is damaged easily during muscle contraction that allow extracellular Ca^{+2} influx and release of endogenous ligands. The upregulated Ca^{+2} in DMD leads to calpains activation, which

degrades IκB (inhibitory of NF-κB) and then activates NF-κB inflammatory pathway, which stimulates cytokine release such as TNF-α and IL-1β which in turn further augment the activity of NF-κB and impair muscle regeneration. In inactive condition, NF-κB is retained in the cytoplasm binding to the inhibitory protein IκB. The activation of NF-κB is regulated by IκB kinase that stimulates translocation of NF-κB to the nucleus, which then regulates transcription of cytokine genes (Kumar and Boriek, 2003, Acharyya et al., 2007).

A number of studies showed a higher expression of genes involved in inflammatory responses in DMD muscles such as TNF-α, IL-1β and IL-6. TNF-α can further stimulate production of ROS and therefore create positive feedback loop where ROS can increase production of NF-κB (Whitehead et al., 2006). Hodgetts et al., showed the role of neutrophils in dystrophic myofibres by depleting them using antibodies, and results in reducing fibre necrosis and inflammatory cells (Hodgetts et al., 2006). Mast cells are infiltrating inflammatory cells, which surrounds injured muscle. They can contribute to fibre necrosis by releasing histamine and TNF-α and mediate necrosis through producing pro-inflammatory cytokines (Tidball, 2005).

A pro-inflammatory cytokine, TNF-α has been reported to induce a shift towards more glycolytic myofibres in skeletal muscles, reduce mitochondrial and ATP contents, thus compounding dystrophic metabolic stress. The activation of TNF-α reduces the expression of regulatory genes of skeletal muscle oxidative phenotypes for example; PGC-1α, PGC-1β, PPARα and TFAM and the activation of NF-κB by TNF-α reduced expression of TFAM, NRF-1 which are regulators of mitochondrial biogenesis. In addition, activation of IL-1β induces the expression

of NF-κB and hence reduced expression and activity of slow oxidative fibres. Therefore, activation of NF-κB signalling results in impairment of cellular oxidative phenotype (Remels et al., 2010, Remels et al., 2013). Gene therapy using AAV to inhibit NF-κB via the over-expression of dominant-negative forms of IKKα and IKKβ showed significant results through reducing necrosis and enhancing muscle regeneration in older *mdx* (Tang et al., 2010).

1.7.6. Autophagy:

Autophagy is a critical homeostasis process in clearing defected and damaged organelles from the cells and it has been found to be severely impaired in muscle biopsy from DMD patient and *mdx* mice (De Palma et al., 2012). A reduced expression of autophagy markers were shown in *mdx* compared to wild type in (TA) and diaphragm muscles. For example, the level of LC3II in *mdx* mice, which is the network form of the microtubule-associated protein-1 light chain 3, was found significantly lower than in normal muscles. On the other hand, the level of p62 was increased in muscles from *mdx* mice (De Palma et al., 2012). Activation of autophagy improves dystrophinopathy in *mdx* mice where maximal force generating capacity was improved by AICAR (5-aminoimidazole-4- carboxamide-1-β-d-ribofuranoside) (Pauly et al., 2012).

1.7.7. Fibrosis:

Fibrosis is the deposition of extracellular matrix components; collagen and fibronectin during repair of the damaged fibres which leads to loss of tissue structure, function and replacement of normal tissue with connective tissues in response to inflammation and chronic injury which in turn impairs tissue function (Goyenvalle et al., 2011). The imbalance of different cell types lead to production

of growth factors, angiogenic factors, proteolytic enzymes and fibrogenic cytokines that destroy, remodel and replace normal tissue with connective tissue elements (Serrano et al., 2011). Accumulation of connective tissue has negative impact on therapeutic intervention as the amount of target tissue available for therapy is reduced. A superfamily of TGF-β cytokines contribute to pathogenesis associated with muscular dystrophy where TGF-β1 signalling disrupts muscle membrane by blocking nutrients from reaching to myofibres (Zhou and Lu, 2010) through stimulating interleukin 11 (IL-11) (Johnstone et al., 2015). During chronic damage in DMD, increased and persistence of different inflammatory-macrophages cells types could modify the kinetics level of cytokines, resulting in altered satellite cells function with progressive fibrosis. Fibro/adipogenic progenitor (FAP) cells are thought to persist if the regeneration fail and therefore they differentiate into adipocytes and control pro-differentiation signals with great tendency to generate adipose cells (Mann et al., 2011).

1.7.8. Impact on muscle function in the absence of dystrophin:

In normal myofibres, dystrophin and associated proteins are found in a rib like structure called costameres linked to sarcomeres' Z disc of the myofibrils located all along the whole fibre (Pardo et al., 1983). Costameres are located ideally to transmit the forces developed by activated fibres throughout a muscle (Brooks and Faulkner, 1988). The DPC provides the connection between the sarcomeres, laterally through the sarcolemma and basement membrane into the extracellular matrix (ECM) (Goldstein and McNally, 2010). In aged and *mdx* mice, the lateral force is severely impaired and correlated to the loss of dystrophin, which highlighted the critical role of DPC in lateral force transmission in skeletal muscles (Ramaswamy et al., 2011). A number of investigators have proposed

the important role of dystrophin in the stability of muscle fibres. For example, the skeletal muscle from *mdx* and humans exhibit high levels of contraction induced injury following the protocol of lengthening contraction. *Ex-vivo* assessment of force deficit following eccentric contractions in normal muscles showed a 10% reduction compared to *mdx* muscles which showed a round 70% decrease (Petrof et al., 1993a) that reflect the compromised lateral force transfer between fibres and the critical role of costameres in the maintenance of sarcomere stability (Rybakova et al., 2000, Bloch et al., 2004). This reduction was attributed to loss of dystrophin and hence disorganized costameres that enhanced membrane leak of cytosolic Ca^{+2} and consequently increased mitochondrial production of ROS and NADPH oxidase which contribute to muscle force loss (Whitehead et al., 2006). ROS are thought to directly oxidize contractile proteins or sarcolemmal lipids and they may activate signalling via NF-κB leading to inflammation and altered cytoskeleton (Goldstein and McNally, 2010, Whitehead et al., 2008). In total, the exacerbated microenvironment of the DMD muscles with increased inflammatory markers, increased oxidative and metabolic stress, the replacement of contractile tissue with fibrotic scar tissue make the extracellular matrix stiffer, leading to a reduction in the force capacity of the muscle (Lieber and Ward, 2013).

As mentioned before, due to absence of dystrophin, nNOS delocalize from the sarcolemma to the cytosol. As a result, the activity of cytosolic nNOS is elevated (Lai et al., 2009). Opposing studies shown differential effects of NO on muscle force and pathology associated with DMD. For example; several studies revealed a beneficial effect of NO releasing agents (arginine) in *mdx* mice (Voisin et al., 2005) and DMD patients (Hafner et al., 2016), however, supplementation of

arginine has exacerbates fibrosis in *mdx* mice (Wehling-Henricks et al., 2010), whereas convincing data has suggested that NO inhibits muscle force (Kobzik et al., 1994). Specifically, NO impair muscle function through nitrosylation of RYR1 (Bellinger et al., 2009, Bellinger et al., 2008), as it has been proposed that nitrosative stess induced by delocalized nNOSμ in *mdx* mice inhibits muscle force. When nNOSμ activated by Ca^{+2}, nNOS generates excessive NO. ROS in dystrophic muscle convert NO to reactive nitrogen species (RNS) that lead to global dysregulated nitrosylation state. Specifically, s-nitrosylation of RYR compromises the contractile proteins that reduces the already compromised force (Li et al., 2011). S-nitrosylation of RYR-1 causes depletion of calstabin1 (FKBP12), resulting in leaky channel (Lamb and Stephenson, 1996). Deletion of calstabin1 specifically in skeletal muscles, can cause a loss of depolarization-induced contraction and impaired excitation-contraction coupling because of reduced maximal voltage-gated SR Ca^{+2} release (Tang et al., 2004) (figure 1.8).

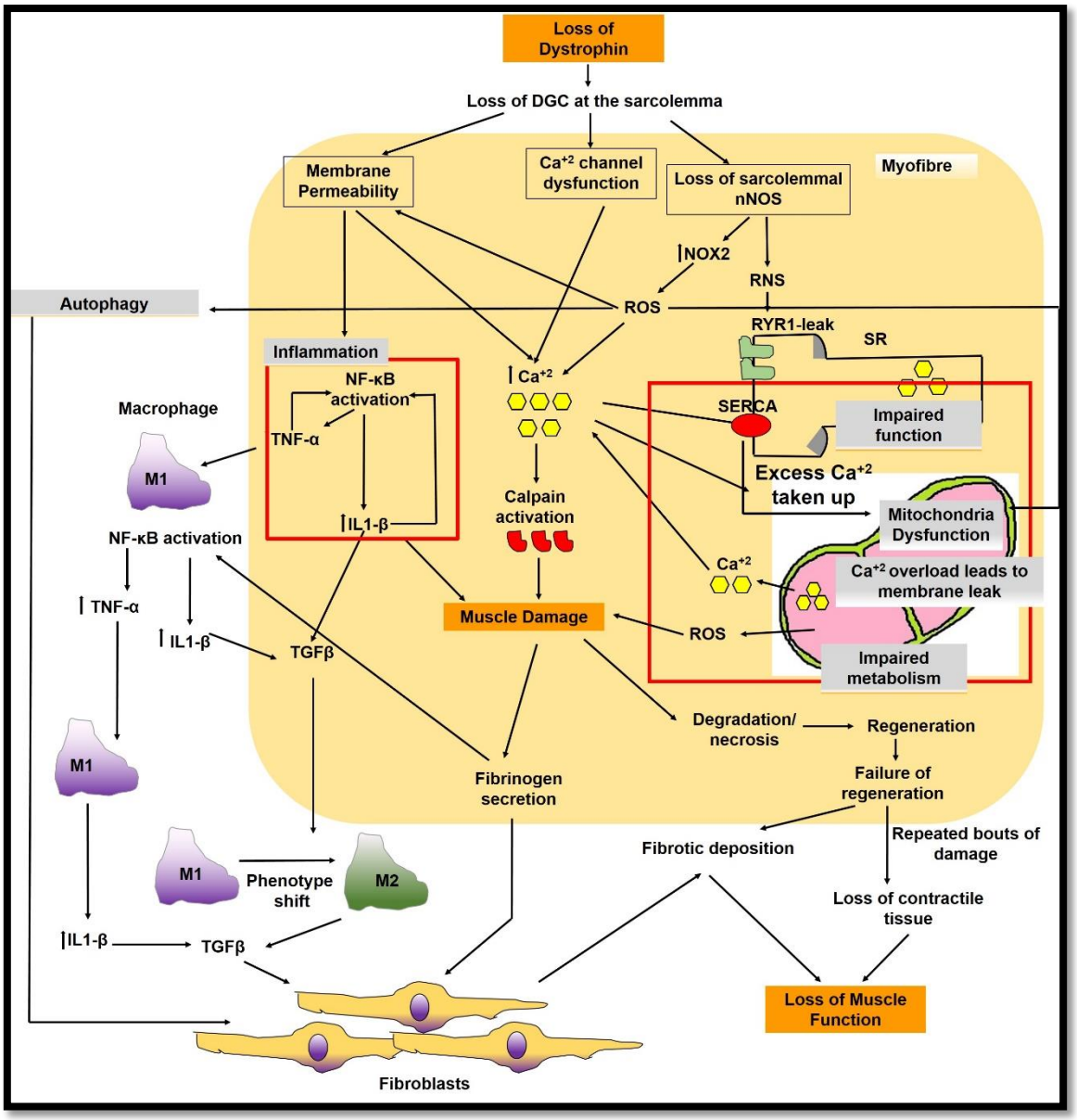

Figure 1.7. Pathways involve in loss of muscle function

1.8. *Mdx* mice as a model of DMD:

In 1984, Bulfield et al., first described the existence of a mutation in the dystrophin gene of C57BL/10 strain, with elevated levels of serum pyruvate kinase and creatin kinase, which they proposed as a possible investigatory animal model of X-linked human disease of DMD (Bulfield et al., 1984). Analysis of cDNA from *mdx* and wild type muscles revealed single base substitution in exon 23 in the

mdx mice. In the *mdx*, a cytosine is replaced by a thymine at nucleotide position 3185, resulting in a termination codon (TAA) in place of a glutamine codon (CAA) (Sicinski et al., 1989).

mdx mice have minimal clinical symptoms comparing to human DMD and their life span is reduced by 25% where the individual life span reduced by 75% (Chamberlain et al., 2007). Severe dystrophic phenotypes such as heart failure do not occur until mice are 17 months or older (Quinlan et al., 2004). The *mdx* muscle degeneration appears in waves not a continuum. Skeletal muscles in *mdx* exhibit different phases; in the first 2 weeks they are not distinguishable from normal muscles, then between 3-6 weeks of age, the limb muscles become hypertrophic, they undergo extensive degeneration/regeneration cycle, indicated by newly differentiated fibres with centralized nuclei (as a sign of regeneration) and heterogeneity in fibre size. In parallel, the muscles undergo necrosis at this early stage which then decreases around 10 weeks of age (McGeachie et al., 1993).

Despite sharing the same genetic defect as DMD, *mdx* mice have a slowly progressive pathology which does not lead to loss of muscle mass and spread formation of fibrous connective tissue that characterize human disease. The diaphragm is the only exception and shows progressive deterioration with extensive replacement of muscle fibres with fibrous connective tissue, similar to what seen in DMD patients. In addition, *mdx* mice do not loss their ability to walk (Chamberlain et al., 2007). On the other hand, pathology in DMD boys is difficult to diagnose during the first years of life, but they show symptoms of pseudo-hypertrophy followed by onset of muscle wasting around 4 years of age. Pseudo-

hypertrophy means damage of muscle fibres accompanied by necrosis followed by the activation of satellite cells, which play a role in muscle fibre regeneration. The poor cycle of regeneration and degeneration, produce large but weak muscles. Muscle wastage occurs as the degeneration process overtakes the capabilities of satellite cells for muscle regeneration (Morgan and Zammit, 2010). DMD boys loss the ambulation around 10 years of age and die as a result of respiratory or cardiac failure (McGreevy et al., 2015, Chamberlain et al., 2007).

The slowly progressive phenotype of *mdx* mice is explained by four different reasons; first, the active process of regeneration due to the ability of satellite cells to divide rapidly and allow repair of damaged fibres (McGreevy et al., 2015). Second, the increased expression of utrophin, a homolog to dystrophin, which is suggested to compensate for the loss of dystrophin in these mice (Tinsley et al., 1998). Third, the presence of the cytidine monophosphate sialic acid hydroxylase gene (CMAH) in mice; this gene is inactivated in humans and appeared to worsen the consequence of dystrophin absence in humans (Chandrasekharan et al., 2010). Fourth, the protective small size of mice where the force produced by muscle fibres are reduced and then muscle damage is reduced as well (Bodor and Mcdonald, 2013). In *mdx* mice, the percentage of oxidative type I fibres in the oxidative soleus muscles is reduced. Moreover, the percentage of type IIa in the fast, more glycolytic EDL muscle and TA muscles is also lower in *mdx* mice (Ljubicic et al., 2014). On the other hand, the percentage of glycolytic type II fibres is increased in *mdx* muscles (Selsby et al., 2012, Whitehead et al., 2015).

Recently, another mouse model of DMD carrying the *mdx* 23 mutation on the DBA2/J background (DBA/2-*mdx*) showed more severe skeletal muscle damage,

reduced muscle function by 7 weeks, and an earlier onset of cardiac disease at 28 weeks when compared with *mdx* mice. Moreover, D2-*mdx* showed less central nuclei and increased calcification in the skeletal muscle, heart and diaphragm (Coley et al., 2016). DBA/2-*mdx* mice are better representing human disease because they exhibit increased fat, fibrosis, TGFβ signalling and inflammation (Fukada et al., 2010). Note that the DBA/2 *mdx* mice are a poor model for cardiomyopathy (Hakim et al., 2017). However, they were available after my study has started.

Despite the histopathological differences between *mdx* and DMD patients, the *mdx* mouse has been the cornerstone of pre-clinical research for DMD and remains an appropriate mouse model.

1.9. Gene therapeutic approaches for DMD:

Gene therapy is the complementation of the defective gene by a functional copy using gene transfer. Over the last decade, adeno associated virus (AAV) emerged as one of the promising approach for DMD therapy. Several studies showed improvements in muscle functions following reinsertion of full or partial length of dystrophin, utrophin into *mdx* mice using viral gene therapy (Konieczny et al., 2013, Wang, 2010, Hirst et al., 2005, Phelps et al., 1995, Chakkalakal et al., 2003). Different approaches are used to ameliorate dystrophic diseases, for example; non-viral, such as plasmid or antisense oligonucleotides (AON) and viral, such as adeno virus (AV) and AAV. For gene therapy, a number of challenges remain to overcome; addressing advantages and disadvantages of gene replacement, immune challenges, determination of optimal mode of gene delivery and also the disease advancement (Rodino-Klapac et al., 2007).

1.9.1. Non-viral gene therapy

Non-viral therapy relies on introducing the transgene without using a viral vector. Non-viral gene approaches are based on replacement and repair of the defective gene. The replacement involves delivery of dystrophin by using plasmid whereas the repair approaches are based on injection of antisense oligonucleotides (Rando, 2007). Although, there is limited immune response due to absence of viral proteins, the transfection efficiency is limited with the transgene size (Pichavant et al., 2011).

1.9.1.1. Plasmid-based therapy

Plasmid-based approach acquires several advantages; simplicity, cheaper and easier to produce in larger a mounts (Mali, 2013). In DMD, the simplest way is directed intramuscular injection of full length or micro-dystrophin, however, the transfection efficiency obtained was very low with full length dystrophin (Pichavant et al., 2011). Transfection efficiency of intramuscular injection of plasmid in combination of electroporation leads to 50% gene expression (McMahon et al., 2001). The difficulty of the previous method has directed the attention to a systemic or regional delivery of plasmid, where intra-arterial delivery into *mdx* mice showed 1-5% expression of dystrophin in limb muscles (Zhang et al., 2004). A phase I clinical trial of DMD used the full length dystrophin resulted in rare dystrophin positive fibres in six out of nine patients only with no adverse immunological effects (Romero et al., 2004). However, the main issue remains to be resolved is to the maximize persistence of the plasmid (Fairclough et al., 2011). Plasmid-DNA has established methodology for DNA vaccinations as economic factors are more favourable compared to recombinant-protein vaccines. DNA-based vaccination exhibit features of live-attenuated, synthetic

peptides or proteins (Hasson et al., 2015). DNA vaccination involves introduction of nuclei acid into host cells where it directs the synthesis of its own polypeptides to stimulate immune response. The immune response can be directed to elicit either cellular or humoral immune response or both. Further, DNA-based vaccine is highly specific and the immunized antigen underwent the same modification as natural viral infection. DNA-vaccination differ from DNA-based gene therapy in that the former is designed to permit localised, short term expression of the target antigen (Hasson et al., 2015).

1.9.1.2. Antisense oligonucleotides induce exon skipping for dystrophin restoration:

Antisense oligonucleotides (AON) is an RNA based approach, designed on synthesizing oligonucleotides with different chemical backbones that hybridize to the complementary target. Specifically for DMD, AONs can target a section of the pre-messenger mRNA and lead to exclusion of the specific exons from the dystrophin mRNA transcripts to circumvent mutations, restore the open reading frame and then protein production (Scully et al., 2013). As 60-80% of DMD patients have a frame-shifting deletion, exon skipping approach results in production of truncated, yet functionally dystrophin protein (Aoki et al., 2012). It has been noted that exons 45-55 cover the main mutation in DMD (hot spot region), therefore, in theory, any therapy able to skip the entire 45-55 exon region can rescue more than 60% of deletion mutation and generate mild symptoms like BMD (Aoki et al., 2012). AONs are 20-30 nucleotides in length and complementary to regions in mRNA transcripts to skip specific exons either by blocking splice enhancer sequence or by modifying secondary mRNA structure folding. Examples of differing AONs chemistries include; 2'O-methyl-

phosphorothiate-AONs (2OMePS), phosphorodiamidate morpholino oligomer (PMO) (Scully et al., 2013, Fairclough et al., 2011). Both drugs target dystrophin exon 51 and both elicited the expected skipping of exon 51 (Hoffman and McNally, 2014). Preclinical studies in *mdx* mice showed that intravenous and intramuscular injections of 2MePS have successfully induced dystrophin expression (Mann et al., 2001, Lu et al., 2005). Surprisingly, in 2013, a large phase III study of (PRO51/Drisapersen) running by (GSK and Prosensa therapeutic; Netherlands) based on 2OMePS failed to show any improvements in the primary outcome measure of 6 minutes walking test at primary endpoint, in the presence of detectable dystrophin (Goemans et al., 2011, Goemans et al., 2018). Interestingly, most preclinical studies have reported higher efficiency of exon skipping with the PMO chemistry than with 2OMePS chemistry (Wu et al., 2010, Lu et al., 2005, Wu et al., 2011). 3 dogs were tested with the same approach and showed enhancement in the protein levels in all skeletal muscles up to 20% with no toxicities (Hoffman et al., 2011). A phase I/II clinical trials of AVI-4658/Eteplirsen, initiated by (Sarepta, Bothwell, WA, USA) using (PMO) showed no adverse effects with variable restoration of dystrophin-positive fibres expression in 7 out of 19 patients enrolled in the trial with no improvement in a 6 minutes walking test. This finding was associated with increased expression of α-sarcoglycan and NOS (Cirak et al., 2011). Another clinical trial based on (Eteplirsen) by Sarepta resulted in a 20% dystrophin expression of normal levels (Mendell et al., 2013). Although, concerns on clinical efficacy and limited dystrophin level delayed the approval, Food and drug administration (FDA) recently approved Eteplirsen in 2016 to be the first oligonucleotide to be commercialized (Aartsma-Rus and Krieg, 2017). Despite these successful

restorations of deficient dystrophin expression, there are hurdles that still remain, for instance; the poor uptake to muscle and the lack of uptake to other affected tissues; heart and brain (Nakamura, 2017).

1.9.2. Viral gene therapy-adeno associated virus (AAV):

AAV is a small, single stranded member of *Parvoviridae* family which requires a helper virus for replication and life cycle completion, is now received a major attention for DMD treatment. Interest in AAV for gene therapy research began with awareness of its potential advantages for example; non-pathogenicity, long term persistence, diverse tissue tropism, ability to transduce dividing and non-dividing cells, lower immunological response comparing to other viral vectors for example adeno-virus and non-pathogenic to human (Kay, 2011, Daya and Berns, 2008, Chakkalakal et al., 2005, Konieczny et al., 2013).

Wild type (WT) AAVs have a non-enveloped icosahedral capsid of about 25 nm in diameter. The capsid contains a single strand DNA of 4.7 kb with three open reading frames (ORF), which composed of; 1) *Rep* that encodes Rep78, Rep68, Rep52, and Rep40, responsible for viral DNA replication , 2) *Cap* gene composed of three capsid protein; VP1, VP2 and VP3 and 3) Assembly activating protein (AAP), which acts along the capsid proteins to localize and facilitate capsid assembly in the nucleus (Daya and Berns, 2008). They are flanked with two inverted terminal repeats (ITRs), which are base-paired hairpin structures of 145 nucleotides length. They are required for priming the single stranded to double stranded DNA conversion during replication and package the viral DNA into the capsid (Xiao et al., 1997). They are naturally defective in replication, which mean

they require the presence of an auxiliary virus to achieve their productive cycle for example; AV or herpes simplex virus (Merten et al., 2005) (figure 1.9).

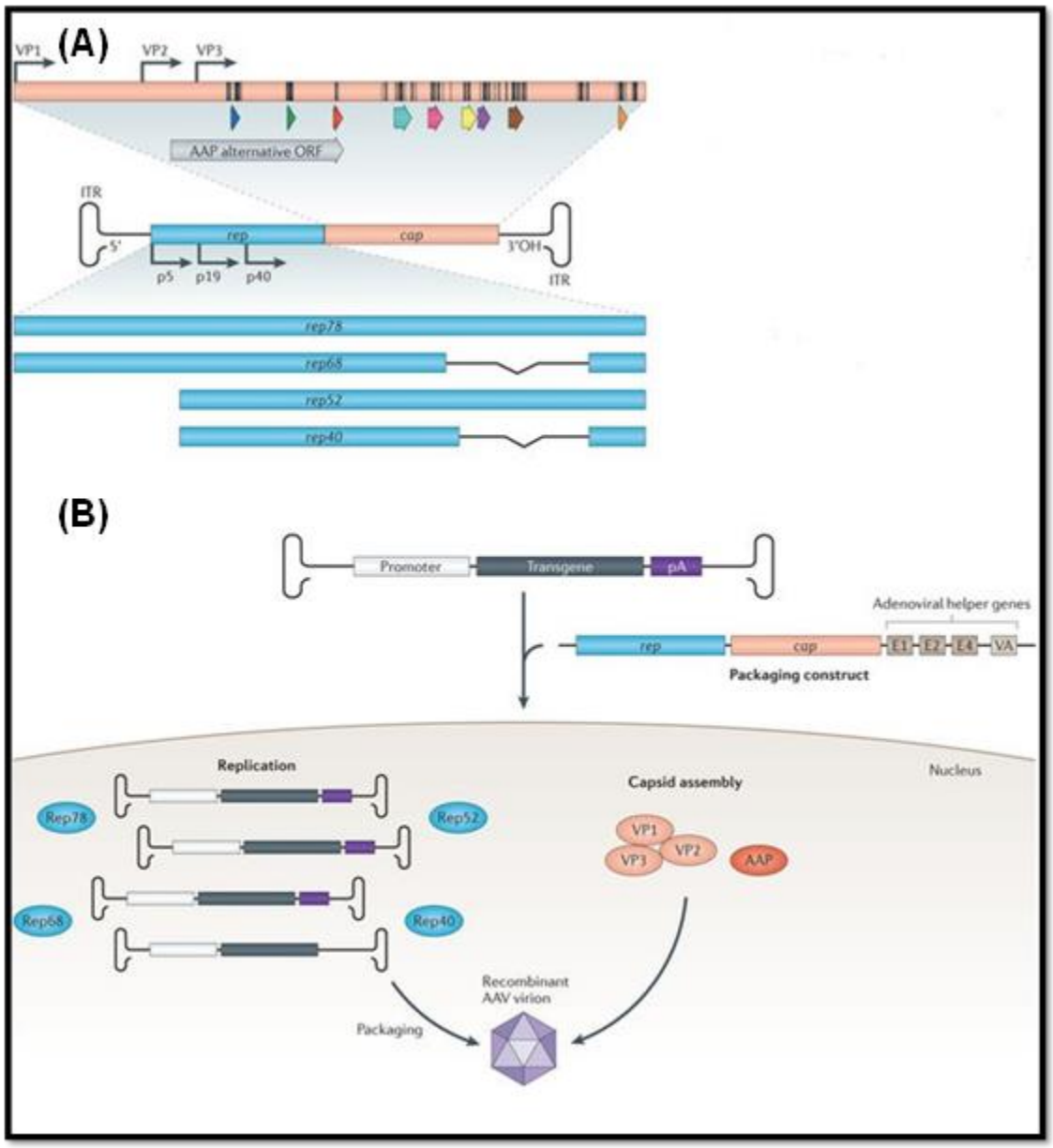

Figure 1.8. Structure of adeno associated virus

(A) The 4.7-kb single-stranded DNA genome of adeno-associated virus (AAV). The AAV genome contains three open reading frames (ORFs) flanked by inverted terminal repeats (ITRs). The rep ORF encodes (Rep40, Rep52, Rep68 and Rep78) that are essential for viral replication and transcriptional regulation. The Cap ORF encodes 3 proteins (VP1, VP2 And VP3) that form viral capsid. (B) Recombinant AAV is generated by inserting a gene of interest between the ITRs and replace both rep and cap, which are provided in adenoviral helper gene that are necessary for replication. The viral capsid determines

the ability of the resulting AAV vector to transduce cells, from binding to cell surface receptor to nuclear entry and genome release, which lead to stable transgene expression in post mitotic tissue. Adapted from (Kotterman and Schaffer, 2014).

The concerns about the ability of AAV to integrate specifically into chromosome 19 as a function of integration efficiency element (IEE) and the ability of *rep* gene to express cellular genes led to construction of recombinant AAV rAVV that lack both *rep*, *cap* genes and IEE. Therefore, *rep* and *cap* can be replaced by a therapeutic expression cassette, with the ITRs being retained as they are essential for packaging. Thus, the (rAVV) are considered as extrachromosomal elements that ensure long term transgene expression in post mitotic tissues such as skeletal muscle (Daya and Berns, 2008). The limited cloning capacity of only 4.7 Kb has restricted the application of rAAV for DMD as the full length dystrophin cannot be packaged, which represent the major limitation of rAAV (Konieczny et al., 2013, Wang, 2010). However, all of the rAAV advantages make it more resourceful for muscle therapy. AAV binds to the host cells by using heparin sulphate proteoglycan structure on the cell surface and utilize (FGFR1), co-receptor on the cell surface to internalize via receptor-mediated endocytosis (Konieczny et al., 2013). Different AAV serotypes are produced to date targeting specific tissues and organs (Chahal et al., 2014). Currently, rAAV capsid serotype selection for a specific clinical trial is based on effectiveness in animal models. However, preclinical animal studies are not always predictive of the human outcome (Manno et al., 2006, Nietupski et al., 2011). As shown by preclinical and clinical trials, rAAV2 vectors transduced mouse and human hepatocytes at equivalent but relatively low levels. However, rAAV8 vectors, which are effective in many animal models, transduced human hepatocytes

relatively poorly at about 20 times less than mouse hepatocytes (Lisowski et al., 2014).

Different rAAV candidates employed in diverse clinical trails are reviewed in (Naso et al., 2017). In human clinical trials, AAV vectors is a promising approach for gene delivery into post mitotic tissues for instance; retina and brain. AAV8 has been used for years in liver clinical trials for hemophilia B (Nathwani et al., 2011). The first AAV clinical trial was conducted in the subject of cystic fibrosis, today more than 70 approved clinical trials worldwide for different diseases (Clément and Grieger, 2016). In 2012, based on the safety profile and outcomes, Glybera, an rAAV1 based drug for treatment of familia lipoprotein lipase (LPL) deficiency was this first rAAV to be market-approved in Europe (Gaudet et al., 2010, Clément and Grieger, 2016). In 2017, Luxturna, which is developed by Sparks Therapeutic to treat patients with an inherited retinal disease (IRD), that may lead to blindness, was the first AAV2 gene medicine to be approved by FDA (Smalley, 2017). However, in the area of DMD, due to limited carrying capacity of AAV, a new mini or micro-dystrophins that lack multiple regions of the rod domain and maintain amino and carboxyl domains including the nNOS binding site was synthesized (Gao and McNally, 2015). These constructs can be inserted into AAV and delivered into *mdx* mice where they can induce expression and reduced pathology associated with DMD (Wang et al., 2009, Zhang and Duan, 2012).

Although, phase I clinical trial on mini-dystrophin gene using optimised AAV2.5 vector has been completed, minimal expression of dystrophin was detected and immune response was reported against minidystrophin (Mendell et al., 2012, Rodino-Klapac et al., 2013). Because AAV is approved medicine in multiple

conditions as mentioned earlier with no known disease association, it becomes one of the leading gene delivery approach.

1.10. Viral gene therapy approaches that target oxidative capacity and mitochondrial biogenesis in DMD:

Energy is vital to all living organisms. In human and mammals, the vast majority of energy is generated by oxidative metabolism in the mitochondria. The cellular demand for energy varies under different physiological conditions in different cells. There is great interest in mitochondrial oxidative metabolism in general biomedical field. Therefore, a regulatory network of transcription factors controls the quantity and activity of mitochondria. Understanding these molecular mechanisms regulating mitochondrial biogenesis and function provides potentially important therapeutic targets in mitochondrial dysfunction associated with pathogenesis of numerous conditions such as aging, type 2 diabetes and DMD, which is the main focus in this thesis (figure 1.10).

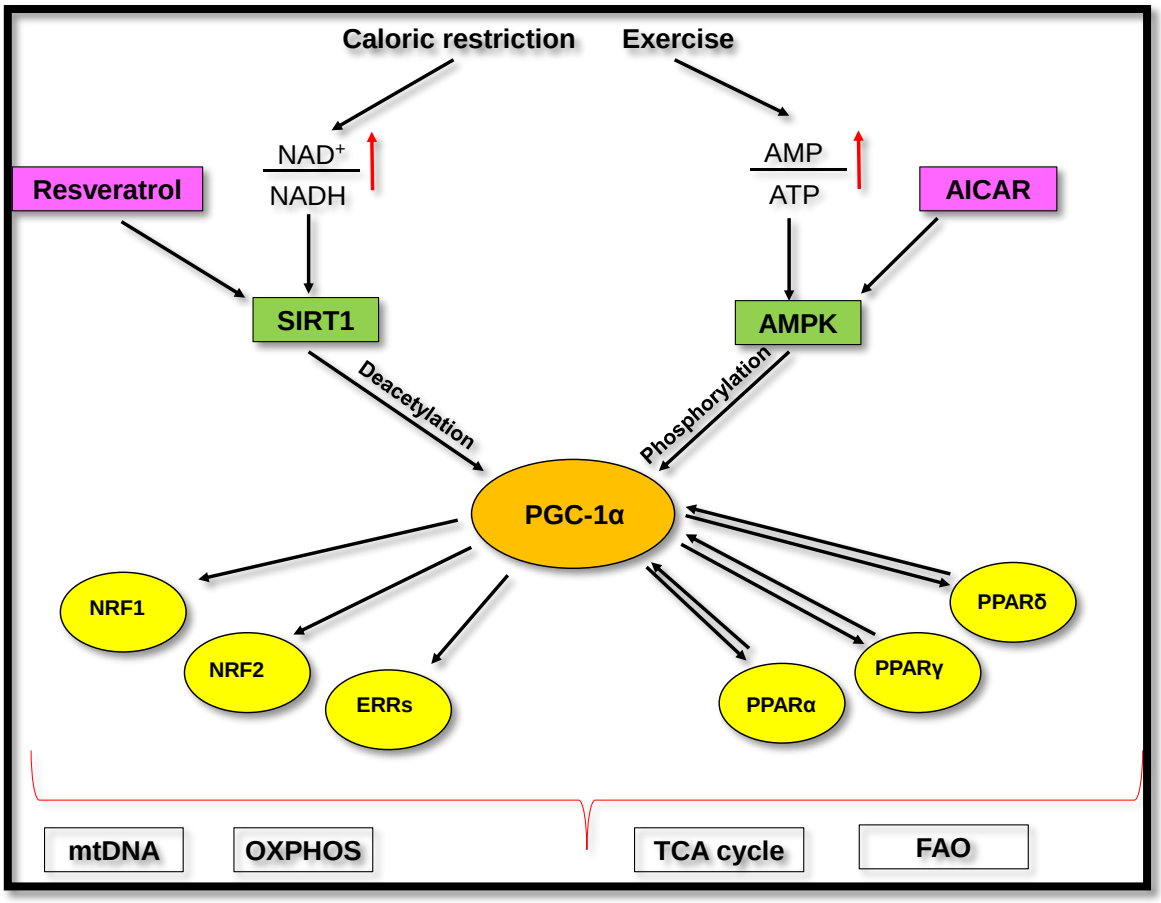

Figure 1.9. Schematic representation of signalling pathways that target oxidative metabolism and mitochondrial biogenesis

Adapted from (Komen and Thorburn, 2014)

1.10.1. PGC-1α

Peroxisome proliferator-activated receptor (PPAR) s (PPAR α, δ and γ) is a large family of nuclear receptors that interact with transcriptional coactivator PGC-1α and binds to wide numbers of transcription factors known to be involved in mitochondrial biogenesis, glucose and fatty acid metabolism, adaptive thermogenesis, heart development and muscle fibre types transition (Liang and Ward, 2006). According to the above mentioned biological response, PGC-1α is highly expressed in tissues active in oxidative metabolism and where mitochondria are abundant for example; the heart, slow-twitch skeletal muscle,

kidney, brain and brown adipose tissue (BAT) (Puigserver et al., 1998, Liang and Ward, 2006, Finck and Kelly, 2006). PGC-1α is a protein that induce the probability of gene transcription through binding to transcription factors (Puigserver and Spiegelman, 2003). However, it has been shown that PGC-1α also plays as a coactivator of NRF-1 and -2 (nuclear respiratory factor) which are required for regulating expression of genes essential in mitochondrial structure (TFAM) (Wu et al., 1999). In terms of skeletal muscle, over-expression of PGC-1α is well known in switching glycolytic fibres into oxidative types I and IIa and the level of PGC-1α gene is increased by endurance and short-term exercise as shown in human and rodents models (Baar et al., 2002). Moreover, transgenic mice with overexpressed PGC-1α showed more resistance to contraction-induced fatigue (Lin et al., 2002) and deficient mice of PGC-1α exhibited reduced number of mitochondria and low level of oxidative capacity (Leone et al., 2005). Therefore, PGC-1α has been investigated as a therapeutic approach in treating DMD. Using *mdx* mice, administration of rAAV- PGC-1α drives more expression of dystrophin homologue (utrophin), increases expression of myosin type 1 heavy chain (Pendrak et al., 2012). Moreover, increased over-expression of oxidative proteins for example; cytochrome C, UCP-1 and Cox IV compared to the control, indicates the enhanced ability of the treated muscles to produce more ATP and increased either number or size of mitochondria which suggested increased endurance capacity following over-expression of PGC-1α (Pendrak et al., 2012). PGC-1α is regulated by numbers of upstream pathway in skeletal muscle, calcineurin A, calcium calmodulin-dependent protein kinase (CaMK) and AMP-activated protein kinase AMPK (Finck and Kelly, 2006). PGC-1α exerts its regulatory functions by interacting with transcription factors such as NRF1,

estrogen related receptor α (ERRα) and GA-binding protein, and subsequently activating the expression of the genes targeted by these factors (Handschin and Spiegelman, 2006).

1.10.2. PERM1

The pathways targeted by PGC-1α and ERRs include genes working either downstream or in parallel, for example; PGC-1/ERR-induced regulator in muscle 1 (PERM1) gene which is expressed selectively in muscles and is required for the expression of selective genes involved in mitochondrial biogenesis and oxidative metabolism (Cho et al., 2016). In C_2C_{12} cells myotubes, PERM1 has been shown to induce a subset of genes involved in oxidative metabolism induced by PGC-1α and estrogen related receptor γ (ERRγ) (Cho et al., 2013). However, gene based therapy of AAV mediated expression of PERM1 into 4 weeks old C57BL/6J mice increased expression of genes involved in oxidative function (PGC-1α and ERRα) but not (ERRγ), mitochondrial biogenesis (TFAM, SIRT3,Tf2bm), angiogenesis (VEGFa), glucose metabolism (Glut4), and fatty acid metabolism (Cpt1b). In addition, over-expression of PERM1 via AAV enhanced capillary density and im proved fatigue resistance without altering fibre types in wild type mice (Cho et al., 2016). As PERM1 shares overlapping actions to those of PGC-1α, it is a possible targeted therapy for DMD.

1.10.3. SIRT1

In *mdx* mice, the level of nicotinamide adenine dinucleotide (NAD^+) is significantly reduced and repletion provides protection from metabolic disease and mitochondrial dysfunction in a SIRT1 dependent manner (Ryu et al., 2016). Sirtuins is an NAD^+-dependent histone/protein deacetylase that play role in

cellular antioxidant stress, metabolism and cell survival and are highly conserved within species. There are seven members of sirtuins where SIRT1 is the best characterized member them (Horio et al., 2011). SIRT1 senses changes in intracellular NAD^+ levels, which reveal energy level, and uses this information to adapt the cellular energy output to matches cellular energy requirements (Cantó and Auwerx, 2012). In DMD, multiple studies showed the beneficial effect of SIRT1 activation on metabolic, degenerative and inflammatory diseases (Tonkin et al., 2012, Vinciguerra et al., 2010, Lavu et al., 2008). Transgenic mice specifically overexpress SIRT1 in skeletal muscle exhibited a fast to slow fibre types conversion, induced expression and activity of PGC-1α, induced utrophin expression, increased mitochondrial contents and mitigated pathology associated with dystrophic muscles such as fibrosis, centrally nucleated fibres and creatine kinase level (Chalkiadaki et al., 2014). For DMD, specifically, the activity of SIRT1 is attenuated in *mdx* mice as shown in a study using resveratrol and found the deacetylation target of SIRT1, the histone H3 acetylation at lys9/Lys14 was increased in *mdx* mice and resveratrol can reverse this effect (Imai et al., 2000). Resveratrol treatment of *mdx* mice resulted in inducing a shift towards more oxidative fibres in soleus muscles and a restoration of type IIa in EDL and TA muscles, through increasing SIRT1 expression which reduce PGC-1α acetylation level (Ljubicic et al., 2014). These findings suggested that over-expression of SIRT1 results in deacetylation of PGC-1α which then mediate the induction of mitochondrial biogenesis (Chalkiadaki et al., 2014). Therefore, SIRT1 has been suggested as a potential target in DMD.

1.10.4. PPARδ

Peroxisome proliferator-activated receptors (PPARs) are a class of nuclear receptors that play important roles in energy metabolism. There are three different isoforms (α, γ and δ) with specific roles in metabolism. However, PPARδ has been shown to play a role in skeletal muscle metabolism as shown in studies of gain and loss of- function (Angione et al., 2011). Knockdown of PPARδ specifically in skeletal muscle resulted in metabolic disorders and impaired oxidative capacity as it showed a reduction in the expression of PGC-1α (Luquet et al., 2003), whereas mice overexpress PPARδ showed a shift towards oxidative type I fibres and consequently resulted in promoting oxidative capacity (Schuler et al., 2006). However, *mdx* mice treated with GW501516 agent (a PPARδ agonist) showed an increase in the forelimb and hind limb grip strength in addition to the increase in mitochondrial mass and over-expression of PGC-1α and Cyt c, together with an increase in type I/IIA oxidative fibres (Jahnke et al., 2012). Therefore, PPARδ is another possible target for DMD.

1.10.5. Estrogen related receptors:

Nuclear receptors are ligand-dependent transcription factors that regulate the expression of specific genes related to metabolism, reproduction and development. Orphan nuclear receptors are those which no physiological ligands. Three known receptors belong to this family have been identified to date; estrogen related receptors (ERR) α, β, γ (Giguère, 1999). None of these receptors binds estrogen due to the presence of amino acid side chain within the ligand-binding pocket (LBD), which maintains transcription without addition of exogenous ligand in converse with the other typical nuclear receptors (NRs) that

require ligands to enable gene activation. The amino acid mimic a ligand bound conformation, which is essential for cofactor binding (Giguère, 1999).

Selective estrogen receptor modulators such as tamoxifen, 4-hydroxytamoxifen and diethylstilbestrol (DES) have been identified as synthetic ligands to one or more ERRs and act as agonist or inverse agonists. Diethylstilbestrol (DES) and 4-hydroxytamoxifen (4-OHT) function to inhibit ERRγ activity (Greschik et al., 2004). In addition, bisphenol A, 2,2-bis (hydroxyphenyl) propane (BSA) has strong interaction with ERRγ and functions as an inverse agonist on ERRγ to maintain its highly constitutive activity (Liu et al., 2007).

Structural studies provided evidence that ERRs are active constitutively. As shown in (figure 1.11), ERRs contain N-domain, a transcription activation function domain (AF)-1 that is involved in the transcriptional regulation of the receptor through a conserved motifs (Tremblay et al., 2008). ERRs contain zinc finger DNA-binding domain (DBD), a highly conserved in all three receptors which may explain that several genes can be targeted by more than one of the ERR isoforms. They bind to the same DNA element which is known as the ERR response element (ERRE), TCAAGGTCA. ERRE involves in DNA recognition and protein-protein interaction. Structure also contains ligand-binding domain (LBD) and a C-terminal AF-2 domain that interacts with co-activators and co-repressors (Huss et al., 2015). Diverse roles of ERRs are determined by variations in both DNA and ligand binding specificities in addition to specific interaction with co-activator and co-repressor that mediate transcription.

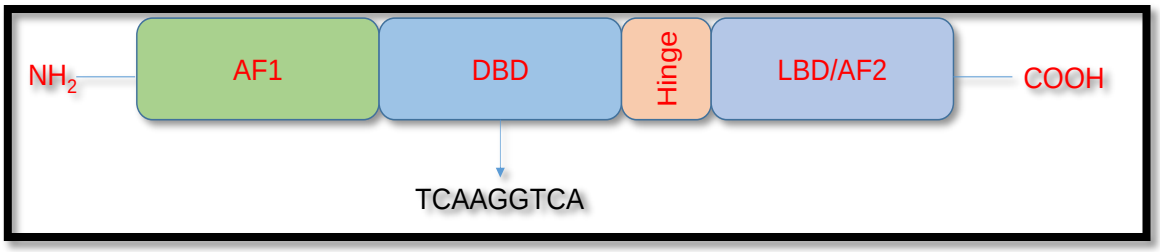

Figure 1.10. Structure of Estrogen related receptor

ERR contains NH2 terminal region which contains transcriptional activation factor 1 (AF1), DNA-binding domain (DBD), a hinge region that anchored the protein flexibility required for receptor dimerization and ligand binding domain LBD) which contains a conserved AF-2 helix motif. Modified from (Huss et al., 2015).

Although ERRα and ERRγ are expressed in tissues associated with metabolic activity, ERRγ is more selectively expressed in metabolic and vascularized tissues such as; brain, liver, kidney, adipose, placenta, and skeletal muscle tissues. ERRα and ERRγ modulate cellular energy metabolism by directing mitochondrial biogenesis and function (Huss et al., 2015, Deblois and Giguère, 2011, Giguere, 2008). They promote oxidative capacity in skeletal and cardiac muscles (Alaynick et al., 2007, Wang et al., 2015). They are crucial components of cellular glucose metabolism by regulating genes involved in glycolysis, including glucose uptake, glucose to pyruvate conversion and pyruvate entry in the Krebs cycle (Zhang et al., 2006, Deblois and Giguere, 2013). Further, they regulate lipid synthesis through fatty acid oxidation in the mitochondria and importantly they target genes involved in mitochondrial biogenesis and activity, including genes of electron transport chain (Giguere, 2008).

ERRβ functions during development of placenta, endolymph of the inner ear and retina and mutations have been associated with hearing loss in humans (Collin et al., 2008, Onishi et al., 2010). ERRβ also involves in the expression of genes important in self-renewal (Chen et al., 2008). In addition, the increase in their

expression causes an increase in mitochondrial biogenesis and activity, which stimulates oxidative capacity (Eichner et al., 2010, Cai et al., 2013, Huss et al., 2004, Rangwala et al., 2010).

Studying ERRs-null mice showed different phenotypes for example; ERRγ-null mice die shortly after birth (Alaynick et al., 2007), ERRα-null mice are viable and fertile and the mouse embryonic fibroblasts exhbit normal growth and proliferation, suggesting that ERRα by itself is not essential for mitochondrial biogenesis (Luo et al., 2003b) and ERRβ-null mice results in embryonic lethality at day 10, however, ERRγ can substitute for ERRβ to promote mouse fibroblasts and prevent the need for ERRβ during embryonic lineage (Luo et al., 1997). Because these receptor share similar target genes (Giguere, 2008), it is likely there is some functional redundancy between ERRs. Interestingly, ERRs are shown to work in a compensatory manner in heart, for example, ERRγ is upregulated in ERRα-null mice; furthermore, in ERRγ$^{-/-}$ mice, ERRα and ERRβ are upregulated. A complete inhibition of individual ERR isoform does not prevent mitochondrial biogenesis or activity due to presence of a compensatory mechanism through increased expression of other isoforms (Murray et al., 2013, LaBarge et al., 2014). The functions of ERRβ and ERRγ are overlapping by controlling genes important for ion homeostasis in the trophoblast, skeletal muscle, kidney, liver and stomach (Alaynick et al., 2007, Luo et al., 2013, Gan et al., 2013).

Significantly, ERRγ regulate metabolic processes, which do not involve ERRα and β. For example; specific over-expression of ERRγ ameliorates impaired hepatic insulin signalling via increasing expression of LIPIN1 gene (Kim et al.,

2011). Moreover, ERRγ stimulates expression of fibroblast growth factor (FGF) in hepatocytes, which is important regulator of angiogenesis (Jung et al., 2016).

In skeletal muscle, ERRα and ERRγ are both positively associated with mitochondrial biogenesis. However, the effects of ERRα is dependent on PGC-1α to activate the transcription of mitochondrial genes such as ATP-synthase (Atp5) and cytochrome c oxidase (Cox5), whereas ERRγ exert its effect independent of PGC-1α and rather linked to activation of AMPK (Narkar et al., 2011). When ERRγ is expressed ectopically in glycolytic muscle, it drives a switch towards oxidative fibres and induces mitochondrial biogenesis and angiogenesis. This is accompanied by induction of genes associated with fatty acid oxidation, TCA and OXPHOS (Narkar et al., 2011). In the basal state, knockout of ERRα in skeletal muscle, does not lead to any phenotypic changes (Luo et al., 2003b), whereas ERRγ-null mice are lethal (Alaynick et al., 2007), suggesting that ERRγ is potentially required for basal mitochondrial function. Therefore, the next section will discuss the regulation of ERRγ.

1.10.5.1. Regulation of ERRγ:

Expression and activity of ERRγ is controlled by different cellular stress and membrane receptors, such as, insulin and glucagon receptors. These two receptors play opposite roles in regulating ERRγ expression. For example; in response to nutrient availability, hypoxia, endoplasmic reticulum stress, pro-inflammatory cytokine interleukin (IL-6) and energy demands, these two receptors have been speculated to regulate ERRγ expression (Misra et al., 2017). As a result, ERRγ could be instrumental in cellular energy surveillance.

Moreover, post-translational modification functions as a major mechanism regulating activities of orphan nuclear receptors independent of ligands. ERRγ activity is altered by phosphorylation, ubiquitination and sumoylation; that inhibit, increase or stabilize the transcriptional activity of ERRγ during various physiological conditions (Misra et al., 2017). Furthermore, ERRγ transcription depends on co-regulators that respond to different cell signals. PGC-1α functions as transcriptional coactivators for ERRγ in various metabolic pathways. It binds to AF-2 domain of ERRγ ending up in a conformational change that maintain the assembly of an active transcriptional complex (Sever and Glass, 2013). Wang et al., suggested a feed-forward loop where ERRγ activates PGC-1α by activating the latter promoter, and PGC-1α then activates ERRγ (Wang et al., 2005). Likewise, GRIP-1 enhances the transcriptional activity of ERRγ (Hong et al., 1999). In addition, there are co-repressors, which inhibit ERRγ activation by competing with the binding of co-activators to the AF-2 domain. SHP, DAX-1, SMILE and GNL3L repress ERRγ transcriptional activity. Furthermore, receptor-interacting protein 140 (RIP140) acts as co-activator and co-repressor depending on the target genes (Misra et al., 2017).

1.10.5.2. Downstream targets of ERRγ (Mitochondrial biogenesis, oxidative transformation and angiogenesis):

An integral part of skeletal muscle differentiation is a dramatic increase in mitochondrial number and oxidative capacity, which are hallmark features of myocyte differentiation (Murray et al., 2013). Gene array analysis run by Narkar's group showed that in the absence of exercise, ERRγ from transgenic mice regulated a total of 1123 genes in skeletal muscles, of which 623 genes were induced. The majority of the upregulated genes belong to either mitochondrial

biology (90) or oxidative metabolism (43) encoding several components of fatty acid oxidation pathway, oxidative respiratory chain, contractile genes especially those associated with slow fibres (Narkar et al., 2011). In skeletal muscles, ERRγ is exclusively and highly expressed in oxidative myofibrils and control an induction of genes associated with oxidative metabolism (LPl, Cytc, Pdk4, Ucp3) (Huss et al., 2002, Narkar et al., 2011). On the other hand, *mdx* mice showed reduced expression of ERRγ by (60-85%) in addition to compromised gene network regulating oxidative metabolism and angiogenesis. However, transgenic over-expression of ERRγ in *mdx* mice reprogram the induction of genes involved in oxidative metabolism such as pyruvate dehydrogenase (Pdk4), Ucp3, cytochrome C (Cytc) and lipoprotein lipase (Lpl). In addition, there is an induction of angiogenesis program; VEGF-189, VEGF-165 and FGF and promoting switch towards more slow oxidative fibres, which are rich in mitochondria and capillary density in the absence of exercise. All these changes are independent of PGC-1α by recruiting the alternative factor AMPK, which is upregulated in the transgenic muscle of ERRγ (Matsakas et al., 2012, Matsakas et al., 2013).

ERRγ heterozygous mice ($ERR\gamma^{+/-}$) compared to wild type exhibited reduced expression of genes related to fatty acid oxidation and fatty acid uptake such as cpt1b, and lpl and oxidation gens such as Idh3a which indicate impairment in utilizing fatty acids as fuel (Rangwala et al., 2010). Furthermore, ERRγ null mice ($ERR\gamma^{-/-}$) die shortly after birth and showed defects in cardiac oxidative capacity as an example of pathways controlled by PGC-1α. Characteristics of cardiac muscle from completed knockout mice showed reduced expression of genes involved in TCA and ETC complex I enzymes (Alaynick et al., 2007). Therefore, ERRγ has important roles in energy metabolism and skeletal muscle growth.

Further, angiogenesis induction in skeletal muscle possibly occurs in response to paracrine signals following ERRγ activation. Conditioned medium from ERRγ overexpressing C_2C_{12} cells was able to induce formation of endothelia cell tube in culture (Liang et al., 2013, Narkar et al., 2011), which indicate that ERRγ induce angiogenic factors in a paracrine fashion. ERRγ has important roles in angiogenesis as muscle specific ERRγ over-expression in a murine model of hind limb vascular occlusion showed enhancement in re-vascularisation and neoangiogenesis, which contribute to the reparative function in skeletal muscle ischemia and maximize restoration of blood perfusion (Rangwala et al., 2010). Thus, taken together, ERRγ is a possible target in *mdx* mice to overcome ischemic issues.

Furthermore, ERRγ stimulates the VEGF promoter containing putative ERR binding sites which is known to transcribe all VEGF isoforms (Arany et al., 2008). However, induction of angiogenesis by ERRγ is not dependent on VEGF induction only as there are other factors induced such as FGF1, known to control endothelial cell migration and proliferation (Forough et al., 2006), along with Efnb2, possibly recruit mural cells such as vascular smooth muscle cells and pericytes, required for vessel formation (Foo et al., 2006). Interestingly, this effect of ERRγ in angiogenesis is PGC-1α independent and not involved hypoxia inducible factor (HIF-1α), which negatively regulates oxidative metabolism (Mason et al., 2007) and showed unchanged expression in transgenic muscle of ERRγ (Narkar et al., 2011). Conversely, HIF-2α was upregulated in response to exercise of ERRγ transgenic muscle, which is then proposed as a downstream target of ERRγ (Rangwala et al., 2010) (figure 1.12).

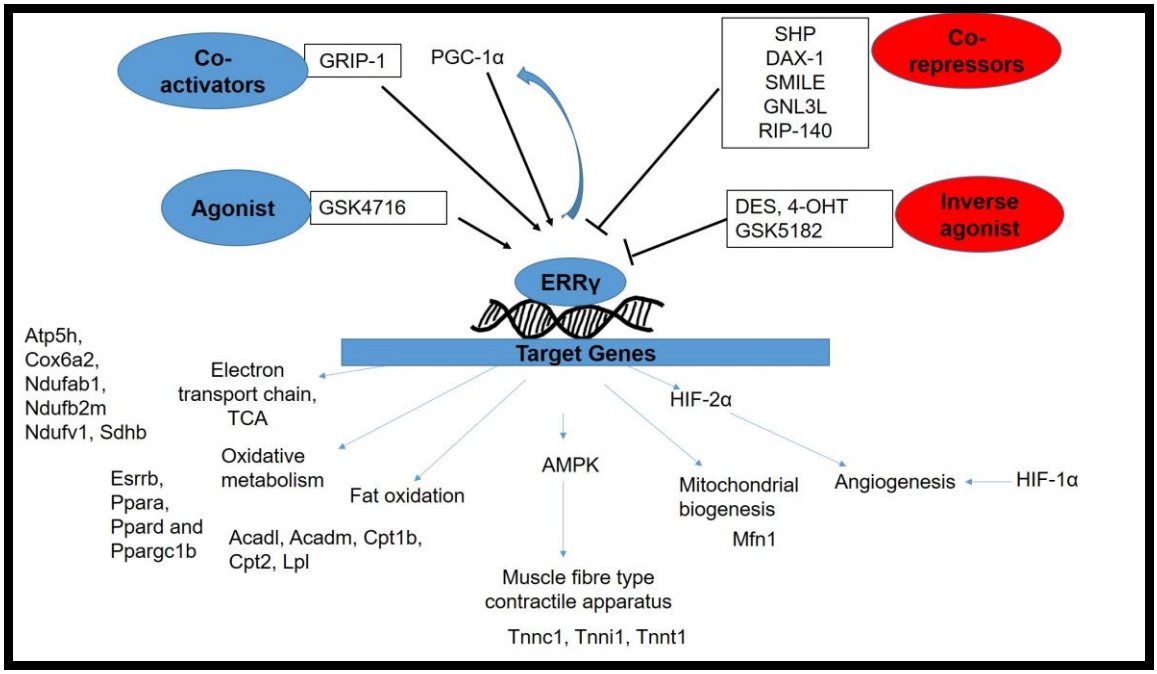

Figure 1.11. Schematic representation showing the role of ERRγ in the transcriptional network regulating muscle oxidative capacity and angiogenesis

1.11. The potential impact of ERRγ in DMD:

In vivo ERRγ loss or gain of function studies show changes in mitochondrial ETC/ OxPhos gene expression and oxidative capacity (Narkar et al., 2011, Rangwala et al., 2010). ERRγ$^{-/-}$ myocytes showed increased reliance on medium chain fatty acid (MCFA) as a substrate for energy production, which generates fewer ATPs per molecule than long chain fatty acid (LCFA). However, increased flux of fatty acid through ETC would cause more ROS production (Murray et al., 2013). Therefore, downstream pathways are induced in response to elevated ROS; Foxo1, NF-κB and their downstream targets, Atrogin-1 and MuRF1 (Murray et al., 2013). In normal physiological condition of elevated ROS, NF-κB directly activate antioxidant genes such as superoxide dismutase (SOD1 and SOD2) (Morgan and Liu, 2011). Foxo1 activation is known to reduce type I fibres and decrease muscle mass (Kamei et al., 2004). Thus, over-expression of ERRγ may have a protective role in these pathways during dystrophin loss.

Activation of other nuclear receptors such as PGC-1α and PPARδ have been shown to improve pathology associated with DMD by eliciting a fast to slow muscle fibres, stimulate utrophin expression, affecting neuromuscular junction and activating metabolic reprogramming in *mdx* mice (Handschin et al., 2007, Selsby et al., 2012, Hollinger et al., 2013, Jahnke et al., 2012). Activation of AMPK has also been reported to reverse mitochondrial deficit and induce a switch towards oxidative fibres ameliorating the dystrophic phenotype (Ljubicic et al., 2011). In parallel, induction of molecules that regulate angiogenesis/ vascular density for example VEGF and FGF and vasorelaxation/ blood flow such as NO, PDE5 inhibitor have shown to promote regeneration and improve the dystrophic phenotype of *mdx* mice (Messina et al., 2007, Tidball and Wehling-Henricks, 2004).

However, to date, a simultaneous rescue of both metabolic and angiogenic gene networks by any of the factors has not been established yet. Therefore, ERRγ is the only identified transcription factor that regulate both metabolism and angiogenesis in the skeletal muscle based on data obtained from transgenic *mdx* mice, demonstrating a significant advantage over other approaches (Narkar et al., 2011, Matsakas et al., 2013). Together, ERRγ can be considered as a 'gatekeeper' of transcriptional program controlling the activation of oxidative metabolism, mitochondrial biogenesis and angiogenesis genes and its over-expression becomes an appropriate pipeline in an attempt to ameliorate muscular dystrophy pathologies.

1.12. Hypothesis:

The general hypothesis is that adeno associated virus delivery of ERRγ, a key enhancer of the oxidative metabolism and angiogenesis is able to restore muscle function and improve oxidative capacity and angiogenesis in *mdx* mice (a model of duchenne muscular dystrophy) during postnatal life.

1.13. Aims:

Study 1: Assess the gene expression profile following intramuscular administration of AAV8-ERR*γ* into 6 week-old *mdx* and assess the short-term changes of pathology, biomarker profiling in dystrophic skeletal muscle following AAV8 mediated ERRγ expression using intramuscular administration of $1X10^{10}$ vg into two cohorts of 6 and 12 week-old *mdx* and recover 4 weeks post administration.

Study 2: Assess the short-term changes of pathology, function and biomarker profiling in dystrophic skeletal muscle following AAV mediated ERRγ expression using intravenous administration of AAV8-ERRγ of $1X10^{12}$ into 6-week old *mdx* and recovered 4 weeks later.

Study 3: Assess the short-term changes of pathology, function and biomarker profiling in dystrophic skeletal muscle following AAV mediated ERRγ expression using intraperitoneal administration of AAV8-ERRγ of $2X10^{12}$ into 3-week old *mdx* and recovered 6 weeks later.

Study 4: Develop a sequence-optimized form of ERRγ and assess the short-term effect of pathology, function and biomarker profiling in dystrophic skeletal

muscle following intraperitoneal administration of AAV9-ERRγ of $2X10^{12}$ into 3-week old *mdx* and recovered 6 weeks later.

2. Chapter 2
Materials and Methods

2.1. Tissue culture:

Murine skeletal muscle cells (C_2C_{12}) (Yaffe and Saxel, 1977) and human embryonic kidney cells (HEK-293T) were cultured in Dulbecco's modified Eagles medium (DMEM), 10% Fetal calf serum (FCS) in a humidified incubator at 5% CO_2, 37^oC.

2.1.1. Sub-culture of cell lines:

Aseptically, (10% FCS, DMEM) growth medium was discarded and cells were washed twice with 10 ml phosphate buffered saline (PBS). Then, PBS was discarded aseptically and 2.5 ml of trypsin/EDTA (0.05%) was added. Cells were incubated for 5 minutes at 37^oC and monitored under the microscope until most of the cells have detached and free in the media. Sometimes, gentle tapping the sides of the flasks aids in detaching the cells (depending on the surface area, degree of confluence and cell types). Immediately, 10 ml of 10% FCS, DMEM was added and gently pipetted up and down to obtain homogenous cell suspension which was transferred into 50 ml tube and spun down for 5 minutes, 1000 rpm at room temperature (RT). The supernatant was discarded and 1 ml of 10% FCS DMEM medium was added to the pellet and re-suspended. For cell counts, 10 µl of the cells was mixed with 10 µl of trypan blue dye and counted using Countess Cell Counter machine. Depending on the required number of cells, the required volume was transferred to a flask in appropriate volume of media, incubated at 37 ^oC in 5% CO_2 incubator.

2.1.2. Evaluation of transfection efficiency:

In 6 well plates, 50,000/cm^2 of C_2C_{12} cells were seeded per well in 2 ml of 10% FCS DMEM and grown for 24 hour. Subsequent, cells were transfected with 4 µg

of eGPF plasmid using linear polyethylenimine (PEI) (linear, MW=25000). Different ratios were used from (1:1-1:6) by changing the amount of PEI. In a total volume of 200 µl of serum free DMEM, eGFP plasmid and PEI were diluted together, mixed well and incubated for 15 minutes at RT. Then, 200 µl of the mix were added to each well. The next day, the transfection efficiency was visualized with fluorescent inverted microscopy (figure 2.1).

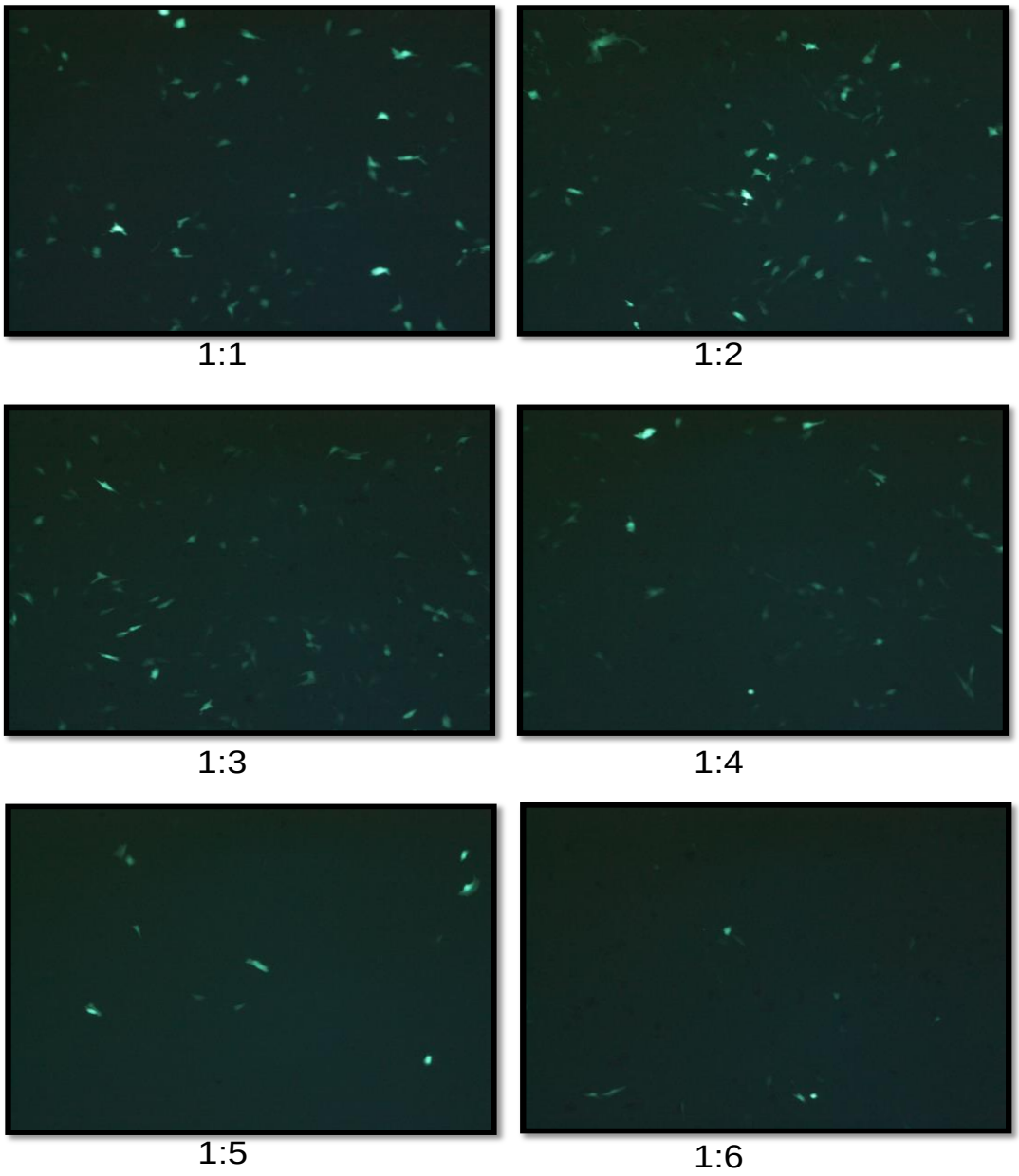

Figure 2.1. Optimization of transfection efficiency

Evaluation of transfection efficiency showed (1:2) of (DNA: PEI) ratio is highly efficient in transfection compared to other ratios. C_2C_{12} cells were seeded per well in 2 ml of 10% FCS DMEM and grown for 24 hour. Following that, cells were transfected with 4 ug of eGFP plasmid using PEI. After 24 hour, the transfection efficiency was visuliazed using fluorescent inverted microscopy.

2.2. Proliferation assay (MTS):

C_2C_{12} cells were seeded as 3000/cm^2 in 96-well plates with 100 µl of 10% FCS DMEM and grown for 24 hours. Cells were transfected with (0.2 µg) of a murine estrogen related receptor-gamma plasmid under the control of spc5-12 promoter plasmid (ERRγ) PEI. The ratio was (1:2), plasmid DNA: PEI. After 24 hrs, the proliferation assay was performed following manufacturer's instructions. Briefly, 20 µl of CellTiter 96® AQueous one solution reagent was added into each well of the 96-well assay plate. The plate was incubated for 1 hour, 5% CO_2. Subsequently, the absorbance was recorded at 490 nm using 96-well plate reader. The control cells were received the same amount of PEI and there were wells with DMEM 10% FCS only, used as a blank.

2.3. C_2C_{12} viral transduction:

Cells were plated 3000/cm^2 in 96-well plates until they were 70% confluent. Then, they were induced to differentiate by changing serum to 2% horse serum. Later, virus was added to the medium at $1x10^{10}$ vg for three days.

2.4. Plasmid production:

pDP8 helper plasmid was transformed into XL-10 competent bacterial cells via heat shock, where 50 ng of plasmid was added to bacteria on ice for 5 minutes and then heat shocked for 1 minute (42°C), then on ice again for 1 minute. Then, bacteria was grown in 1 ml of LBSOC medium (20 mM glucose, 10mM $MgSO_4$,

10Mm $MgCl_2$, 2.5 mM KCl, 10 mM NaCl, 2% Tryptone and Yeast extract) for 45 minutes with shaking. 200 µl of bacterial culture was plated on ampicillin (50 µg/ml) LB agar (LB broth and agar) plates and incubated overnight at 37°C. Next day, one colony was picked and grown in 5 ml starter culture of LB (ampicillin) and grown through the day. Overnight a large 2.5 L culture was inoculated at 1/1000 with the starter culture. Qiagen Giga preparation kit (endotoxin free) was used to purify the plasmids. To confirm the identity of the pDP8 helper plasmid, 1% agarose gel (0.8 g of agar, 80 ml of TAE buffer and SYBR safe dye) was prepared. Restriction enzyme (RE) (HindIII) was used to check the pDP8 helper plasmid fragments. Restriction digestion reaction contained 10 µg of the plasmid DNA, 1 unit/µg of RE, 3 µl of buffer and make the total volume to 20 µl with water. All of them were mixed and incubated for 1 hour at 37°C. Loading dye of 5 µl was added to the sample and 1 Kb ladder was used. Gel was run at 90 V, 400 Am for 1 hour.

2.5. AAV8-ERRɣ virus:

2.4.1. AAV production:

Virus production included several steps, firstly HEK-293T cells were plated to reach 80% confluency in DMEM 10% FCS. Then, the cells were transferred to roller bottle with 200 ml of 10% FCS DMEM. The bottles were incubated in roller incubator with rotor at 0.5 rpm overnight. Then, the rotor was turned up to 1 rpm for two more days. The second step was transfection, which firstly included changing medium in the cells to DMEM/ free of serum (SF) and preparation of the complex which included 500 µg of plasmids; pPDP8 (375 µg) and pAAV-Ha-ERRγ (125 µg) in (1:1) ratio, diluted in SF DMEM. The transfection of the cells

was carried out using PEI. The ratio was (5:1) PEI to plasmids (pDP8 and pAAV8-ERRγ) in DMEM/SF. 20 ml of the mix was added to the bottle and cells were cultured for 3 days. AAV was harvested by shaking the flasks to detach all cells and the supernatant was decanted to 250 ml corning tubes. Cells were pelleted and frozen. Then to every 200 ml of supernatant, 50 ml of 40% PEG was added, mixed, inverted 10-20 times and put overnight at 4°C. Following, the supernatant was centrifuged for 30 minutes at 3000 rpm at 4°C. The supernatant was then removed and the pellet was re suspended in 9 ml lysis buffer. This lysate was then added to the cell pellet. Then, the lysate was frozen, thawed three times using dry ice/ethanol. After these freze/thaw cycles, benzonase was added to the final concentration of 50 U/ml and incubated for 30 minutes at 37°C. The lysate was clarified by centrifugation at 3700 *g* for 20 minutes at RT and passed through 0.45 um filter. The lysate was layered to an iodixanol gradient into a Beckman Quick-Seal Ultra-Clear 25X77mm tube. The iodixanol solution was layered using a pasteur pipette in the following order; 6.9 ml of 15% iodixanol, 4.6 ml of 25% iodixanol, 3.84 ml of 40% iodixanol and 3.83 ml of 60% iodixanol (Table 2.1).

Table 2.1. Layers components of iodixanol

Layer	Iodixanol	5M NaCl	5x PBS-MK	H_2O	Phenol Red
15%	12.5 ml	10 ml	10 ml	17.5 ml	100 ml
25%	20.8 ml	10 ml	10 ml	19.2 ml	100 ml
40%	33.3 ml	10 ml	10 ml	6.7 ml	100 ml
60%	50 ml	10 ml	10 ml	6.7 ml	100 ml

Then, the lysate was layered on the top and the tube was filled to the bottom of the neck with lysis buffer using a syringe fitted with a small gauge needle to avoid bubbles formation, the tube was then sealed with a Beckman tube heat sealer,

and centrifuged for 1 hour at 18ºC in a type 70Ti rotor at 69000 G. After centrifugation, the tube was clamped in a stand and a 18-19 gauge needle was inserted into the interface between the 60 and 40% iodixanol layers and removed the AAV fraction (40% layer) which then can be stored in fridge overnight. Desalting and concentration was the third step which was carried out in Amicon Ultra-15 100,000K (PL100) (Millipore) centrifugal filter device. Firstly, the filter was rinsed with 5 ml of PBS-MK by centrifuge at 4000 *g* for 15 minutes. Then, 5 ml of PBS-MK was added to AAV fraction and the total volume was added to the filter device, centrifuged for 20 minutes at 4000 *g* until the volume was reduced to 2 ml. Another 15 ml of PBS-MK was added to the filter and the step was repeated 3 times to desalt AAV preparation. During the last step, the volume was reduced to 1-2 ml. Finally, the concentrated, desalted AAV was collected by rinsing the sides of the filter after removing the retentant from the filter. The virus was aliquoted in 100 µl volumes and stored at -80 ºC.

2.4.2. AAV titre by Dot blot quantification

The last step in preparing the virus was quantification by dot blot and it is divided into two steps; preparation of viral DNA and preparation of dot blots. 1 and 5 µl sample of AAV were treated with DNase I (5 U) I in a final volume of 200 µl of SF DMEM for 1 hr at 37ºC. The sample was then treated with 100 µg of proteinase K for 1 hr at 37ºC to digest viral capsid. Double extraction/ purification of viral DNA was accomplished by using an equal volume of 25:24:1 of phenol/chloroform/ isoamyl alcohol, mixed and centrifuged at 13000 rpm for 10 minutes at 4ºC, then the top layer was removed to a new tube. The DNA was precipitated with 40 µl of 3 M sodium acetate, 40 µg glycogen (2 µl) and 2.5 volumes of 100% ethanol and incubated at -80ºC for 30 minutes followed by

centrifugation at 13000 rpm for 20 min at 4ºC. The DNA pellet was washed in 70% ethanol and re suspended in 400 µl of 0.4 M NaOH/10 mM EDTA. A 2-fold serial dilution of AAV vector plasmid corresponding to the AAV virus stock to be titred, was prepared in a volume of 20 µl (160 ng-0.3125 ng). All dilutions were mixed with 400 µl of 0.4 M NaOH/10 mM EDTA (pH 8.0) solution. The samples were denatured at 100ºC for 5 minutes and then cooled on ice for 2 minutes. To prepare the blot, wet a single sheet of 3MM paper and hybridization membrane (Hybond N^+) with water. Then, they were placed in dot-blot apparatus and secured with clips. All denatured DNA was added and then vacuum was applied. The wells were washed with 400 µl of 0.4 M NaOH/10 mM EDTA and vacuum was applied to dry. After that the membrane was rinsed with 2X SSC and placed in bottle with hybridization buffer for 1 hour at 42ºC. A HRP labelled nucleic acid probe was prepared by diluting the probe of a promoter (Spc5-12), which were PCR fragments to a concentration of 10 ng/ul in sterile water (10 µl) followed by denaturation for 5 minutes in a boiling water bath. Immediately DNA was cooled on ice for 5 minutes. An equal volume of DNA labeling reagent was added and mix with 10 µl glutaraldehyde and added to the cooled probe and incubated for 10 minutes at 37ºC. The probe was added to the hybridization buffer. The hybridization was run overnight at 42ºC. Blot was washed in primary wash buffer for 40 minutes and washed twice with 2X SSC for 5 minutes. Using ECL chemiluminescence, the blot was developed by adding a volume of 1:1 ratio from each solution in the ECL chemiluminescence kit.

The virus was titered by serial dilution (12.5, 6.25, 3.125, 1.56 and 0.78 µl). To calculate the number of AAV particles number; first we calculated the MW of pAAV8-ERRγ plasmid in Daltons by multiplied the size of the molecule in base

pair (bp) which is (7700 bp) by 650 (average MW of one bp in Daltons). For example; for pAAV8-ERRγ plasmid (7700 bp) MW=7700 X 650 =5.01 $X10^6$ Daltons. Then, we calculated the number of particles present in gram of DNA using Avogadro's number (6.023 $X10^{23}$). For example; there were 6.023 $X10^{23}$ molecules in 5.01 $X10^6$ g of this DNA which translated as 1.20 $X10^{17}$ pAAV8-ERRγ molecules per g DNA (6.023 $X10^{23}$/ 5.01 $X10^6$). Then, to calculate the number of molecules in ng of this DNA, divided 1.20 $X10^{17}$ by 10^9 which gave 1.20 $X10^8$ molecules per ng of pAAV8-ERRγ DNA.

We compared the intensity of the control and sample dots, then we estimated the amount of DNA in ng of the sample dots. The resulted number was multiplied by calculated number of molecules/ng and then by a factor of two, as the control plasmid is double stranded. Standard curve obtained was used to measure the amount of virus.

2.6. Generation of Sequence-optimised ERRγ plasmid and viral vector:

Optimized ERRγ sequence of mouse was generated by Geneart (Regensburg, Germany). We theoretically designed two plasmids expressing the same sequence-optimized ERRγ construct. We modified the plasmids to include; 3-FLAG sequence (ATG-GAC-TAC-AAA-GAC-CAT-GAC-GGT-GAT-TAT-AAA-GAT-CAT-GAT-ATC-GAT-TAC-AAG-GAT-GAC-GAT-GAC-AAG) either at 5' or 3'end, a consensus Kozak sequence, GC content was increased to promote RNA stability and codon usage was modified according to transfer RNA frequency. Then, the two different plasmids expressing the same optimized sequence of ERRγ were sent for synthesis to Geneart Eurofins Company. Then, the two new plasmids of 5'Flag and 3'Flag codon optimized ERRγ were returned back with a vector backbone (PEX-K4). Both plasmids were

amplified following manufacturer instruction using (EndoFree Plasmid Maxi Kit, QIAGEN). pAAV vectors were made by excising sequence optimized genes from parental plasmid using (AgeI and PacI) restriction enzymes and cloned into pAAV vector of non-optimized sequence.

To synthesize the codon-optimized 5'F and 3'F plasmids, double restriction digestion was carried out using (AgeI and PacI) restriction enzymes of noncodon-optimized ERRγ and the two codon optimized plasmids in order to use the back bone from the noncodon construct and the insert of the codon-optimized ERRγ.

2.5.1. Restriction digestion:

20 µg of non-optimized ERRγ plasmid and 5'F and 3'F ERRγ plasmids were double digested with AgeI (1 unit/ug) and PacI (1 unit/ug) restriction enzymes with 7 µl of buffer and make the total volume to 70 µl with water. The reaction was either incubated either for 1 hour or overnight at 37°C and then the fragments were separated on 1% gel (0.8 g agarose, 80 ml 1% TAE and 8 µl of syBR safe). After that, the bands of the backbone (6155 bp) from the non-optimized ERRγ plasmid and the insert (1466 bp) from the two codon-optimized plasmids were extracted following gel extraction kit.

2.5.2. Ligation:

Different ratios of the backbone to the insert were mixed with (1 µl) of ligase, (2 µl) of T4DNA ligase buffer and make the total volume to 20 µl with water. The ligation reaction was incubated for 2 hr at 14°C.

2.5.3. Transformation:

On ice, the ligation mix was transformed into XL-10 gold competent cells by heat shock (as described in section 2.3). Bacteria were plated on ampicillin agar plates overnight. The following day colonies were picked and added into 5 ml LB medium with ampicillin and incubated overnight at 32^{o}C with shaking. 2 ml of the mix was run on miniprepration kit, following manufacturer instructions.

2.5.4. Confirmation of the plasmids:

Confirmation of the plasmids was carried out using different restriction enzymes. Firstly, to confirm the linearized product, single digestion using XhoI restriction enzyme was run and the expected size was 7617 bp. To further confirm the size, BsrgI and BstxI restriction enzymes were used to differentiate between the new codon-optimized constructs and the non-optimized plasmid. BsrgI showed two bands at 5587 and 2030 bp for the new constructs and single band for the non-optimized. BstxI resulted in two bands at 4117 bp and 3583 bp for the non-optimized plasmid and three bands at 4177 bp, 2592 bp and 908 bp for the sequence optimized plasmids. To confirm the presence of ITRs; the following restriction enzymes were used; MscI, XbaI, BsHII and SmaI. All restriction enzymes have been ordered from New England Biolabs.

2.5.6. Sequencing:

Codon-optimized ERRγ plasmids were sent to source bioscience for sequencing and ApE Software was used to check the sequence.

2.7. β-galactosidase assay:

HEK-293T cells were seeded for 24 hours (as described in section 2.1) and then co-transfected with either non-codon-optimized mouse ERRγ plasmid or codon-optimized 5'Flag or 3'Flag ERRγ and β-gal plasmid using PEI (as described in section 2.2). Using the kit β-galactosidase assay was performed following manufacturer instructions. Firstly, the cells were washed for three times with pre-cooled PBS after removing the DMEM medium. Then, lysis buffer was added to the cells and incubated for 30 minutes at RT to extract all cell components. After that, the cell extracts were transferred to a microfuge tube and centrifuged for 15 minutes at maximum speed to remove any cellular debris. Then, an aliquot of the supernatant was used for protein concentration measurement using BSA assay (kit) and the rest was frozen at -80^{o}C. To run the assay, six concentrations in duplicate were prepared to obtain a standard curve using β-Gal stock solution and sample buffer using the concentrations recommended by the manufacture. Then, 200 µl of the β-Gal standard working dilutions and cell extracts were pipetted per well using the microplate provided with the kit and then covered with the adhesive cover and incubated for 1 hour at 37^{o}C. The solutions were then removed and the wells were washed 3 times with 250 µl of washing buffer for 30 seconds and removed washing buffer carefully. Then, 200 µl of anti- β-Gal-DIG working dilution were added to each well and the plate was covered with foil and incubated for 1 hour at 37^{o}C. Then, the washing step was repeated. Following that by pipetted 200 µl of anti-DIG-POD working dilution per well, covered the plate with foil and incubated for 1 hour at 37^{o}C. Then, another washing step was performed. Next, 200 µl of substrate with enhancer were pipetted into each well and incubated at RT until colour development was detectable for photometric

detection (approximately 30 minutes). The absorbance was measured at 405 nm using a microplate (ELISA) reader. For results interpretation, the β-Gal concentration (ng/ml) of the calibration standards were calculated and plotted on the x-axis against the absorbance values on the y-axis. The result was a linear calibration curve and used to measure the concentration for the unknown samples.

2.8. Animal Housing:

Wild type (C57BL/10 ScSnOlaHsd) and dystrophin-deficient mice (C57BL/10 ScSn-DMD^{mdx}/J mice) were housed in a temperature-controlled environment with water and food *ad libitum*. *In vivo* experimentation was conducted under statutory Home Office recommendation, regulatory, ethical and licensing procedure, and under the Animals (Scientific Procedures) Act 1986. All the animals were bred in the Biological Resources Unit, University of Reading.

2.8.1. *In-vivo* gene delivery:

The system was checked to ensure adequate amounts of gas supply and isoflurane for the duration of the procedure and the flow was set to induction chamber. The recovery box was adapted to 35^{o}C. The solution to be injected was prepared in 19G, 1 ml syringe. The oxygen valve was adjusted to 3 L/min. The isoflurane was turned on to 4.5% and mouse was monitored until recumbent and then isoflurane flow was adjusted to 2.5% during the procedure. The mouse was then removed from the chamber and put gently on tissue where the oxygen flow was adjusted to the mouse mouth. In all experiments, no empty vector control was used. For intramuscular administration, skin covering mouse *tibialis anterior* (TA) muscles was shaved to allow more accurate orientation.

The first injection was carried out with $2.5X10^{10}$ vg of AAV8 ERRɣ in 50 µl of saline solution, contra-lateral TAs were injected with 50 µl of saline solution. Animal was moved to the recovery chamber.

For intravenous administration, mice were warmed for 10 minutes in a hot box at 40°C. Then, a mouse was removed and placed inside a tail-vein animal restrainer and the tail was sterilize with 70% ethanol. $1\ X10^{12}$ vg if AAV8-ERRγ in 100 µl of saline solution was injected in the treated animals and similar volume of saline in the control animals using a 1.0 mL syringe with a 27G needle. After removing the needle, to stop any bleeding, the site of injection was held with gauze before the mice were returned to their cages.

For intraperitoneal experiment. Mice were injected with $2\ X10^{12}$ vg of AAV8 ERRɣ in 100 µl of saline solution just off the midline in the lower left quadrants. Control *mdx* were injected with 100 µl of saline solution. Sex and age of mice will be mentioned in each experiment.

2.8.2. Tissue processing:

Mice were sacrificed via cervical dislocation. Muscles were excised from tendon to tendon, weighed, blocked on a cork disc using (OCT) and rapidly frozen in liquid nitrogen-cooled iso-pentane. The frozen blocks were stored in -80ºC. To assess muscle pathology, 10 µm transverse cryo-sections for each muscle were obtained and transferred to a clean slide and stored at -80ºC. For intramuscular experiment, tissues were collected for RNA and protein analysis from frozen blocks used for histology. For all systemic experiments, one muscle leg was used for histology purposes and the second one was frozen for RNA and protein analysis. Muscles were stored at -80ºC.

2.8.3. Muscle Function:

Experiment was performed on EDL muscles from 9 weeks old *mdx* (6 weeks post-AAV administration) for intraperitoneal experiment and from 10 weeks old *mdx* (4 weeks post-AAV administration) for intravenous experiment. Mice were killed according to Schedule 1 of the animals (Scientific procedures) Act 1986, United Kingdom. Muscles were bathed in oxygenated Ringer solution containing (137 mM NaCl, 24 mM $NaHCO_3$, 5 mM KCl, 2 mM $CaCl_2$, 1 mM $MgSO_4$, 1 mM NaH_2PO_4, 11 mM Glucose; pH 7.4) kept at 25°C and continuously perfused with 5% CO_2/95% O_2. Muscles were mounted in the organ bath, flanked by plate electrodes and attached between an adjustable clamp and a dual-mode muscle lever (Aurora Scientific), and were stimulated using a computer-controlled stimulator (Aurora Scientific). Muscles were electrically stimulated to twitch and gradually increased the stimulation voltage to establish supramaximal stimulation and then the voltage was set to 110% for the remainder of the experiment. Optimum length (L_o) was determined with twitch stimulation (pulse duration: 100 msec), and muscle length was altered gradually until maximum twitch force was reached. A digital caliper was used to measure the distance between the proximal and distal myotendinous junctions (L_{opt}). To determine maximal isometric muscle force (F_{max}), each muscle perform 500 msec tetanic contraction with 2 minutes between each contraction. EDL muscles, then, were subjected to ten lengthening contractions (150 Hz for 500 msec, followed by 200 msec at a 110% L_o). After completion of the muscle measurements, muscles were weighed and frozen in liquid nitrogen-cooled isopentane. Force traces were analyzed with Dynamic Muscle Analysis v5.100 software (Aurora Scientific).

2.9. Creatine kinase assay (CK):

Serum CK was assayed in blood collected from mice via cardiac puncture while the mice under terminal anaesthesia induced by CO_2. Blood was allowed to clot on ice and then serum has been collected by centrifuge the blood at 8000 rpm for 15 minutes and stored at -80^{o}C. The assay was run in 96 well plate using spectrophotometry plate reader at 37^{o}C. 6 µl of the blood samples and 300 µl of the buffer (from the kit) were added into each well. The absorbance was measured was measured at 340 nm and readings were taken at 4 intervals; 0 min, 1 min, 2 mins, 3 min and 4 minutes. The first reading was ignored and then, the absorbance was blotted against the time points. Finally, the CK level for each sample was measured using the following equation; CK level= (Δab/min) X 8095.

2.10. Histology:

2.10.1. Succinate dehydrogenase staining:

The largest sections from the midportion were selected for all analysis. Firstly, sections were air dried for 30 minutes and incubated with incubation medium; NBT stock, succinate stock and phenazine methanosulfate. The medium should be prepared freshly. NBT stock; phosphate buffer, 6.5 mg KCN,185 mg EDTA and 100 mg nitroblue tetrazolium, succinate stock (500 mM sodium succinate). For each 2 ml of NBT stock, 0.2 ml of succinate stock was added in addition to tiny crystal of nitroblue tetrazolium. Muscles were incubated with the stain until a purple colored developed. Then, sections were washed for 1 minute with distilled water followed by fixation in formol calcium for 15 minutes. Slides mounted with hydro-mount medium.

2.10.2. Haematoxylin and Eosin Staining:

Sections were dried at RT for 30 minutes, then they were placed in Mayers haematoxylin solution for 3 minutes, slides were bluied up by washing them in running tap water for at least 3 minutes. Slides were then placed in 1% eosin for 3-5 minutes. Sections were dehydrated in 100% alcohol for 3 times for 1 minute and cleared in xylene for minimum of 10 minutes and mounted in DPX.

2.10.3. Immunohistochemistry protocol:

The following protocol was used to stain laminin, IgG, embryonic myosin (MYH-3) and myosin heavy chain (MHC) type I, IIA and IIB. Generally, sections were air dried for 30 minutes. Slides were washed twice in PBS-T for 5 minutes. Then, permeabilization buffer was added for 15 minutes. Slides were washed three times with PBS-T followed by incubation in washing buffer for 30 minutes. Primary antibody was diluted in washing buffer for 30 minutes and added to the sections for 1 hour at RT. After that, primary antibody was washed with washing buffer. Then, secondary antibody was diluted in washing buffer for 30 minutes and added to the section for 45 minutes at RT in the dark. Secondary antibody was removed by performing 3 washes with washing buffer. Following the same protocol, MHC type IIA and IIB myofibres were stained together on the same slide, however, MHC type I myofibres was stained on a serial section. The first primary antibody was incubated overnight and the next day the secondary antibody was added followed by the same procedure for the second primary antibody. Finally, sections were mounted with fluorescent mounting medium (Dako fluorescent medium).

Capillary density was investigated with an antibody against CD31, as a marker of endothelial cells and was performed by firstly blocking the sections with avidin for 15 minutes followed by biotin blocking solution for another 15 minutes (Vector Labs). Then, sections were washed with PBS-T for 5 minutes and then blocking the non-specific binding with 3% milk-PBS for 30 minutes. After that, the sections were incubated with CD31 antibody for 1 hr at RT following by washing with PBS-T and then incubation with biotinylated secondary antibody (rabbit anti rat HRP), followed by washing as mentioned above. Sections were incubated with ABC-HRP for 10 minutes, followed by washing. Sections were developed for 6 minutes using DAB kit (2 drops from and 4 drops from DAB substrate reagent). Next, the substrate was washed off with water for 1 minute and dehydrated in 100% ethanol three times, each for 1 minute, cleared in xylene and mounted in DPX, List of antibodies (Table 2.2).

Table 2.2. List of immunohistochemistry antibodies

Primary antibody	Species	Dilution	Supplier	Secondary antibody	Dilution	Supplier
Laminin	Rabbit	1.200	L9393 (Sigma)	Goat anti rabbit (Alexa 633)	1.200	A11037 (Life Technology)
IgG	Rabbit	1.200	AB6709 (Abcam)	Goat anti rabbit (Alexa 488)	1.200	A11034 (Life Technology)
MYH-3	Mouse	1.200	F1.652 (Santa Cruz)	Goat anti-mouse (Alexa 488)	1.200	A11029 (Life Technology
CD31	Rat	1.150	MCA2388GA	Polyclonal Rabbit anti rat Immunoglobulins/ HRP	1.200	(P0450) Dako
Type I (A4.840)	Mouse	1:1	DSHB	Goat anti-mouse (Alexa 633)	1.200	A11037 (Life Technology
Type IIb (BF-F3)	Mouse	1:1	DSHB	Goat anti-mouse (Alexa 633)	1.200	A11037 (Life Technology
Type IIA (A4.74)	Mouse	1:1	DSHB	Goat anti-mouse (Alexa 488)	1.200	A11029 (Life Technology

2.11. Laminin image analysis:

To calculate the cross sectional area of the muscle fibres, analysis was performed on the largest muscle cross sectional area using SigmaScan software. The intensity threshold was set to identify the area of interest. From the software, the number of pixel, smallest length and area were highlighted to count and identify each object. Then, all identified objects have individual identified number and the area represented by the number of pixels is determined. Then, the smallest fibre was identified to define its area. The spread sheet generated by the software contained the number of fibre with their corresponding pixels. All objects which were not larger than the area of the smallest fibre were disregarded. In the object, all objects identified by the software and did not corresponded to a fibre were deleted. Finally, the smallest length of each muscle in pixel was used to find out the area in um^2. Firstly, the length was divided by two to calculate the radius. Secondly, the radius was multiplied by 1.255 which is the power of the 5X object used in the microscope and the value was used in the equation. Finally, the area was calculated using the equation [3.14 X $(radius)^2$].

2.12. RNA extraction:

First, muscles were grounded using cooled pestle and mortar and then transferred into a clear tube with a flat base. After that, 500 µl of TRI reagent was added into each tube and homogenized using homogenizer. RNA was extracted Tri-reagent according to manufacturer's instructions.

2.13. Complementary DNA (cDNA) synthesis:

RNA concentration was determined by spectrophotometry using Nanodrop. According to the RNA concentrations, 0.5 to 1 µg of RNA was reverse transcribed

with oligo DT using QScript cDNA Synthesis Kit following manufactory instruction.

2.14. Quantitative real time polymerase chain reaction PCR (Qpcr):

Housekeeping genes were obtained from (Primerdesign). 6 housekeeping genes were tested to select the highly two stable genes. 5 treated samples and 5 control were run for each gene. The most stable Housekeeping genes were chosen using (qbase Biogazelle) software, with best stability of less than 0.5. Two primers with highest stability were used to normalize the genes of interest. *TA* and *EDL* muscles were normalized to Htatsf1 and Csnk2a2, Diaphragm and gastrocnemius muscles to Csnk2a2 and cdc40, heart to Csnk2a2 and AP3d1, quadriceps to Paklip1 and Htatsf. From each sample, 5 µl are used to prepare arbitrary dilutions of 5 standards. Set of six primers were checked to choose the most stable genes among all samples. In brief, for each reaction, 7.5 µl of the master mix (5 µl of syprgreen, 0.5 µl of primer and 2 µl of RNAse/DNAse free water) and 2.5 µl of the template are run in X25 thermofast96 FastPCR Nuetral plates. The optimal efficiency of all primers (Housekeeping genes or gene of interest) falls between 90 and 110%. Relative mRNA levels were determined by Quantitative PCR following the cycling protocol; 3 minutes at 95^{o}C, 15 seconds at 95^{o}C and 60 seconds at 60^{o}C, using the Perfecta SYBR Green Fast Mix). Primers were designed using the Blast software.

2.15. Western blotting:

Muscles were powdered on dry ice and lysed using RIPA lysis buffer.

2.15.1. Determination of protein concentration:

Protein concentration was measured with Bio Rad DC Lowery Assay. Protease and phosphatase inhibitors were added to the lysis buffer. Briefly, to prepare the standard curve assay, two fold serial dilutions was prepared of BSA (1.4 mg/ml) (Bovine serum albumin) containing from 0.12mg/ml to 1.0mg/ml apart from one standard without BSA in order to calibrate the absorbance to zero. Into each standard, 2 µl of lysis buffer was loaded and the total volume make up to 20 µl with water. The samples were prepared with 1:10 dilution.

200 µl of reagent A' (200 µl and 4 µl of reagent A and reagent S) were added to each sample and standards followed by 800 µl of reagent B. The samples were left for 15 minutes then absorbance of protein samples were measured using spectrophotometer at 750 nm absorbance. The BSA concentration (mg/ml) of the standards were blotted on the x-axis against the absorbance values on the y-axis. The resulted linear curve was used to measure the concentration of the unknown protein samples.

2.15.2. Western blot protocol:

The samples were vortexed and boiled for 5 minutes at 95^{o}C before loading into the gel. Protein ladder was run alongside the samples. 20-40 µg of protein samples were separated by electrophoresis on TruPAGE Precast Gel for 1 hour at 170 volt. For transfer step, nitrocellulose membrane was used and run for 2 hours at 50 volt. To visualize the total protein per lane, the blot was covered in

methanol for 1 min and then in ponceau stain for 5 minutes with shaking. Followed by washing in distilled water for another 5 minutes and then imaged using Image J software. Then, blocking buffer of non-fat milk in Tris buffered saline tween 20 (TBST) was used for 1 hour to block unspecific proteins. Immunoblotting was performed using primary antibodies against; ERRγ, Flag, PGC-1α, Oxpho cocktail and PERM1 diluted in 5% non-fat milk-TBST overnight at 4^{o}C. The next day, blots were washed three times for 5 minutes in TBST followed by addition of HRP labelled secondary antibodies diluted in 5% non-fat milk TBST at RT for 1 hour (Table 2.3). The blots were then visualized with Clarity western ECL substrate detection system using Image quanta and densitometry analysis were then performed using Image J software.

Table 2.3. List of western blot antibodies

Primary antibody	Species	Dilution	Supplier	Secondary antibody	Dilution	Supplier
ERRγ	Rabbit	1.1000	Proteintech Rosemont, USA) (14017-1)	Polyclonal Goat anti-rabbit immunoglobulins/HRP	1.2000	AP307p Merck Milipore
Flag	Mouse	1.1000	Sigma, F1804	Polyclonal Rabbit anti-mouse immunoglobulins/HRP	1.2000	P0260 Dako
Oxphos cocktail	Mouse	1.2000	Abcam, ab110413	Polyclonal Rabbit anti-mouse immunoglobulins/HRP	1.5000	P0260 Dako
PGC1α	Rabbit	1.1000	Abcam, 54481	Polyclonal Goat anti-rabbit immunoglobulins/HRP	1.2000	AP307p Merck Milipore
PERM1	Rabbit	1.1000	Sigma, C1orf170	Polyclonal Goat anti-rabbit immunoglobulins/HRP	1.2000	AP307p Merck Milipore

2.16. Microarray analysis:

Total RNA was extracted using the Stratagene MicroRNA kit and RNA resuspended in nuclease-free water. The integrity of the RNAs were assessed using a Bioanalyser and 5 ng used for the preparation of biotin-labeled cell extract using the Nugen Ovation amplification system (www.nugen.com). For each

representative biological replicate group, 7 µg of labeled extract was hybridized to Affymetrix Chicken GeneChips for 20 hours. The hybridized arrays were washed, stained, and scanned according to the protocols set out by Nugen and Affymetrix.

2.17. Statistical analysis:

Statistical comparison between treated and control groups for all experiments except fibre sizing was performed by 2-tailed student's t test on paired samples in muscles from the same animal and un-paired when comparing muscles from different animals using sigma plot software (version 12.3). *P* values<0.05 were considered significant (* indicates $p<0.01$, ** $p<0.001$, *** $p<0.0001$. Fibre size results were performed by chi-square test.

3. Chapter Three

Intramuscular administration of AAV8-ERRγ into 6 and 12 week-old *mdx*

3.1. Introduction

DMD is a genetic disorder with impaired energy homeostasis in which the capacity of mitochondria to produce ATP is impaired in skeletal muscles of human DMD and *mdx* mice (Even et al., 1994, Kuznetsov et al., 1998, Austin et al., 1992, Timpani et al., 2015). ATP is synthesized via the creatine phosphagen system, metabolism of glucose via glycolysis, and fatty acid oxidation. Pyruvate generated by glucose metabolism and acetyl CoA generated by fatty acid metabolism are shuttled into tricarboxylic acid (TCA) cycle and electron transport chain (ETC) in the mitochondria and ATP is produced by oxidative phosphorylation (OXPHOS) process (Rybalka et al., 2015). Dystrophin deficient skeletal muscles exhibit a reduction in the availability of glucose due to loss of NO signalling regulated by neuronal nitric oxide synthase (nNOS) due to reduced expression of nNOS (Ennen et al., 2013). nNOS becomes a target of calpain in dystrophic muscles, leading to reduced levels of NO, which is a strong regulator of glucose uptake and flux during muscle contraction (Hong et al., 2014). In addition to defects in glycolysis, dystrophic muscles exhibit defects in the TCA cycle, fatty acid oxidation, mitochondrial electron transport chain and the purine nucleotide cycle (PNC), have all been reported leading to 50% reduction in resting ATP level (Rybalka et al., 2015). Furthermore, loss of dystrophin disrupts sub sarcolemma mitochondria pool density (SSM) which in turn impair the control of mitochondrial localization and the capacity to generate ATP that serve to diminish ATP availability and promote cell death (Percival et al., 2013).

In addition to diminished level of ATP, dystrophic muscle of *mdx* mice also have an abnormal vasculature density and an impaired blood flow. Vascular abnormality occurs as a result of; lower NO-dependent flow in endothelial cells

(EC), reduced nNOS and endothelial nitric oxide synthase (eNOS) expression and decreased vascular density (Loufrani et al., 2004, Palladino et al., 2013, Asai et al., 2007). Data have shown that the loss of (nNOS) from the sarcolemma caused a reduction in nNOS activity in the cytosol and a significant reduction in the level of NO (Tidball and Wehling-Henricks, 2014). Many mechanisms have been identified through which nNOS deficiency contributes to miss regulation of muscle development, fatigue, blood flow, inflammation and fibrosis. In skeletal muscle, NO could diffuse to nearby arterioles, resulting in vasodilation and increasing blood flow by antagonizing α-adrenergic vasoconstriction via cGMP mediated pathway. Therefore, NO production has been suggested to play roles in blood flow, vasorelaxation and angiogenesis (Tengan et al., 2012). However, in dystrophic muscles, due to inadequate level of NO, the sympathetic vasoconstriction unopposed, and the muscle is subject to ischemia (Tidball and Wehling-Henricks, 2014).

Furthermore, vascular abnormality occurs in response to lower expression of dystrophin in vascular smooth muscle cells and EC (Ito et al., 2006). NO produced by (eNOS), expressed in EC, is involved in the regulation of blood pressure through relaxation of vascular smooth muscle cells and vasodilation of blood vessels (Palmer et al., 1987, Suhr et al., 2013).

However, intracellular free calcium concentrations within SMC controls vascular tone. Contraction of SMC is triggered by receptor-mediated generation of the second-messenger inositol 1,4,5-trisphosphate (IP_3). IP_3 mediates release of Ca^{+2} from intracellular stores and stimulates influx of extracellular Ca^{+2} via voltage and non-voltage-gated Ca^{+2} channels (Tsai and Kass, 2009). The elevation in intracellular calcium

activates calcium/calmodulin-dependent myosin light chain kinase (MLCK) which phosphorylates myosin light chain (MLC) to activate myosin ATPase and trigger SMC contraction, thus increasing blood flow (Tsai and Kass, 2009). Therefore, the vasculature depends on the level of free Ca^{+2} in the cytosol of vascular smooth muscle cells and the sensitivity of the contractile proteins to Ca^{+2}, which is determined by the extent of myosin light chain phosphorylation. It has been hypothesized that in vascular smooth muscle cells, the reduction in intracellular Ca^{+2} due to a defect in L-type channel leads to the hyperpolarization of the SMC membrane potential, followed by a reduction in the sensitivity of the contractile machinery by decreasing the Ca^{+2} sensitivity of myosin-light chain phosphorylation, this in turn decreases the vascular tone of SMC (Perez-Zoghbi et al., 2009). In addition, dystrophin deficiency in vascular endothelial cells has been implicated in impaired NO-dependent flow (shear stress). Consequently, an impaired blood flow results in ischemia and a decreased capacity of the vasculature to respond to flow. Shear stress is the main stimulus inducing the release of vasoactive agents by vascular endothelial cells for angiogenesis, vascular remodelling and vascular cell growth (Ando and Kamiya, 1993, Wragg et al., 2014). However, dystrophin was found to form a complex with caveolin-1 calcium channel and eNOS in EC (Palladino et al., 2013). In vascular endothelial cells, cGMP-PKG regulates angiogenesis and vascular permeability. In the absence of dystrophin, the NO production and cGMP-PKG signalling are impaired in EC of *mdx* mice, leading to low responsiveness to shear stress (Palladino et al., 2013). Therefore, new blood vessel formation could be downregulated due to defects in mechanotransduction (Thomas et al., 2003, Sander et al., 2000, Palladino et al., 2013).

Moreover, NO was shown to improve protein level of VEGF in cardiomyocytes following treatment with NO donor, S-Nitroso-N-acetylpenicillamine (SNAP) via HIF-1α (Kuwabara et al., 2006). As a consequence of diminished NO in *mdx* mice, the expression of VEGF is reduced. Further, reduced blood flow leads to low eNOS expression, which normally exert feedback loop to induce VEGF expression (Baum et al., 2004); thus compounding vascular flow in dystrophic muscle. Together, there is a close association between reduced blood flow and defected angiogenesis leading to insufficient vascular density in *mdx* mice that mismatched to the metabolic need of the muscles. Augmenting angiogenesis by inducing the density of vascular architecture would be one way to improve muscle perfusion and potentially positively impact on dystrophic pathology (Loufrani et al., 2001, Matsakas et al., 2012).

In skeletal muscle, dystrophin is involved in the arrangement of the microtubule lattice. In dystrophic muscle, the pattern of microtubule is disorganised and becomes denser due to absence of dystrophin. It is thought that in response to membrane stress such as eccentric contraction, *mdx* myofibres induce ROS production by activation of NADPH (reduced-form nicotinamide adenine dinucleotide phosphate) oxidase 2 (NOX2). Further, NOX2 amplify Ca^{+2} influx through stretch activated channel (SAC) (Khairallah et al., 2012). ROS production has also been identified following Ca^{+2} entry into the mitochondria (Whitehead et al., 2006).

Other consequences of poor Ca^{+2} homeostasis in dystrophic muscle is an activation of necrosis. The necrotic fibres activate and release neutrophils and damage-associated molecular patterns (DAMPs) that promote inflammation

process. Then, M1 macrophage attack the necrotic myofibres and increase the secretion of pro-inflammatory cytokines such as tumour necrosis factor alpha (TNF-α), interleukin-1β (IL-1β) and interleukin-6 (IL-6). It has been reported that serum of the DMD patients shows over-expression of pro-inflammatory cytokines with the presence of the two phenotypes of macrophages; M1 and M2. Pro-inflammatory cytokines play roles in regenerating myofibres which ultimately replaced by connective and adipose tissues when the capacity of regeneration is exhausted (De Paepe and De Bleecker, 2013). In addition, increased levels of ROS in dystrophic tissues induce pro-inflammatory cytokines, for example NF-κB leading to activation of TNF-α and IL-1β (Figari et al., 1987, Remels et al., 2010).

As a consequence of the dysregulation of redox signalling and calcium homeostasis, the system is under high demand of ATP production for Ca^{+2} buffering, satellite cell cycling and muscle regeneration which together with reduced capacity for ATP synthesis, reduced glucose transport and the reduced level of NAD results in metabolic stress in dystrophic muscle (Rybalka et al., 2014). Therefore, it is important to improve ATP synthesis as dystrophin-deficiency-mediated damage could be mitigated if the availability of ATP is improved.

However, targeting metabolism as a therapy may have a beneficial effect on the pathophysiological course of DMD. Improving the oxidative phenotype of muscle fibres may overcome many of the pathological changes in DMD, as glycolytic fibres are more prone to damage due to the faster and larger accumulation of force during contractile activity, thus increasing susceptibility to sarcolemma

damage. The lower abundance of mitochondria might also accelerate the degeneration of glycolytic fibres due to decreased capacity to maintain Ca^{+2} homeostasis (Webster et al., 1988, Pedemonte et al., 1999), as slow, oxidative muscle fibres are more resistant to the dystrophic pathology (Head et al., 1992, Webster et al., 1988). In this context, selective transgenic over-expression of ERRγ, PGC-1α, PPARγ in skeletal muscles of *mdx* mice allowed transition of the muscle phenotype into more slow, oxidative fibres and hence more protection against damage and DMD pathology (Matsakas et al., 2013, Reilly and Lee, 2008, Summermatter et al., 2012).

The muscles of *mdx* mice exhibit diminished expression of ERRγ. Matsakas et al demonstrated that ERRγ is expressed in highly metabolic tissues and that the over-expression of ERRγ in skeletal muscle of *mdx* mice resulted in a mitigation of the muscle pathology, such as a shift towards a more oxidative phenotype, upregulation of angiogenic factors, improved perfusion and a reduction of centrally nucleated fibres (Matsakas et al., 2013). Therefore, the key question in this study is to address the impact of the post-natal over-expression of ERRγ by AAV gene transfer on the muscle pathology of *mdx*.

Despite the fact that (DMD) is caused by mutations in the dystrophin gene (Hoffman et al., 1987), the understanding of the molecular pathogenesis of disease and the responses to therapy remain incomplete. Hence, large scale parallel gene expression analysis allows the investigation of the molecular pathophysiological pathways and comparison of how these pathways are differed from healthy muscle (Haslett et al., 2002). The analysis of gene expression in the *mdx* mouse has the potential to identify potential therapeutic targets, novel genes

involved in disease pathology and candidates disease biomarkers relevant to DMD. Many expressing profiling techniques have been developed, which include quantitative polymerase chain reaction (Qpcr), microarray and RNA sequencing (RNAseq) (Roberts et al., 2015).

Nowadays, there is increasing desire to find a connection between diseases, their mode of action, pathophysiology and the impact of therapeutic molecules on them. A connection map (cMap) is a developing technique designed to find connections between genes, drugs, and diseases. It is based on implying genomic signature such as mRNA levels, protein expression or metabolic patterns (Lamb et al., 2006). In other words, the effect of each selected molecule has been robustly defined by the cognate change in the transcriptome of the treated cells. Given that characteristic alterations in gene transcription (a signature) underpins most diseases, drugs that can ameliorate or reverse these transcriptional shifts will have therapeutic potential. In this way, a series of readily-available drug candidates can be bio-informatically generated, scored and ranked by their likelihood of ability to restore the normal biological state, or, in case of muscular dystrophy protect against further muscle loss. Accordingly, the c-Map resource has the potential to connect human diseases and the drugs that treat them (Huang et al., 2015). The main advantage of cMap is that cMap is agnostic to the drug targets or drugs mode of actions, as historically described; thus allowing a reductive process of candidate drugs that have already had regulatory approval. On the other hand, gene expression microarrays allows the measurement of genome-wide transcriptional expression levels (Yap et al., 2007). The C-Map approach maximizes the chances of success by basing the search on defined factors (changes in gene transcription). This approach

demonstrates the power of transcriptional signature-based drug repurposing and highlight several advantages over other drug discovery methodologies including reduced time to clinic, known tolerability and toxicity profiles, non-target dependent mechanisms as well as potentially identifying new pathways for future discovery (Lamb et al., 2006).

In this chapter, we aim to assess the effect of overexpressing ERRγ on metabolic activity *in vitro* and *in vivo*. Firstly, we used the mouse myoblast C_2C_{12} cell line to assess the metabolic capacity of the cells following transfection with a plasmid expressing a murine ERRγ transgene under the control of the spc5-12 promoter. At the *in vivo* level, firstly, 6-week old *mdx* has been used for microarray analysis (n=3) to assess short term effect of ERRγ over-expression on global gene expression profiles in dystrophic muscle and to create a cMap. Then, we aim to assess the short term changes in pathology such as oxidative capacity, angiogenesis in *tibialis anterior* (TA) muscles following intramuscular administration (IM) of $2.5X10^{10}$ vg AAV8 ERRγ expression under the control of the spc5-12 promoter. (TA) is one of the most active, fast-twitch skeletal muscles. TA is a well defined muscle with a strong connective tissue fascia that retain fluid injected into the muscle. The muscle is also easy to inject percutaneously, thus avoiding the need for surgical exposure. Moreover, the muscle lies in the anterior compartment in the lower region of the hind limb. The ability to evaluate the effect of a treatment provides a significant rationale to demonstrate the efficacy of a treatment in high scale (Dellorusso et al., 2001). TA exhibits high resistance to fatigue during periods of intense running, making it interesting system to investigate the secondary consequence in DMD (Jones et al., 2009). Here, AAV8-ERRγ was injected into the TA muscle and recovered after 4 weeks of

treatment in order to examine the effect of overexpressing ERRγ on oxidative capacity and angiogenesis. Two main cohorts of *mdx* males were used; 6 week old (during active necrosis) and 12 week old (after the peak of active necrosis), (n=6). TA muscles from 12 week old mice (n=6) were blocked in groups (mounted on the same piece of cork) of three and TA muscles of 6 week old mice were blocked in groups of two. Therefore, histological analysis for *mdx* and *mdx*-ERRγ had n=6. However, as molecular analysis was performed on samples from the blocked tissues, the effective n value for this analysis is n=2. All genes in both aged groups (n=2) showed similar pattern of increase or decrease. Therefore, for molecular analysis, we grouped the data from *mdx* and *mdx*-ERRγ of 6 and 12 weeks ending up in (n=5). Following the first study and based on the observations from microarray and histological analysis, another study was carried out using 6 week-old male *mdx* only (n=6). Intramuscular administration of $2.5X10^{10}$ vg AAV8 ERRγ was carried out into TA muscles. Muscles were recovered 4 weeks post injection and were blocked individually to assess the changes at the molecular level in a large number of samples.

3.2. Results:

3.2.1. C_2C_{12} cells treated with pAAV-ERRγ plasmid or AAV8-ERRγ virus increase NADPH activity without increasing the cell number:

A proliferation/MTS assay was run to examine whether over-expression of ERRγ using the pAAV ERRγ plasmid had an effect on increasing either the metabolic activity or proliferative capacity of mouse myoblast C_2C_{12} cells. The impact on metabolic activity of over expression of ERRγ was also assessed in C_2C_{12} myotubes following transduction with AAV8-ERRγ.

C_2C_{12} cell proliferation assay is based on the conversion of tetrazolium compound into formazan product in the presence of NADH or NADPH produced in the metabolically active cells by dehydrogenase enzyme. C_2C_{12} cells myoblast transfected with ERRγ plasmid (p=0.001) and C_2C_{12} myotubes transduced with AAV8-ERRγ virus (p=0.001) showed a significant increase in the cell activity represented by the increase in the NADPH activity compared to the myoblasts/myotubes treated with control (eGFP) plasmid/virus under the same conditions (figure 3.1). Cell counting resulted in no difference in the number of cells between the control and treated myoblast groups following treatment (figure 3.2).

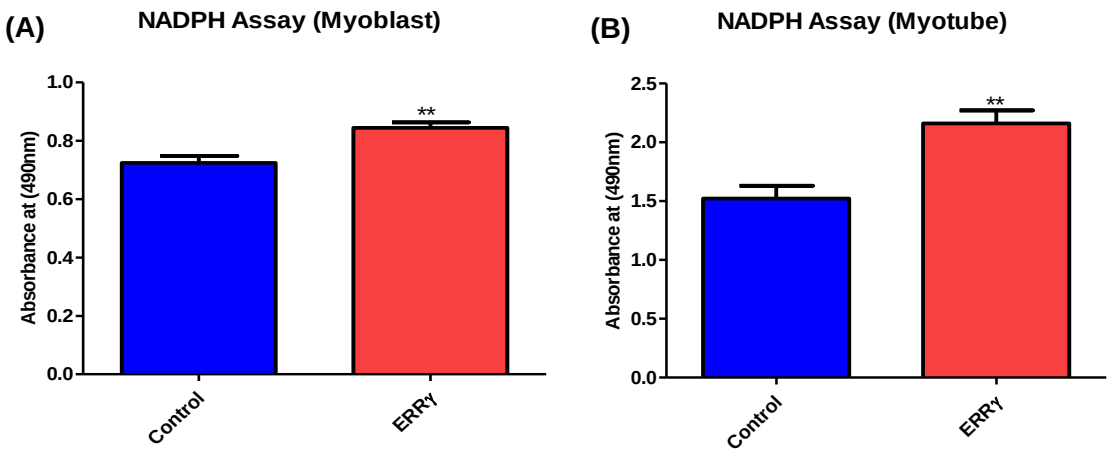

Figure 3.1. MTS assay of C_2C_{12} cells

A) Transfection of C_2C_{12} cells with (1:2) pAAV-ERRγ: PEI induced NADPH activity of C_2C_{12} myoblast cells compared to control cells transfected with pAAV-GFP plasmid, (n=8, *p*=0.001). B) C_2C_{12} myotubes were transduced either with 1 $X10^{10}$ vg/well of AAV8-ERRγ or AAV8-GFP virus for three days and showed increase in the NADPH activity of the transduced myotubes with AAV8-ERRγ (n=8, *p*=0.001, un-paired student t-test).

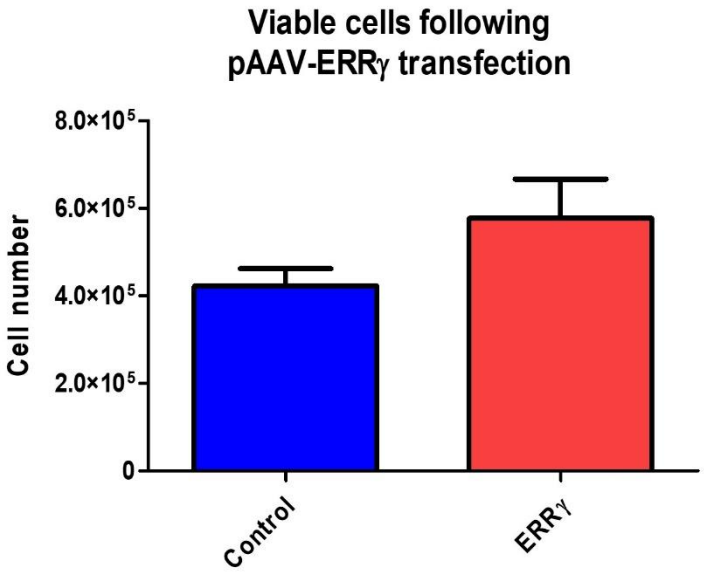

Figure 3.2. C_2C_{12} myoblast cells viability

Transfection of C_2C_{12} cells with (1:2) pAAV-ERRγ: PEI compared to the cells transfected with pAAV-GFP plasmid showed no difference in the number of cells between the two treatments (n=8, *p*=0.131, un-paired student t-test).

3.2.2. Principal component analysis (PCA) showed distinct expression profiles of *mdx*-ERRγ treated TA's compared to *mdx*:

Every signal from each GeneChip represented a gene expression value. Scatter plots of fluorescent intensity of cDNA products analysed by microarray hybridization (figure 3.3). Figure 3.3 A showed 0.9669 to 0.9680 interval of spread for *mdx* vs wild type; however, the interval of spread of *mdx*-ERRγ vs wild type is 0.9760 to 0.9769 (figure 3.3 B). Then, the suitability of the expression data sets for inclusion in the analysis and the overall relationship between and within the biological replicates is assessed using principle components analysis (PCA). Comparing the signature of the *mdx* and *mdx*-ERRγ muscles showed clear difference between the two groups, demonstrating that they have distinctive profiles (figure 3.4). From this data set one cannot be unequivacol that the *mdx*-ERRγ muscles are 'tending towards' the wild type muscle, just simple stating that *mdx*-ERRγ muscles are distinct from *mdx* muscles.

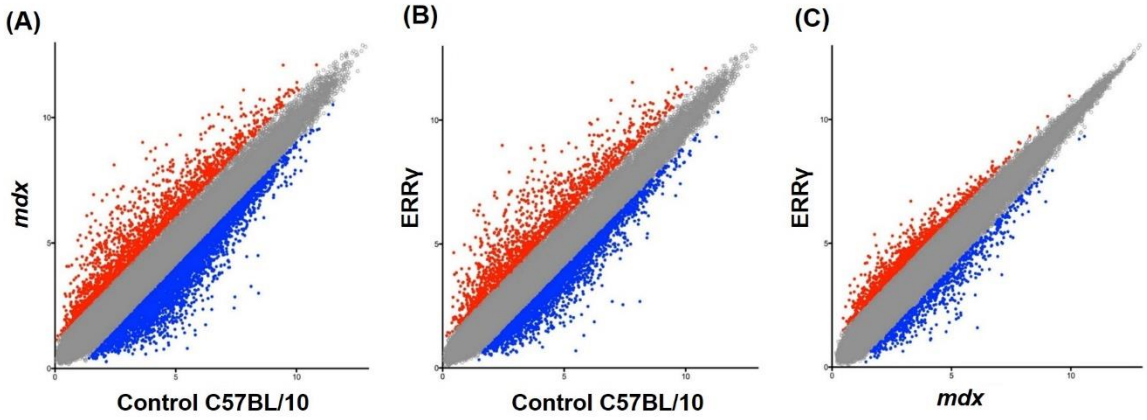

Figure 3.3. Scatter plot analysis of wild type, *mdx* and *mdx*-ERRγ following IM-AAV8-ERRγ into 6 week-old *mdx*

Scatter plot showing the log ratios of the means of differentially regulated transcripts between (A) *mdx* and control, (B) *mdx*-ERRγ and control and (C) *mdx*-ERRγ and *mdx*. All genes are represented in these plots. (Red dots represent upregulation, blue dots downregulation; n=3, male *mdx*.

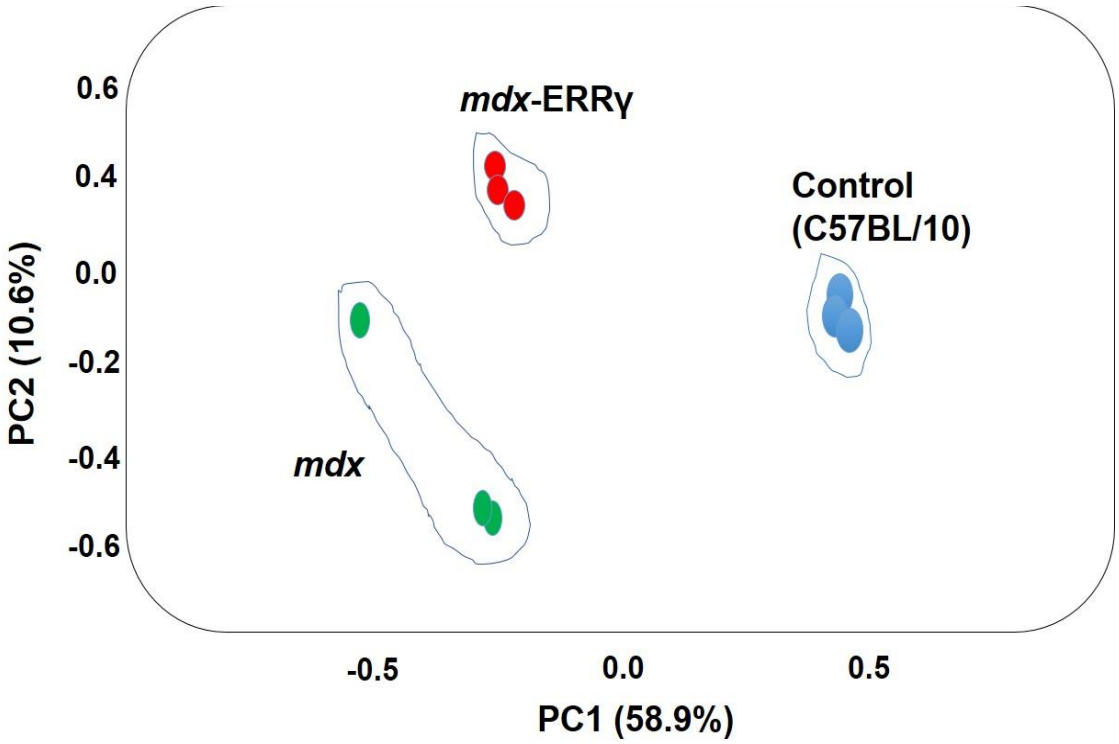

Figure 3.4. Principle components analysis of individual experimental samples

Principal component analysis (PCA) scores plots comparing wild type, *mdx* and *mdx*-ERRγ. Each dot represent a muscle sample from the respective groups (% variance in the parenthesis; n=3).

3.2.3. Alterations in gene ontogeny following ERRγ over-expression in *mdx*

To verify the biological meaning of observed changes in the expression of many genes, statistically different genes can be functionally classified using a combination of Gene Ontology (GO) criteria and other molecular descriptions. GO biological processes were grouped into general categories, like metabolic process, cell proliferation, biological regulation and cell communication. The analysis showed that the most significant enriched pathways are related to metabolic process. The distributions of these categories are represented in pie charts (figure 3.5 A). These genes were also classified into different categories

according to their contribution in different molecular functions. Accordingly, analysis showed that the most enriched genes are involved in protein binding. The distributions of these categories are represented in pie charts (figure 3.5 B). Although, using an identical approach we found that 1429 transcripts significantly changed their expression greater than 2-fold between *mdx* and *mdx*-ERRγ. For example; CoA4 gene (cytochrome c oxidase assembly factor 4) showed 29 fold increase in the treated muscles, which is an enzyme involve in the maturation of mitochondrial complex IV. Acadl, acyl-CoA dehydrogenase, involves in β-oxidation of fatty acid and increased by 19 fold increase. Another example is Fabp1 that increase by 6 fold.

(A)

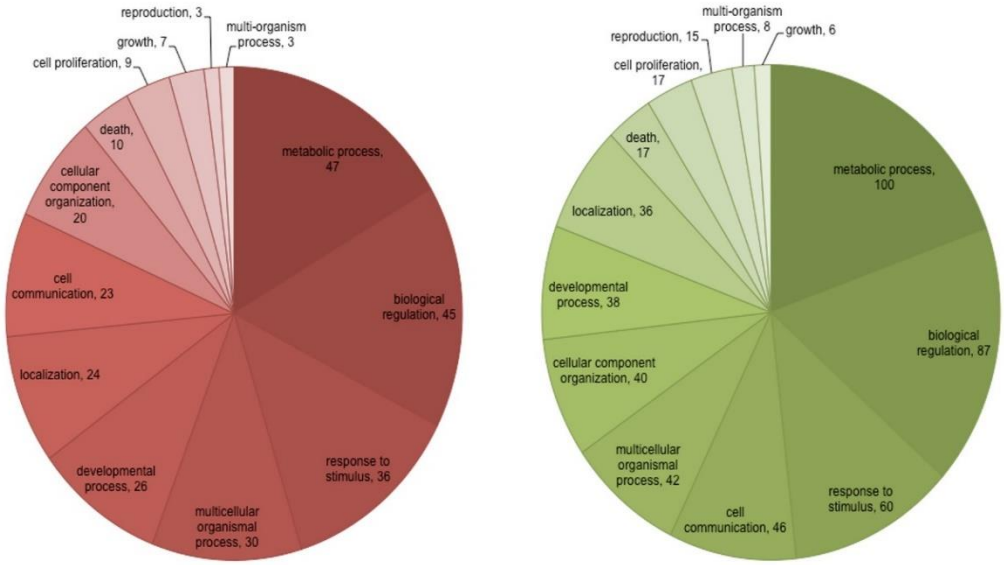

(B)

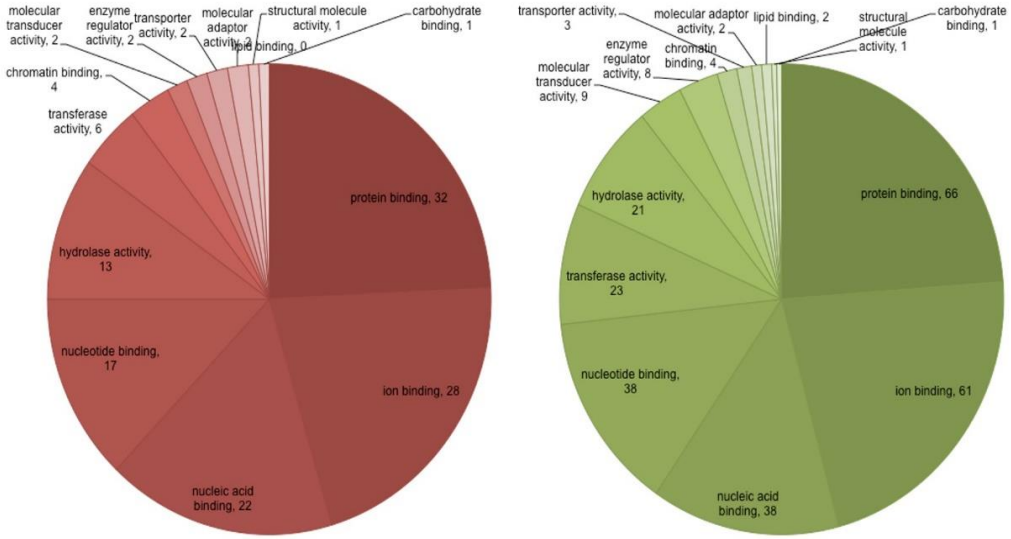

Figure 3.5. Gene ontology following ERRγ over-expression in *mdx*

A) Changes of biological processes associated with over-expression of ERRγ. The red colour represents the up-regulated functions and green colour shows the down-regulated functions. B) Changes of molecular functions associated with over-expression of ERRγ. The red colour represents the up-regulated functions and green colour shows the down-regulated functions.

3.2.4. Expression level of ERRγ in the TA of *mdx* muscles following AAV8-ERRγ gene transfer:

To assess the change in the expression of ERRγ following AAV8-ERRγ gene transfer into TA muscles of *mdx* mice, quantitative real time PCR (qRT-PCR) was performed using specific primers for each gene of interest and the relative expression was normalized to the house keeping genes; Csnk2a2 and Htatsf1. ERRγ mRNA was over-expressed 3 fold in the treated muscles compared to the control (n=5, p=0.02) (figure 3.6 A). However, despite the increase in the mRNA level, no increase in the levels of ERRγ protein was detectable (figure 3.6 C), although the quality of ERRγ antibodies are notoriously poor.

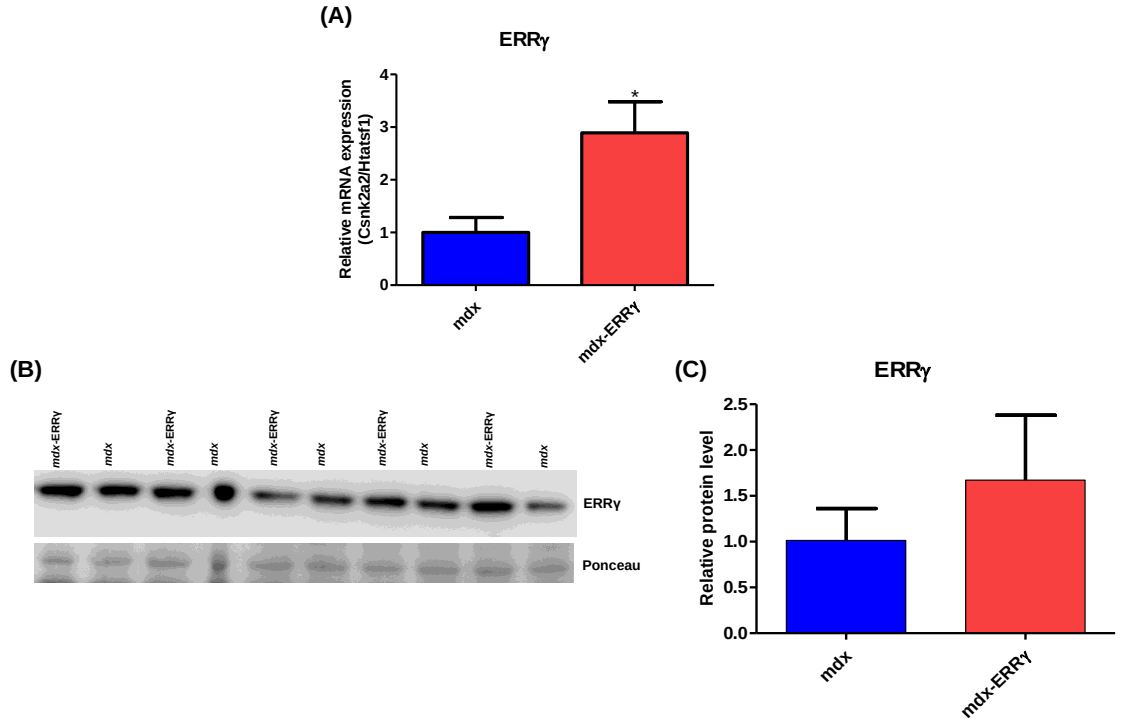

Figure 3.6. Quantitative analysis of ERRγ using qRT-PCR and western blot

A) Data were generated from samples of both cohorts; 6 and 12 week old mice and were recovered 4 weeks post administration. 3 fold increase in the expression of mRNA relative transcript of ERRγ in in treated TAs muscles compared to TAs injected with saline (n=5, *p*=0.02, paired student's t-test). The level of ERRγ was expressed relative to the housekeeping genes; Htatsf1 and Csnk2a2. The levels of ERRγ protein in TA muscles were determined by western blot analysis using 25 µg of protein and Ponceau stain was used for normalization. The total ERRγ was determined using ERRγ antibody. B) The intensity of the bands was quantified using ImageJ software. C) The values showed no difference in the protein level of ERRγ between the treated and control TAs, (n=5 male *mdx*, *p*=0.429, paired student's t-test).

3.2.5. Expression of ERRγ in transgenic muscle:

To compare the level of ERRγ over-expression between the transgenic TA muscles from transgenic mice specifically express ERRγ and TA muscles from our experiment, qRT-PCR was performed using ERRγ primer and the relative expression was normalized to the house keeping genes; Csnk2a2 and Htatsf1. Analysis showed 170 fold over-expression of ERRγ in transgenic TA muscles compared to *mdx*-ERRγ muscles from this

experiment (figure 3.7). This supraphysiological over-expression is relevant with respect to how the data from this study, that demonstrated a modest 3 fold over-expression, is interpreted

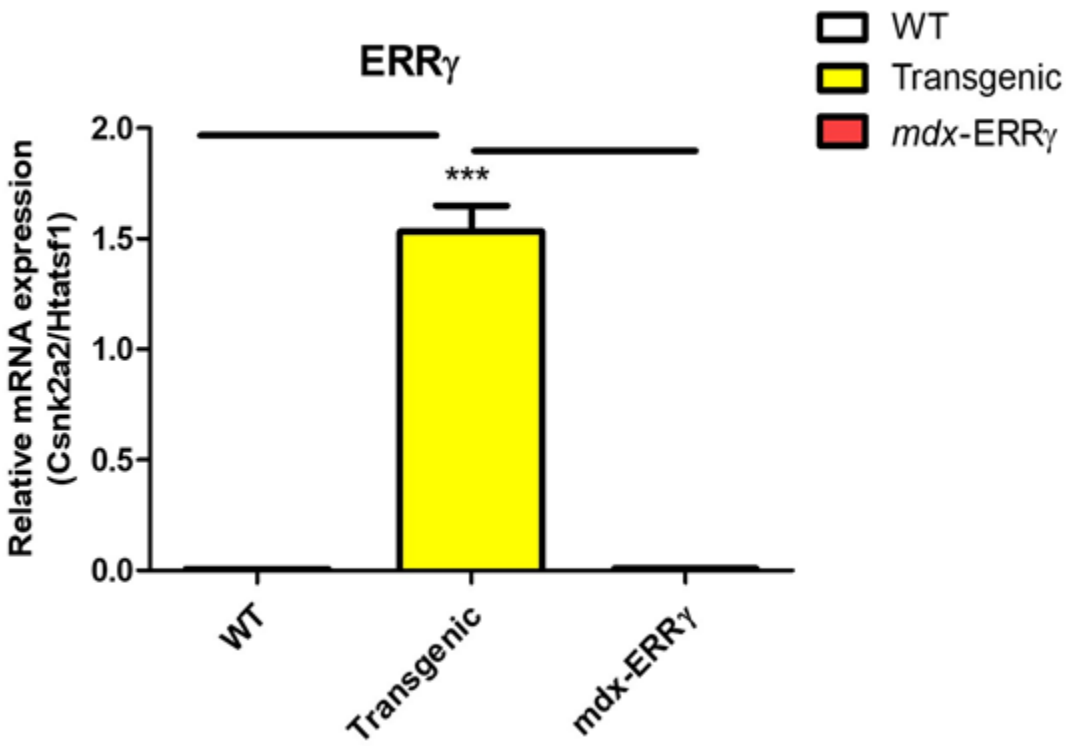

Figure 3.7. Relative mRNA expression of ERRγ in transgenic TA muscles
Expression of mRNA relative transcript of ERRγ in *tibialis anterior* muscles (TA) of the transgenic mice compared to TA muscles from gene transfer experiment and wild type. 170 fold increase in the expression of ERRγ in *mdx*-ERRγ TA muscles (n=5 male *mdx*, One way Anova, p=0.0001).

3.2.6. Impact of ERRγ over-expression on markers of oxidative metabolism:

Succinate dehydrogenase staining (SDH) was performed to assess whether overexpressing ERRγ influenced the oxidative capacity of the myofibres within the TA muscles. We differentiate between oxidative and glycolytic fibres based on the intensity of the SDH stain, those fibres with a strong dark stain were accounted as oxidative fibres and the fibres with weak or faint stain were called

glycolytic fibres. The percentage of oxidative fibres was expressed by the number of oxidative fibres related to the total fibres per muscle. Following ERRγ over-expression, the percentage of oxidative fibres increased in the treated TA muscles compared to those injected with saline only. This shift in oxidative capacity was found in all experimental groups with 100% increase in SDH positive fibres in 6 week-old *mdx* (p=0.0002) and 58% increase in 12 weeks old *mdx* (p=0.001) (figure 3.8 A-B).

In order to assess whether overexpressing ERRγ has an impact on mitochondrial oxidative metabolism and biogenesis, we quantified the expression of a panel of genes related to these processes. However, all genes related to mitochondrial oxidative metabolism, mitochondrial biogenesis and fatty acid oxidation were unaffected between two groups (figure 3.8 C).

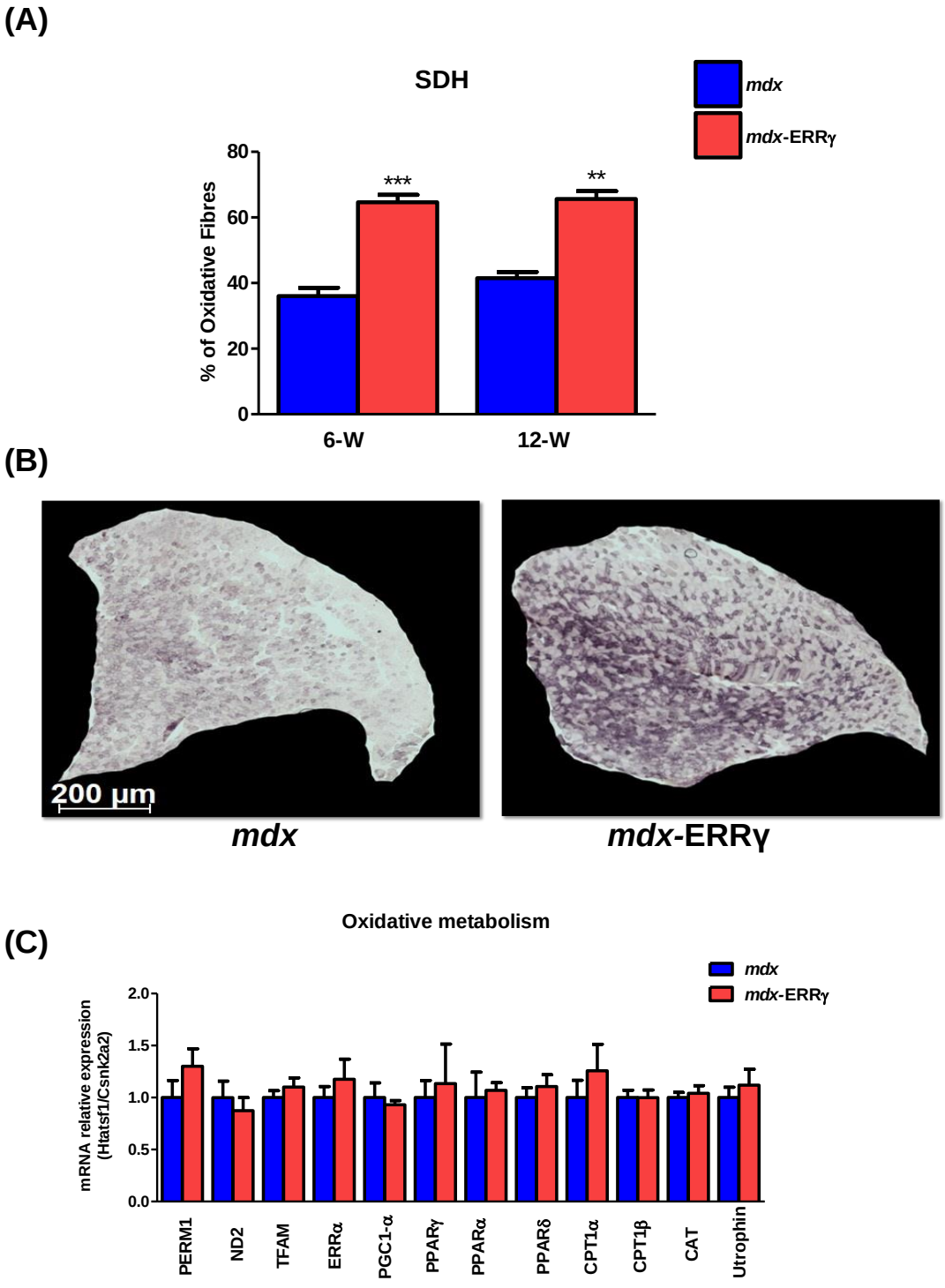

Figure 3.8. Oxidative metabolism of TA muscles and qRT-PCR analysis of genes related to Oxidative metabolism, mitochondrial biogenesis and fatty acid genes into TA muscles following ERRγ expression

A) The relative abundance of oxidative fibres in *mdx* mice treated either at 6 (p=0.002) or 12 weeks (p=0.001) and samples were recovered 4 weeks later, based on quantification of an entire TA section. Data are expressed as a percentage (%) of total fibres, (n=6 per group, male *mdx*). B) Representative images of cross sections of *mdx*

and *mdx*-ERRγ TA muscles stained for SDH activity. Scale bar, 200 μm. C) Relative mRNA expression of genes involved in mitochondrial oxidative metabolism, mitochondrial biogenesis and fatty acid metabolism were unchanged with the over-expression of ERRγ. The level of the test genes were expressed relative to the housekeeping genes; Htatsf1 and Csnk2a2. PERM1 (p=0.08), ND2 (p=0.499), TFAM (p=0.211), ERRα (p=0.455) and PGC-1α (p=0.696), PPARγ (p=0.757), PPARα (p=0.888), PPARδ (p=0.493), CPT1α (p=0.543), CPTβ (p=0.993), CAT (p=0.416) and utrophin (p=0.407), (n=5, paired student's t-test).

3.2.7. Moderate over-expression of ERRγ does not affect fibre typing

Tibialis anterior muscle is a mixture of type IIA, IIB and IIX myofibres. To assess whether ERRγ gene delivery has any impact on the distribution of muscle fibre types, we stained muscle cross sections with antibodies against different MHC isoforms to quantify the relative fibre type content. Based on this approach, ERRγ has no effect on fibre type composition either in *mdx* mice treated at 6 week or at 12 weeks old (figure 3.9).

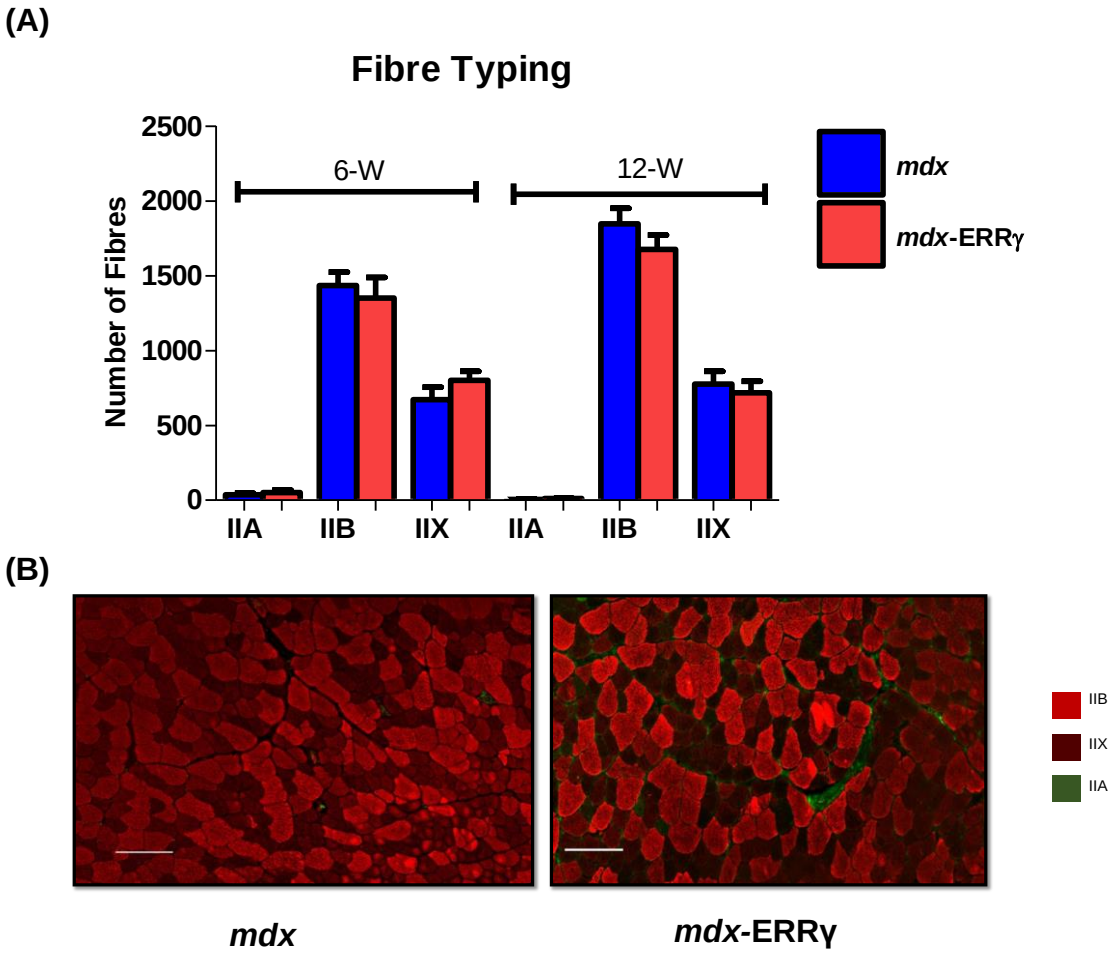

Figure 3.9. Myosin heavy chain analysis in TA muscles following IM of AAV8-ERRγ
A) The relative abundance of different fibre types in TA, based on quantification of an entire TA section. Myosin heavy chain (MHC) analysis in *mdx* and *mdx*-ERRγ shows no difference in the number of fibre types in *mdx* mice treated at 6 weeks IIA (p=0.52), IIB (p=0.25) and IIX (p=0.35) or 12 weeks cohort IIA (p=0.10), IIB (p=0.25) and IIX (p=0.617), (n=6 per group, male *mdx* paired student's t-test). B) Representative images of cross sections show the midportion of *mdx* and *mdx*-ERRγ TA muscles stained with antibodies against MHC isoforms, as indicated. Scale bar, 200 µm.

3.2.8. Moderate over-expression of ERRγ does not affect fibre size

Laminin was used to assess the cross sectional area (CSA) of individual fibres. Individual fibre size was determined in the entire muscle cross section. Although, *mdx* mice have a high distribution of type IIB fibres which exhibit the largest CSA, however, the administration of the AAV8-ERRγ in all experimental groups did not result in any change in fibre size compared to control muscles. Analysis did not show any significant shift in the CSA of the fibres in all groups (figure 3.10).

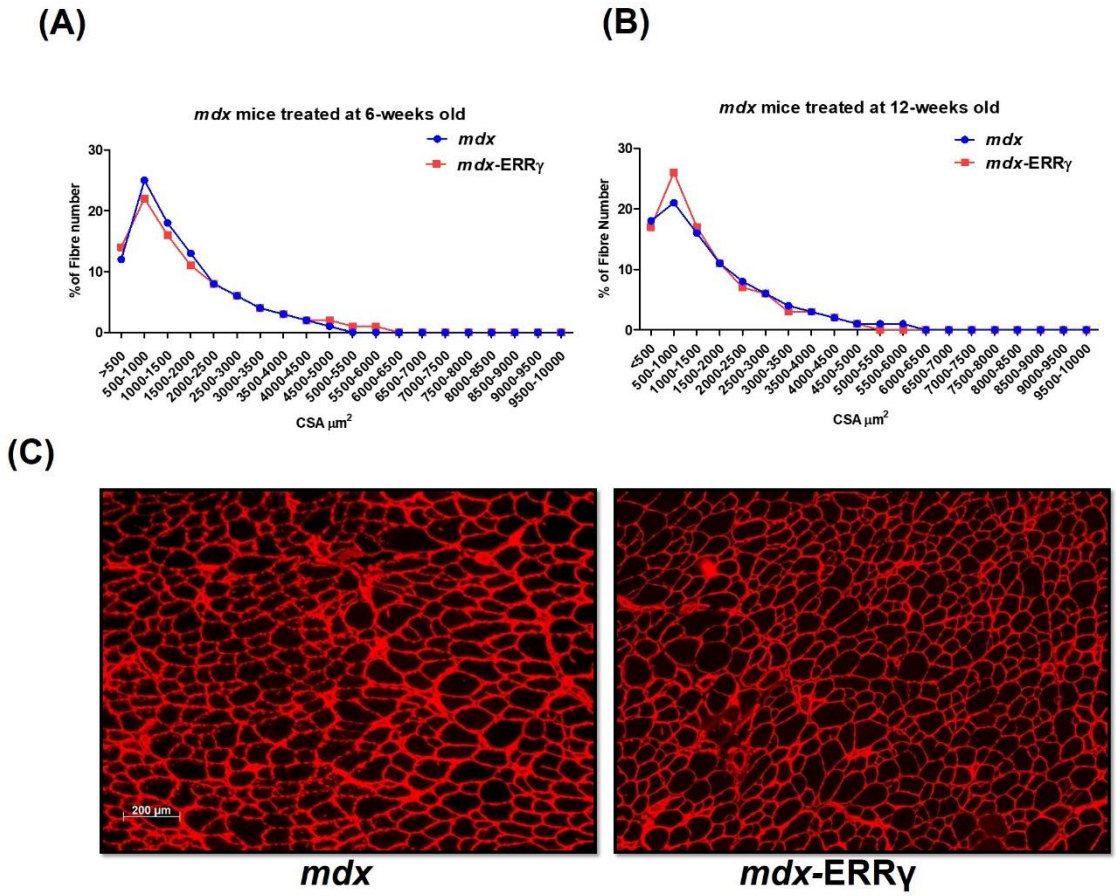

Figure 3.10. Cross sectional area of TA muscles following IM of AAV8-ERRγ
A and B) Distribution of fibre cross-sectional area of *mdx* and *mdx*-ERRγ TA muscles treated at 6 (p=0.323) and 12 weeks of age (p=0.15), respectively with no shift in fibre size, (n=6 per group, male *mdx*, Chi square). C) Representative images of cross sections of *mdx* and *mdx*-ERRγ TA muscles immunostained with anti-laminin antibody. Scale bar, 200 µm.

3.2.9. Effect of ERRγ over-expression on angiogenesis:

The impact of ERRγ over-expression on angiogenesis markers and capillary density was investigated by assessing angiogenic factors and CD31 staining. VEGF-165 isoform is one of the angiogenic factors, increased by 1.6 fold in the *mdx*-ERRγ compared to the control *mdx* (p=0.018). Moreover, CD31 is a vascular endothelial marker was used to assess the capillary number. However, Intramuscular administration of the virus into TA muscles does not increase the capillary number neither in mice treated at 6 nor in 12-week old (figure 3.11).

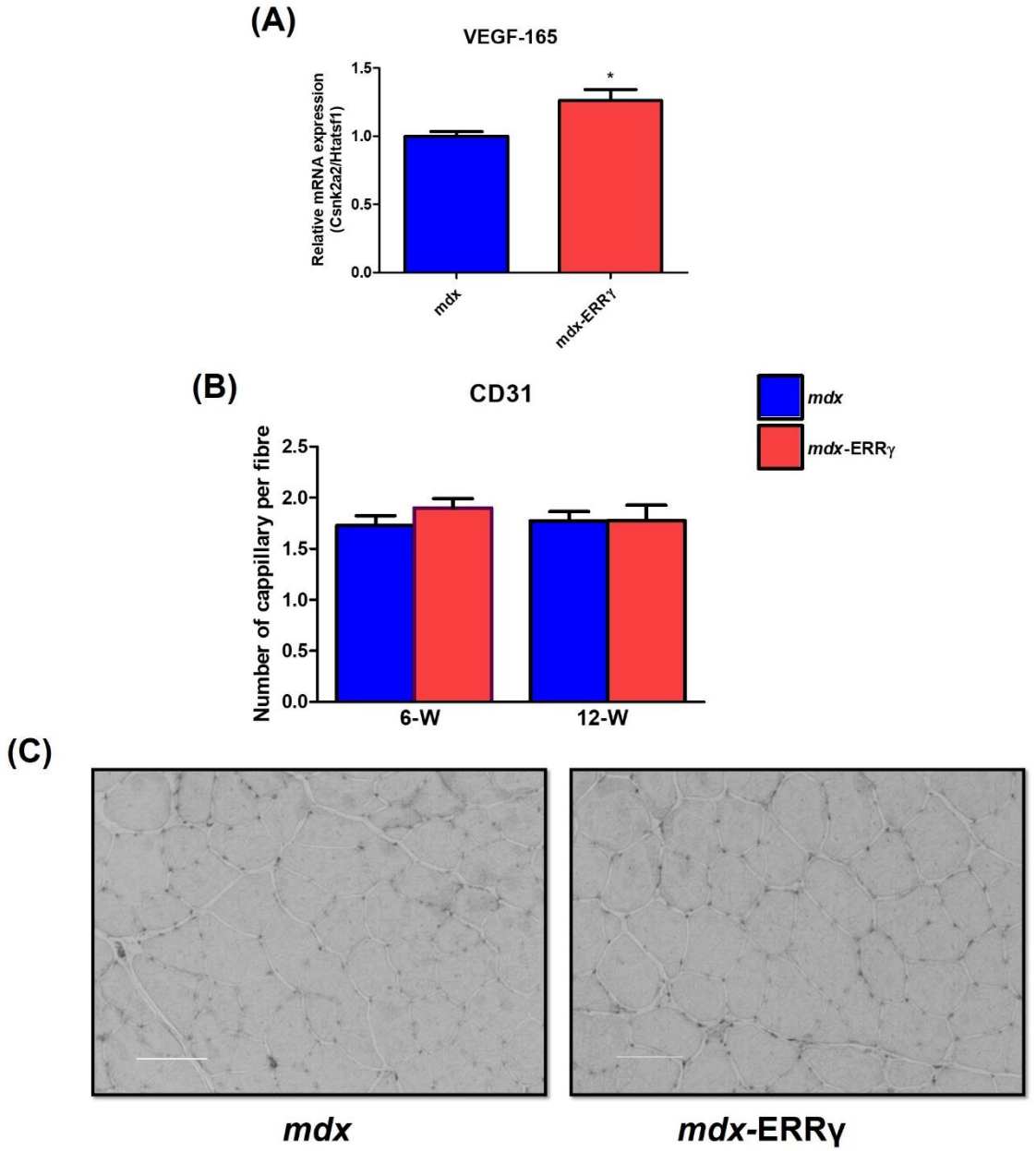

Figure 3.11. Effect of ERRγ over-expression on angiogenesis in TA muscles following IM of AAV8-ERRγ

A) VEGF-165 mRNA levels were determined by qRT-PCR, normalized to Htatsf1 and Csnk2a2. VEGF-165 expression was increased by 1.6 fold compared to untreated muscle, (n=5, male *mdx, p*=0.018, paired student's t-test). B) Capillary density of *mdx* and *mdx*-ERRγ TA muscles, quantified by CD31-stained muscles, using ImageJ software shows no increase in the number of capillary number per fibre either in *mdx* mice treated at 6 weeks (*p*=0.233) or 12-weeks of age (*p*=0.983), (n=6 per group, male *mdx*, paired student's t-test). C) Representative images of cross section of *mdx* and *mdx*-ERRγ TA muscles stained with anti-CD31 antibody. Scale bar, 100 μm.

3.2.10. Haematoxylin and Eosin analysis:

The percentage of centrally nucleated fibres was calculated using ImageJ software. It was found that administration of AAV8-ERRγ in the treated muscle was able to decrease the level of central nucleation from 81% to 73% in the mice treated at 6-weeks of age (p=0.006). However, there was no reduction in the number of central nuclei in the 12-week cohort as shown in (figure 3.12).

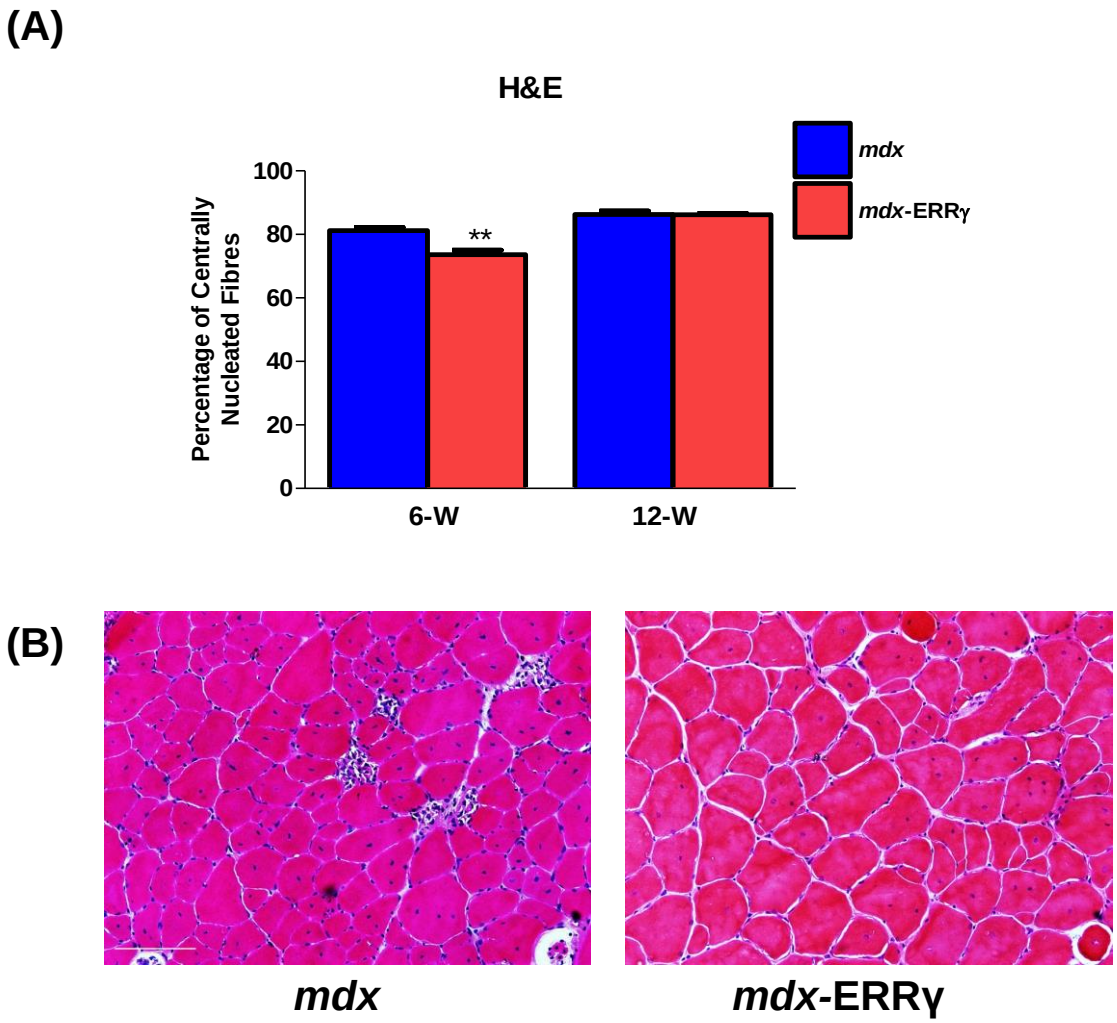

Figure 3.12. H&E stain of centrally nucleated fibres in TA muscles following IM of AAV8-ERRγ

A) Percentage of centrally nucleated fibres in *mdx* and *mdx*-ERRγ TA muscles of *mdx* mice treated at 6 or 12 weeks of age shows 10% decrease in centrally nucleated fibres in 6 week old *mdx*-ERRγ compared to *mdx* (p=0.006) but no change in the 12 weeks old

mice cohort (p=0.935), (n=6 per group, paired student's t-test). B) Representative images of cross sections of *mdx* and *mdx*-ERRγ TA muscles stained with H&E. Scale bar, 50 μm.

3.2.11. Embryonic myosin analysis (MYH-3):

Myofibre regeneration was assessed by assessing expression of embryonic myosin heavy chain (MYH-3) within the muscles (Haslett et al., 2002). MYH-3 is expressed mainly during the embryonic stage of skeletal muscle development and is re-expressed during muscle regeneration. However, over-expression of ERRγ resulted in 2% significant reduction in the percentage of regenerating fibres in 6 week old cohort (p=0.001) but was not significant in 12 week old cohort (p=0.092) (figure 3.13).

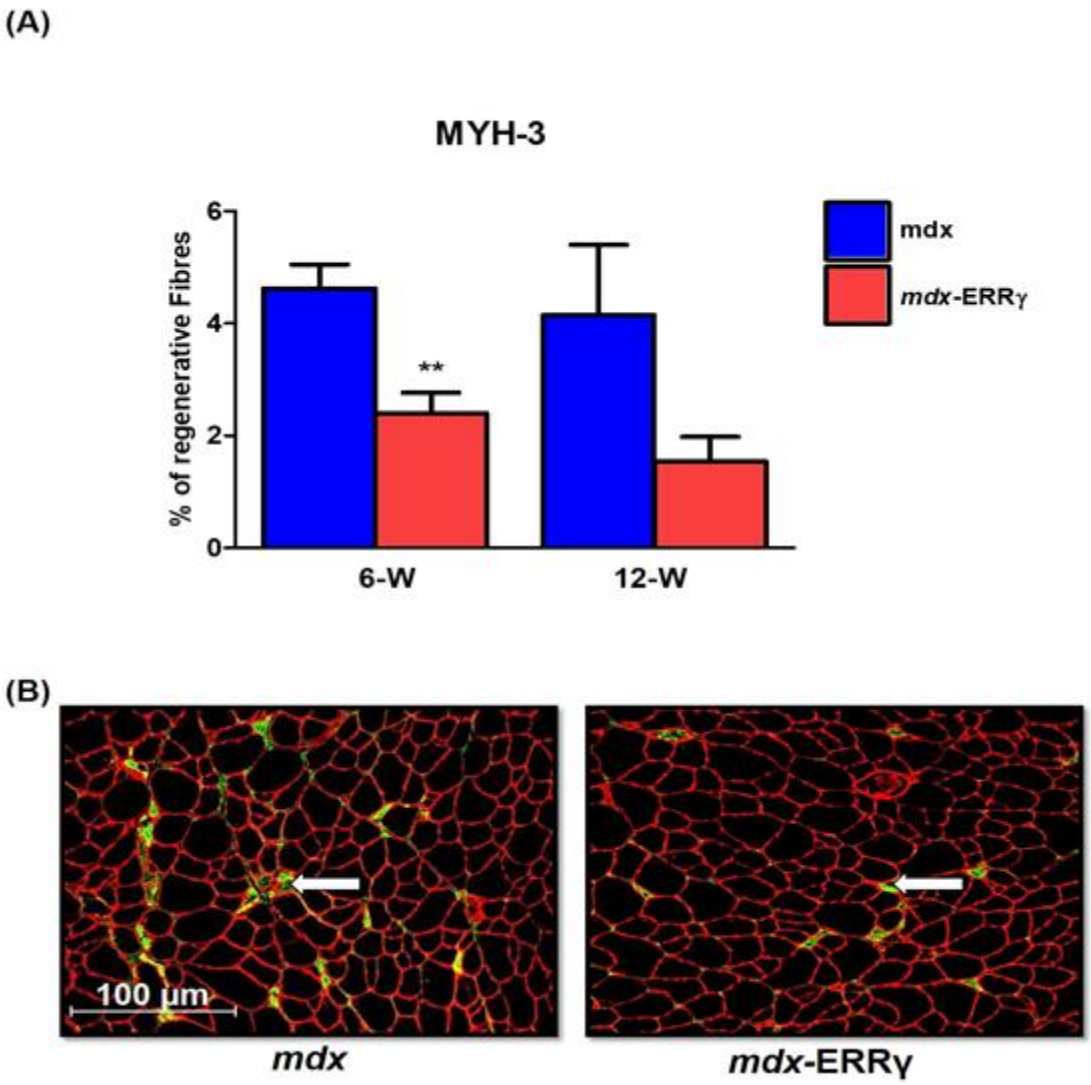

Figure 3.13. Embryonic myosin heavy chain (MYH-3) analysis in TA muscles following IM of AAV8-ERRγ

A) Percentage of positive fibres expressing MYH-3 in the entire TA from *mdx* and *mdx*-ERRγ shows significant reduction in the MYH-3 positive fibres in TA of *mdx*-ERRγ from the group treated at 6 weeks old compared to *mdx* (p=0.001) but not in 12 weeks cohort (p=0.092), (n=6 per group, paired student's t-test). B) Representative images of cross section of *mdx* and *mdx*-ERRγ TA muscles immunostained with anti-MYH-3 antibody. Scale bar, 100 µm.

3.2.12. Moderate over-expression of ERRγ is not sufficient to reduce necrotic muscle fibres

Muscle fibre necrosis was assessed by scoring for IgG positive fibres to assess the sarcolemma integrity. However, the percentage of necrotic fibres was not different between *mdx* and *mdx*-ERRγ neither in 6 weeks nor in 12-weeks cohorts (figure 3.14).

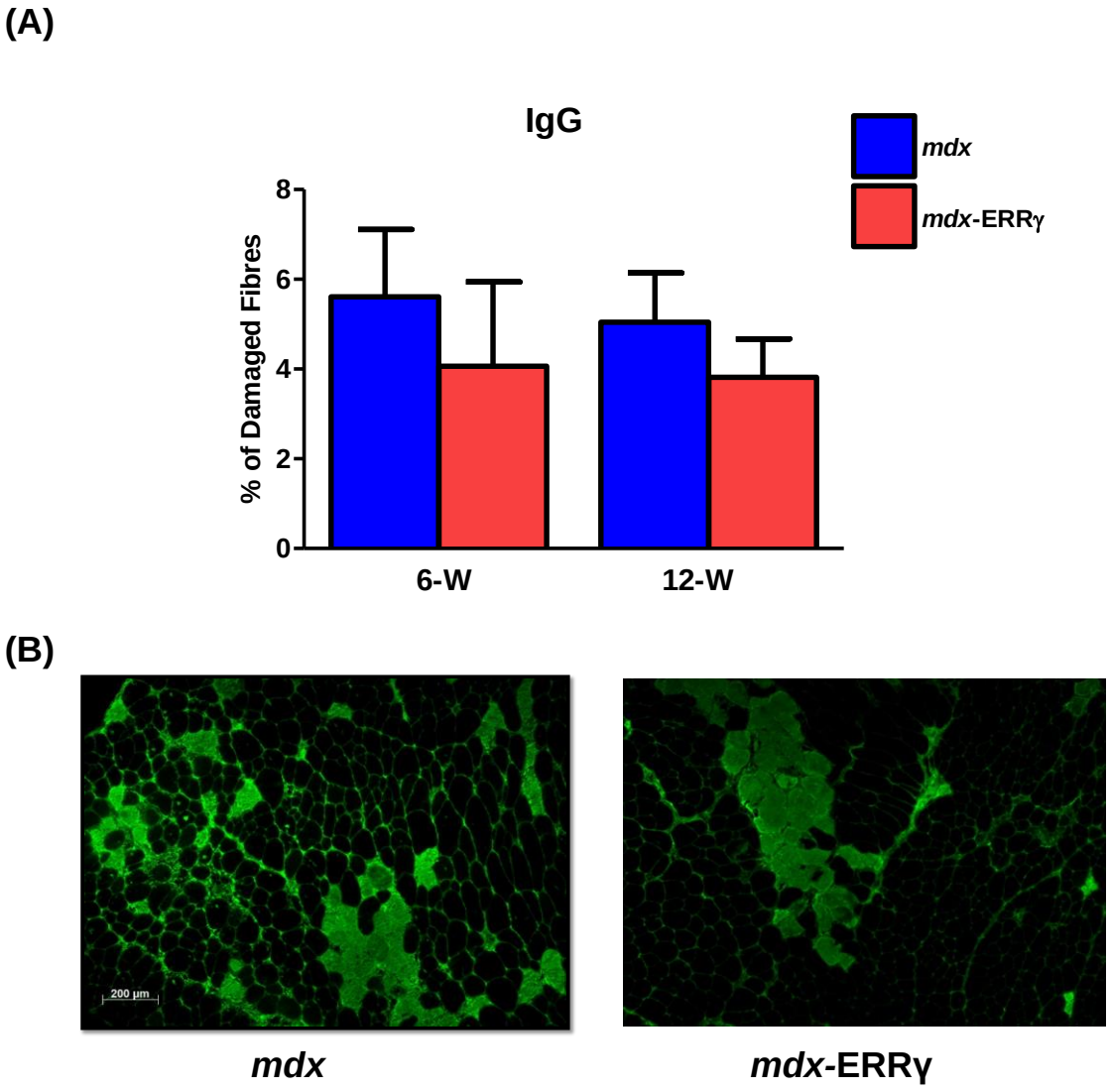

Figure 3.14. IgG staining of damaged fibres in TA muscles following IM of AAV8-ERRγ

A) The percentage of IgG positive fibres in the entire TA from *mdx* and *mdx*-ERRγ shows no reduction in the percentage of damaged fibres in the *mdx* mice treated at 6 (p=0.529)

or 12-weeks old (p=0.401), (n=6 per group, male *mdx* paired student's t-test). B) Representative images of cross section of *mdx* and *mdx*-ERRγ TA muscles immunostained with anti-IgG antibody. Scale bar, 200 µm.

3.2.13. The impact of AAV8-ERRγ gene transfer in 6 weeks old *mdx* on oxidative capacity, angiogenesis and inflammation in the second study:

From the histological observations, intramuscular administration at 6 weeks of age showed reduced pathology associated with an increase in the percentage of oxidative capacity by SDH staining, reduced central nucleated fibres and the level of regeneration by embryonic myosin MYH-3. Therefore, we carried out similar experiment at 6 week-old male *mdx* in order to analyse genes at molecular level in a larger number of samples because the previous data of qRT-PCR were based on pooled samples of 6 and 12 weeks. SDH staining activity showed a significant increase in the TA muscles treated with AAV8-ERRγ as shown previously (figure 3.15).

However, microarray data showed less than 2 fold difference in some genes of interest, the only gene that showed significant difference was IL-6 (inflammatory cytokine). Therefore, we analysed the key genes of interest related to oxidative angiogenesis and inflammation markers using qRT-PCR. Analysis was performed on TA muscle obtained from *mdx* mice treated at 6 weeks of age, (n=6) and run to assess the effect of ERRγ over-expression on genes related to oxidative metabolism, angiogenesis and inflammation. Relative transcript mRNA level of ERRγ showed significant increase following intramuscular administration of AAV8-ERRγ by 5 fold (figure 3.16 A; p=0.01). However, genes related to oxidative metabolism or angiogenesis showed no difference between the treated

and the contralateral TAs as observed previously. Pro-inflammatory markers; IL-1β and TNF-α were significantly reduced in the treated TAs (p=0.039), (p=0.046) respectively, but not with IL-6 (figure 3.16 D).

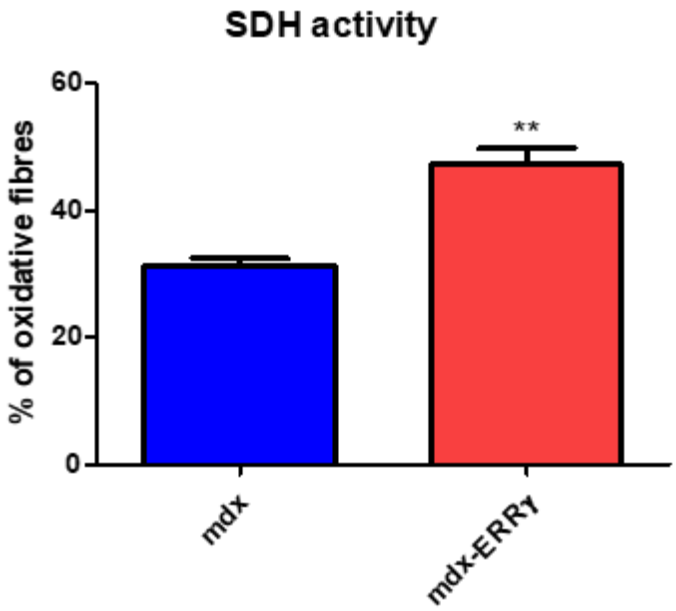

Figure 3.15. SDH staining activity of TA muscles following over-expression of ERRγ at *mdx* mice treated at 6 weeks-old

The relative abundance of oxidative fibres in *mdx* and *mdx*-ERRγ in *mdx* mice treated at 6 weeks old, based on quantification of an entire TA section. Data are expressed as a percentage (%) of total fibres, (n=6, male *mdx*, paired student's t-test, p=0.003).

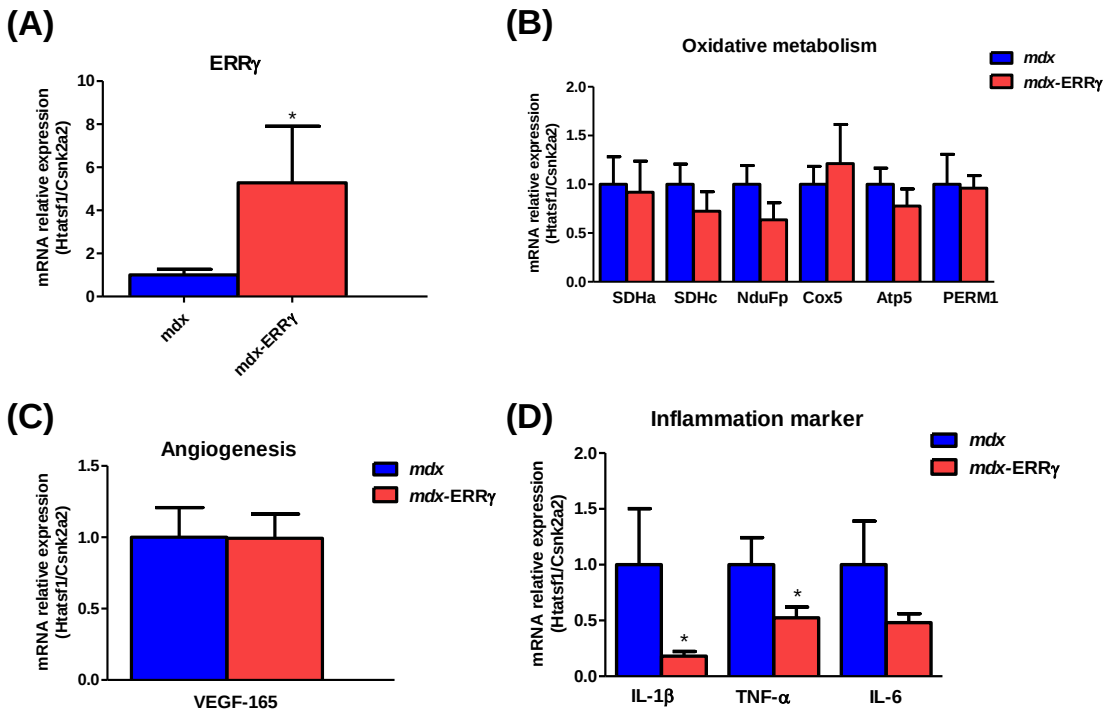

Figure 3.16. Real time PCR analysis of genes involved in oxidative metabolism, angiogenesis and inflammation

RNA levels for the indicated genes were determined by qRT-PCR, normalized to housekeeping genes; Htatasf1 and Csnk2a2 levels *mdx*, (n=6, male *mdx*, paired student's t-test). A) 5 fold increase in the expression of ERRγ (p=0.01). B) Relative expression of oxidative metabolism markers revealed no significant difference to control; Sdha (p=0.671), Sdhc (p=0.417), NduFp (p=0.288), Cox5 (p=0.711), Atp5 (p=0.214) and PERM1 (p=0.915). C) Expression of VEGF-165 angiogenesis marker was unaffected following ERRγ over-expression (p=0.892). D) Inflammatory markers; IL-1β and TNF-α were significantly decreased by 5.5 fold (p=0.039) and 1.9 fold (p=0.046) respectively, IL-6 was unaffected (p=0.468)

3.2.14. Connectivity map (cMap):

The gene expression core signature was uploaded to cMap in order to identify substances that cause either similar or opposite effects on the expression of the core signature genes. In other words, we screened for compounds that result in a similar (agonistic) or dissimilar (antagonistic) expression profile. The resulting compounds were ranked based on their enrichment score. This value is a

measure for the strength of the correlation of the gene expression profile provided and the profile of the substances deposited in the database. This resulted in 94 drugs with a highly positively correlated and 35 substances with a highly negatively correlated gene expression profile (Appendix). The list showed drugs with anti-inflammatory, anti-apoptotic properties that positively correlated the genomic profiles of ERRγ over-expression. However, the screening approach successfully identified substances that 1) have already been shown to be useful in human diseases; diflorason and pancuronium bromide 2) under current investigation; benfotiamin and ebselen and 3) are so far unknown but promising candidates; eucatropine.

3.3. Discussion:

The data has shown here represent the first evidence of the effect of post-natal over-expression of ERRγ in *mdx* mice. Data has shown an increase in SDH activity, a decrease in centrally nucleated fibres and a reduction in the inflammation markers in the 6 week-old *mdx*.

Initially, C_2C_{12} myoblast cells were transfected with murine p-AAV8-ERRγ plasmid and C_2C_{12} myotubes cells were transduced with AAV8-ERRγ virus. The MTS assay results suggested a role of ERRγ in increasing the metabolic activity of the cells and is further confirmed by cell counts, where no change in the number of cells was observed. Rangwala et al., showed upregulation of mitochondrial function in response to over-expression of ERRγ in primary mouse myotubes represented by induced expression of fatty acid metabolism genes (Cpt1b and fabp3) and citrate synthase activity. Moreover, genes of mitochondrial ETC, fatty acid oxidation and TAC were increased (Rangwala et al., 2010).

Therefore, since number of the cells unchanged and MTS assay increased in myoblast and myotubes, therefore MTS assay has to be due to increased activity per cell not more cells.

Scatter plots of the transcriptomic data demonstrates that *mdx* TA muscle overexpressing ERRγ has different distribution of genes expression compared to the *mdx*-control. Following over-expression of ERRγ, 1429 transcripts significantly changed their expression greater than 2-fold between *mdx* and *mdx*-ERRγ. Based on global gene expression, the range of spread following ERRγ over-expression has been narrowed down by 1% compared to the *mdx*. Principal component analysis (PCA) was run to study the relationship within and between biological replicates and to study the overall distribution of gene expression. PCA has demonstrated a clear difference between the wild type and *mdx* as expected. More importantly, treated TA muscles are distinct from *mdx*, such that these muscles are moved away from diseased phenotype. This shift means that treated muscles do not exhibit the same gene expression pattern as *mdx* and therefore over-expression of ERRγ may play a role in rescuing the disease pathology. PCA analysis provides further support that over-expression of ERRγ at 6 weeks of age may improve the pathology associated with the disease. The distinct difference between the expression patterns of *mdx* and *mdx*-ERRγ does not imply the differences are positive per se, however other data, disclosed herein, and the gene ontology data give confirmatory evidence that this shift is positive.

As mentioned earlier, the loss of dystrophin in both *mdx* and DMD, ultimately results in impaired oxidative phosphorylation and reduced expression of mitochondrial genes, leading to defects in ATP production, which is hypothetically

involved in disease pathogenicity (Kuznetsov et al., 1998, Even et al., 1994, Timpani et al., 2015). Previously, it has been shown that a selective over-expression of ERRγ in transgenic *mdx* mouse muscle, reprogram defects in *mdx* mice by restoring the metabolic and angiogenic program through upregulation of mitochondrial oxidative capacity (SDH activity) angiogenesis factors (VEGF-165 and VEGF-189) as they are downregulated compared to wild type (Matsakas et al., 2013). Further, ERRγ induced a shift towards slow-oxidative fibres, improved vasculature and blood flow which ameliorated muscle damage in *mdx*. A limitation to that work, however, is that the beneficial effects of ERRγ were demonstrated in transgenic animals and perform at supraphysiological levels and in the context of disease prevention rather than treatment. Although using genetically modified mouse model is a powerful tool in understanding the molecular mechanism underlying specific gene, however, there are significant limitations of genetically modified mouse. The presence of a phenotypic outcome does not always reflect the function of the modified genes and can be influence by other environmental and genetic factors for example; the potential functional alteration of neighbouring genes and therefore the interpretation of the findings is not always straightforward. In addition, the transgenic mice allow stable expression of the transgene from the embryonic life (Lin, 2008, Babinet, 2000). In this chapter, we assessed the short term effect of postnatal over-expression of ERRγ on two ages of *mdx* mice; active degeneration/regeneration period at 6 weeks and the period after crisis at 12 weeks of age.

Subsequent to the *in vitro* analysis, we assessed the impact of over expression of ERRγ on mitochondrial function and angiogenesis in *mdx* mice. Mice treated with AAV8-ERRγ via intramuscular administration route lead to a 3 fold increase

in the transcript level of ERRγ and increased muscle oxidative capacity as showed by SDH staining in all treated groups either at 6 or 12 weeks of age. Despite the increase in the oxidative capacity of the fibres which is represented by SDH staining, none of the genes related to oxidative metabolism and mitochondrial biogenesis (PERM1, ND2, TFAM1, ERRα, PGC-1α, utrophin) or fatty acid oxidation (PPARα, PPARγ, PPARδ, CTP1α, CTP1β, CAT) were affected at the transcript level. Similarly, in the second study on 6-week old *mdx*, SDH activity was increased. Further, expression of ETC genes (Sdha, Sdhb, NduFp, Cox5, Atp5) and down stream target of ERRγ (PERM1) were not affected with the 5 fold over-expression of ERRγ. Compared to our results, transgenic mice which specifically overexpress ERRγ in *mdx* mice, resulted in remodelling the oxidative capacity of the fibres as shown by increasing the number of oxidative fibres represented by SDH staining. Moreover, transgenic over-expression of ERRγ in wild type mice showed an increase in PPARα and δ, the latter is a metabolic regulator known to involve in a shift towards slow-oxidative fibres and is downregulated in *mdx* mice. Further, the genome wide expression showed upregulation in the genes of fatty acid metabolism (CTP1α, CTP1β, CAT) and ETC (Sdha, Sdhb, NduFp, Cox5, Atp5) (Narkar et al., 2011), however, sarcolemmal utrophin expression was not different (Matsakas et al., 2013, Rangwala et al., 2010, Narkar et al., 2011). These results suggest the tremendous difference in the supraphysiological over-expression of ERRγ in transgenic mice with 170 fold compared to the modest over-expression we achieved in this study could be one of the factors that result in unchanged level of the expression of the genes examined in our study. Moreover, treatment of mouse myoblasts with GSK4716, an agonist for ERRβ/γ resulted in over-

expression of oxidative metabolism genes; ERR α, β, γ, PGC-1α, β and key genes of mitochondrial pathways; Cpt1b, fatty acid metabolism gene, Atp5b, ETC genes and Idh3, function in Krebs cycle (Rangwala et al., 2010). These results could be time dependent since the effect of agonist in tissue culture was assessed 48 hours following treatment only. It is important to consider that the response may changed following different lengths of treatments. In the same way, effect of adiponectin of fatty acid utilization was shown to be time-dependent as the expression of PPARα target genes; CPT1 and AcO peaked at 3 hours following treatment of adiponectin and then slowly reduced to basal level after 24 hours (Yoon et al., 2006). Therefore, it would be better to investigate the effect at different time points to give better understanding if the response is time dependent. Another comparison to our results is the upregulation of transcriptional coactivator peroxisome proliferator-activated receptor (PPAR)-γ coactivator-1α (PGC-1α) that ameliorated DMD pathology, promoted fast to slow fibre type transition and increased mitochondrial genes using transgenic model (Handschin et al., 2007) and gene transfer approach (Selsby et al., 2012). The results of the previous two studies are different to the outcomes presented in this chapter following over-expression of ERRγ, possibly due to different time of intervention and exposure time as they inject neonatal mice in order to prevent disease, whereas, the injection here take place at 6 weeks as a strategy to protect muscle from further decline. PGC-1α was downregulated in primary mouse myotubes transduced with adenovirus (AD) mediated expression of ERRγ (Rangwala et al., 2010) and was not affected in the *mdx* transgenic muscle of ERRγ (Matsakas et al., 2013), despite being a coactivator of ERRs (Godin et al., 2012), which suggest that ERRγ works independent of PGC-1α. Moreover, in

contrast to our result, induced expression of peroxisome proliferator-activated receptor γ coactivator 1 and estrogen-related receptor induced regulator in muscle-1 (PERM1) via AAV approach in cultured C_2C_{12} myotubes and in C57BL/6J mice regulate mitochondrial biogenesis and oxidative capacity as well as angiogenesis via the transcriptional induction of VEGF (Cho et al., 2016, Cho et al., 2013). These results are different possibly due to the use of wild type mice rather than *mdx*, in which fibrosis may interfere with the virus delivery and hence limit the amount of available tissue to target with gene therapy (Bernasconi et al., 1999), as well as the amount of oxidative and metabolic stress may influence the outcomes. In addition, active cycle of degeneration/regeneration at 6 weeks of age may result in virus cargo loss. Previously, it has been shown that AAV mediated expression of U7 for dystrophin exon skipping were lost from *mdx* mice within 3 weeks after intramuscular injection (Le Hir et al., 2013). It is possible the virus has been lost in this study as another reason of unchanged protein level of ERRγ. Herein, unaffected expression of the previous tested genes in this study may be due to the modest over-expression of ERRγ compared to transgenic muscle or the time of intervention where the active cycle of regeneration and degeneration at 6 weeks of age diminishes the activation of ERRγ pathway due to AAV loss. However, the increase in the SDH activity could be due to the fact that protein level is not a representation of the transcript level. Therefore, it is important to consider that all genes were measured at one time point only, which suggest the need to check other time points in which the genes may showed a difference. In the same pattern, ND2 gene in H2K dystrophic cells showed no effect following 24 hours CBD treatment. However, assessing its expression at different time points (1-24) hours showed a peak of over-expression at 12 hours

and then it returns back to normal (Foster *et al*., personal communication). Therefore, we could speculate that all of these genes were upregulated at some point during (4 weeks) of expressing ERRγ and resulted in adaptive responses in terms of enhancement of SDH activity and then reverse back to their basal level.

In DMD, more oxidative slow skeletal muscle fibres are known to be more resistant to the dystrophic pathology compared with faster, glycolytic fibres (Head et al., 1992). An abundance of recent evidence shows that induction of slow myofibre program, whether via transgenic (Matsakas et al., 2013), pharmacological (Ljubicic et al., 2014), physiological (Ljubicic et al., 2011) or gene therapy (Selsby et al., 2012) methods ameliorates the dystrophic pathology in *mdx* mice possibly due to their capability to generate more ATP as they are rich in mitochondria. Generally, loss of dystrophin leads to progressive increase in oxidative fibre content because of a selective loss of fast fibres; IIB and IIx (Webster et al., 1988, Petrof et al., 1993b). In contrast to the previous works where *mdx* mice specifically transgenically overexpress ERRγ in skeletal muscles (Matsakas et al., 2013, Rangwala et al., 2010), gene delivery of ERRγ into TA muscles does not result in an increase in type IIA and IIX myofibres and no change between the treated and the control in type IIB myofibres within all cohorts. In transgenic mice, the development of the myosin heavy chain isoform takes place during embryogenesis while in this experiment specifically the administration was delivered postnatally. On the other hand, over-expression of PGC-1α using an AAV approach, induced a shift towards slow twitch type I fibres in soleus muscle when PGC-1α was over-expressed prior to the initial onset of myofibre damage when they were injected as neonates (Selsby et al., 2012),

whereas in this work we sought to determine the impact of ERRγ in TA muscles during the early regenerative phase, which follows the first wave of necrosis. This difference could be due to the use of different muscles in which soleus muscle contained predominantly slow twitch (type I) fibres (Gollnick et al., 1974). In contrast, TA muscle is considered glycolytic with type IIB fibres being predominant (Kammoun et al., 2014). In turn, over-expression of ERRγ either at 6 or 12 weeks has no effect on fibre type distribution.

Rangwala et al., showed a decrease in the size of fast twitch muscle parallel to the shift towards slow twitch muscles which have smaller size in transgenic mice specifically overexpressing ERRγ (Rangwala et al., 2010). However, our data demonstrated no difference in the fibre size in all aged animal which is consistent with the MHC data. However, it is important to note that there was no increase in the total number of the fibres in the treated muscles compared to the control, thus confirming that the postnatal shift in the oxidative capacity was due to increase in oxidative potential of the muscles not the number of the fibres.

We then evaluated the potential of vascular differences in *mdx* muscles following the over-expression of ERRγ. Compared to wild type muscle, vascular density has been shown to be reduced in *mdx* mice as a result of reduced availability of NO in the muscle cells due to miss-localization of nNOS and leads to muscle ischemia and impaired blood flow (Loufrani et al., 2004, Messina et al., 2007). Also, satellite cells isolated from *mdx* mice exhibit decreased expression of hypoxia inducible factor 1 α (HIF-1α), VEGF and a decreased ability to induce angiogenesis (Rhoads et al., 2013). Previously, it was shown that adenovirus mediated expression of ERRγ increased the expression of VEGF gene and

induced the secretion of VEGF in C_2C_{12} myotubes. Further, incubating human umbilical vein endothelial cells (HUVECs) with the condition medium from ERRγ-overexpressing C_2C_{12} myotubes, increased proliferation, migration and tube formation of HUVECs (Liang et al., 2013). These results propose that VEGF is a downstream target of ERRγ over-expression and hence, proliferation, migration and tube formation of endothelial cells were mediated by VEGF. Furthermore, transgenic over-expression of ERRγ in *mdx* mice upregulate angiogenic factors; VEGF-165 and VEGF-189 (Matsakas et al., 2013). Our results showed different outcomes on VEGF-165 expression. For example; when muscles from the two groups were combined, the expression of VEGF-165 increased. Thereafter, the moderate upregulation of VEGF-165 was not supported by an increase in the number of capillary per fibre in both groups possibly due to the fact the data of qRT-PCR was generated from pooled samples of two different ages and does not represent the direct effect of overexpressing ERRγ on each cohort, as it mentioned earlier that samples were mounted on the same cork for each group which then require large number of samples to perform proper statistical analysis, therefore pooled samples were used. It is important to consider that single 4 weeks timepoint in this study is possibly not sufficient to detect these changes and adaptive responses may still be ongoing. Nevertheless, assessing over-expression of VEGF-165 on higher number of muscles from 6 weeks old *mdx* demonstrated unchanged expression following 5 fold over-expression of ERRγ. Therefore, over-expression of ERRγ has no effect on the level of angiogenesis when administered at the stage of active cycle of regeneration and degeneration (6 weeks). Previous studies conducted in wild type mice with transgenic over-expression of PGC-1α, PGC-1β or ERRγ (Arany et al., 2008, Chinsomboon et

al., 2009, Narkar et al., 2011) and in *mdx* mice with transgenic over-expression of ERRγ (Matsakas et al., 2013) showed upregulation in the expression level of angiogenic markers in contrast to postnatal over-expression of ERRγ in *mdx*. Possibly, the expression of ERRγ here is much more moderate comparing to transgenic models and the virus only expressed for short length of time, hence is not enough to increase expression of VEGF-165 and capillary number in *mdx* fibres. Furthermore, in comparison to our result, intramuscular administration of AAV mediated expression of VEGF into 4 week old *mdx* mice induced the capillary number per fibre following 3 fold increase in the VEGF protein level (Messina et al., 2007). Since the length of VEGF expression in that study was 4 weeks, similar to the length of expressing ERRγ in our study, the different time of intervention is the main difference between the two studies.

A cumulative index of pathology that measures muscle damage and regeneration over the life of the mouse is reflected in the presence of centrally nucleated fibres (Deasy et al., 2009). Non-centrally nucleated fibres are an indicator of those spared from damage. Between 3-4 weeks of age, *mdx* mice start the first wave of fibre necrosis followed by a regeneration process, featured by a centrally nucleated fibres and results in replacement of a large proportion of the damaged fibres by 5-6 weeks of age (Gillis, 1999). In our study, the reduction in the number of fibres with central nucleation suggest that degeneration/regeneration has been slowed by the over-expression of ERRγ at 6 weeks of age but not at 12 weeks whereby the over-expression has no effect on reducing the centrally nucleated fibres. It has been reported that between 12-24 weeks of age, the cycle of degeneration/regeneration reaches a steady state level (Gillis, 1999). Previous study on treating *mdx* of 12 weeks with GW501516 and AICAR agonists of

PPARγ and AMPK separately or in combination, for 4 weeks, reduced centrally nucleated fibres which is opposite to our result (Jahnke et al., 2012). The difference to our study was possibly due to the level of activation of PPARγ and AMPK, as the GW501516 and AICAR agents were injected more than once per week and as a consequence induced the reduction in central nucleated fibres compared to the modest over-expression of ERRγ with a single injection only. This reduction in centrally nucleated fibres was further supported by the reduction of embryonic myosin heavy chain involved in muscle regeneration.

Expression of MYH-3 is a hallmark of muscle regeneration dystrophy (Haslett et al., 2002) and regeneration was assessed because it is an indicator of damage previously experienced by the muscle. Regenerative fibres were significantly lower in the 6 weeks treated muscles but not in12-week in consistent with central nucleation results. In general, decreased number of embryonic myosin heavy chain positive fibres could be explained as an indicator of decreased capacity for repair or decreased damage (Hollinger and Selsby, 2015). As centrally nucleated fibres were less following ERRγ over-expression in 6 weeks treated mice, MYH-3 data supported the idea that over-expression of ERRγ decreased muscle degeneration. Possibly, the over-expression of ERRγ drive an impact on membrane integrity and hence the reduction in central nucleation and MYH-3 is an indication of less muscle turnover and less damage. Increased expression of PGC-1α in 12 month old *mdx* mice using AAV approach showed functional improvements and an increase of MYH-3 positive fibres with no change in the expression of the genes examined (Hollinger and Selsby, 2015). Therefore, we could argue that reduced level of MYH-3 and a reduction in the percentage of

central nucleation in this study is an example of an initial adaptive response to the AAV8-ERRγ, despite no change was observed in the protein level of ERRγ.

In this study, necrotic muscle fibres were observed in larger groups of fibres in muscle tissue, whereas in the treated mice, the necrotic fibres were observed as scattered small groups or individual fibres within the muscle tissue, however, there was no significant reduction in the IgG uptake by muscle fibres following the over-expression of ERRγ neither in 6 nor in 12 week old treated *mdx*, which is inconsistent with the observed reduction in the central nucleation and MYH-3 positive fibres. We anticipated that a reduction in central nucleation and regenerated fibres as an adaptive response to the presence of the vector before being lost due to active degeneration/regeneration, which cannot be definitive as has not assessed. However, the integrity of the membrane was not maintained due to loss of dystrophin, which highlight the need to recue dystrophin for any gene therapy for DMD (Le Hir et al., 2013). It has been demonstrated that optimal restoration of dystrophin is required to protect against pathology. If not, the loss of the therapeutic gene will, at best, establish transient improvement. Compared to our study, over-expression of PGC-1α at 3 weeks of age reduced the necrotic area in soleus muscle with no difference in the centrally nucleated fibres (Hollinger et al., 2013), possibly because different muscles exhibit different degree of damage and that soleus-oxidative muscle is less prone to damage than TA, glycolytic muscle (Webster et al., 1988, Pedemonte et al., 1999). However, multiple factors are involved in muscle fibre necrosis, where disruption of Ca^{+2} homeostasis activates proteases such as calpain which are involved in protein degradation, including cytoskeletal and membrane proteins that lead to necrosis. Previous studies on treating *mdx* with GW501516 and AICAR agonists of PPARγ

and AMPK separately or in combination reduced levels of central nucleation, the number of regenerated fibres and gene involved in degeneration, *e.g.* miRNA-31. That reduction was combined with decreased expression of FOXO-1, involved in muscle atrophy and IgM uptake by the fibre (Jahnke et al., 2012). Therefore, it is possible that a reduction in regeneration fibres (MYH-3) in this study is due to reduced expression of genes involved in atrophy. However, further investigation on genes related to repair process such as; paired box 7, myocyte enhancer factor 2c and myogenic factor 5 will give better understanding on the role of ERRγ on muscle repair.

It has been reported that levels of TNF-α and IL-1β are upregulated in DMD serum compared to healthy muscles (Kumar and Boriek, 2003, De Paepe and De Bleecker, 2013, Barros Maranhao et al., 2015). Matsakas et al., showed increased expression of pro inflammatory cytokines; TNF-α, IL-1β and IL-6 in the *mdx* muscles compared to C57 wild type muscles (Matsakas et al., 2013). Here we demonstrated that over-expression of ERRγ in TA muscles of *mdx* mice at 6 weeks of age resulted in a reduction in the expression level of pro-inflammatory cytokines; IL-1β and TNF-α. Previously, it has been demonstrated that downregulation of TNF-α and IL-1β pathways improves the dystrophic phenotype in *mdx* mice (Hodgetts et al., 2006). For example; partial blocking of IL-1β in *mdx* mice via Kineret, which is a recombinant IL-1 receptor antagonist approved by the FDA for treating rheumatoid arthritis, has improved forelimb grip strength (Benny Klimek et al., 2016). In contrast to our study, over-expression of PGC-1α in 12 month old mdx mice showed increased expression of IL-1β (Hollinger and Selsby, 2015). On the other hand, TNF-α is known to inhibit contractile function of skeletal muscle, induce muscle wasting and increase production of ROS via

NF-κB signaling pathway, which in turn can influence catabolic processes in dystrophic muscles (Morrison et al., 2000). Further, TNF-α and IL-1β cytokines are required for muscle repair as demonstrated in multiple literatures (Chen et al., 2007). In chronic obstructive pulmonary disease (COPD) which is characterized by muscle wasting, TNF-α mRNA expression is elevated and shown to have a direct negative effect on muscle fibre oxidative phenotype by inducing a shift from type I to type IIB. In addition, mitochondrial biogenesis markers such as TFAM and NRF-1 were down regulated in response to elevated level of TNF-α (Remels et al., 2010). These detrimental effects of increasing expression of TNF-α on mitochondrial respiration suggest a link between a reduction in the inflammation marker observed following over-expression of ERRγ and the increase in the percentage of oxidative fibres. Speculatively, decreased expression of pro-inflammatory cytokines in this study is possibly linked to increased SDH activity of the fibres.

Reduced expression of these cytokines may suggest that muscles under less stress that means less infiltration of inflammatory cytokines. This point could support, in part, the unchanged expression of IL-6, which is known to involve in muscle repair (Pedersen, 2007, Fujimori et al., 2002, Serrano et al., 2008, Scheller et al., 2011). Interestingly, IL-6 was shown to induce expression of VEGF (Cohen et al., 1996). Our results supported this interaction as there is no difference on VEGF expression. Further, we could suggest that over-expression of ERRγ improves the inflamed environment by decreasing the pro-inflammatory cytokines. Therefore, decreased expression of pro-inflammatory cytokines in this study highlights again the importance of the time of intervention and how that may change the experimental outcomes. In DMD, muscles have a complex

immune environment, where the muscles are under constant damage and that eventually prevent the transition from M1 to M2 macrophage phenotype. Therefore, despite the reduction in pro-inflammatory cytokines, the transition from M1 to M2 will never happen as the muscle will start overexpressing pro-inflammatory cytokines when the second cycle of degeneration is initiated. However, the drawback of the second experiment, when we assessed the effect of overexpressing ERRγ in 6 week-old *mdx* in large number of samples, is that we do not have a conclusion on the level of ERRγ protein as the samples have been lost.

Based on the global gene expression and scatter blot generated from microarray in this study, over-expression of ERRγ shows alterations in the gene ontogeny profiles. Analysis of the cMap data shows that many of the drugs that gives the greatest correlation with ERRγ over-expression are steroid based, which is known to have anti-inflammation properties. Noteworthy, an increase in oxidative stress drives inflammation response, whereas a reduction in oxidative stress drives anti-inflammation properties, therefore, drugs that are naturally anti-inflammatory fully expect to be in the top of the list. This finding highlight the pro-oxidative and anti-inflammatory properties of ERRγ upregulation. In the cMap list, diflorason and pancuronium bromide, which has been used for neuromuscular diseases (Giostra et al., 1994) and epitiostanol that has been used for breast cancer (Dembitsky et al., 2017) are examples of steroid-based drugs. However, we would not prioritize them due to side effects of steroid. Numerous clinical trials have recognized both the effect of steroids in DMD and the recognized risk of side effects associated with their daily use, such as weight gain and decreased bone mineral density (Angelini and Peterle, 2012). We highlighted some of the compounds with non-

steroid, anti-inflammatory application to emphasize the presence of other drugs with clinical applications that possibly mimics ERRγ over-expression. For example; benfotiamin, is one of the most effective treatment for preventing diabetes. It is known as a chemical derivative of thiamine nutrient (vitamin B1), which is known to regulate level of glucose metabolism (Arora et al., 2006). Type 2 diabetic (T2D) patients are characterized by oxidative stress, an impaired glucose tolerance, a reduced skeletal muscle oxidative capacity and mitochondrial dysfunction (Phielix and Mensink, 2008). Emerging evidence suggested that boosting oxidative capacity through improving mitochondrial function might be beneficial to patients. A study on patients of type II diabetic showed that two weeks treatment with benfotiamine has an ability to reduce heart failure, decreased oxidative stress and restore heart cell function (Ceylan-Isik et al., 2006). Moreover, we identified compounds with high scores as Heat shock protein 90 (Hsp90) inhibitor, for example; tanespimycin, monorden, geldanamycin and alvespimycin. Therapeutic Hsp90 inhibitors have been developed as anti-inflammatory therapy. In cancer, for example; Hsp90 is a molecular chaperon responsible for folding many proteins directly involved in progression of cancer and therefore, inhibition of Hsp90 protein folding mechanism leads to attack numerous oncogenic pathway (Liu et al., 2018). Binding of these compounds to Hsp90, leads to degradation and reduction of the target proteins. Specifically, alvespimycin is an analogue to geldanamycin and tanespimycin, with high affinity to Hsp90 and Phase I clinical trial using alvespimycin in acute myeloid leukemia (AML) showed that alvespimycin is well tolerated and showed signs of clinical activity (Lancet et al., 2010). In parallel, Hsp proteins are also important factors in skeletal muscle physiology and

adaption to stress and exercise. They involve in maturation and activation of inflammatory cells and regulate expression of pro-inflammatory factors (Paepe et al., 2012). For example; overexpression of Hsp72 in dystrophic muscles, through administration of a pharmacological inducer (BGP-15), preserve muscle strength and ameliorates the dystrophic pathology (Gehrig et al., 2012).

In addition, compounds with antioxidant and anti-inflammatory properties were identified from the cMap, such as ebselen, known to mimic glutathione peroxidase (GPx1). Ebselen has anti-inflammatory and antioxidant properties (Muller et al., 1984). Historically, it has been evaluated pre-clinically for diabetes, ischemic stroke and hearing loss. It is well characterized to reduce oxidative stress in noise-related hearing loss. In preclinical study of the hearing loss, treatment with ebselen has been shown to stimulate protein expression of GPx1 and the phase I clinical trial approved safety for the prevention of noise-induced hearing loss (Kil et al., 2007). Based on this outcomes, Ebselen could be used in the prevention and management of oxidative stress-linked to DMD and importantly, it highlight the beneficial effect of ERRγ over-expression in regulating oxidative stress associated with DMD. Among the list, GW8510 is another compound that has highly significant correlation with gene expression profile. GW8510 is a 3′-substituted indolone and is known to inhibit cyclin-dependent kinases 2 and 5 (CKD2 and 5), which regulate the cell cycle (Johnson et al., 2005). GW8510 has been shown as a neuroprotective agent for Parkinson disease. The neuroprotective properties has been evaluated in human neuronal cells treated with neurotoxin (MPP), in the presence of different concentration of GW8510. The results showed protection against cell death and the exact mechanism remains to be elucidated (Wimalasena et al., 2016). MPP is known

to target mitochondrial function and to induce endoplasmic reticulum stress response in neurons (Kim-Han et al., 2011). These effects are parallel to the effects induced by transgenic over-expression of ERRγ, where it showed remodeling of oxidative metabolism in *mdx* mice to the normal level (Matsakas et al., 2013).

Based on these data, we should take into account that overexpression of ERRγ by AAV gene transfer is a valid approach, but conscious that it is not the only approach; cross correlation of pharamaceuticals can lead to the identification and repurposing of approved drugs, with a faster timeline to clinic.

In conclusion, this first study has provided histological analysis of TA muscles 4 weeks post administration of AAV8-ERRγ into 6 and 12 week old *mdx* mice. We have shown improvement in the SDH activity of the muscle fibres in both groups. The increase in the SDH activity of the muscles treated at 6 weeks of age was supported by a reduction in the centrally nucleated fibres and regenerative fibres. Despite these changes, none of the genes related to oxidative metabolism, mitochondrial biogenesis were affected when the samples of both groups were analyzed together. The second study was run to check the expression of genes on larger number of samples and hence we demonstrated no effect of ERRγ over-expression on the tested genes. Although, the data from qRT-PCR does not showed any difference between the treated and control TA muscles. The data from histology analysis, GO and PCA analysis give an arguments for exploring the effect of ERRγ over-expression in different ages of *mdx* mice and at different doses.

4.Chapter Four

Systemic administration of AAV8-ERRγ into 3 and 6 week-old *mdx*

4.1. Introduction:

In the previous chapter, we showed an intramuscular administration of AAV8-ERRγ in 6 week-old *mdx* led to an improvement in the succinate dehydrogenase activity (SDH) and a reduction in the centrally nucleated fibres. In addition, PCA analysis showed a distinct profile expression of treated samples from the control. CMap was further support that overexpression of ERRγ in 6-week old mdx is an encouraging strategy in dystrophic tissues. Here, to assess the potential for achieving systemic transduction of skeletal muscle with AAV8-ERRγ, we studied the short-term effect of systemic administration of AAV8-ERRγ into 6 weeks old *mdx* male mice.

It has been suggested that *mdx* gender influenced physiological and pathological outcomes. Assessing histopathology demonstrated male to be severely more affected than female at 6 weeks of age by quantifying damaged fibres using Evans blue dye (EBD). At 24 weeks of age, females tended to have more damaged fibres (Salimena et al., 2004). Two studies have suggested that skeletal muscles of male *mdx* are more severely affected at younger age (4-12 weeks of age), where they showed more inflammation, increased sarcolemmal permeability and higher deposition of extracellular matrix, whereas age matched females showed more regenerating fibres. These differences are possibly due to the accepted fact that both innate and adaptive immune responses of females are more robust than in males (Verthelyi, 2006) and also attributed to female estrogen level and the regulation of nitric oxide by estrogen (Verthelyi, 2006). Later, at 6 months of age, female *mdx* showed greater specific force compared to aged match male. After 6 months, female become more affected and at 20 months, they showed lower tetanic force (Salimena et al., 2004, Yoshida et al.,

2006). Evidence of different innate and adaptive immune responses in post-pubertal male and female mice influence these striking difference in dystropathology between male and female (Yoshida et al., 2006). Further, later in adult life, hormonal changes during the estrus cycle affect stress, motor activity and immune status (Hakim and Duan, 2012). Therefore, female hormones play a role in the pattern of myogenesis and repair since adult female *mdx* performed better than males, but aged females performed worse than males. While such gender issues appear to be important in the *mdx* mouse and since DMD affect boys, it might be more appropriate to use male mice for DMD research. All experiments in this study were performed on young male *mdx* mice at a range of ages to assess the effect of systemically overexpressing ERRγ on active pathology of *mdx*.

In DMD, gene based therapy was developed as an efficient, safe systemic approach to deliver dystrophin to the muscle fibres with a viral vector. Systemic administration of viral vector mediated expression of a gene of interest should achieve efficient and widespread expression of the transgene in vast majority of skeletal muscles, where they represent around 40% of body weight. Adeno associated viruses (AAV) represent one of the viral vectors with attractive advantages, for example; no known pathogenicity, ability to transduce a wide variety of tissues including dividing and non-dividing cells, presence of serotypes that exhibit tropism for striated muscles, such as 1, 2, 8 and 9 and a lower ability to elicit immune response than adenoviral vectors (Hareendran et al., 2013). The main challenge in gene therapy is the selection of an appropriate serotype, which require knowledge of performance in the target species of interest and cells type. Although, small number of serotypes have been evaluated in small and large

animals, the knowledge of tissue and target cell tropism is limited (Lisowski et al., 2015). To date, there are 12 different serotypes (1-12), with more than 100 AAV variants have been described in the literature, although most gene transfer experiments are performed with AAV1-9 (Hareendran et al., 2013). In skeletal muscle and liver, AAV2 showed therapeutic efficacy, but other comparative studies using AAV1 and AAV8 support improved gene delivery to skeletal muscle and liver, respectively (Lisowski et al., 2015). Also, AAV2, AAV4, AAV9 and AAVrh10 have been delivered to target eye (Boye et al., 2013) and AAV1, 6, 8 and 9 show strong cardiac transduction, with AAV9 to be the most cardiotropic in rodents (Tilemann et al., 2012).

Currently, rAAV capsid serotype selection for a specific clinical trial is based on effectiveness in animal models. However, there are still significant concerns of the translatability to humans because pre-clinical results have been proved to be poorly predictive in humans (Manno et al., 2006, Nietupski et al., 2011, Naso et al., 2017). AAV8 which transduce many animal models very effectively, showed low transduction efficiency in human (Jiang et al., 2006). For example; using AAV8 targeting IX deficiency in mice achieved about 100% transduction in liver (Nakai et al., 2005), but clinical trial in human using the same vector showed low level of transduction efficiency (Nathwani et al., 2014). To date, there are more than 70 approved clinical trials, for example; AAV8 has been shown to transduce liver of rodents and non-human primates and is now being explored in clinical trials to deliver genes for hemoglobinopathies and other disease (Kattenhorn et al., 2016). Engineered AAV1 is now being explored in clinical trails for heart failure (Naso et al., 2017).

Skeletal muscle exhibits several advantages, such as, stability and susceptibility to transfection, which make it an attractive target tissue for gene therapy (Lu et al., 2003b). However, there are several obstacles for rAAV delivery that may limit the potential of the vector. The major barriers are 1) Limited capacity of rAAV of 4.7 kb, excluding delivery of large genes such as dystrophin. However, this is not an issue in the studies included in this thesis as ERRγ fits into AAV. The observations of mildly affected BMD patients with very large dystrophin deletions, led to understanding that truncated dystrophin is functional and shown to completely prevent disease in *mdx* mice. Such findings encourage researchers to develop mini and micro dystrophin genes based on the deletion of non-essential regions and keeping the essential regions of the gene, resulting in short but functional dystrophin that overcome the limited capacity issue of AAV (Gregorevic et al., 2004, Gregorevic et al., 2006, Harper et al., 2002), which suggest the requirement of re-administration strategies. 2) Unexpected immune response, which represent the main challenge facing AAV gene delivery. Immune response can be developed against the AAV capsid or the transgene product and can prevent prolonged transgene expression (Daya and Berns, 2008). Immune response directed against AAV can be divided into; innate and adaptive immunity (Hareendran et al., 2013). Innate immunity is the first non-specific defence mechanism, involves limited response of cytokines and chemokines. Innate immune response can cause local or systemic toxicity with higher dose of AAV, whereas adaptive immune response can be divided into humoral and cell-based immune response. Humoral response is mediated by neutralizing antibodies, preventing the re-administration of vector and limiting AAV transduction. Cells-mediated response functions at the cellular level, eliminating

the transduced cells using cytotoxic T cells (Nayak and Herzog, 2010, Kay, 2011).

To avoid immune response, immunosuppression regime or modifying AAV vectors have been used with different levels of efficiency. The advantage in the context of gene therapy is that, the duration of the intervention is relatively short. Using a combination of anti-CD4 antibodies and cyclosporine prevent neutralizing antibodies formation and allow vector re-administration (McIntosh et al., 2012). Repeated administration of AAV1 in *mdx* mice combined with immunosuppression using two specific agents (CTLA-4/Fc and anti-mouse CD40L monoclonal antibody) to block B-T cells interaction, results in preventing formation of neutralizing antibodies against AAV1 (Lorain et al., 2008). However, the main limitation is the absence of antigen specificity, which raises concerns over the risk of serious infection by hypogammaglobulinemia (Ginzler et al., 2012). Modification of AAV capsid is another strategy to improve transduction and prevent immune response. It is based on shielding AAV from recognition by antibodies or T cells by masking their immunogenic epitopes. Genetic modification of the capsid works by mutating neutralizing antibodies epitopes. It was done by scanning for the peptides to map neutralizing epitopes for antibodies present in human or mice. Then, AAV variant libraries were generated by either insertion of peptides at specific positions to disrupt the antibody binding site of viral capsid or by site directed mutagenesis of specific residues of immunogenic peptides on AAV capsid (Hareendran et al., 2013). The main advantage of this strategy is that no need for immunosuppression to reduce antibody titres, however, the novel AAV may reduce transduction efficiency of the target tissue and may alter tissue tropism (Masat et al., 2013).

Dystrophic muscles are characterized by increased susceptibility to damage, impaired Ca^{+2} homeostasis, increased ROS production and oxidative stress (Whitehead et al., 2010, Gervásio et al., 2008, Allen et al., 2016). ROS are potent pro-inflammatory mediators which activate NF-κB leading to activation of TNF-α activity and derive fibrosis (Figari et al., 1987, Kim et al., 2007). Moreover, impaired mitochondria and ATP production have also been reported (Rybalka et al., 2014, Kuznetsov et al., 1998, Percival et al., 2013, Timpani et al., 2015). In addition, dystrophic deficiency is characterized by accumulation of damaged proteins/organelles such as dysfunctional mitochondria, further contribute to muscle pathology (De Palma et al., 2012), impaired vasculature and blood flow (Loufrani et al., 2004, Ennen et al., 2013, Matsakas et al., 2013). Further, in the absence of dystrophin, normal localization of nNOSμ is prevented, which is required for NO production, leads to defective nNOS signalling, resulting in impaired muscle contraction due to excessive muscle ischemia damage that possibly impair recovery from muscle fatigue (Thomas et al., 1998, Percival et al., 2010). These deficiencies contribute to pathology and excessive accumulation of fibrotic tissues that drastically reduce the motility and contractile function of dystrophic muscle and ultimately decreases the amount of muscle tissue that can be targeted by gene therapy (Mann et al., 2011).

As a consequence, targeting energy producing pathways by therapeutic intervention seems logical. In the absence of efficient therapeutic strategies that address the primary genetic defect, treatments which target the mitochondrial dysfunction and muscle perfusion could ameliorate disease progression. To stimulate respiratory capacity in muscle tissues, inducing expression of different mitochondrial biogenesis regulators has been addressed previously. For

example; transgenic over-expression of PGC-1α increased utrophin expression (Handschin et al., 2007) and the post-natal over-expression of PGC-1α induced a fast to slow fibre type shift and an increase in mitochondrial proteins in the *mdx* mouse (Selsby et al., 2012). Moreover, PGC-1α has been shown as an angiokine in ischemic skeletal muscle (Arany et al., 2008). In addition, induction of PERM1 in cultured C_2C_{12} myotubes and in C57BL/6J mice regulated mitochondrial biogenesis and oxidative capacity as well as angiogenesis via the transcriptional induction of VEGF (Cho et al., 2013, Cho et al., 2016).

Moreover, increasing expression of the angiogenic factor (VEGF) via AAV gene transfer, enhances muscle function in *mdx* mice and induces muscle regeneration (Messina et al., 2007). AMPK is known as a regulator of cellular metabolism in response to cellular stress in muscles. Further, activation of AMPK pharmacologically with AMP analogue (AICAR) increases VEGF transcription and protein and capillarization in skeletal muscle *in vitro* (Ouchi et al., 2005) and in wild type mice (Zwetsloot et al., 2008). Inhibiting expression of AMPK using dominant negative mutant of the α2-subunit of AMPK lead to inhibiting vascularisation *in vitro* by inhibiting endothelial cell migration towards VEGF (Nagata et al., 2003).

Estrogen-related receptors (ERRs) are orphan nuclear receptors of which ERRα and γ are highly expressed in tissues associated with metabolic activity such as brain, liver, kidney, placenta, adipose tissues and skeletal muscle (Pearen and Muscat, 2012). However, in skeletal muscle, ERRγ is found to be expressed exclusively in highly vascularized aerobic muscles, specifically in type I fibres (Narkar et al., 2011). Moreover, ERRγ controls the induction of genes associated

with oxidative metabolism, fatty acid oxidation pathway, oxidative respiratory chain, angiogenic genes and contractile genes especially those associated with slow fibres which raises the possibility of fibre type transition from fast to slow linked to metabolic demands (Narkar et al., 2011, Huss et al., 2004, Huss et al., 2002). More interestingly, transgenic over-expression of ERRγ in a murine model of hind limb vascular occlusion shows enhancement in re-vascularisation and neo-angiogenesis which assists the repair damage of ischemic skeletal muscle and maximizes the restoration of blood perfusion (Matsakas et al., 2012).

Based on this background and the results obtained from previous chapter, we aim to assess the effect of post-natal over-expression of ERRγ on skeletal muscle pathology of *mdx* mice systemically. Here, we investigate the effect of post-natal over-expression of ERRγ in *mdx* using AAV8 to determine the extent to which systemic ERRγ gene transfer can rescue dystrophic muscle from disease-related decline. We assess the effect systemic administration of AAV8-ERRγ under the control of spc5-12 promoter into 6 weeks of age (during the active regenerative cycles). Six week-old *mdx* mice were injected with $1x10^{12}$ vg delivered in 100 µl to the tail vein, while the control *mdx* mice were injected similarly with an equal volume of saline (n=7), samples were collected post-mortem at 4 weeks post administration. A summary of all tabulated data will be provided at the end of the results.

4.2. Results:

4.2.1. Evaluation of ERRγ over-expression in different muscles following ERRγ gene transfer into 6 week-old *mdx*:

Following intravenous administration of AAV8-ERRγ into 6 week-old *mdx*, the expression of ERRγ was assessed by quantitative real time PCR (Q-PCR) in different muscles using specific primer for ERRγ. EDL, gastrocnemius, TA, diaphragm and quadriceps showed over-expression of ERRγ mRNA by 3, 10, 6, 5 and 3 fold respectively with no change in the soleus expression of ERRγ (figure 4.1 A-F). However, the protein analysis showed no increase in the relative protein level of ERRγ in EDL muscle and 2 fold increase in gastrocnemius (figure 4.1 G-I).

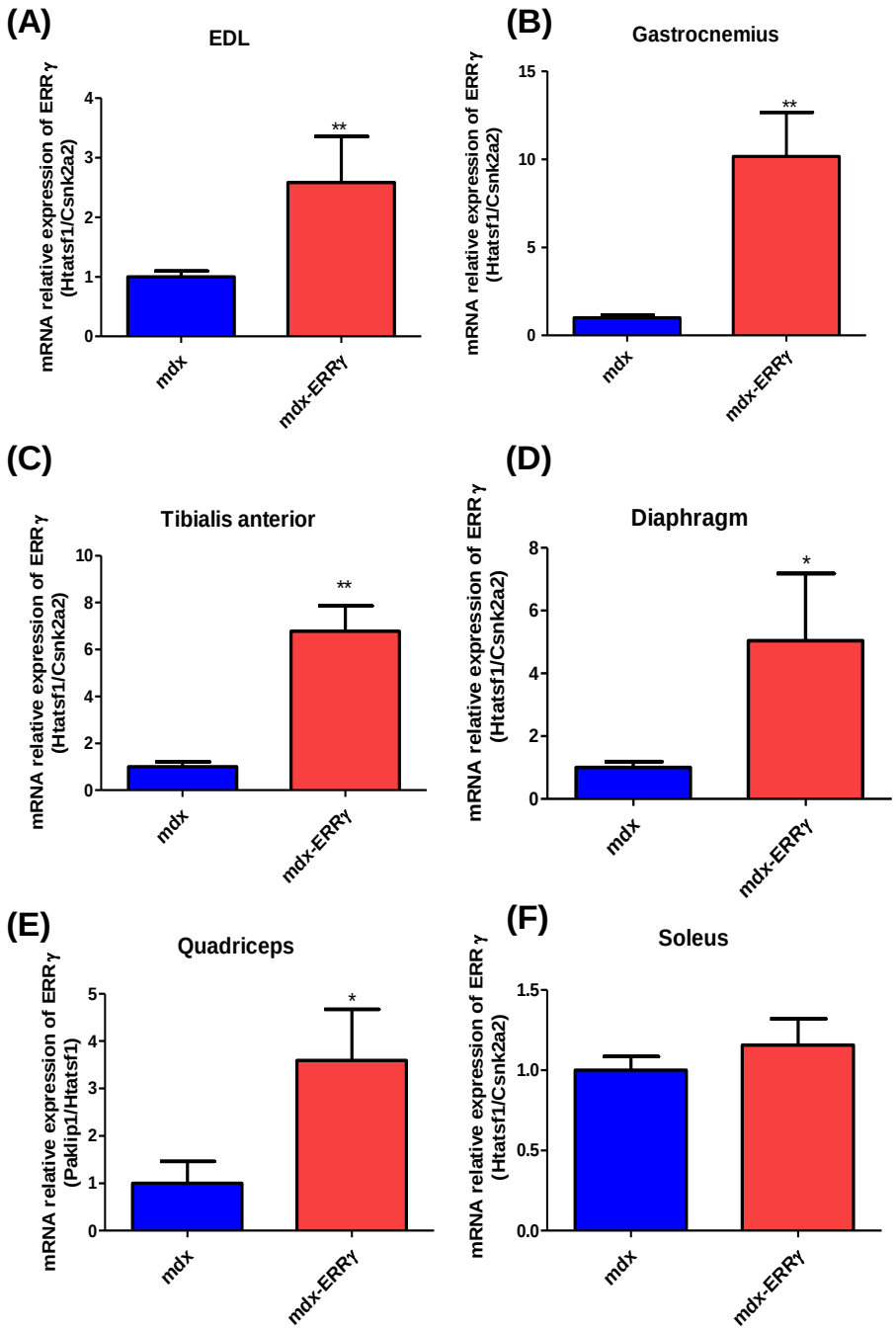
(A)
EDL
mRNA relative expression of ERRγ (Htatsf1/Csnk2a2)
0
1
2
3
4
**
mdx
mdx-ERRγ
(B)
Gastrocnemius
mRNA relative expression of ERRγ (Htatsf1/Csnk2a2)
0
5
10
15
**
mdx
mdx-ERRγ
(C)
Tibialis anterior
mRNA relative expression of ERRγ (Htatsf1/Csnk2a2)
0
2
4
6
8
10
**
mdx
mdx-ERRγ
(D)
Diaphragm
mRNA relative expression of ERRγ (Htatsf1/Csnk2a2)
0
2
4
6
8
*
mdx
mdx-ERRγ
(E)
Quadriceps
mRNA relative expression of ERRγ (Paklip1/Htatsf1)
0
1
2
3
4
5
*
mdx
mdx-ERRγ
(F)
Soleus
mRNA relative expression of ERRγ (Htatsf1/Csnk2a2)
0.0
0.5
1.0
1.5
mdx
mdx-ERRγ

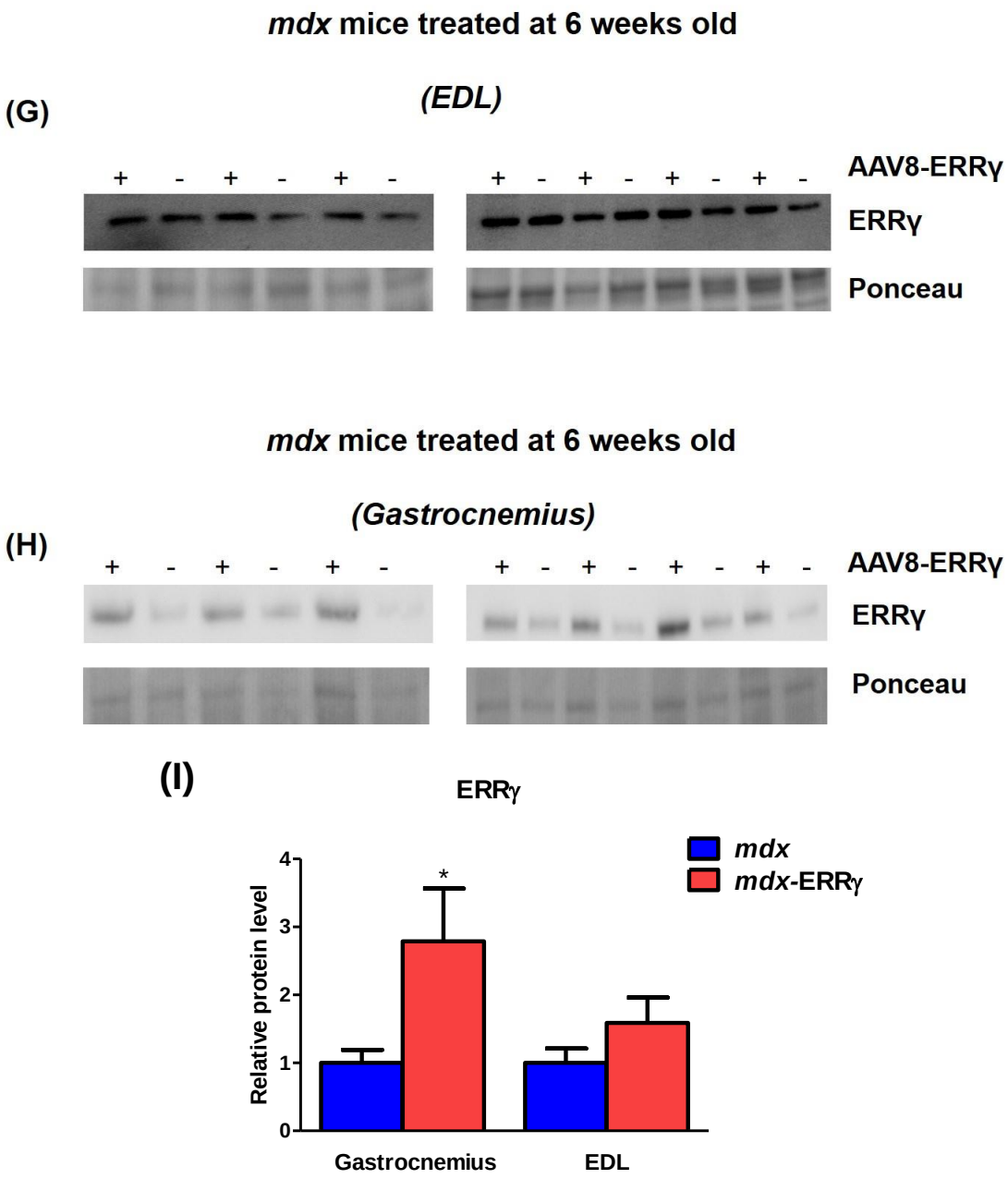

Figure 4.1. ERRγ gene transfer increases expression of ERRγ in *mdx* mice treated at 6 weeks old

Intravenous administration of $1X10^{12}$ vg AAV8-ERRγ into 6 week old *mdx* and samples were collected 4 weeks later increased expression of ERRγ in some assessed muscles. Total RNA was harvested from *mdx* and *mdx*-ERRγ muscles. (A-F) Relative mRNA levels of ERRγ for the indicated muscles were determined by qRT-PCR, normalized to the indicated housekeeping genes levels. EDL muscles show 3 fold increase (p=0.001), gastrocnemius muscles show 10 fold (p=0.001), TA muscles show 6 fold (P=0.001), diaphragm muscles show 5 fold (p=0.011), quadriceps muscles show 3 fold (p=0.006) and no difference in soleus muscles (p=0.437). The levels of ERRγ protein in gastrocnemius and EDL muscles respectively were determined by western blot analysis,

using 30 µg of protein and Ponceau stain was used for normalization. The total ERRγ protein was determined using ERRγ antibody. G) The intensity of the bands in EDL muscles from 6 week old *mdx* study was quantified using ImageJ software. H) The intensity of the bands in gastrocnemius muscles from 6 week old *mdx* study was quantified using ImageJ software. I) ERRγ gene transfer increases ERRγ protein levels in gastrocnemius muscle by 2 fold (p=0.04) with no increase in EDL muscle (p=0.239), (n=7, un-paired student's t-test).

4.2.2. Gene transfer of AAV8-ERRγ has no effect on muscle function in EDL muscles of *mdx* mice treated at 6 weeks old:

To test the effect of ERRγ gene transfer on physiological function of freshly recovered EDL muscles, tetanic force, specific force and specific force following lengthening contractions were assessed. EDL muscles were used due to its ideal size and geometry, including definitive tendons (Brooks and Faulkner, 1988). In the experiment of *mdx* mice treated at 6 weeks of age and recovered 4 weeks post administration, there was no difference in the EDL muscle mass (figure 4.2 A). Neither the tetanic force of the AAV8-ERRγ EDL muscles nor the specific forces differed from those of the control (figure 4.2 B-C). In order to assess to which extent ERRγ gene transfer improve resistance to eccentric contraction, muscles underwent a series of 10 lengthening contractions. ERRγ failed to improve resistance to contraction induced injury (figure 4.2 D).

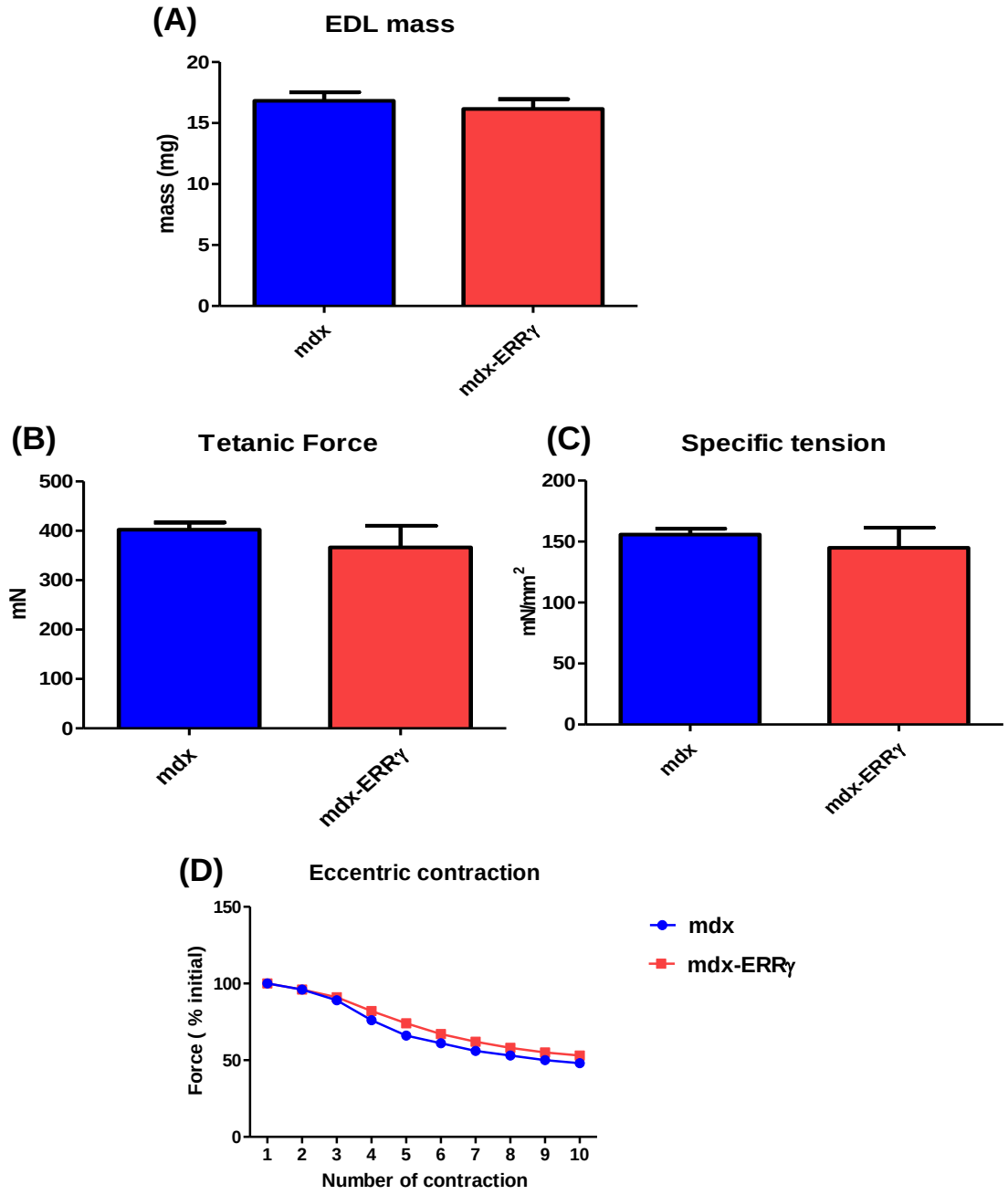

Figure 4.2. Gene transfer of ERRγ into 6 week old *mdx* has no effect on muscle force

Intravenous injection of 6 week old *mdx* mice with $1X10^{12}$ vg of AAV8-ERRγ and recovered 4 weeks later has no impact on A) EDL muscle mass (p=0.539). Muscles were stimulated according to standard techniques in order to assess tetanic force and specific force. B) Tetanic force was unaffected with ERRγ gene transfer (p=0.449). C) Tetanic force normalized by muscle cross sectional area is specific force. Cross sectional area (mm^2)= mass (mg)/ [(L_o mm)* (L/L_o)* (1.06 mg/mm^3)], where L/L_o is the fibre to muscle length ratio (0.45 for EDL) and 1.06 is the density of muscle. However, specific force is not different between *mdx* and *mdx*-ERRγ (P =0.541), (n=7 for *mdx* and *mdx*-ERRγ, un-

paired student's t-test). D) EDL muscles were given a series of 10 lengthening contractions (150 Hz for 500 msec, followed by 200 msec at a 110% L_o). Eccentric contraction shows no difference between the two groups of muscle, (n=7 for *mdx* and *mdx*-ERRγ, p=0.320, two-way Anova).

4.2.3. Impact of ERRγ over-expression on oxidative metabolism in muscles of *mdx* mice treated at 6 weeks old:

In the experiment of 6 week-old *mdx*, gastrocnemius was chosen to assess the effect of over-expression of ERRγ on histology as these muscles showed the highest over-expression of ERRγ by 10 fold. An enzymatic succinate dehydrogenase (SDH) stain was used to assess whether over-expression of ERRγ has an effect on the percentage of oxidative fibres as a representation of oxidative activity. Based on counting the fibres in the entire muscle cross section, over-expression of ERRγ in gastrocnemius muscles from 6 weeks experiment showed a 14% increase in the percentage of oxidative fibres (p=0.001) (figure 4.3 A). In order to assess the effect of ERRγ over-expression on genes related to oxidative metabolism and mitochondrial biogenesis, specific primers were used to evaluate the relative expression of these genes. Gastrocnemius muscle from 6 week old *mdx* study was analysed for some parameters as it showed a higher level of ERRγ over-expression. In addition, EDL muscles since it is used for functional assessment. However, none of the examined genes related to oxidative metabolism or mitochondrial biogenesis showed any difference between *mdx* and *mdx*-ERRγ in the 6 week-old mice of either gastrocnemius or EDL muscles (figure 4.3 B-C).

mdx mice treated at 6 weeks old

(A)

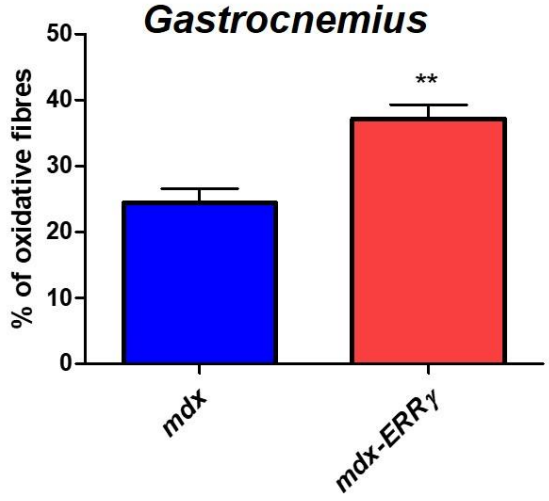

(B)

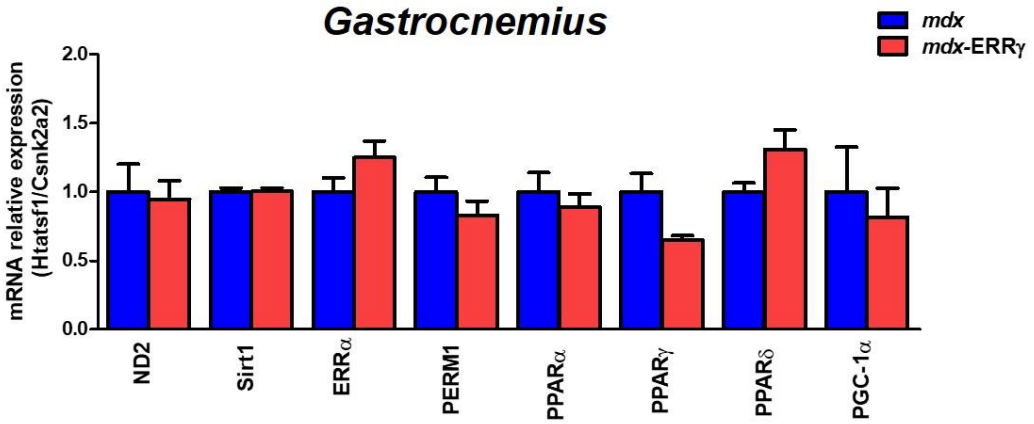

(C)

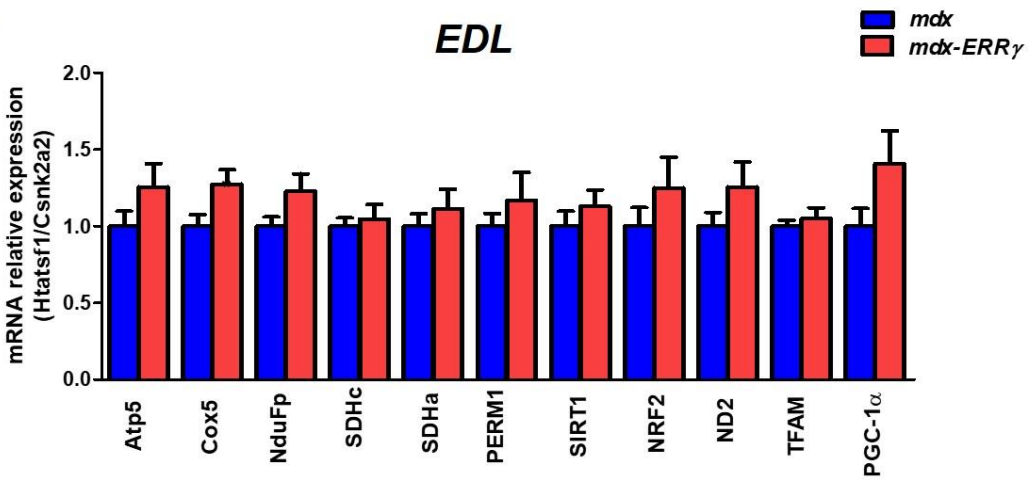

Figure 4.3. Effect of ERRγ over-expression on oxidative capacity

Over-expression of ERRγ in gastrocnemius muscles from 6 week study showed increased SDH activity. A) The relative abundance of oxidative fibres in *mdx* and *mdx*-ERRγ in 6 weeks study based on quantification of an entire cross section of gastrocnemius. Data are expressed as a percentage (%) of total fibres. SDH activity is increased by 14% in gastrocnemius muscles (p=0.001). B) ERRγ over-expression in gastrocnemius muscle from 6 week-old *mdx* shows no difference in the relative mRNA *level* of oxidative metabolism genes; ND2 (p=0.830), SIRT1 (p=0.928), ERRα (p=0.137), PERM1 (p=0.274), PPARα (p=0.532), PPARγ (p=0.059), PPARδ (p=0.07) and PGC-1α (p=0.1). C) Relative mRNA expression of the indicated genes related to oxidative metabolism and mitochondrial biogenesis in EDL muscles from 6 week study. No difference in the expression level of any indicated genes Atp5 (p=0.181), Cox5 (p=0.063), NduFp (p=0.1), sdhc (p=0.675), sdha (p=0.475), PERM1 (p=0.416), SIRT1 (p=0.165), NRF2 (p=0.305), ND2 (p=0.191), TFAM (p=0.535), PGC-1α (p=0.121), (n=7, un-paired student's t-test).

4.2.4. Increasing expression of ERRγ does not significantly alter myosin isoforms in gastrocnemius muscle of *mdx* mice treated at 6-weeks old:

We asked whether postnatal over-expression of ERRγ shift the muscle fibre type. We used staining of muscle cross section with antibodies against the different MHC isoforms to quantify the fibre type content. However, we found that over-expression of ERRγ has no effect on fibre type composition in gastrocnemius from 6 weeks experiment (figure 4.4).

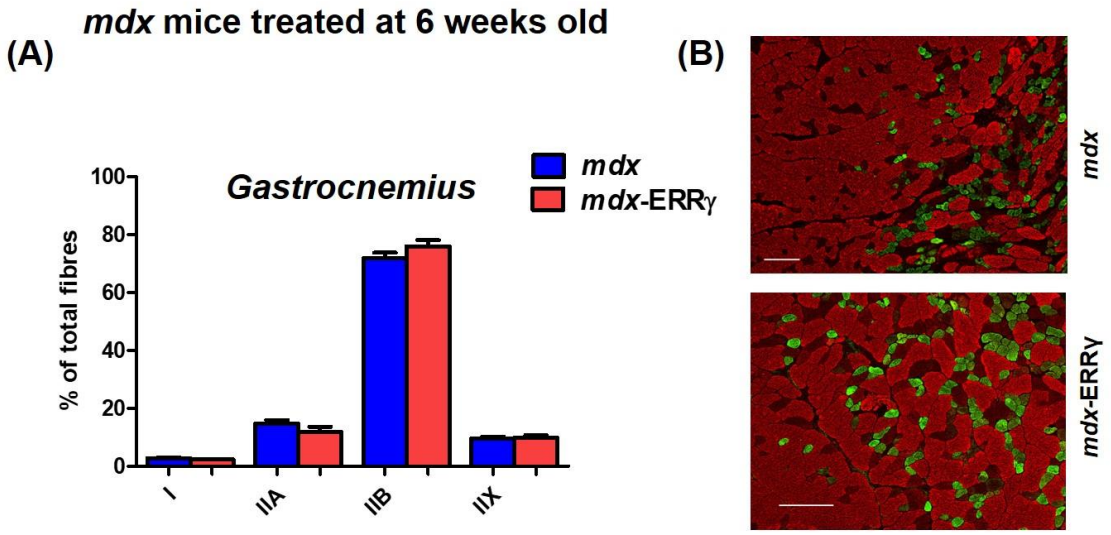

Figure 4.4. Over-expression of ERRγ in gastrocnemius muscles has no impact on muscle fibre typing

A) The relative abundance of different fibre types in gastrocnemius from 6 week old *mdx* based on quantification of an entire muscle sections. Myosin heavy chain (MHC) analysis in *mdx* and *mdx*-ERRγ shows no difference in the number of fibre types in gastrocnemius, type I (p=0.10), IIA (p=0.212), IIB (p=0.161) and IIX (p=0.844). B) Representative images of cross sections show the mid-portion of *mdx* and *mdx*-ERRγ muscles stained with antibodies against MHC isoforms, as indicated. Scale bar, 200 μm, (n=7, un-paired student's t-test).

4.2.5. Impact of ERRγ over-expression on angiogenesis in *mdx* mice treated at 6 weeks-old:

In order to assess the effect of ERRγ over-expression on genes related to angiogenesis, specific primers were used to evaluate the relative expression of these genes. Over-expression of ERRγ in 6 week old *mdx* shows no difference in the transcript levels of angiogenesis markers neither in gastrocnemius nor in EDL muscles (figure 4.5 A-B).

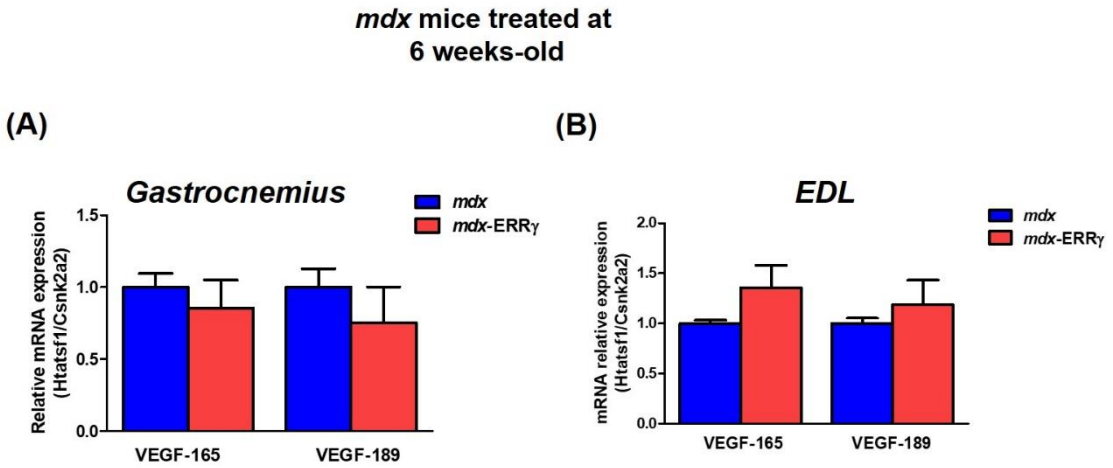

Figure 4.5. Over-expression of ERRγ has no effect on angiogenesis in *mdx* mice treated at 6-weeks old:

Relative mRNA levels of angiogenic markers shows no difference in the expression of A) VEGF-165 (p=0.519) and VEGF-189 (p=0.396) in gastrocnemius muscles or B) VEGF-165 (p=0.259) and VEGF-189 (p=0.10) in EDL muscles between *mdx* and *mdx*-ERRγ from 6 weeks study, (n=7 for *mdx* and *mdx*-ERRγ, un-paired student's t-test).

4.2.6. Effect of ERRγ over-expression on myofibre central nucleation in gastrocnemius muscle of *mdx* mice treated at 6-weeks old:

Haematoxylin and eosin staining was used to assess whether over-expression of ERRγ decreased central nucleation. Gastrocnemius muscles from mice treated at 6 weeks of age showed 8% reduction in the percentage of centrally nucleated fibres (p=0.007) (figure 4.6).

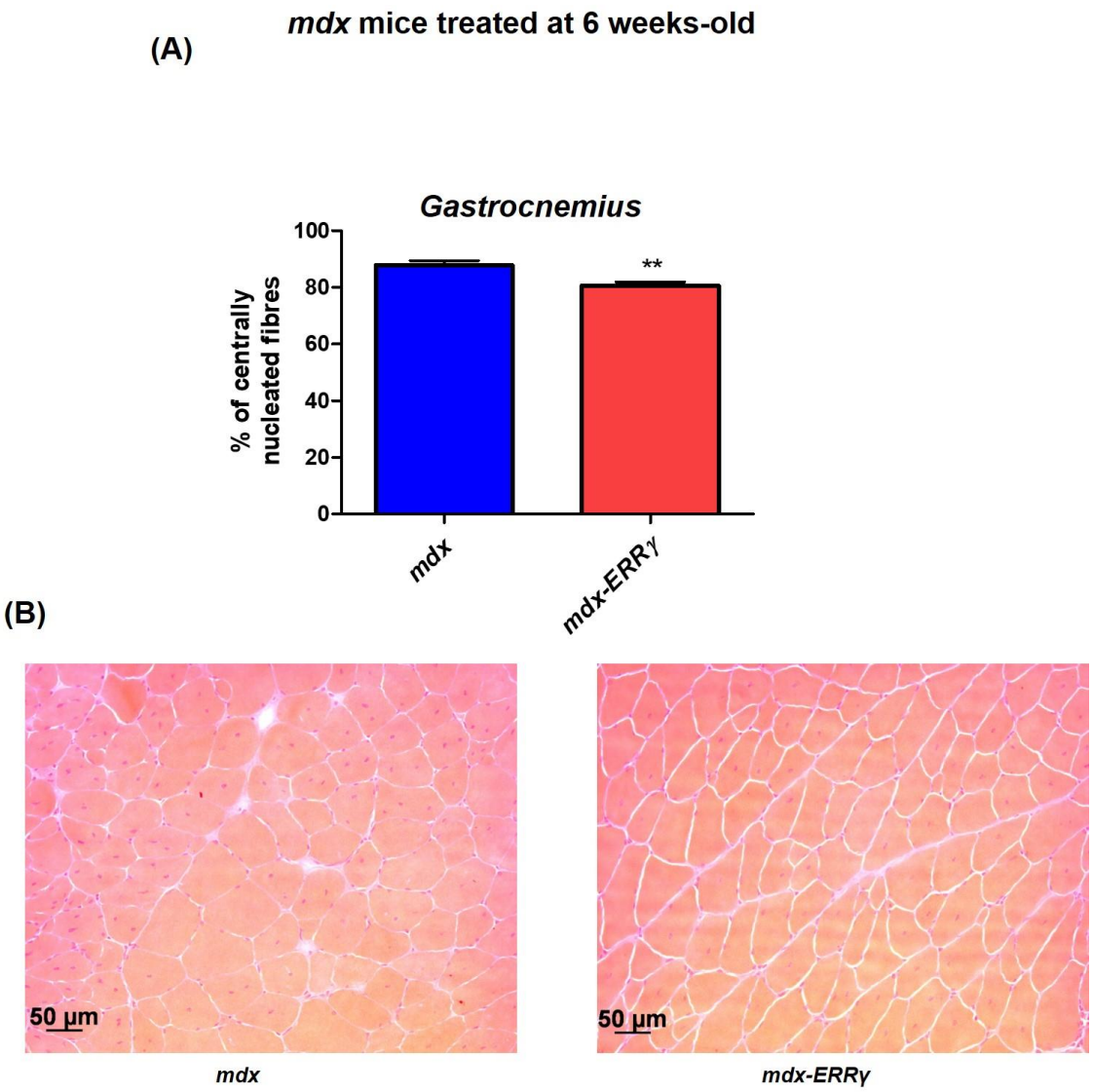

Figure 4.6. Over-expression of ERRγ reduces central nucleation in gastrocnemius muscle of *mdx* mice treated at 6-weeks old

A) Percentage of centrally nucleated fibres in *mdx* and *mdx*-ERRγ of gastrocnemius from 6 weeks study shows 8% reduction of centrally nucleated fibres (p=0.007). B) Representative images of cross sections of *mdx* and *mdx*-ERRγ gastrocnemius stained with H&E. Scale bar, 50 µm, (n=7, un-paired student's t-test).

4.2.7. Effect of ERRγ over-expression on muscle damage of *mdx* mice treated at 6-weeks old*:*

To determine the effect of ERRγ over-expression on muscle damage, serum CK level was assessed. The level of CK in the blood serum was higher in *mdx* serum compared to WT serum as demonstrated previously (Matsakas et al., 2013).

However, the over-expression of ERRγ does not reduce the serum CK in 6 week old mice (figure 4.7 A). In addition, muscle damage was assessed by scoring for IgG positive fibres as an indicator of sarcolemmal integrity. In the 6 week study, over-expression of ERRγ in gastrocnemius had no effect on the number of IgG infiltrated fibres (figure 4.7 B). To further assess the level of regeneration, the number of fibres expressing embryonic myosin (MYH-3) was assessed in an entire muscle cross section, the percentage of fibres expressing MYH3 was not different between the *mdx* and *mdx*-ERRγ in gastrocnemius from the 6 weeks study (figure 4.7 D).

***mdx* mice treated at 6 weeks old**

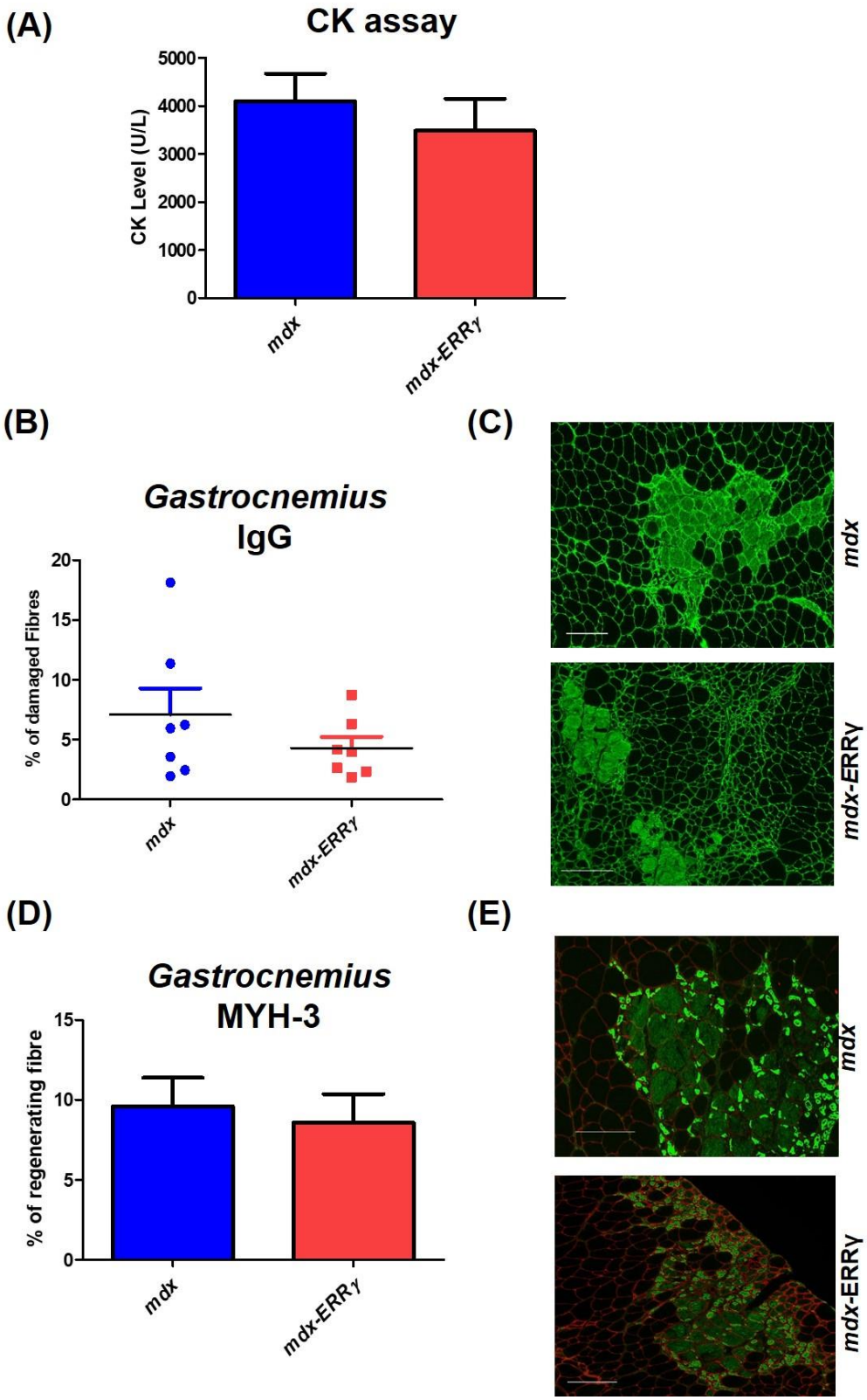

Figure 4.7. ERRγ gene transfer has no effect in CK levels, IgG infiltration or MYH-3 positive fibres in *mdx* mice treated at 6 weeks old

A) Creatine kinase assay measurement shows no difference in the blood serum of *mdx* and *mdx*-ERRγ in 6 weeks (p=0.495). B, D) The percentage of IgG and MYH-3 positive fibres in the entire gastrocnemius muscles of *mdx* and *mdx*-ERRγ show no difference of the damaged fibres in 6 week study (p=0.262) or MYH-3 positive fibres (p=0.685). C, E) Representative images of cross section of *mdx* and *mdx*-ERRγ gastrocnemius muscles immunostained with anti-IgG antibody, anti-MYH-3 antibody, respectively. Scale bar, 200 μm, (n=7, un-paired student's t-test).

4.2.8. Impact of ERRγ over-expression on inflammation, degradation, translation, ubiquitination calcium and antioxidant markers in EDL muscle of *mdx* mice treated at 6-weeks old:

To find out whether increasing expression of ERRγ affects the expression levels of markers related to pro and anti-inflammatory pathways, degradation, translation, ubiquitination, calcium and antioxidant markers, specific primers were used. EDL muscle was used for these assessments. 3 fold over-expression of ERRγ in EDL from the 6 week study has no effect on the expression of genes related to inflammation (TNF-α, IL-1β, IL-6 and IL-10) except a 1.6 fold increase of NF-κB which is expected to increase in the dystrophic muscles (p=0.006) (figure 4.8 A). In addition, none of the autophagy related genes (P62, Beclin-1, Bnip3) or apoptotic marker; chathespin-L *or* atrophy gene; FOXO-1 were affected (figure 4.8 B). Furthermore, to determine if the over-expression of ERRγ had any impact in the calcium handling, two markers were assessed. However, over-expression of ERRγ in the 6 weeks old *mdx* did not change expression of RYR-1 Ca^{+2} release channel or SERCA-1, a Ca^{+2} pump channels (figure 4.8 C). Genes involved in the translation pathways (Gadd34 and 4EBP-1) were unchanged (figure 4.8 D), ubiquitination genes; Atrogin-1 was reduced by 1.4 fold (p=0.026)

and MuRF-1 was unaffected (figure 4.8 E). Finally, SOD2 was used as an antioxidant marker and showed no change (figure 4.8 F).

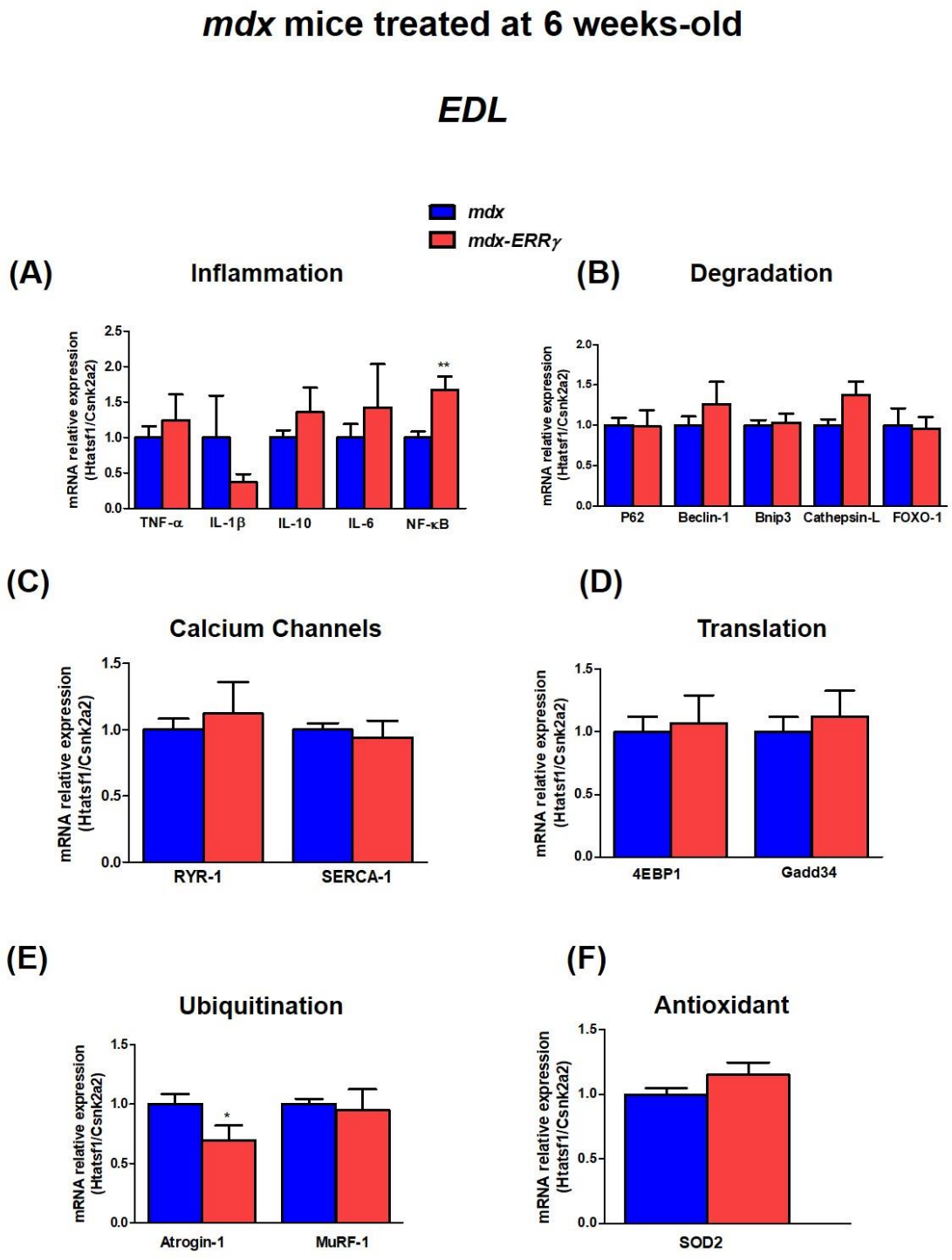

Figure 4.8. Impact of ERRγ over-expression on inflammation, degradation, translation, ubiquitination calcium and antioxidant markers in EDL muscle of *mdx* mice treated at 6-weeks old

Relative mRNA levels for the indicated genes in the EDL muscles of of *mdx* and *mdx*-ERRγ from 6 weeks study A) Relative mRNA levels for the indicated inflammatory markers; TNF-α (p=0.552), IL-1β (p=0.628), IL- 6 (p=0.902) and 1.6 fold increase of NF-κB (p=0.006) IL-10 (p=0.535). B) Relative mRNA levels for the indicated autophagy markers; P62 (p=0.383), Beclin-1 (p=0.710), Bnip3 (p=0.824), chathepsin-L (p=0.07), FOXO-1 (p=0.877). C) Over-expression of ERRγ in EDL muscle of 6 week-old *mdx* has no effect on the expression of calcium receptors; RYR-1 calcium channel (p=0.629), SERCA-1 (p=0.678). D) Relative mRNA levels for the indicated translation markers; 4EBP-1 (p=0.788) and Gadd34 (p=0.624). E) Relative mRNA levels for the indicated ubiquitination markers; 1.4 fold decrease of Atrogin-1 (p=0.026) and MuRF1 (p=0.78). F) Relative mRNA levels for the antioxidant marker; SOD2 (p=0.183), (n=7, un-paired student's t-test).

4.3. Evaluation of administration of AAV8-ERRγ at earlier (pre-crisis) timepoint in *mdx* mice:

Observation from earlier study on 6 week-old *mdx* showed modest output following over-expression of ERRγ. These results were particularly surprising as it was an age/sex matched study consistent with the transcriptomic study in which the PCA and gene ontology data was particularly encouraging. Therefore, we thought to determine if a similar protocol, but delivered to an earlier age and for a longer timepoint would have a better impact on the dystrophic pathology. In fact, the onset of pathology begins at 3 weeks of age where *mdx* undergo severe myofibre necrosis and subsequent regeneration in limb muscles (Grounds et al., 2008). The timing of the age of onset of muscular dystrophy corresponds to the disappearance of utrophin around the sarcolemma (Clerk et al., 1993). Also, it could be the result of huge disruptions in intracellular signalling and excessive inflammation (Evans et al., 2009a), or a result of an increase in motor activity at the time of weaning (Mokhtarian et al., 1995). The high level of necrosis between 21 and 28 days provides an excellent model to assess therapeutic interventions

aimed at preventing or decreasing muscle necrosis (Grounds and Torrisi, 2004, Radley et al., 2008, Radley and Grounds, 2006, Hollinger et al., 2013). Muscle necrosis peaks at 4 weeks of age and then becomes stable, where low level of damage was observed as approximately 6% of each skeletal muscle being actively necrotic. However, discrepancies in the literatures have been reported about the stable period of necrosis. Some have reported 8-12 weeks (McGeachie et al., 1993, Heier et al., 2014), others reported 10-12 weeks of age (Godfrey et al., 2015, Muntoni et al., 1993, Dangain and Vrbova, 1984). Following 12 weeks of age, muscles exhibit a low level of muscle necrosis and reduced creatine kinase levels. After 20 months of age, they exhibit a more severe pathology with the general replacement of skeletal muscle with fibrous connective tissue, diminished cardiac and respiratory function and reduced life span (Chamberlain et al., 2007). In *mdx* mice, the major wave of necrosis occurs between 3-4 weeks of age and is followed by a regenerative process between 5-6 weeks of age, which results in the replacement of a large proportion of the damaged fibres (Gillis, 1999). This study was carried out in 3 week-old *mdx* and recovered 6 weeks post administration to better evaluate the over-expression of ERRγ in dystrophic tissue. Intraperitoneal administration with $1x10^{12}$ vg administered in 50 µl just off the midline in the lower left quadrants, while the control mice were injected with an equal volume of saline solution, n=12 (*mdx* control) and n=10 (*mdx*-ERRγ). The number of animals herein was changed to improve the power of this study. In both studies; 6 and 3 weeks of age, samples were collected around the stable period of degeneration/ regeneration process (9-10 weeks of age).

4.3.1. Evaluation of ERRγ over-expression in different muscles following ERRγ gene transfer into 3 week-old *mdx*:

Following IP AAV8-ERRγ gene transfer, assessing the over-expression of ERRγ mRNA in different muscles showed increased expression in EDL muscle by 2 fold (p=0.002) and TA muscle by 3 fold (p=0.02) respectively, with no change in the expression of ERRγ in the other examined muscles (figure 4.9 A-E). Protein level was found to increase by 2 fold in EDL muscle (p=0.013) (figure 4.9 F-G).

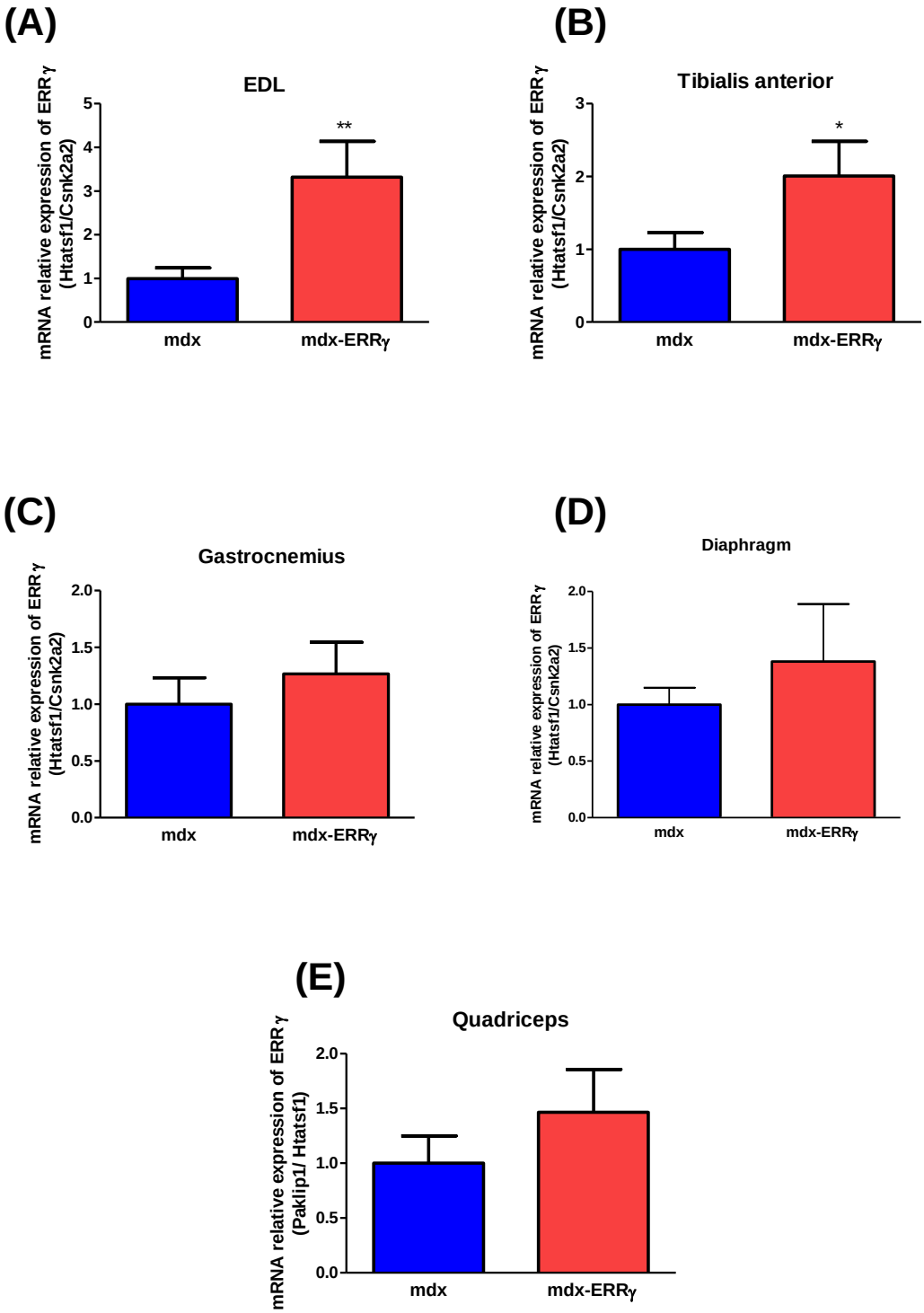
(A)
EDL
mRNA relative expression of ERRγ
(Htatsf1/Csnk2a2)
5
4
3
2
1
0
**
mdx
mdx-ERRγ
(B)
Tibialis anterior
mRNA relative expression of ERRγ
(Htatsf1/Csnk2a2)
3
2
1
0
*
mdx
mdx-ERRγ
(C)
Gastrocnemius
mRNA relative expression of ERRγ
(Htatsf1/Csnk2a2)
2.0
1.5
1.0
0.5
0.0
mdx
mdx-ERRγ
(D)
Diaphragm
mRNA relative expression of ERRγ
(Htatsf1/Csnk2a2)
2.0
1.5
1.0
0.5
0.0
mdx
mdx-ERRγ
(E)
Quadriceps
mRNA relative expression of ERRγ
(Paklip1/ Htatsf1)
2.0
1.5
1.0
0.5
0.0
mdx
mdx-ERRγ

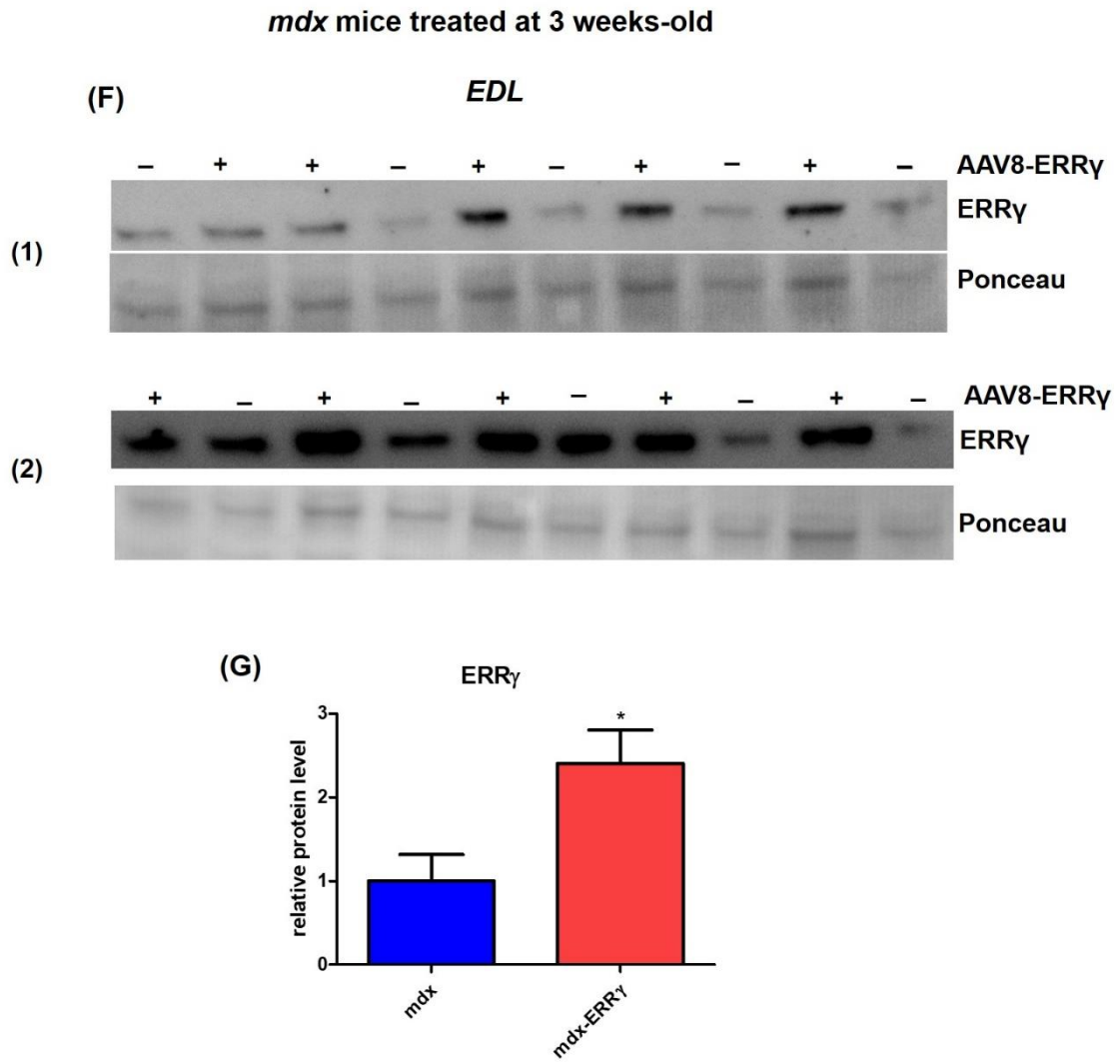

Figure 4.9. ERRγ gene transfer increases over-expression of ERRγ mRNA in EDL and TA muscles of *mdx* mice treated at 3 weeks-old

Intraperitoneal administration of $2X10^{12}$ vg AAV8-ERRγ into 3 week old *mdx* and samples were collected 6 weeks later increased levels of ERRγ mRNA in some assessed muscles. Total RNA was harvested from the *mdx* and *mdx*- ERRγ muscles. (A-E) Relative mRNA levels of ERRγ for the indicated muscles were determined by qRT-PCR, normalized to the indicated housekeeping gene levels. Results show 3 fold increase of ERRγ mRNA in EDL (p=0.002), 2 fold increase in TA (p=0.02) and no change in gastrocnemius (p=0.467), diaphragm (p=0.446) and quadriceps (p=0.321), (n=12 for *mdx*, n=10 for *mdx*-ERRγ, un-paired student's t-test). The levels of ERRγ protein in EDL muscles were determined by western blot analysis, using 30 µg of protein and Ponceau stain was used for normalization. The total ERRγ protein was determined using ERRγ antibody. F) The intensity of the bands was quantified using ImageJ software. G) ERRγ gene transfer increases ERRγ protein levels in EDL muscle by 2 fold (p=0.013), (n=10 for *mdx* and *mdx*-ERRγ, un-paired student's t-test), samples were run in two blots.

4.3.2. Gene transfer of AAV8-ERRγ improves specific force in EDL muscles of *mdx* mice treated at 3-weeks old:

In order to assess the functional benefits of ERRγ over-expression in dystrophic mice at 3 weeks of age and recovered at 9 weeks, EDL was examined for muscle function. EDL muscles treated at 3 weeks of age showed no difference in the mass following treatment (figure 4.10 A). The tetanic isometric force generated from EDL muscles of treated *mdx* was unaffected compared to the control, however the specific force was significantly greater than that of the control by 14% (p=0.043) (figure 4.10 B-C). Similar to 6 weeks experiment, ERRγ has failed to improve resistance to contraction induced injury (figure 4.10 D). Cross sectional area showed no difference between the two groups (figure 4.11 A).

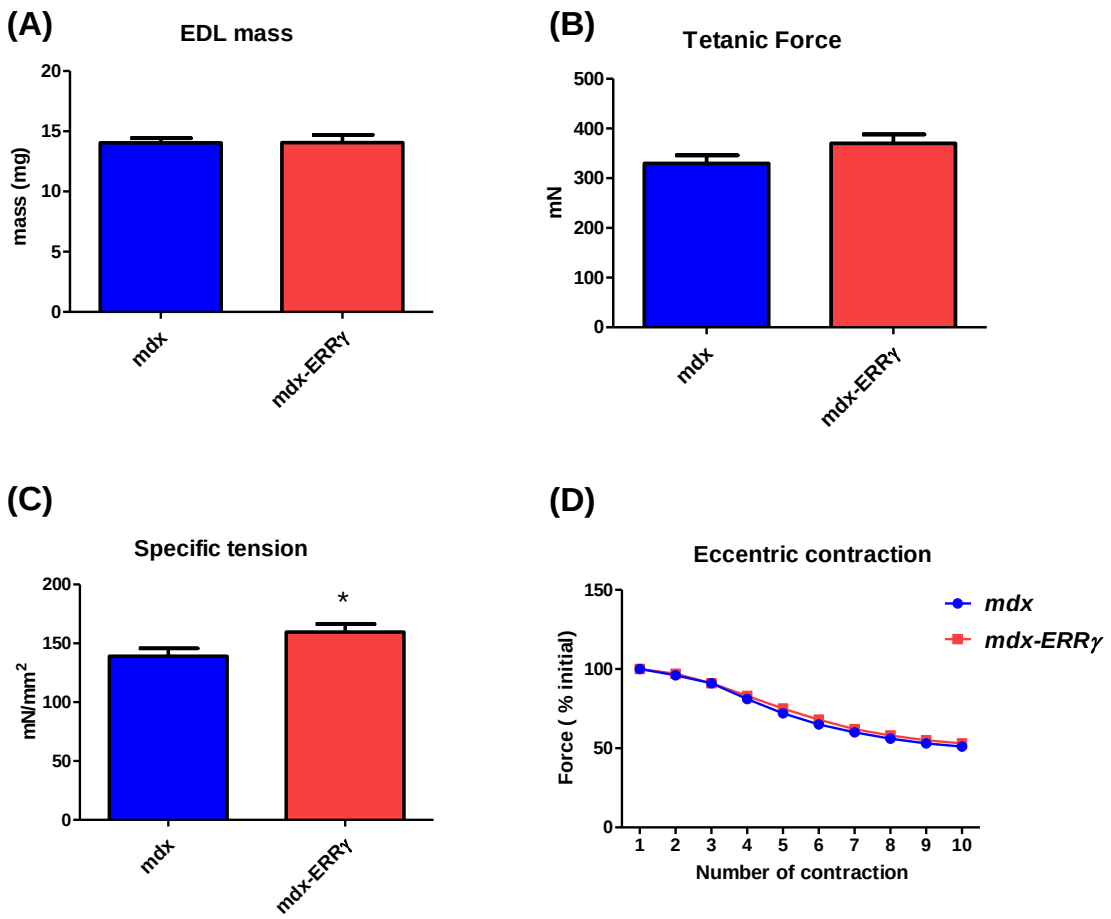

Figure 4.10. Gene transfer of ERRγ improves specific force in dystrophic muscle treated at 3 weeks of age by 14%

Intraperitoneal administration of $2X10^{12}$ vg of AAV8-ERRγ into 3 week old *mdx* mice and recovered 6 weeks later has no impact on A) EDL muscle mass (p=0.991). Muscles were stimulated according to standard techniques in order to assess tetanic force and specific force as described in (figure 4.1). B) Tetanic force is unaffected with ERRγ gene transfer (p=0.112). C) ERRγ gene transfer into 3 week old-*mdx* led to a 14% improvement of specific tension in EDL muscles (p=0.043). D) EDL muscles were given a series of 10 lengthening contractions (150 Hz for 500 msec, followed by 200 msec at a 110% L_o), eccentric contraction shows no difference between the two groups, (n=12 for *mdx* and n=10 for *mdx*-ERRγ, p=0.211, two-way Anova).

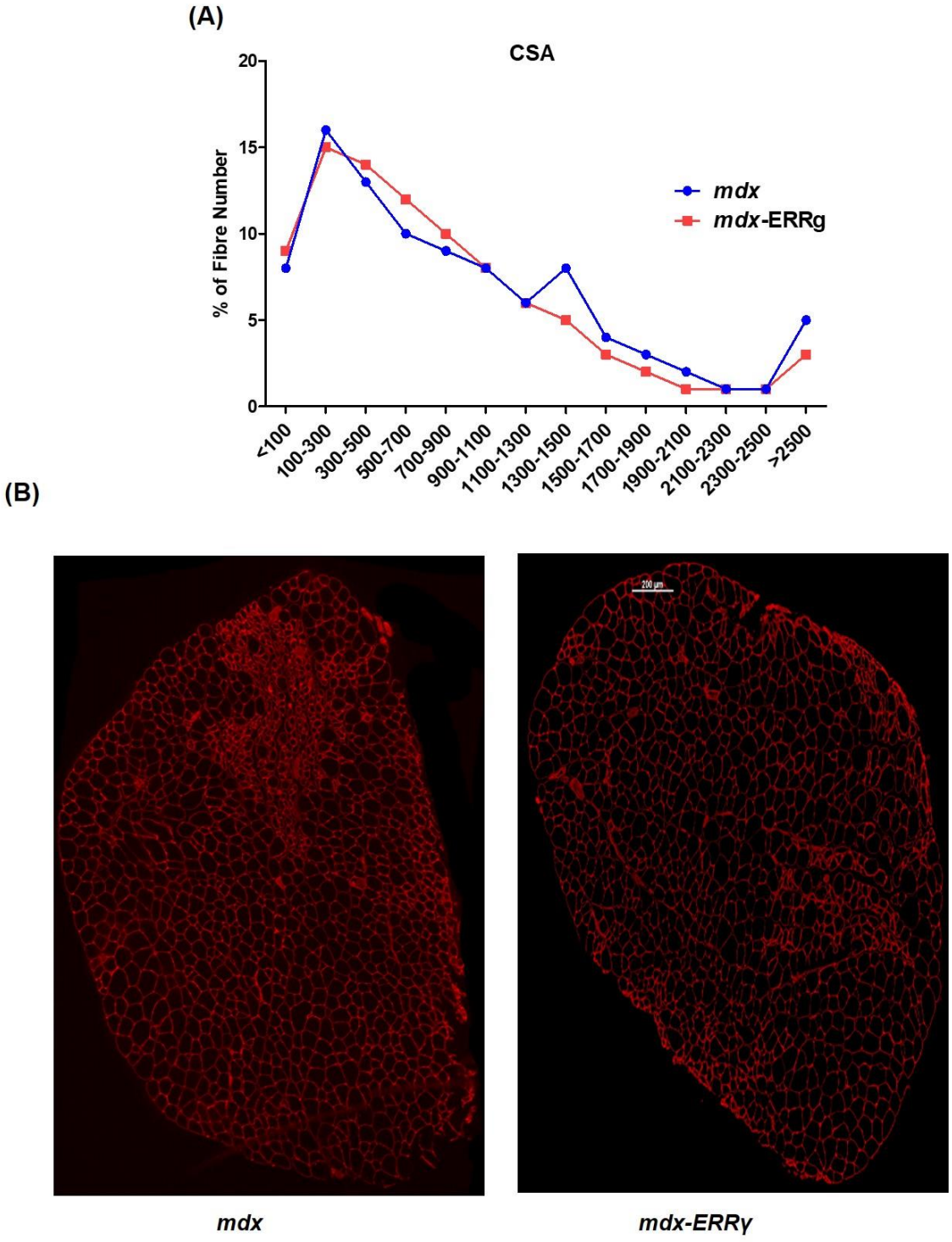

Figure 4.11. Cross sectional area of EDL muscle treated at 3 weeks of age.

A) Distribution of fibre cross sectional area of *mdx* and *mdx*-ERRγ EDL muscles, calculated from laminin stained images and shows no difference between the two groups of muscles, chi square (p=0.242), B) Representative images of cross sections of *mdx* and *mdx*-ERRγ immuno-stained with anti-laminin antibody, scale bar, 200 µm, (n=12 for *mdx* and n=10 for *mdx*-ERRγ, un-paired student's t-test).

4.3.3. Impact of ERRγ over-expression on oxidative metabolism in EDL muscles of 3 week old *mdx* mice:

In this experiment, EDL muscle was chosen as it showed the highest over-expression of ERRγ. An enzymatic succinate dehydrogenase (SDH) stain was used to assess whether over-expression of ERRγ has an effect on the percentage of oxidative fibres as a representation of oxidative activity. EDL muscles from mice treated at 3 weeks of age which exhibited a 3 fold over-expression of ERRγ resulted in a 60% increase in the percentage of oxidative fibres (p=0.008) (figure 4.12 A). In order to assess the effect of ERRγ over-expression on genes related to oxidative metabolism and mitochondrial biogenesis, specific primers were used to evaluate the relative expression of these genes. Sdha gene was upregulated by 2 fold (p=0.006) and PGC-1α, which is the upstream inducer of mitochondrial biogenesis genes was upregulated by 2 fold (p=0.006) at the mRNA level following over-expression of ERRγ. However none of the other analysed genes related to oxidative metabolism showed a difference at the transcript level (figure 4.12 C).

We then determined the relative expression levels of mitochondrial complex I, II, III and V using antibodies specific to protein subunits of each complex in EDL muscle lysates from *mdx* mice treated at 3 weeks old. Relative protein level of complex I was increased by 2.7 fold (p=0.006), II was increased by 1.3 fold (p=0.013) and III was increased by 1.7 fold (p=0.019) following ERRγ over-expression. In contrast, complex V was unaffected (figure 4.12 D-E). However protein analysis of PGC-1α resulted in insignificant difference between the treated EDL and the control (figure 4.12 F-G). Moreover, the relative protein level

of the induced regulator of PGC-1α and ERR, muscle 1 gene (PERM1) was not different between the two groups (figure 4.12 H-I).

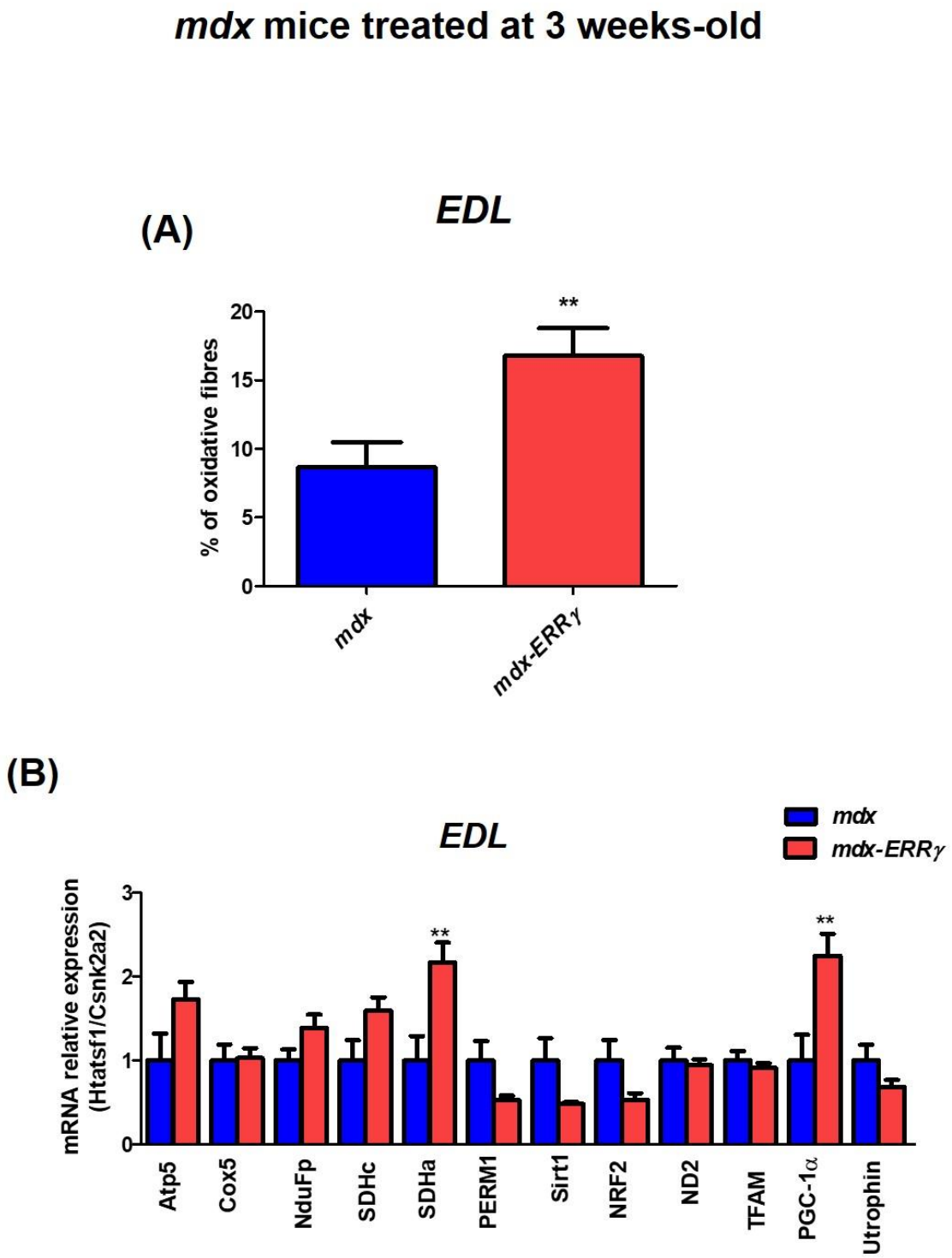

(C)

***mdx* mice treated at 3 weeks-old**

EDL

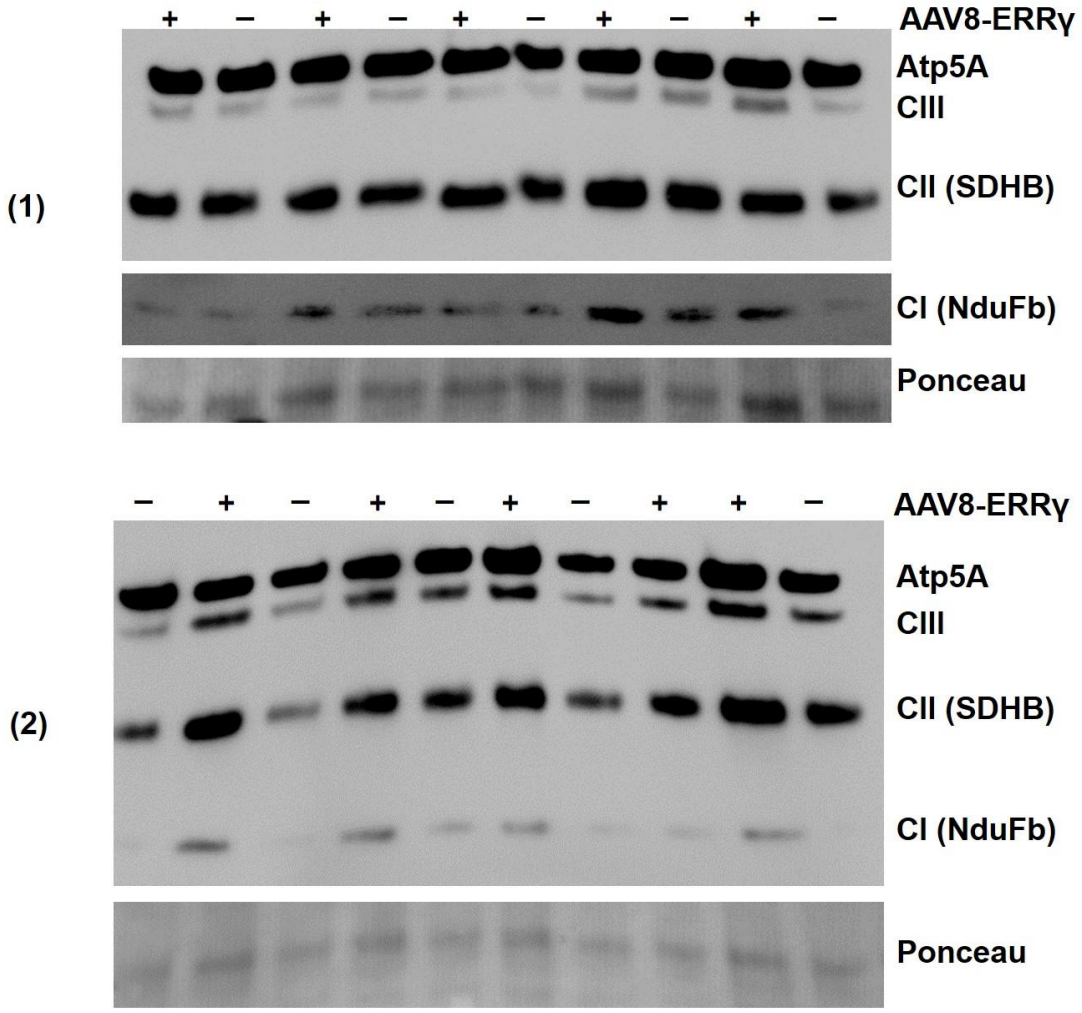

(D)

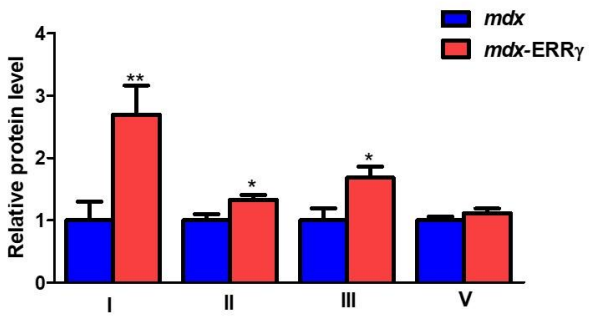

(E) ***mdx* mice treated at 3 weeks-old**

EDL

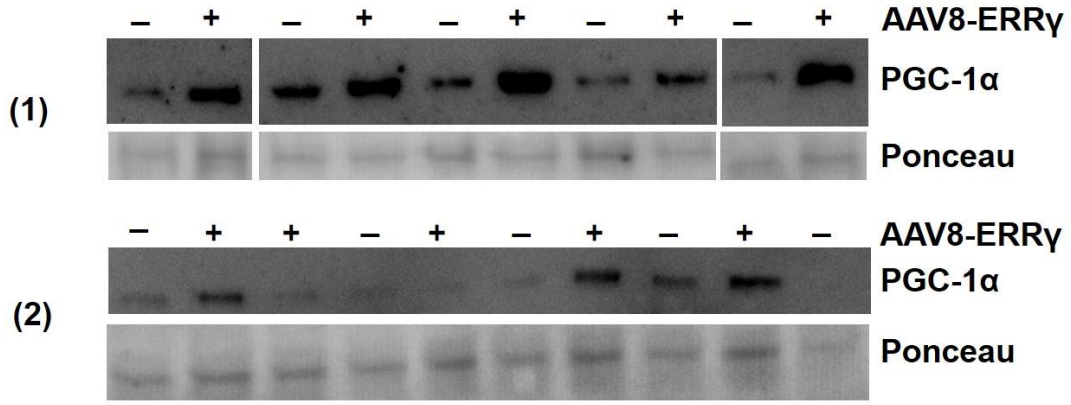

(F)

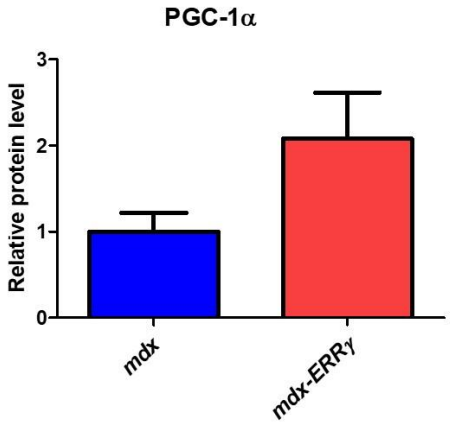

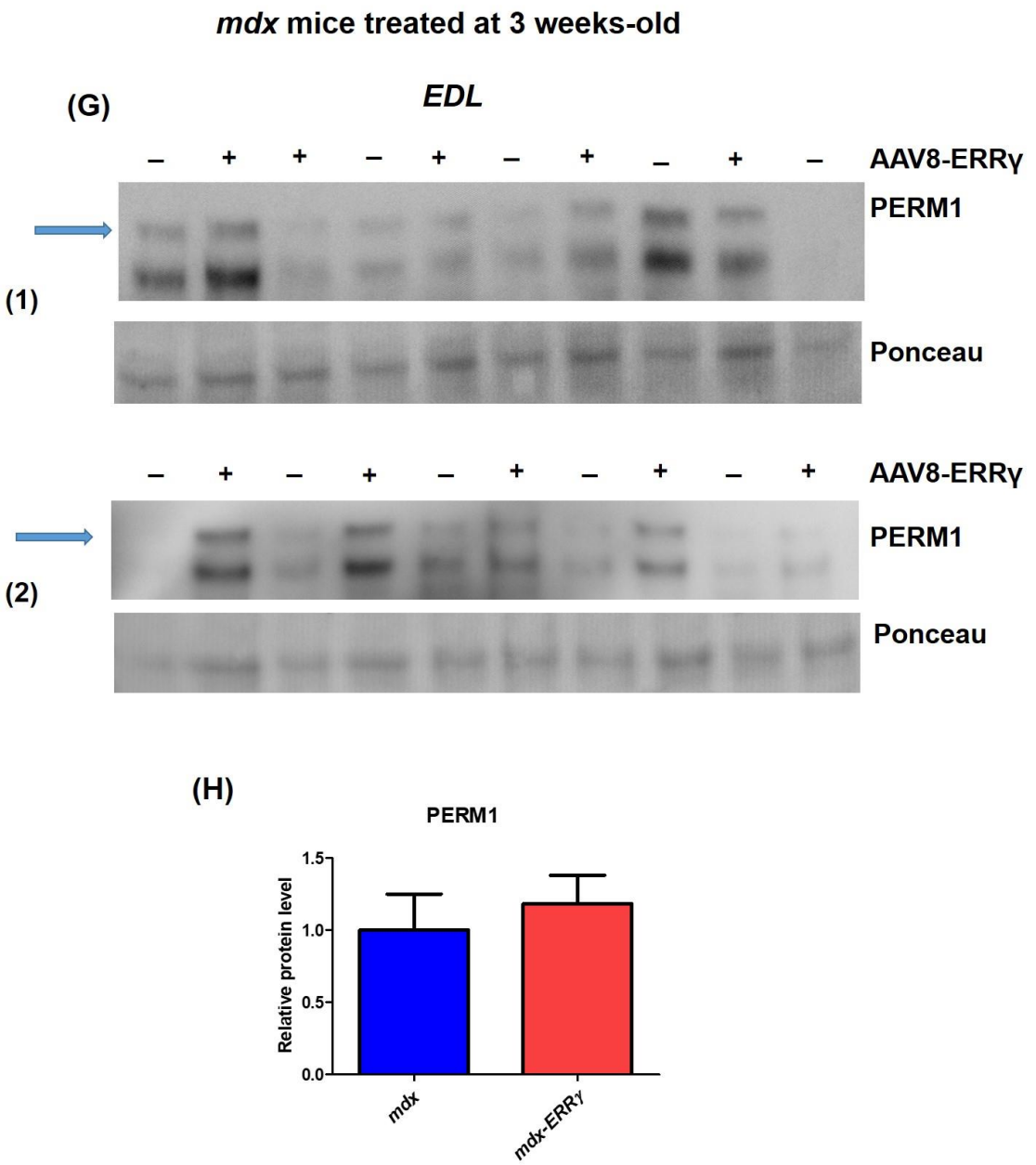

Figure 4.12. The potential of ERRγ over-expression to increase oxidative capacity in *mdx* mice treated at 3 weeks of age

A) The relative abundance of oxidative fibres in *mdx* and *mdx*-ERRγ in 3 weeks study based on quantification of an entire cross section of EDL muscles. Data are expressed as a percentage (%) of total fibres. SDH activity is increased by 60% (p=0.008). B) Relative mRNA expression of the indicated genes related to oxidative metabolism and mitochondrial biogenesis in EDL muscles from 3 weeks study. Atp5 (p=0.07), Cox5 (P-0.903), NduFp (p=0.067), sdhc (p=0.059), sdha (p=0.006), PERM1 (p=0.418), SIRT1 (p=0.249), NRF2 (p=0.621), ND2 (p=0.751), TFAM (p=805), PGC-1α (p=0.006) and utrophin (p=0.155). RNA levels for the indicated genes were determined by qRT-PCR,

normalized to the house-keeping genes; Htatsf1 and Csnk2a2. 30 µg of protein was loaded per lane and Ponceau stain was used for normalization. C) The total OxPhos complex protein was determined using OxPhos complex antibodies. D) The intensity of the bands was quantified using ImageJ software; Atp5, a maker of complex V (p=0.214), complex I (p=0.006), complex II (p=0.013), complex III (p=0.019). E) The total PGC-1α protein was determined by PGC-1α antibody. F) Analysis of PGC-1α bands shows no difference between *mdx* and *mdx*-ERRγ (p=0.07). G) The total PERM1 protein was determined by PERM1 antibody. H) Analysis of PERM1 bands shows no difference between *mdx* and *mdx*-ERRγ (p=0.10), (n=10 *mdx* and *mdx*-ERRγ, un-paired student's t-test).

4.3.4. Increasing expression of ERRγ does not significantly alter myosin isoforms EDL muscles of *mdx* mice treated at 3 weeks old:

To assess the effect of ERRγ over-expression in EDL muscles treated at 3 weeks of age on the fibre type distribution, we used staining of muscle cross section with antibodies against the different MHC isoforms. We found that over-expression of ERRγ has no effect on fibre type composition (figure 4.13).

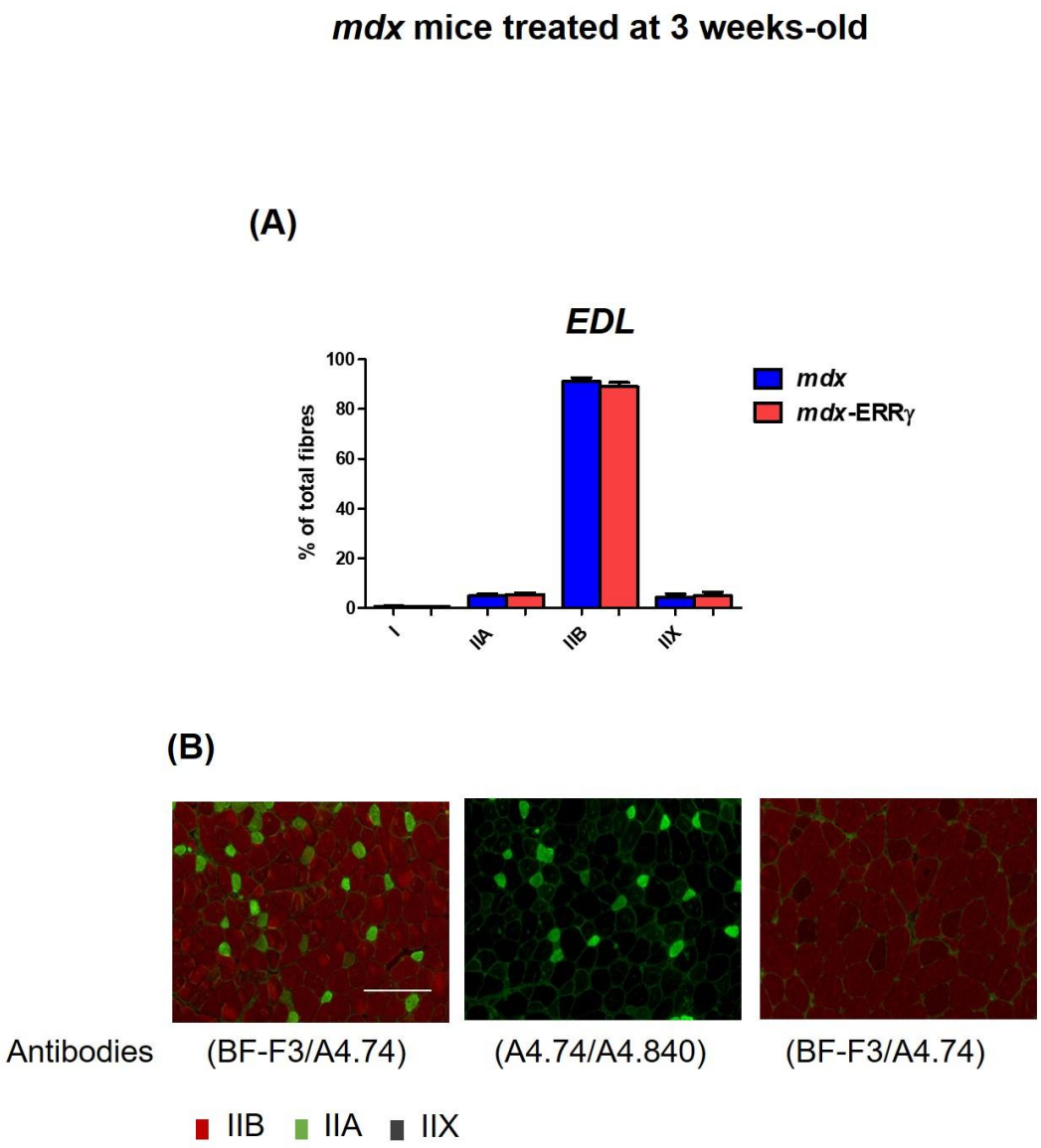

Figure 4.13. Over-expression of ERRγ in 3 week-old *mdx* has no impact on muscle fibre typing

A) The relative abundance of different fibre types in EDL muscles from *mdx* mice treated at 3 weeks old, based on quantification of an entire muscle sections. Myosin heavy chain (MHC) analysis in *mdx* and *mdx*-ERRγ shows no difference in the number of fibre types; type I (p=0.838), IIA (p=0.658), IIB (p=0.388) and IIX (p=0.843). B) Representative images of cross sections show the mid-portion of *mdx* and *mdx*-ERRγ muscles stained with antibodies against MHC isoforms, as indicated. Scale bar, 200 μm, (n=10 for *mdx* and *mdx*–ERRγ, un-paired student's t-test).

4.3.5. Impact of ERRγ over-expression on angiogenesis in *mdx* mice treated at 3 weeks-old:

To evaluate the effect of ERRγ over-expression in angiogenesis, specific primers were used to check the transcript level of genes involved in angiogenesis using qRT-PCR. In addition, muscle capillary density was assessed on muscle sections using the vascular endothelial marker CD31. Interestingly, moderate over-expression of ERRγ in 3 week old treated EDL resulted in 1.6 fold and 2 fold increase in the transcript levels of vascular endothelial growth factors VEGF-165 (p=0.02) and VEGF-189 (p=0.0008), respectively (figure 4.14 A) and a significant increase in the number of capillaries per fibre by 46% increase (p=0.005) (figure 4.14 B-C).

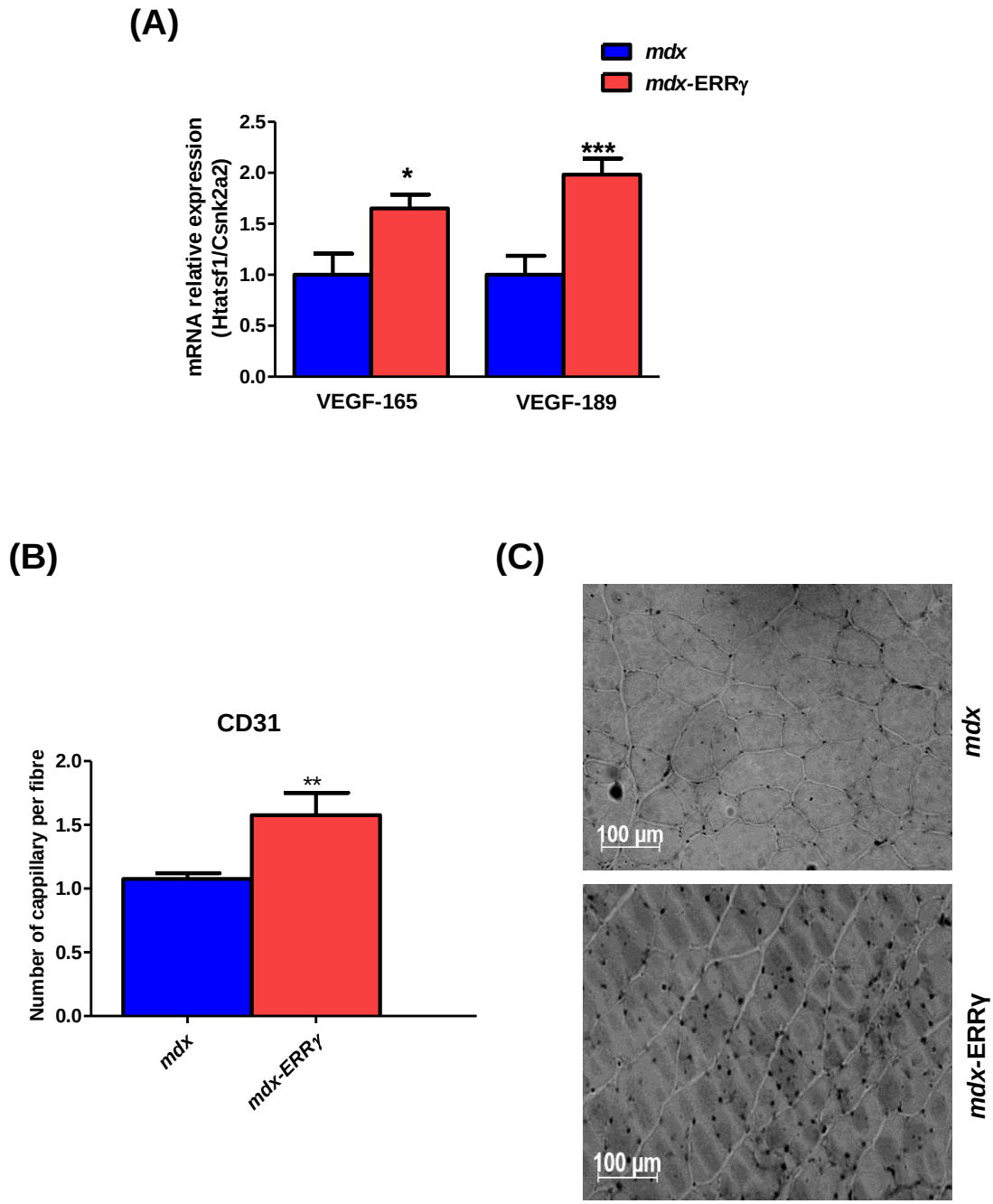

Figure 4.14. Over-expression of ERRγ improves angiogenesis in *mdx* mice treated at 3-weeks old

A) In EDL muscles from *mdx* mice treated at 3 weeks old, expression of VEGF-165 and VEGF-189 increases by 1.8 fold (p=0.02) and 2 fold (p=0.0008), respectively. B) CD31 analysis of capillary number per fibre based on quantification the whole EDL muscle shows 46% increase (p=0.005). C) Representative images of *mdx* and *mdx*-ERRγ EDL stained with CD31 antibody, scale bar, 100 µm, (n=12 for *mdx*, n=10 for *mdx*-ERRγ, un-paired student's t-test).

4.3.6. Reduction in central nucleation following ERRγ over-expression in EDL muscles treated at 3 weeks of age:

Haematoxylin and eosin staining was used to assess whether over-expression of ERRγ has an effect on central nucleation. EDL muscles from mice treated at 3 weeks of age exhibited a 17% reduction in central nucleation following ERRγ over-expression (p=0.006) (figure 4.15).

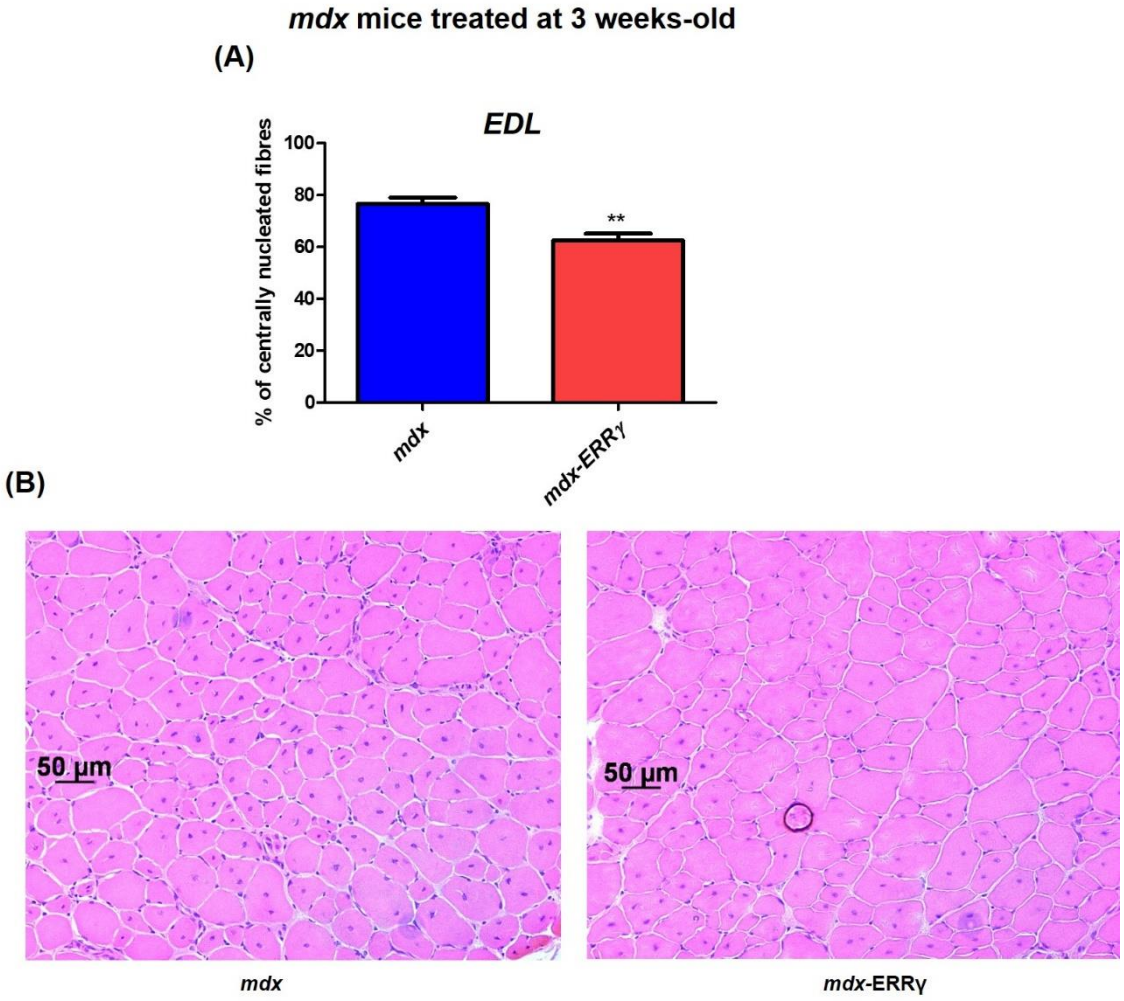

Figure 4.15. Over-expression of ERRγ in *mdx* mice treated at 3 weeks-old reduces central nucleation

A) Percentage of centrally nucleated fibres in *mdx* and *mdx*-ERRγ of EDL muscles from 3 weeks study shows 17% reduction (p=0.006). B) Representative images of cross sections of *mdx* and *mdx*-ERRγ EDL muscles stained with H&E, scale bar, 50 µm. (n=12 for *mdx*, n=10 for *mdx*-ERRγ, un-paired student's t-test).

4.3.7. Effect of ERRγ over-expression on muscle damage in *mdx* mice treated at 3-weeks old*:*

To determine the effect of ERRγ over-expression on muscle damage, serum CK level was assessed. Similar to the previous study, no difference was found in CK level, IgG or MYH-3 positive fibres in EDL treated at 3 weeks of age (figure 4.16).

mdx mice treated at 3 weeks-old

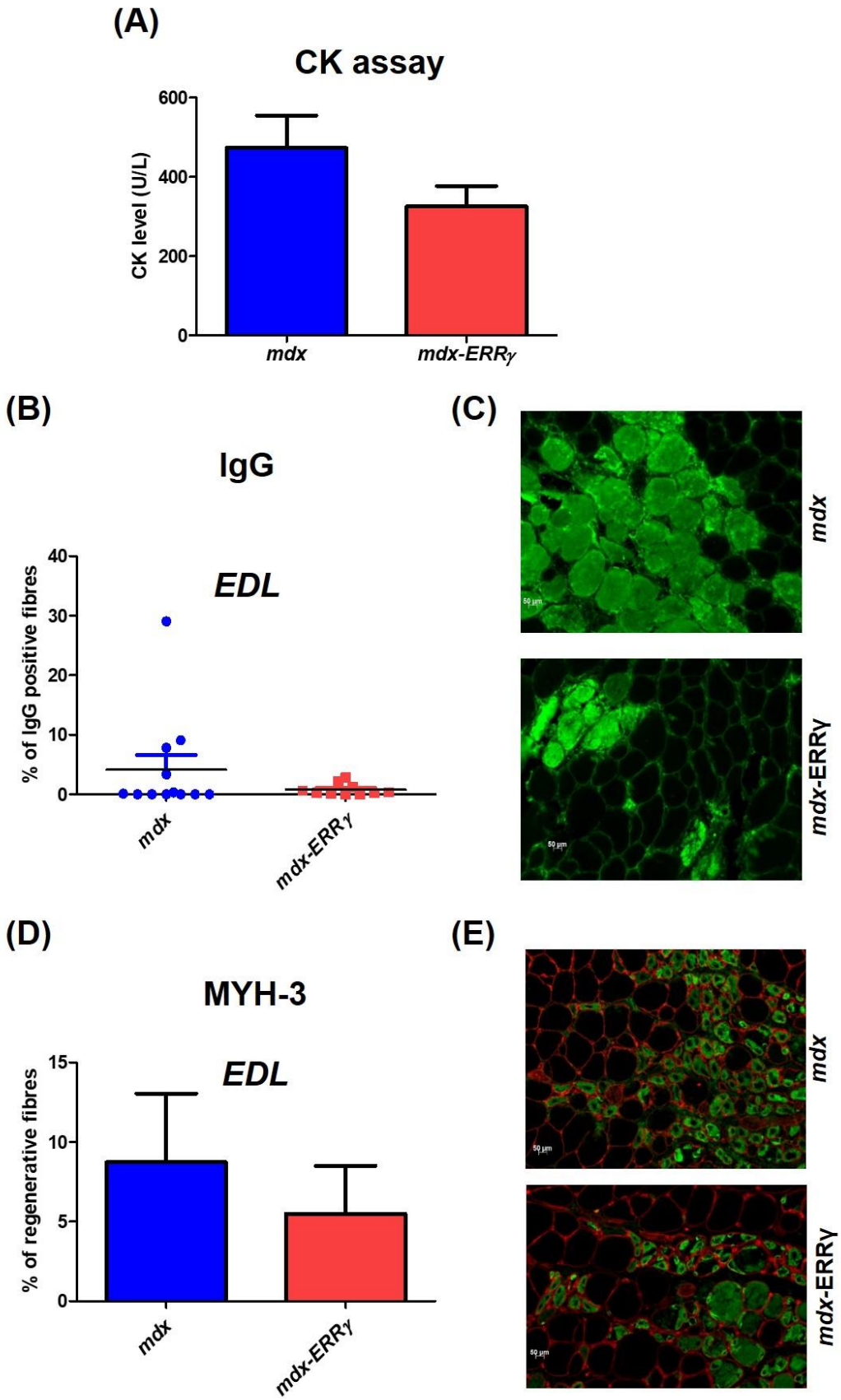

Figure 4.16. ERRγ gene transfer has no effect in CK levels, IgG infiltration or MYH-3 positive fibres in *mdx* mice treated at 3-weeks old

A) Creatine kinase assay measurement shows no difference in the blood serum between *mdx* and *mdx*-ERRγ (p=0.161). B, D) The percentage of IgG and MYH-3 positive fibres in the entire EDL muscles of *mdx* and *mdx*-ERRγ show no difference of the damaged fibres (p=0.228) or MYH-3 positive fibres (p=0.831). C, E) Representative images of cross section of *mdx* and *mdx*-ERRγ EDL muscles immunostained with anti-IgG antibody, anti-MYH-3 antibody, respectively. Scale bar, 50 μm, (n=12 for *mdx*, n=10 for *mdx*-ERRγ, un-paired student's t-test).

4.3.8. Impact of ERRγ over-expression on inflammation, degradation, translation, ubiquitination calcium and antioxidant markers in EDL muscle of *mdx* mice treated at 3-weeks old

EDL muscle was used to assess the relative mRNA expression of inflammatory markers, degradation, translation, ubiquitination, calcium and antioxidant markers using specific primers for qRT-PCR for inflammatory markers; TNF-α (p=0.02), and IL-1β (p=0.04), were increased by 2 fold, whereas IL-6 was increased by 3 fold (p=0.03) and NF-κB was increased by 1.6 fold (p=0.01) with no difference in the expression of IL-10 (figure 4.17 A). None of the autophagy related genes; P62, Beclin-1, Bnip3, apoptotic marker; chathespin-L or atrophy gene; FOXO-1 were affected in the 3 week-old *mdx* (figure 4.17 B). Interestingly, there was a difference found in calcium receptor RYR-1 with 2 fold increase (p=0.03), with no difference in SERCA-1 expression following over-expression of ERRγ (figure 4.17 C). Genes involved in translation showed a decreased expression following ERRγ over-expression. Gadd34 was decreased by 0.26 fold (p=0.025) and 4EBP-1 was decreased by 0.69 fold (p=0.006) (figure 4.17 D). In addition, ubiquitination markers; Atrogin-1 and MuRf-1 were assessed and the transcript level of the latter was increased by 2 fold (p=0.045) (figure 4.17 E). The

expression of antioxidant gene SOD2 in the 3 weeks old *mdx,* tended to be increased but failed to reach significant (*p*=0.051) (figure 4.17 F).

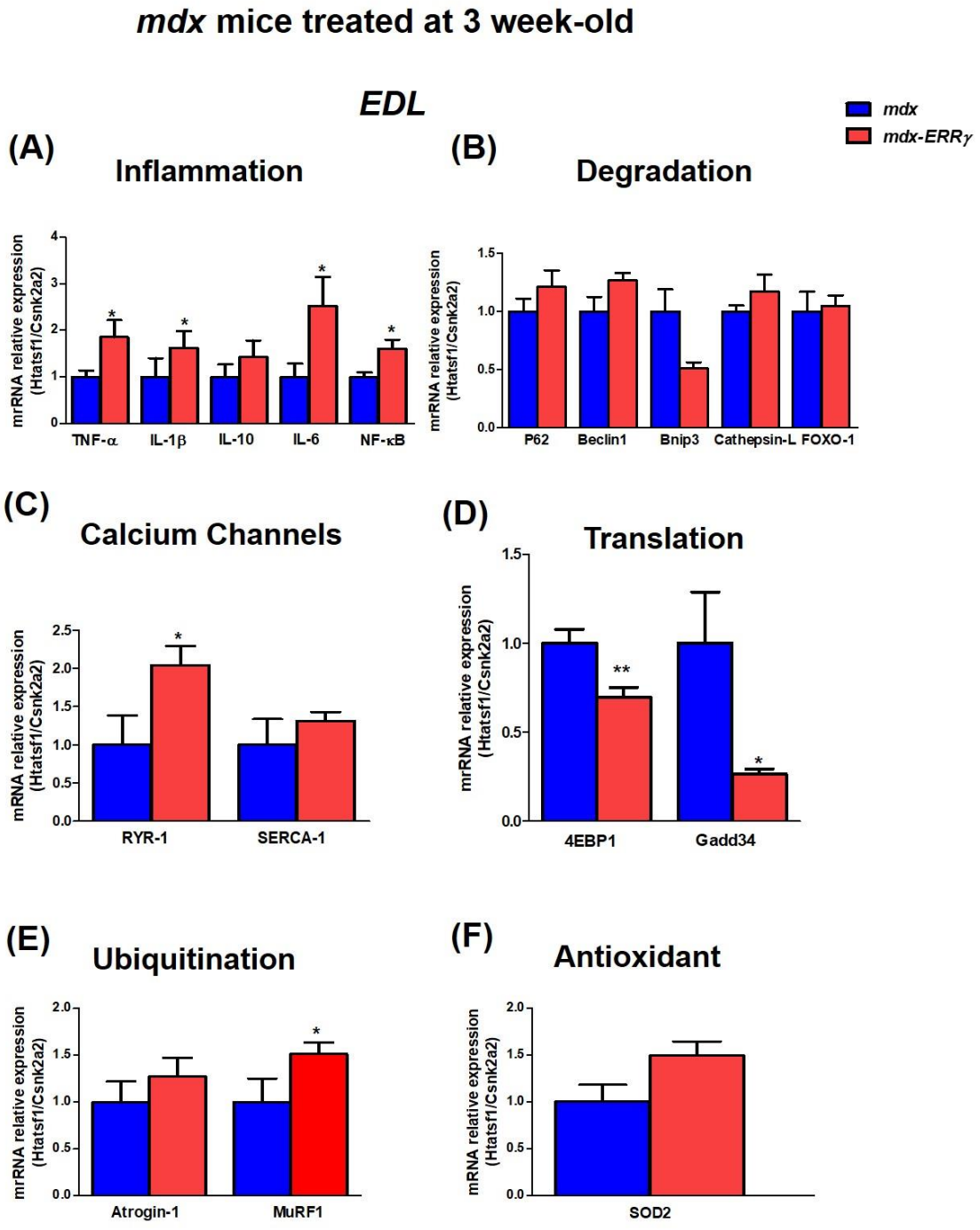

Figure 4.17. Impact of ERRγ over-expression on inflammation, degradation, translation, ubiquitination calcium and antioxidant markers in EDL muscle of *mdx* mice treated at 3-weeks old

Relative mRNA levels in the EDL muscles of *mdx* and *mdx* -ERRγ from 3 weeks study A) Inflammatory markers; 2 fold increase of TNF-α (p=0.02), 2 fold increase of IL-1β (p=0.04), IL-10 (P=0.348), 3 fold increase of IL-6 (p=0.03) and 1.6 fold increase of NF-κB (p=0.01). B) Autophagy markers; P62 (p=0.342), Beclin-1 (p=0.08), Bnip3 (p=0.170), chathepsin-L (p=0.379), FOXO-1 (p=0.807). C) Indicated calcium markers; 2 fold increase in RYR-1 calcium channel (p=0.03), SERCA-1 (p=0.08). D) Relative mRNA levels for the indicated translation markers showed a 0.69 fold decrease of 4EBP-1 (p=0.006) and 0.26 fold decrease of Gadd34 (p=0.025). E) Relative mRNA levels for the indicated ubiquitination markers, Atrogin-1 (p=0.383) and 1.5 fold increase of MuRF1 (p=0.045). F) Relative mRNA levels for the antioxidant marker SOD2 (p=0.051), (n=12 for *mdx*, n=10 for *mdx*-ERRγ, un-paired student's t-test).

Table 4.1. Summary of the data for 3 and 6 week-old *mdx* experiments

			3 week-old Experiment	6 week-old Experiment	
			EDL muscle	EDL muscle	Gastrocnemius muscle
Muscle function	Muscle mass		No difference	No difference	
	specific force		*	No difference	
	maximum force		No difference	No difference	
	CSA		No difference	No difference	
qRT-PCR		ERRγ	**	**	**
	Angiogenesis	VEGF-165	*	No difference	No difference
		VEGF-189	***	No difference	No difference
	Inflammation	IL-10	No difference	No difference	
		1L-1β	*	No difference	
		IL-6	*	No difference	
		TNF-α	*	No difference	
		NF-κB	**	**	
	Mitochondrial biogenesis	PGC-1α	**	No difference	No difference
		TFAM	No difference	No difference	
		ND2	No difference	No difference	No difference
		NRF2	No difference	No difference	
		PERM1	No difference	No difference	No difference
		SIRT-1	No difference	No difference	No difference
		Atp5	No difference	No difference	
		cox5	No difference	No difference	
		NduFp	No difference	No difference	
		Sdhc	No difference	No difference	
	Degradation	FOXO-1	No difference	No difference	
		P62	No difference	No difference	No difference
		Cathepsin-l	No difference	No difference	
		Beclin-1	No difference	No difference	
		Bnip3	No difference	No difference	
	Ubiquitination	Atrogin	No difference	*	No difference
		murf-1	*	No difference	No difference
	Translation	4EBP-1	**	No difference	No difference
		Gadd34	*	No difference	
	Ca+2 receptor	RYR-1	*	No difference	
		SERCA-1	No difference	No difference	
	Antioxidant	SOD2	No difference	No difference	
Pathology	SDH		**		**
	H&E		17% reduction **		8% reduction **
	MYH-3		No difference		No difference
	IgG		No difference		No difference
	MHC		No difference		No difference
	CD31		**		
western blot	ERRγ		*	No difference	*
	PGC-1α		No difference		
	PERM-1		No difference		
	Complex I		**	No difference	
	Complex II		*	No difference	
	Complex III		*	No difference	
	Complex IV		No difference	No difference	

Colour guide: Red=increase, green=decrease, $^{*}p<0.01$, $^{**}p<0.001$, $^{***}p<0.0001$

4.4. Discussion

The only published work on the impact of ERRγ on *mdx* pathology was addressed in transgenic mice, which showed 170 fold over-expression of ERRγ, however, did not permit determination of whether this approach has beneficial effects when initiated after the onset of muscle necrosis (Matsakas et al., 2013). In this chapter, we investigated the effect of postnatal over-expression of ERRγ in skeletal muscle of *mdx* mice and whether the gene delivery helps improving the defects in oxidative metabolism and angiogenesis and thereafter will help in delaying the disease pathology and improving muscle function. Two different ages of *mdx* mice were used in different studies; 6 week old, where mice experience cycles of degeneration and regeneration, consistent with previous work and earlier when mice start to exhibit early signs of muscle injury, at 3 week old, but for longer time.

Over-expression of ERRγ in transgenic muscles of 170 fold is massively high comparing to the modest increase in all examined muscles in these two studies. However, the soleus muscles from 6 week-old *mdx* study, showed no change in the expression of ERRγ. Unchanged expression may be due to low transduction of AAV in soleus muscles which is composed by type 1 and type IIA fibres. A study using AAV8/*lac*Z in utero showed rare transduction of slow-twitch fibres (Koppanati et al., 2009); this demonstrate preferential transduction of AAV8 into fast-twitch muscle fibres.

Muscle from *mdx* mice has been shown previously to experience force deficit due to loss of dystrophin (Brooks and Faulkner, 1988). Here we demonstrated that, EDL muscles from *mdx* mice treated with AAV8-ERRγ at 3 weeks of age showed

an increase in specific force in addition to an increase in oxidative capacity, angiogenesis markers and increased number of capillary density. They also have shown upregulation of inflammatory markers and down regulation of genes involved in translation. On the other hand, although EDL muscles from *mdx* mice treated with AAV8-ERRγ at 6 weeks of age showed similar over-expression of ERRγ, however, no improvement in specific force or any of the other parameters were observed. It is important to mention that gastrocnemius muscles showed the highest level of ERRγ over-expression in the 6 weeks study, therefore, we used it to assess pathology and some of the genes.

It is important to consider that skeletal muscle represents about 40% of body mass. Therefore, under the condition of dystrophic pathology, metabolic rate is decreased compared to the control and varies during mice life. For example, different studies have assessed the effect of *mdx* age on energy requirement. Two studies on 6-12 months old *mdx* showed no difference in energy expenditures (Dupont-Versteegden et al., 1994, Mokhtarian et al., 1996). In contrast, at 4-6 weeks of age, the metabolic rate was less compared to the control, which was attributed indirectly to the increased rate of muscle degeneration and regeneration, disturbance of Ca^{+2} homeostasis, ultimately decreased physical activity. Interestingly, effect of time of intervention on the outcomes of gene therapy was addressed by different studies using AAV mediated expression of PGC-1α. Administration of AAV6-PGC-1α into neonatal or 3 weeks or 12 months old *mdx* resulted into different outcomes, which highlight the effect of time as an essential parameter to account for when discussing the results of gene therapy. For example; AAV-PGC-1α into neonatal *mdx* showed an increased expression of mitochondrial genes and an improvement in muscle

function. On the other hand, no effect on histology or gene expression were observed when the virus administered at 12 months of age. In addition, treated *mdx* at 3 weeks of age with the same vector showed an increase in the genes related to inflammation, metabolism, sarcomere, but no change in the number of fibres with central nucleation. The results of these studies will be discussed throughout this chapter as a comparison to our results and to emphasize the effect of time of intervention on the outcomes obtained in this chapter (Hollinger and Selsby, 2015, Hollinger et al., 2013, Selsby et al., 2012). Further, administration of quercetin into 3 months old *mdx* for 6 months decreased histopathological injury in the heart and diaphragm and decreased inflammation (Hollinger et al., 2015), however, administration for long term showed different outcomes. In a study of 2 months old *mdx*, respiratory function was protected for the first 4-6 months of treatment, but later become insensitive. These results again highlight the importance to consider factors such as age and length of treatment on the outcomes (Selsby et al., 2016).

In dystrophic muscle, oxidative stress leads to mitochondrial dysfunction and to 50% reduction in ATP availability (Kuznetsov et al., 1998, Even et al., 1994). Loss of NO disturb glucose metabolism, as there is a reduced expression of Glut4, responsible for glucose uptake, therefore, represents one of the causes of energy deficit in dystrophy (Olichon-Berthe et al., 1993, Schneider et al., 2018). Reduced ATP production in *mdx* mice has been demonstrated previously to disturb Ca^{+2} buffering and diminish satellite cell repair mechanisms (Onopiuk et al., 2009). It is also associated with a reduction in the ability of a muscle to produce force and altered cross bridge mechanics (Fitts, 1994). Dystrophic mitochondria are more susceptible to damage as they are more fragile at both the inner and outer

mitochondrial membranes (Scholte and Busch, 1980). It is though that mitochondrial dysfunction results from 1) Ca^{+2} overload which lead to inhibition of ATP synthesis and continued permeability of transition pore (PTP) (Ascah et al., 2011). 2) Mitochondrial mis-localization is another reason, as proper mitochondrial localization is important to function. Mitochondrial pool work in a system that allows them to translocate to the sites of increased metabolic demand and they are extremely responsive to changes in regions of intracellular environment. However, loss of dystrophin has negatively impact the localization and density of sub-sarcolemmal mitochondria (Percival et al., 2013). 3) Impaired mitophagy and accumulation of damaged mitochondria that are not perform properly in energy production and have increased chance to undergo opening of PTP complex which leads to mitochondrial swelling, collapse of mitochondrial membrane potential that induce apoptosis (Grumati et al., 2010). All of this leads to further elevation of ROS, which then further impacts on calcium dysregulation and mitochondrial function.

It is well established that mitochondrial ATP synthesis depends on normal respiratory chain function, which is known as the oxidative phosphorylation system that coordinates electron transfer with the proton gradient to generate ATP. Defects in mitochondrial respiratory chain by mean of impaired function of mitochondrial enzymes can cause skeletal muscle weakness in *mdx* muscle (DiMauro, 2006). Here, specific force produced from muscle of 3 week-old *mdx* overexpressing ERRγ was greater than the control. Accordingly, protein levels of mitochondrial protein complex, OXPHOS enzymes as complex (I, II and III) were increased in 3 week-old *mdx*, as well as expression of sdha, which is the active subunit of the SDH enzyme that links two important pathways within

mitochondria; the Krebs cycle and oxidative phosphorylation. As part of the Krebs cycle, sdha converts succinate to fumarate and transfers electron to oxidative phosphorylation (Comim et al., 2016). Succinate dehydrogenase (SDH) enzyme activity in the muscle cross sections were increased in *mdx* mice treated at 3 and 6 weeks of age following 3 and 10 fold over-expression of ERRγ in EDL and gastrocnemius muscles, respectively. Interestingly, lower over-expression of ERRγ in EDL muscles resulted in higher improvement in SDH. The difference in the distribution of muscle fibre types between EDL and gastrocnemius muscles is potentially the reason for this difference, which may affect the response of these fibres to ERRγ over-expression. Using mATPase method, EDL muscles shows predominance with type IIB fibres and a lower proportion of type I fibres. Gastrocnemius muscle has higher proportion of IID fibres and less with type IIB fibres (Cornachione et al., 2011).

Recently, it has been demonstrated that dystrophic muscles exhibit deficiency in the capacity of mitochondrial oxidative phosphorylation, specifically, a deficiency in mitochondrial complex I function, which limit the ATP producing capacity of mitochondrial. The problem was with NADH influx into ETC, whereby NADH is unable to be oxidized by complex I or is being sequestered away from complex I to establish proton motive force (Rybalka et al., 2014, Godin et al., 2012). In addition, *mdx* mitochondrial encountered decreased mitochondrial biomass which underscores loss of ETC function (Rybalka et al., 2014, Percival et al., 2013, Godin et al., 2012). Transgenic over-expression of ERRγ in skeletal muscles of *mdx* mice increase mitochondrial enzyme activity and enhance expression of genes involved in electron transport chain (Narkar et al., 2011, Matsakas et al., 2013). Phenotypic characterization revealed that ERRγ whole

body knockout demonstrated reduced expression of tricarboxylic acid cycle (TCA) and electron transport chain (ETC) complex I enzymes (Alaynick et al., 2007). These results were based on gain-and-loss of function, therefore, we hypothesize that over-expression of ERRγ postnatally will improve expression of defective genes in *mdx* mice. In the study of 3 week-old, mRNA expression of the other nuclear encoded genes NduFp, Atp5, sdhc subunits showed a trend of increase, however, failed to reach significant difference. Moreover, expression of the cytochrome c oxidase Cox5, complex IV, was not different between the two groups in this study. However, discrepancy in the literature about Cox expression has been reported. Kuznetsoz et al., has reported that activity of Cox was reduced in *mdx* quadriceps muscles compared to the control (Kuznetsov et al., 1998). Alternatively, others have reported unchanged activity of Cox in *mdx* and DMD patients (Percival et al., 2013, Sperl et al., 1997, Rezvani et al., 1995). We could speculate that the time for increased Cox expression is not yet to respond to the ERRγ over-expression, or, perhaps the increased expression has peaked earlier, exerted its effect and then reduced to basal level once again. Literatures have reported this type of effect in different fields, for example; AchE expression is time dependent in co-culture of cell line that resemble motor neuron (NG108-15) cells with chick myotubes. The induction reached maximum after 2 days of transfection of luciferase-tagged mouse AchE promoter and then plateau (Jiang et al., 2003). Similarly, C_2C_{12} myoblast treatment with serum shock showed time dependent manner of over-expression of MyoD (myogenic marker), reached maximum over-expression after 16 hours and then lowered to basal level, then upregulated again after 32 hours (Chatterjee et al., 2013). Further, following skeletal muscle injury, markers of immune and satellite cells, factors for muscle

regeneration increased in the early stage of recovery and then all genes returned to normal at 14 days post injury (Xiao et al., 2016). Therefore, we could speculate that similar pattern of expression has occurred in the genes including in this study, where they were overexpressed as a transient adaptation to the over-expression of ERRγ and then return back to basal level.

Furthermore, athletes who stop training after extensive exercise, their muscles show adaptation that maintain the mass and strength of the muscles for some time before complete loss. By assessing SDH activity, analysis showed stabilized SDH activity for the next 12 days of inactivity and then started to reduce (Coyle et al., 1984). In our study, given the improved specific force by 14% and increased protein activity of mitochondrial proteins, it is likely to suggest that the cells are more capable of ATP production and may indicate an increased mitochondrial number or volume. We could also anticipate that over-expression of ERRγ results in the early adaptive responses that have benefits over a more protected time period, which is the increase in specific force. Although, with active cycles of regeneration, the virus has been lost, however, some benefits remains at endpoint. With loss of virus, we can overcome this by the use of the mimetics that overexpress ERRγ, as described in the previous chapter. The virus loss has been addressed previously as one of the major issue encountered with AAV based gene therapy due to the cycles of degeneration and regeneration (Le Hir et al., 2013, Peccate et al., 2016). However, this could be overcome with repeated administration or combined therapy with dystrophin rescue (Peccate et al., 2016, Majowicz et al., 2017). The extent of the metabolic improvements were not seen in 6 week-old *mdx* and so the lack of force improvements. Speculatively, in 3 week-old *mdx*, which showed an increase in specific force, metabolic

improvements increased platform to produce ATP, which possibly match the demand at cross-bridge level and then result in the specific force improvement. Further, increased mitochondrial volume limits the contribution of free radicals and calpain to disease-related muscle injury (Spencer and Mellgren, 2002).

We also assessed the level PGC-1α, co-activator of ERRγ (Sever and Glass, 2013). Interestingly, similar of what has been shown for PGC-1α and other regulators (MEF-2 factors) in skeletal muscle (Hock and Kralli, 2009, Handschin et al., 2003), PGC-1α expression was increased in treated muscles compared to the control in the young treated *mdx*, suggesting the presence of a positive feedback regulatory loop. Despite the increase in the PGC-1α mRNA expression following over-expression of ERRγ in 3 week-old *mdx*, the corresponding protein level was unchanged. This is reminiscent of changes seen in mice fed with resveratrol (Gordon et al., 2013). In contrast to our study, the transgenic mice with 170 fold over-expression of ERRγ has no effect on the expression of PGC-1α (Matsakas et al., 2013). Moreover, this is opposite to what has been shown in myotubes obtained from primary cell line of transgenic muscle of ERRγ, where induction of ERRγ resulted in down regulation of PGC-1α (Rangwala et al., 2010, Matsakas et al., 2013). Hence, these difference between our study and data based on transgenic muscles are possibly due to different level of ERRγ over-expression between transgenic and gene transfer approach. Alternatively, it could be one of these parameter that respond to ERRγ in the first instance and then turn down due to vector loss (Peccate et al., 2016, Majowicz et al., 2017).

As mentioned earlier, there may be a consequence to turn off the expression of these genes that showed no difference, after they did their function (Wan et al.,

2012). Furthermore, massive over-expression does not always lead to an increase in the other family members or genes in the same pathway. They may work in an independent or dependent manner as shown in the family of orphan receptors. For example; ERRs are shown to work in a compensatory manner in heart, where ERRγ is upregulated in ERRα-null mice. Also, a complete inhibition of individual ERR isoform does not prevent mitochondrial biogenesis or activity due to presence of a compensatory mechanism through increased expression of other isoforms (Murray et al., 2013, LaBarge et al., 2014).

In addition to measuring oxidative gene expression, we also assessed PGC-1α pathway change because of increased expression of PGC-1α. However, expression of genes involved in mitochondrial biogenesis (SIRT1, NRF2, ND2 and TFAM) were not affected with the over-expression of ERRγ in our study, possibly due to the fact that ERRγ over-expression is not sufficient to induce such changes or alternatively, these genes were overexpressed at some point, establish an effects and then return back to basal levels. For example; ND2 was shown to increase after 2 hours of CBD treatment. However, at a 24 hour timepoint, its expression return back to control levels (Foster *et al*, personal communication).

SIRT1 is working upstream of PGC-1α, and its expression has been shown to increase following over-expression of PGC-1α by AAV gene transfer in neonatal *mdx* (Selsby et al., 2012). It is generally thought that induction of mitochondrial biogenesis is under the control of transcriptional coactivators PGC-1α and PGC-1β which control the binding of their downstream factors (nuclear respiratory factor); NRF-1, NRF2 (GABP) and ERRα to the promoter of nuclear genes

encoding regulators of oxidative phosphorylation and mitochondrial replication and transcription (TFAM) (Hock and Kralli, 2009, Scarpulla et al., 2012). To test the general changes in mitochondrial biogenesis we measured expression of NRF-2, which was unchanged, may explain unchanged expression of TFAM. In muscle, NRF-2 is believed to control transcription of utrophin gene (Angus et al., 2005). Consistent with this, expression of utrophin was unchanged. Similar to what has been shown in transgenic muscle of ERRγ, where no increase in the localization of utrophin in the sarcolemma (Matsakas et al., 2013). However, activity of PGC-1α is not controlled by increased in protein level only but also through post translational modification (PTM), acetylation, therefore, the expression of PGC-1α target TFAM was unchanged as the activity of PGC-1α protein was not changed. As there is no increase in the mitochondrial biogenesis related genes; ND2, NRF2 and TFAM, in the presence of an increase in the activity of mitochondrial proteins involved in electron transport chain, we could speculatively suggest there is no difference in the mitochondrial number but the function or performance of mitochondria was improved and therefore cause ability to meet cellular ATP demand; given that muscle oxidative capacity not only relies on mitochondrial density but also on mitochondrial function.

Skeletal muscle has mitochondria located beneath the sarcolemmal membrane (subsarcolemmal, SSM) or between the myofibrils (intermyofibrillar, IMF) (Hoppeler and Flueck, 2003). It was demonstrated that despite the reduction in the density of the SSM content, there is no significant difference in the total mitochondrial content between dystrophic muscles and the control. Moreover, the disruption in SSM localization promotes mitochondrial inefficiency and reduce mitochondrial ATP-generating capacity. Therefore, the reduction in energy

available was not due to a reduction in mitochondrial number, per se (Percival et al., 2013, Even et al., 1994, Rybalka et al., 2014, Kuznetsov et al., 1998). Generally, it was demonstrated that mitochondrial performance depends on number, activity and energetic efficiency (Crescenzo et al., 2015). Therefore, unchanged expression of genes associated with mitochondrial biogenesis does not conflict with the improvement of mitochondrial efficiency as it is possible that specific population of mitochondria may be more responsive to ERRγ over-expression. In further studies, the use of mitochondrial fraction rather than the total mitochondria will address this question as whether ERRγ over-expression has specific effect on each population of mitochondria in term of number and performance.

PERM1 has been shown to act as a downstream effector of PGC-1α and ERRs and it is required for maximal oxidative capacity by upregulating genes related to mitochondrial biogenesis (Cho et al., 2013). Unexpectedly, over-expression of ERRγ did not increase the transcript or protein level of PERM1, possibly because the effect of ERRγ over-expression is not sufficient or its expression in *mdx* mice was not decreased to the level that require an upregulation by ERRγ. Further analysis including wild type mice will add more clarity on the level of this gene in dystrophic muscle.

In many transgenic mouse models, an increase in muscle oxidative capacity is closely associated with a shift towards more oxidative muscle fibre type. For example; muscle specific over-expression of ERRγ, PGC-1α, PGC1-β and PPARδ showed increased number of type I, IIA, IIX and a decrease in type IIB (Matsakas et al., 2013, Rangwala et al., 2010, Lin et al., 2002, Arany et al., 2007,

Wang et al., 2004). In addition, rescue of dystrophic muscle by AAV-PGC-1α over-expression in neonatal *mdx* involves fast to slow fibre shift (Selsby et al., 2012). In contrast, postnatal over-expression of ERRγ at 3 weeks of age in *mdx* mice showed enhanced oxidative capacity but no changes in fibre type composition. The lack of change is expected as other studies were performed on transgenic mice; for example transgenic overexpression of PGC-1α, which is known to promote expression of type I and IIa fibres (Lin et al., 2002). As there was no shift towards slow oxidative fibres, we did not observe an increased expression of utrophin which is highly expressed in slow oxidative fibres (Chakkalakal et al., 2003). Since the increase in ERRγ in the current studies are moderate and postnatally compared to other transgenic models where the increase of different transcription factors take place throughout development, possibly the effect of ERRγ is restricted to specific target genes for example; mitochondrial protein to improve energy production, angiogenesis genes but not towards the genes controlling fibre typing.

Besides enhancing oxidative capacity, over-expression of ERRγ in 3 week-old *mdx* showed enhanced vascularisation, which has been seen previously as a muscle adaptation in response to endurance exercise (Chinsomboon et al., 2009). ERRγ increased expression of VEGF-165 and VEGF-189, factors important for angiogenesis (Tammela et al., 2005b). This change suggests that ERRγ promotes angiogenesis to meet the increased muscle oxidative capacity. Alternatively, the oxidative stress in these cells is reduced so metabolic stress is reduced. We could suggest that over-expression of ERRγ has similar effect in vascularisation as seen in mice with transgenic over-expression of PGC-1α, PGC1-β or ERRγ (Arany et al., 2008, Chinsomboon et al., 2009, Narkar et al.,

2011). VEGF over-expression-induced angiogenesis has been show to promote regeneration which is possibly helps in delaying the disease progression (Messina et al., 2007).

In the context of force production, it has been demonstrated that *in vivo* over-expression of VEGF-165 in wild type mice following ischemia decreased skeletal muscle cell apoptosis suggesting a role in muscle cell survival. In addition, *in vitro* over-expression of VEGF-165 in C_2C_{12} cells induced myoblast cell migration possibly by activating signalling which modulate migration (Germani et al., 2003). Messina et al., has demonstrated that over-expression of VEGF has a powerful effect on muscle from *mdx* mice, in which increased number of myogenic positive satellite cells and developmental myosin heavy chain cells suggested a regenerative effect of VEGF. Importantly, VEGF over-expression enhanced forelimb strength (Messina et al., 2007). The question is how increasing angiogenesis marker following ERRγ over-expression may contribute to increased specific force in 3 week-old *mdx*. The fact that studies have demonstrated an association between angiogenesis and myogenesis by an interaction between vascular cells and myogenic progenitor cells and there is a correlation between number of capillary and the number of stem cells (SC) associated with the same myofibre (Latroche et al., 2017). We could anticipate that the angiogenesis markers improve the capacity of SC to activate and proliferate through its regenerative effects. However, because no difference in the percentage of MYH-3 was observed in these mice, we excluded the increase in the repair. Therefore, the increase in the angiogenesis marker could be a response of increased metabolic demand. Alternatively, these stem cells will possibly give rise to myogenic precursor cells (MPCs) that express Pax7 and

then Myf5 and MyoD. These MPS will differentiate and fuse to form new myofibre or fuse to existing damaged fibres (Yin et al., 2013). Later, it is possible these newly formed myofibres exhibit increased expression of sarcomeric protein that maintain muscle contraction. Therefore, increasing expression of angiogenic markers in this study following over-expression of ERRγ may play a role in enhancing muscle function. Interventions that increase vascular density such as exercise is beneficial in the management of muscle ischemia to recruit more blood vessels and enhance the reparative re-vascularisation and reperfusion (Ding et al., 2004, Cheng et al., 2010). ERRγ has been demonstrated previously to reverse muscle ischemia by remodelling the myofibres to be more oxidative, which express high levels of angiogenic factors and increased blood flow (Matsakas et al., 2012). In this study, we showed an increase in the capillary density, which is a measure of neoangiogenesis (Al Haj Zen et al., 2010). Therefore, it is likely to reduce ischemia, which is considered one of the causes of muscle weakness in dystrophic muscles as it impairs recovery from fatigue (Allen et al., 2016). The fact that increased ischemia is associated with reduced activity of electron transport chain complex that impair the ETC, resulting in decreased ATP production, reduction of oxygen, that affect antioxidant system and increase ROS, all make cells more susceptible to oxidative stress (Rouslin, 1983). Speculatively, improved ischemia following increased capillary density and increase activity of mitochondrial complex in 3 week-old *mdx* will reduce metabolic stress, increase the level of ATP available for excitation-contraction-coupling and increase force production.

Defect in vasoconstriction response triggered by muscle-derived NO due to miss-localization of nNOS is observed in *mdx* during muscle contraction resulting in

muscle ischemia (Froehner et al., 2014). In this respect, sildenafil, a phosphodiesterase type 5 inhibitor (PDE-5) was shown to improve blood flow in muscle and improve diaphragm force production by enhancing the NO-cGMP signalling pathway (Percival et al., 2012). NO is known to directly involve in modulation of excitation-contraction coupling and nNOS is the main source of NO in skeletal muscle. Targeting nNOS was shown to be remarkable effective in improving muscle function by using modulated form of nNOS in *mdx* mice (Rebolledo et al., 2016) and clinical trial on inducing NO signalling resulted in improving muscle function in DMD patients (Hafner et al., 2016). In consistence to our finding, transgenic over-expression of nNOS in *mdx* reduce central nucleation without restoring utrophin expression (Wehling et al., 2001). We could speculate that improving muscle function following over-expression of ERRγ occurs in part via restoration of nNOS and NO signalling. Improving angiogenesis and its impact on myogenesis is a new player and a potential therapeutic target in DMD research that should be considered in the future studies.

In *mdx* mice, centrally nucleated fibres are considered an index of muscle fibre regeneration (Ferrari et al., 1998). Our results showed fewer centrally nucleated fibres in 3 week and 6 week old treated *mdx* which suggested less regeneration and hence less damage in these muscles overexpressing ERRγ. However, fibres infiltrated with IgG, embryonic myosin positive fibre and CK level were not decreased in the treated muscles likely due to the high variability between the muscles and possibly due to unchanged level of utrophin expression. Intensive studies were targeted to rescue muscle damage either by dystrophin or utrophin replacement (Rafael et al., 1994, Hirst et al., 2005, Rafael et al., 1998, Tinsley et al., 1998, Phelps et al., 1995). In contrast to our study of young mice, over-

expression of PGC-1α in 3 week-old *mdx* induced utrophin expression with no change in central nucleation (Hollinger et al., 2013). Here, the reduction in central nucleation in both studies following over-expression of ERRγ could indicate a beneficial reduction in muscle cell degeneration or damage or a reduction in muscle regeneration. Previous nNOS-null mice studies showed that CK level were unaffected even though central nucleation was reduced (Froehner et al., 2014), being consistence with both studies discussed in this chapter. The fact that ERRγ carried out at different ages complicates the interpretation of these data. The possible explanation here is that reduced central nucleation in 6 week-old *mdx* results from reduced regeneration. However, in 3 week-old *mdx*, the reduction is possibly results from reduced degeneration, which is supported by the increase in angiogenesis and inflammation markers, known to involve in regeneration and repair (Palladino et al., 2013, Arsic et al., 2004, Li et al., 2005, Karin and Clevers, 2016, Wynn and Vannella, 2016).

Inflammation plays a critical role in the development of pathology of DMD. Disruption of DGC components results in activation of innate immune system and inflammatory signalling pathway that ultimately lead to degeneration and progressive muscle weakness (Evans et al., 2009b). In the study of 3 week-old *mdx* but not in 6 week, over-expression of ERRγ resulted in an increase in the transcript levels of NF-κB, TNF-α, IL-1β and IL-6 with no effect on IL-10. We anticipated the unchanged expression of IL-10 to the effect of intervention time. It is possible that with upregulation of other pro-inflammatory cytokines, it is not the time for this anti-inflammatory cytokine to upregulate. Although, TNF-α is known as pro-inflammatory cytokine, it is thought to have a maintenance role in the muscle fibre where the level of TNF-α was found to be higher in regenerating

muscle fibres. It was hypothesized that generation of double knock out mouse for TNF-α (TNF-*mdx*), would improve pathology associated with dystrophin mutation. However, the results obtained from that model was unexpected as the body weight was reduced and serum CK level and whole body strength was unaffected, suggesting that depletion of TNF-α would be compensated by upregulation of other inflammatory cytokines (Spencer et al., 2000). Speculatively, depletion of *TNF-*α will minimize the level of regeneration which emphasize that at certain point in *mdx* mice life, there is a need to upregulate the level of pro-inflammatory cytokines in order to repair the muscle damage. Moreover, eliminating total TNF-α expression contributed to pathological progression in *mdx* diaphragm muscles (Grounds and Torrisi, 2004). Since differentiating myoblast was shown to increase the release of TNF-α that is correlated with regenerating activity (Chen et al., 2007) and ERRγ is essential in regulating myogenesis (Murray et al., 2013), it is potentially possible to suggest that myogenesis promoted by over-expression of ERRγ is associated with increased level of TNF-α.

IL-6 has both pro and anti-inflammatory properties, involves in inflammation, regulation of regeneration and anti-inflammatory processes by acting through two signalling pathways (Scheller et al., 2011). In one hand, blocking IL-6 with a monoclonal antibody in *mdx* mice led to an increase in muscle inflammation suggesting IL-6 has an anti-inflammatory effect possibly by mediating muscle repair, however, without improving muscle function (Kostek et al., 2012). Further, blockade of IL-6 attenuated the dystrophic pathology of *mdx* mice (Pelosi et al., 2015). In support to anti-inflammatory role of IL-6, it has also been reported to involve in muscle regeneration by inducing myoblast differentiation (Serrano et

al., 2008). Treating various cells for 48 hours with IL-6 results in a significant induction of VEGF, which highlight a role of IL-6 in angiogenesis pathway (Cohen et al., 1996). Therefore, we could suggest a link between increasing mRNA expression of VEGF-165 and VEGF-189 and increased capillary density in 3 week-old *mdx* study, as these changes are a consequence to the increased level of IL-6.

Then, increasing expression of IL-1β has been shown to stimulate hypoxia-inducible factor 1α (HIF-1α), resulting in increased expression of VEGF (Silvestre et al., 2000). Therefore, we may suggest a link between increased expression of IL-1β in 3 weeks study and improved angiogenesis markers. However, all of these interactions require further investigation via assessing HIF-1α to elucidate any direct link between them. Further, growing body of evidence suggested that IL-6 is regulated, in part, by IL-1β through MAP kinase activity as shown in C_2C_{12} cells, treated with IL-1β (Luo et al., 2003a), which may suggest a link between IL-1β and IL-6 over-expression in EDL muscles of 3 weeks study.

IL-10 works as anti-inflammatory cytokine through deactivating M1 macrophages and activating M2 macrophages, which promote angiogenesis and repair, whereas M1 macrophages produce pro-inflammatory cytokines. IL-10 null mutation causes severe reduction of muscle strength possibly due to imbalance between M1 and M2 that may affect muscle repair process (Arnold et al., 2007, Villalta et al., 2010). However, its expression was unaffected by the over-expression of ERRγ, possibly because other cytokines were upregulated and compensate for its role in regeneration. Noteworthy, immune pathology in dystrophic muscle is complex in which full immunological repair, the transition

from M1 to M2 phenotype, is never achieved due to on going asynchronous damage.

A PCR array on muscles from transgenic mice overexpressing ERRγ showed increased expression of IL-6 and IL-1β (Matsakas et al., 2013). Similarly, over-expression of PGC-1α in *mdx* mice via gene transfer approach resulted in increased expression of the same cytokines; TNF-α, IL-6 and IL-1β (Hollinger et al., 2013, Selsby et al., 2012). Likewise, we are reporting similar results following over-expression of ERRγ. These results suggest the possibility that increased inflammation pathway is a direct result of increased these two genes (ERRγ and PGC-1α). All studies of AAV-PGC-1α were recovered 3 weeks post administration, which means the upregulation of inflammatory cytokines was not due to the virus infection per se. Therefore, despite using saline as a control in our studies, the upregulation in the pro-inflammatory cytokines here could not be a result of virus infection because the recovery time in our study was 6 weeks post administration. Also, reports have showed that PGC-1α over-expression activate NF-κB by phosphorylation (Olesen et al., 2012). Whether ERRγ has same effect since they share same target genes, it is for future work to investigate.

Moreover, accumulative evidence suggests an association between inflammation and angiogenesis as a protection against exacerbated pathology. In *mdx* mice; ischemia, hypoxia and inflammation are considered as stimuli of angiogenesis (Shweiki et al., 1992, Silvestre et al., 2000). We could suggest a link between increasing angiogenesis and inflammation markers reported in the same study of overexpressing ERRγ at 3 weeks of age, where these

inflammatory cytokines (TNF-α, IL-1β and IL-6) stimulate expression of angiogenesis following over-expression of ERRγ. Oriana del Rocío Cruz-Guzmán et al., has reported an association between the level of inflammatory cytokines and muscle function in DMD patients. Patients with improved muscle function, they showed increased level of inflammatory cytokines (TNF-α, IL-1β and IL-6) (Cruz-Guzmán et al., 2015). Speculatively, increasing expression of (TNF-α, IL-1β and IL-6) in young mice study could be associated with improved specific force.

However, none of these changes were observed in the study started at 6 weeks of age, in which force was not changed, except the increase of NF-κB, which is expected in dystrophic environment. Since the early life of the *mdx* mouse (3-12) weeks of age is considered the period of highest level of necrosis and inflammation (Grounds et al., 2008), assessing the potential of ERRγ to remodel the cytokines level is appropriate. As we determine the effect at one time point is a limitation in each study, further studies by cell sorting on fresh tissues to quantify inflammation precisely could address the direct effect of ERRγ on inflammation.

The rapid release of Ca^{+2} from the sarcoplasmic reticulum through the ryanodine receptors induces the contraction of myofibrils and the re uptake of Ca^{+2} by the Ca^{+2}ATPase (SERCA pump) induces relaxation. Precise balance between Ca^{+2} release and uptake is required to maintain the functioning of contraction/ relaxation process (Berchtold et al., 2000). In *mdx* mice, a functional defect was identified in the RYR-1 receptor, which contributes to altered Ca^{+2} homeostasis in dystrophic muscle. S-nitrosylation of RYR-1 in dystrophic muscles lead to

depletion of calstabin-1 (FKBP12) from RYR-1. Calstabin-1 is a calcium channel stabilizing binding protein. Deletion of calstabin-1 specifically in skeletal muscle has been shown to cause a loss of depolarization-induced contraction and impaired excitation-contraction coupling because of reduced maximal voltage-gated SR Ca^{+2} release (Tang et al., 2004).

Moreover, in *mdx* mice there is evidence of reduced levels of SERCA-1 expression and impaired capacity of Ca^{+2} pumping by SERCA-1 which leads to impaired Ca^{+2} removal from the sarcoplasm (Divet and Huchet-Cadiou, 2002, Kargacin and Kargacin, 1996). Over-expression of SERCA-1 has been shown to mitigate the dystrophic disease pathology in *mdx* mice as well as the muscle damage induced by contraction (Quinlan et al., 1992, Goonasekera et al., 2011). In our study there is a trend of increased expression of SERCA-1 in *mdx* mice treated with AAV8-ERRγ at 3 weeks of age, however, did not reach a significant difference. In contrary to our results, transgenic over-expression of PGC-1α showed decreased expression of SERCA-1 and RYR-1, which resulted in reduced maximal force production following chronic exercise (Summermatter et al., 2012). Speculatively, we could suggest that the increase in specific force in 3 week-old *mdx* following over-expression of ERRγ may be due to the alteration in the expression of RYR-1 which then involve in the correction of Ca^{+2} handling and reduce the level of ROS. As a result, the stress of reactive nitrogen species (RNS) is reduced and muscle force is subsequently increased. On the other hand, there was no change in the expression of these calcium receptors in 6 week-old *mdx* treated with AAV8-ERRγ, which in away correlated with unchanged muscle function. Further investigation on the effect of ERRγ over-expression on Ca^{+2} handling mechanism is required.

Antioxidant gene expression such as catalase, superoxide dismutase 1 (SOD1), superoxide dismutase 2 (Sod2) (Hollinger and Selsby, 2015) and glutathione (Lu, 2013) were decreased in dystrophic muscle compared to healthy muscle. We demonstrated that expression of (SOD2*)*, a mitochondrial antioxidant enzyme showed a trend of increased expression following over-expression of ERRγ, however, failed to reach significance in 3 week-old *mdx*. Comparable to our result, inducing expression of PGC-1α in *mdx* muscle via AAV at 12 months showed no effect on SOD2 expression (Hollinger and Selsby, 2015). It is possible that level of oxidative stress in the 3 week treated mice has already been reduced through reducing metabolic stress, reducing central nucleation fibres and increasing expression of calcium release channel (RYR-1), hence, no need to increase expression of antioxidant, SOD2 at the same time. In response to oxidative stress, NRF-2 is activated as a general regulator of antioxidant genes (Zhang et al., 2015). Since the expression of NRF-2 was unaffected following over-expression of ERRγ in 3 weeks study, it supports this argument of reduced oxidative stress in these mice. Interestingly, resveratrol induced upregulation of SOD1 but not SOD2 in *mdx* mice when treated at 9 weeks of age (Hori et al., 2011), which attract the attention of investigating other antioxidants to clarify the direct effect of ERRγ over-expression on ROS and detoxifying enzymes and highlight the importance of intervention time and length of studies as these factors lead to different outcomes.

In the past few years, studies have started to emerge on impaired autophagy in DMD as evidenced by the presence of swollen mitochondrial, protein aggregation and distension of sarcoplasmic reticulum (Culligan et al., 2002) and activation of Akt signalling in *mdx* muscles (Dogra et al., 2006) and DMD patients (Peter and

Crosbie, 2006). Activation of Akt-mTOR pathway resulted in inhibition of related autophagy pathways (Dogra et al., 2006, Peter and Crosbie, 2006). Other studies based on pharmacological treatment of *mdx* with AICAR, an agonist of the energy sensor AMPK, resulted in activation of autophagy through inducing activity of LC3 that further impact on improving mitochondrial integrity via increased resistance to PTP opening and improve muscle structure and function (Pauly et al., 2012). Moreover, PGC-1α over-expression through gene transfer into 3 week-old *mdx* enhanced expression of LC3 and Atg12 (Hollinger et al., 2013). As ERRγ share similar target genes with PGC-1α, it was expected that over-expression of ERRγ gene transfer may perform a similar function. Conversely, assessing the expression of genes involved in autophagy showed no effect of ERRγ over-expression on any of these genes. However, a debate exists as Spitali et al., has reported that protein levels of autophagy marker in *mdx* are similar to wild type mice and the regulation of autophagy in *mdx* mice is dependent on the muscle type, where glycolytic muscles exhibit greater autophagy process in terms of vesicles formation than the oxidative muscles (Spitali et al., 2013). Therefore, further investigation of other muscles is required to elucidate the role of ERRγ in autophagy. On other hand, a low protein diet was shown to reactivate autophagy and normalize the level of Akt and mTOR signalling and resulted in recovery of muscle function in *mdx* (De Palma et al., 2012).

Forkhead box O (FOXO-1) transcription factor has been shown to regulate oxidative stress by promoting cellular antioxidant defence. Evidence has shown a role of FOXO-1 in the induction of autophagy process (Zhao et al., 2010). Deletion of FOXO-1 led to defective stem cell number and activity that was associated with increased accumulation of ROS (Tothova et al., 2007). Our

results in both studies showed no change the transcript level of FOXO-1. Similarly, following over-expression of PGC-1α into 12 months old *mdx*, the transcript level of FOXO-1 remain unchanged (Hollinger et al., 2013). Matsakas *et al*., showed the expression of FOXO-1 in *mdx* mice is less than C57BL and increased in the transgenic mice of ERRγ (Matsakas et al., 2013). Compared with the 3 fold modest increase of ERRγ in EDL muscles of both studies including in this chapter, 170 fold increase in the ERRγ over-expression in transgenic muscle compared to the control is possibly the reason of this different change. Therefore, it is necessary to assess the activity of these signalling pathways in order to draw a clear conclusion on the effect of ERRγ on autophagy and muscle function.

Atrogin-1 (F-box only protein 32, FBXO32) and Muscle RING finger-1 (MuRF1) are two main markers of muscle atrophy and mice which lack either of them are considered resistance to atrophy (Sandri et al., 2013). They are both upregulated in muscular dystrophy where they are negatively regulated by AKT kinase (Sandri et al., 2004). MuRF1 is a muscle specific ubiquitin ligase which ubiquitinates and targets damaged proteins for degradation by the 26S proteasome, showed an increased expression in the study of 3 week old *mdx* but not in 6 weeks study. Previously, MuRF1 was found to increase following exercise suggesting increased proteasome-mediated proteolysis and increase in unfold protein response (UPR) flux (Pasiakos et al., 2010). Therefore, it is possible that transcript increase in the level of MuRF1 following ERRγ over-expression is an adaptive response for the increase in oxidative capacity which resulted in an increase in ROS as a normal result of enhanced oxidative capacity. In addition, NF-κB expression was enhanced in the same study, it might also explain the

increased expression of MuRF1, because it was found previously that NF-κB signalling upregulate MuRF1 expression (Cai et al., 2004). Atrogin-1, on the other hand is associated with muscle atrophy. Increased protein synthesis of Atrogin-1 has been shown to accelerate protein degradation and suppress protein synthesis. We showed a reduction in the expression of Atrogin-1 in 6 weeks study but not in 3 weeks, which suggest the impact of age of these two different groups in the measured outcomes. However, it was found that Atrogin-1 level in *mdx* is lower than wild type (Whitehead et al., 2015). Compared to our results, postnatal over-expression of PGC-1α into 3 weeks old *mdx* mice showed increased expression of Atrogin-1 (Hollinger et al., 2013). Therefore, in our study, we could potentially suggest reduced protein turnover in 6 weeks ERRγ-treated EDL muscles compared with the control. However, further investigation of the signalling pathway involved in muscle atrophy would evaluate the difference in muscle atrophy between these two ages following over-expression of ERRγ.

Eukaryotic translation initiation factor 4E binding protein 1 (4EBP1) is a mRNA translation repressor protein that negatively regulates eukaryotic translation initiation factor 4E or eIF4E, which is a protein that forms a complex blocking 5' ends mRNA cap structure, important for protein synthesis (Gingras et al., 1998). 4EBP-1 is a downstream substrate of mTORC1, where phosphorylation of 4EBP-1 resulted in inhibition of its ability to sequester eIF4E complex by repressing the cap-dependent mRNA translation initiation. Nutrient and deprivation of growth factors resulted in 4EBP-1 de-phosphorylation, increased binding to eIF4E and a parallel decrease in cap-dependent translation (Kleijn et al., 1998). In *mdx*, the phosphorylation level of 4EBP-1 was enhanced compared to wild type (De Palma et al., 2012), which led to its activation and inhibition of autophagy in muscles

(Mammucari et al., 2008). It has been demonstrated that enhanced 4EBP-1 activity led to increased oxidative metabolism in skeletal muscle during aging and obesity (Tsai et al., 2015). Regulation of the cross talk between mTOR and AMPK was found to be regulated by resveratrol which was found to down regulate mTOR via AMPK activation to promote autophagy in cancer (Park et al., 2016). Following activation of AMPK, mTORC1 complex was inhibited by phosphorylation and at the same time the kinase was able to induce autophagy by phosphorylating ULK-1 during nutrient deprivation. The two crucial targets of mTOR; ribosomal protein S6 kinase (p70S6) and 4EBP-1 were dephosphorylated, and resulted in blocking protein synthesis (Hay and Sonenberg, 2004). Reduction in the transcript levels of 4EBP-1 is possibly a mechanism to conserve ATP under energy starvation and low metabolic condition (Horman et al., 2002). As we measure the expression at one time point, we could not draw a conclusion of why over-expression of ERRγ results in a reduced expression of these factors involving in pathways controlling protein synthesis. Assessment of AKt- mTOR pathway is required to understand the role of ERRγ in protein synthesis.

Growth arrest and DNA damage inducible protein (GADD34) is a gene that reverse translational repression by de-phosphorylation of eIF2α (Novoa et al., 2001). It has been shown previously that the DMD exhibit increased endoplasmic reticulum (ER) stress which cause apoptosis through different pathways and one of these is through C/EBP-homologous protein (CHOP) pathway. However, CHOP is regulated by activating transcription factors; ATF4 and ATF6. A mechanism of a pro-apoptotic activity of CHOP involves upregulation of Gadd34 (Kim et al., 2014). The reduced expression of GADD34 following over-expression

of ERRγ is a marker of reduced cellular stress and speculatively would lead to less apoptosis. To better elucidate these pathways, it is required to investigate other regulators such as ATF4 and ATF6. However, the mechanism regulating translational control of 4EBP-1 and GADD34 gene expression is not fully understood and the role of these markers in the state of DMD require further investigation.

In the 6 week study, neither gastrocnemius nor EDL muscles showed any results similar to what has been shown in EDL muscle treated at 3 weeks of age. The possible explanation is that, as the 6 weeks old muscle is well into the regenerative phase, the achieved ERRγ over-expression in gastrocnemius was not sufficient to induce change at the molecular level despite the reduction of central nucleation and SDH activity. The main drawback in both studies is that we do not have a conclusion of how many fibres are positive for ERRγ over-expression. Therefore, it is helpful to develop a protocol in order to quantify the positive fibres of the ERRγ over-expression. Moreover, none of the positive changes have been observed in the 6 weeks treated EDL despite similar over-expression of ERRγ to 3 week-old EDL muscles. We could speculate that the active cycle of regeneration during 6-weeks of age may lead to loss of vector (Peccate et al., 2016). Alternatively, different aged groups were treated for different lengths of time, which ultimately lead to different outcomes between them. Time of intervention between these two groups; early in necrotic phase at 3 weeks of age vs regenerative phase at 6 weeks of age represent the main difference between these two studies. It is also possible to suggest that oxidative stress at 9 weeks of age (when these muscle are recovered) is already reduced by over-expression of ERRγ since we showed reduced pathology associated with

improving SDH activity and reducing central nucleation fibres in gastrocnemius muscles. Further, unchanged expression of inflammation markers could be a result of reduced stress because it was shown that pro-inflammatory cytokines are associated with muscle regeneration and repair (Serrano et al., 2008, Scheller et al., 2011). Speculatively, by definition, skeletal muscles overexpressing ERRγ are under less oxidative stress and therefore, do not need to upregulate these inflammatory markers.

In conclusion, our investigation revealed several findings following over-expression of ERRγ that are likely to have an effect on muscle function. Over-expression of ERRγ increased expression of mitochondrial complexes; I, II and III, which possibly has an effect via improving level of ATP production that support the platform to improve excitation-contraction coupling and enhance muscle function. Further, increased expression of angiogenesis markers and vascular density could be another mechanism to explain the improved muscle force. As these factors have been shown to promote muscle regeneration and reduce force deficit in dystrophic muscle (Borselli et al., 2010, Messina et al., 2007, Deasy et al., 2009). Collectively, the exact mechanism by which ERRγ leads to the observed changes in specific force and gene expression is currently unclear.

However, these data demonstrated that early intervention of ERRγ reduced metabolic stress by reducing oxidative stress and pathology leading to improved specific force and hence suggested ERRγ as a candidate therapeutic target in DMD.

5. Chapter Five

Systemic administration of AAV9-ERRγ into 3 week-old *mdx*

5.1. Introduction:

AAV is a small non-enveloped single-stranded DNA virus of 25 nm in diameter that has been detected in several tissues and different animal species (Horowitz et al., 2013). Initially, AAV was discovered as a contaminant of adenovirus preparations (Rose et al., 1966, Hastie and Samulski, 2015), further, Hermonat and Muzyczka run the first AAV gene transfer experiment. They used the virus to infect human Detroit 6 and KB cells, with antibiotic resistance tested with G418 in the presence of a helper virus (adenovirus). The observed transduction efficacy was about 0.4-10% (Hermonat and Muzyczka, 1984). This experiment validate another milestone in vector development and the author highlighted areas that require further investigation and understanding in terms of studies of larger DNA fragments, host range mutants and gene therapy applications. The unique feature of AAV is that, the inverted terminal repeats (ITRs), *cis*-active sequences, of 145 base pairs are the only sequences required for AAV rescue and replication, therefore, most of AAV genome is available for substitution of foreign DNA (Hastie and Samulski, 2015). Therefore, these features of AAV make it an interesting tool for gene therapy. Nowadays, rAAV gene based therapy has been widely used for the potential to treat Duchenne muscular dystrophy (DMD) based on their safety profile, efficiency of transduction, ability to transduce dividing and non-dividing cells, stable expression and its low immunogenicity (Zincarelli et al., 2008, Kotterman and Schaffer, 2014, Wells and Wells, 2002, Calcedo and Wilson, 2013). However, the main difficulty has been found in the use of rAAV for DMD gene therapy is the high titers of rAAV required to transduce the enormous amount of tissue (40% of body mass) and the limited capacity of rAAV vector of 4.7 kb and the need to re-administer (Foster et al.,

2008, McIntosh et al., 2012). It has been found that the therapeutic levels of transduction efficiency have been achieved using $1X10^{15}$ to $1X10^{16}$ vg/kg (Hinderer et al., 2018). Therefore, such systems are invaluable in a research and there is a need to develop rAAV vectors that can successfully attain efficient gene transfer and high expression at lowed viral titre.

Different serotypes of rAAV have been described and those which show high tropism for skeletal and cardiac muscles, are more relevant to DMD due to their ability to transduce these tissues, for example; serotype 6, 8 and 9 (Inagaki et al., 2006). Among different AAV serotypes; 8 and 9 transduce tissues more ubiquitously than other serotypes and 9 showed the most robust tissue expression, highest protein level and the slowest clearance of viral genome from the blood (Zincarelli et al., 2008). AAV9-mediated cardiac gene transfer resulted in high efficient and stable expression in mouse and rat (Bish et al., 2008, Moulay et al., 2015, Haihan and Tang, 2018). Despite the high level of gene transfer achieved following those particular serotypes, high titers of rAAV vector were required (Gregorevic et al., 2004). Therefore, finding a way to transduce the tissues efficiently and reduced viral dose is required for gene therapy.

Increasing the transgene expression from a single virion has been an important development to help reduce the viral load required for translational programs; this can be achieved in a variety of ways for example; sequence optimization (Mauro and Chappell, 2014). A number of ways were used in sequence optimization in order to improve mRNA stability and translational efficiency. For example; codon optimization, inclusion of enhancer elements and WPRE sequence, sequence flanking the AUG start codon that can facilitate its recognition by eukaryotic

ribosomes as consensus Kozak sequence and increased GC content. These features have been shown to enhance transcription efficiencies, initiation of translation and improved translation efficiency.

Codon optimization is resultant from the degenerative nature of the genetic codes, polypeptides chains of most proteins can be encoded by infinite numbers of mRNA sequences, for example; 4 different tRNA molecules encode the codon of valine amino acid. In gene therapy, optimization of cDNA sequence as an attempt to produce more proteins could be one way to reduce the viral dose required for efficient gene transfer. For example; in skeletal muscles, administration of codon optimized microdystrophin gene under the control of a muscle restrictive promoter (spc5-12) increased gene expression, improved muscle function and ameliorate disease pathology (Foster et al., 2008, Kornegay et al., 2010, Le Guiner et al., 2017).

Codon usage and codon bias is observed in all species and for the purpose of codon optimization, it is suggested to select a codon, which correlates with high gene expression. The greatest deviation from random codon usage in organisms occurs in the highly expressed genes and results in a selection against the use of codons specifying tRNA with low proportions and selection of high frequency codons whose binding energy for interactions with anti-codon of the tRNA molecule is suboptimal, hence, maximize the level of expression (Makoff et al., 1989, Bentele et al., 2013, Novoa and de Pouplana, 2012, Foster et al., 2008, Nguyen et al., 2004, Garmory et al., 2003, Ward et al., 2011, Nagata et al., 1999, Radcliffe et al., 2008, Qiao et al., 2011, Wang et al., 2012).

Enhancer elements and nuclear transport enhancers promote transport of genetic materials from cytoplasm to nucleus are also incorporated to enhance vector design. For example; simin virus 40 has been included in the expression cassettes to increase the efficiency of expression (Lu et al., 2003a). Further, to enhance transgene expression at the post-transcriptional and translational levels, the wood chuck post-transcriptional response element (WPRE) has been shown to enhance the levels of transgene expression from both plasmid and viral vectors. WPRE is a 600 bp, non-coding *cis*-acting element, promote RNA stability and transport of mRNA from the nucleus to the cytoplasm. WPRE is most effective when placed downstream of the transgene. Inclusion of WPRE elements into eGFP improved virus titre and transgene expression (Hlavaty et al., 2005). Furthermore, a consensus Kozak sequence has been shown to improve translation efficiency (Kozak, 2005). The mechanism of Kozak sequence recognition and function is not yet explored. However, the possible mechanism is that an interaction with consensus Kozak sequence (GCCACC) could reduce the rate of scanning and facilitate the recognition of AUG start codon by Met-tRNA (Kozak, 1999). It is required for optimal translation of mammalian genes (Garmory et al., 2003). Increasing the percentage of C+G content, also, has resulted in enhanced gene expression in mammalian cells. Genes with high GC contents showed increased expression due to increased mRNA stability (Kudla et al., 2006).

In this chapter we tested the hypothesis that optimization of ERRγ sequence within the ERRγ gene would result in increased level of transgene expression and hence increased protein levels. Two plasmids were modified to include the same optimized ERRγ sequences, 3-FLAG sequence, a consensus Kozak

sequence and WPRE. To include a Kozak consensus sequence at the translation start site, the sequence surrounding the initiation codon was modified to GCCACC. The two plasmids differ in the location of 3-FLAG sequence, one at 5' end and the second at 3' end instead, being conscious that sequence context may affect epitope recognition by antibodies. However, the native non-optimized plasmid expressing non-optimized sequence of ERRγ contained a human influenza hemagglutinin (Ha) tag at 3' end. Plasmids expressing optimized sequence of ERRγ were prepared by (Eurofins Company), the sequences are included in the (Appendix). Then we sub-cloned sequences of sequence optimized ERRγ into pAAV. When that is completed, we assessed the proliferative response of mouse myoblast (C_2C_{12}) cells transfected with the two plasmids expressing sequence optimized ERRγ and compared their proliferative effects with the plasmid of non-optimized sequence of ERRγ. Next, we evaluated the protein level of ERRγ in human embryonic kidney cells (HEK-293T) transfected with the non-optimized pAAV-ERRγ and the plasmid expressing optimized ERRγ sequence. Finally, three week old, male *mdx* mice were injected intraperitoneally with $2X10^{12}$ vg of AAV9 expressing sequence optimized ERRγ in 100 µl of saline and the control *mdx* mice were injected with similar volume of saline. Muscles were obtained after 6 weeks post administration and EDL muscles were used to assess muscle function and ERRγ protein level.

5.2. Results:

5.2.1. The sub-cloning of the sequence optimized sequences into the pAAV backbone:

The two plasmids expressing sequence optimized ERRγ were prepared by (Eurofins Company) in a 5'Pex-k4 and 3'Pex-k4 backbones. To sub-clone each of the transgene of sequence optimized ERRγ into pAAV backbone, the non-optimized pAAV-ERRγ plasmid was used as the backbone, with the native gene excised and the two optimized sequence variants of ERRγ was substituted to generate novel pAAV vectors. The PacI/AgeI double digestion of the non-optimized pAAV-ERRγ (2, 3) showed two bands of the back bone (AAV) at 6155 bp and the insert (ERRγ) at 1420 bp. The double restriction digestion of the plasmids; 5'F SO ERRγ and 3'F SO ERRγ using PacI and AgeI also showed bands at the expected sizes of 900 bp of the backbone and 1466 of the insert. The presence of ITRs in the non-optimized (pAAV-ERRγ); (MscI, XbaI, BssHII and SmaI) were confirmed; 10, 11, 12 and 13. The expected sizes for ITRs fragments are the following; MscI, (4223, 1324, 1221, 993, 685), Xbal, (2751, 2391, 360), BssHII (3101, 3016, 85) and SmaI (3049, 2740, 2729, 298, 309) (figure 5.1).

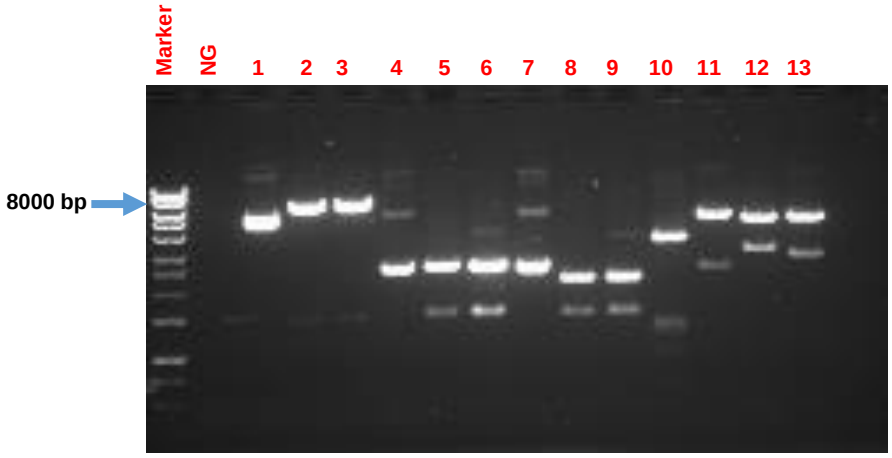

Figure 5.1. Restriction digestion of non-optimized pAAV-ERRγ and plasmids expressing optimized sequence of ERRγ

1, Undigested non-optimized pAAV-ERRγ

2, Cut non-optimized pAAV-ERRγ (PacI/AgeI)-1 hr

3, Cut non-optimized pAAV-ERRγ (PacI/AgeI)-24 hr

4, Undigested Pex K4 So pAAV 5'F ERRγ

5, Cut 5'Pex-k4 sequence optimized ERRγ (PacI/AgeI) (1 hr)

6, Cut 5'Pex-k4 sequence optimized ERRγ (PacI/AgeI)- (24hr)

7, Undigested 3'Pex-k4 sequence optimized ERRγ

8, Cut 3'Pex-k4 sequence optimized ERRγ (PacI/AgeI)- (1hr)

9, Cut 3'Pex-k4 sequence optimized ERRγ (PacI/AgeI)- (24hr)

10, Single digest of non-optimized pAAV-ERRγ (MscI)

11, Single digest of non-optimized pAAV-ERRγ (XbaI)

12, Single digest of non-optimized pAAV-ERRγ (BssHII)

13, Single digest of non-optimized pAAV-ERRγ (SmaI)

5'Pex-k4= back bone of the plasmids from Europhin Company, (SO= Sequence optimized), (5'F= Flag at 5 end), (3'F= Flag at 3 end)

Following ligation, transformation and mini-prep (Described in materials and methods, section 2.5.2 and 2.5.3), XhoI restriction enzyme was used to linearize the plasmids as a first confirmation step to check their sizes (figure 5.2).

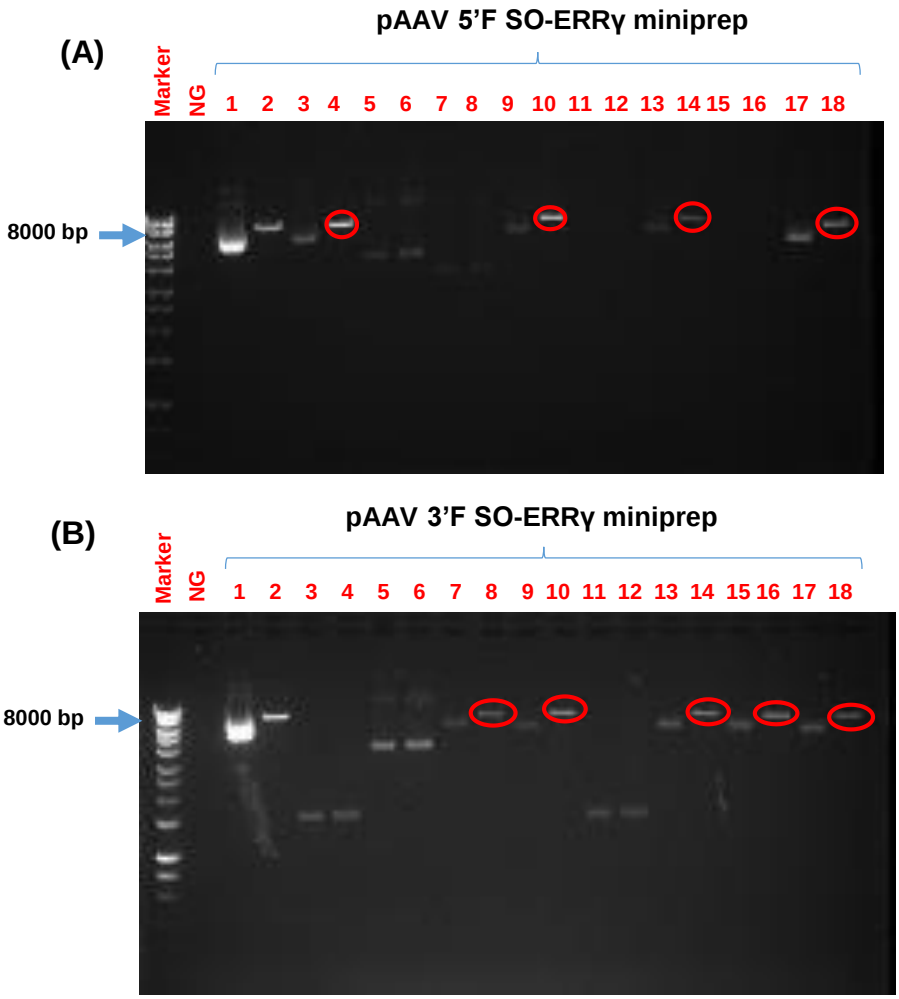

Figure 5.2. Miniprep analysis of pAAV 5'F SO-ERRγ and pAAV 3'F SO-ERRγ

A) Miniprep of the pAAV 5'F SO-ERRγ samples;

1, Undigested non-optimized pAAV8-ERRγ

2, Single digest of non-optimized pAAV8-ERRγ (XhoI)

3, 5, 7, 9, 11, 13, 15, 17, Undigested samples of pAAV 5'F SO-ERRγ miniprep samples

4, 6, 8, 10, 12, 14, 17, 18, Single digest of pAAV 5'F SO-ERRγ miniprep samples (XhoI).

4, 10, 12, 18, Samples showed single band at the right size.

B) Miniprep of the pAAV 3'F SO-ERRγ samples;

1, Undigested non-optimized pAAV8-ERRγ

2, Single digest of non-optimized pAAV8-ERRγ (XhoI)

3, 5, 7, 9, 11, 13, 15, 17, Undigested samples of pAAV 3'F SO-ERRγ miniprep samples

4, 6, 8, 10, 12, 14, 17, 18, Single digest of pAAV 3'F SO-ERRγ miniprep samples (XhoI).

8, 10, 14, 16, 18, Samples showed single band at the right size.

(SO= Sequence optimized), (5'F= Flag at 5 end), (3'F= Flag at 3 end)

Those samples which showed single band were digested with (BsrgI) to differentiate between the non-optimized pAAV8-ERRγ plasmid and the two plasmids expressing optimized sequence of ERRγ. Bsrg1 digestion of pAAV 3'F SO-ERRγ plasmid results in bands of 5587bp and 2030bp, whereas BsrgI digestion of the non-optimized pAAV8-ERRγ results in a single band (figure 5.3).

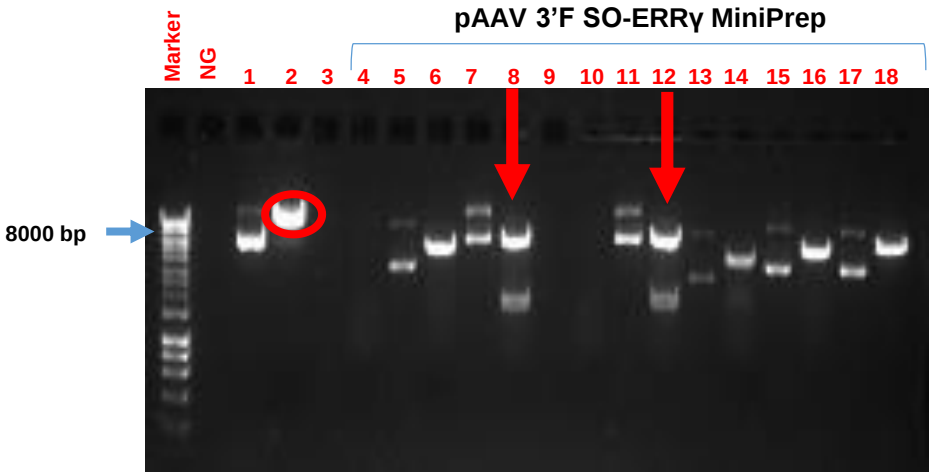

Figure 5.3. Restriction digestion of pAAV 3'F SO-ERRγ plasmid using BsrgI

1, Undigested non-optimized pAAV8-ERRγ

2, Single digest of non-optimized pAAV8-ERRγ (BsrgI)

3, 5, 7, 9, 11, 13, 15, 17, Undigested samples of pAAV 3'F SO-ERRγ samples

4, 6, 8, 10, 12, 14, 16, 18, Single digest of pAAV 3'F SO-ERRγ miniprep samples (BsrgI).

8, 12 samples, showed bands at the expected size (5587 and 2030 bp).

Also, to give more confidence for those samples of pAAV 3'F SO-ERRγ (8, 12), the samples were digested with the restriction enzyme (BstxI) to further differentiate them from non-optimized pAAV-ERRγ plasmid, which should result in 4117 bp and 3583 bp bands. Both plasmids expressing sequences of optimized ERRγ showed three bands; 4177 bp, 2592 bp and 908 bp, confirming their identity. Samples of pAAV 5'F SO-ERRγ were also digested with BsrgI and BstxI to confirm the sequence. The expected bands for the pAAV 5'F SO-ERRγ plasmid digested with BsrgI were 5656 and 1961 confirming the identity of these plasmids (figure 5.4).

The integrity of the ITRs were checked with the following restriction enzymes; MscI, XbaI, SmaI and BsHII. All ITRs are present in both plasmids and therefore, we made a larger scale endotoxin free preparation for further tissue culture analysis and viral preparation (figure 5.5).

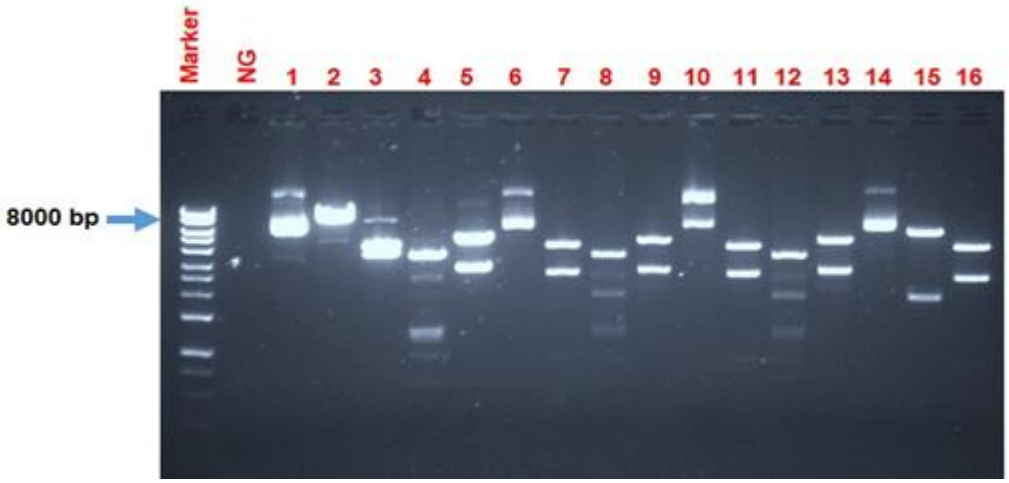

Figure 5.4. Confirmation the sequence of the plasmids expressing optimized ERRγ with BstxI and ITR.

1, Undigested non-optimized pAAV8-ERRγ

2, Single digest of non-optimized pAAV8-ERRγ (BsrgI)

3, Single digest of non-optimized pAAV8-ERRγ (BstxI)

4, Single digest of non-optimized pAAV8-ERRγ (MscI)

5, Single digest of non-optimized pAAV8-ERRγ (SmaI)

6, 10 Undigested samples of pAAV 3'F SO-ERRγ

7, 11, Single digest of pAAV 3'F SO-ERRγ samples (BstxI).

8, 12, Single digest of pAAV 3'F SO-ERRγ samples (MscI).

9, 13, Single digest of pAAV 3'F SO-ERRγ samples (SmaI).

14, Undigested samples of pAAV 5'F SO-ERRγ sample

15, Single digest of pAAV 5'F SO-ERRγ sample (BsrgI).

16, Single digest of pAAV 5'F SO-ERRγ sample (BstxI).

(SO= Sequence optimized), (5'F= Flag at 5 end), (3'F= Flag at 3 end)

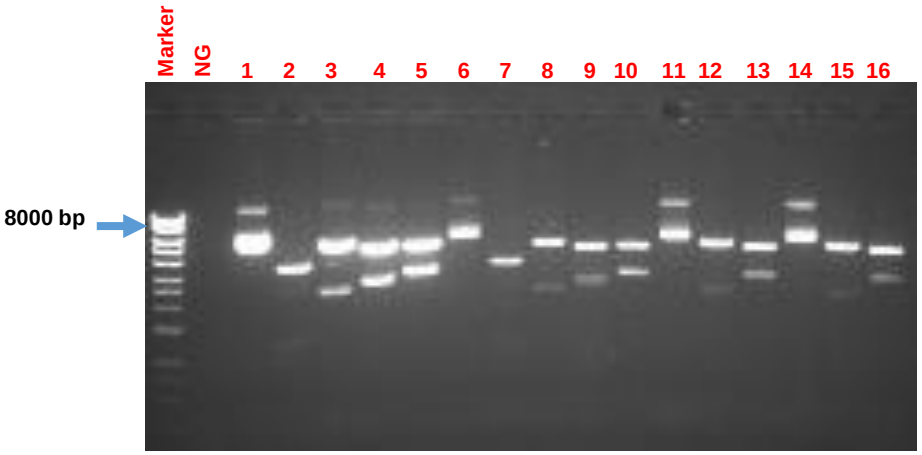

Figure 5.5. Confirmation the ITRs sequence in the pAAV 5'F SO-ERRγ and pAAV 3'F SO-ERRγ

1, Undigested non-optimized pAAV8-ERRγ

2, Single digest of non-optimized pAAV8-ERRγ (MscI)

3, Single digest of non-optimized pAAV8-ERRγ (XbaI)

4, Single digest of non-optimized pAAV8-ERRγ (SmaI)

5, Single digest of non-optimized pAAV8-ERRγ (BsHII)

6, Undigested samples of pAAV 5'F SO-ERRγ samples

7, Single digest of pAAV 5'F SO-ERRγ samples (MscI).

8, Single digest of pAAV 5'F SO-ERRγ samples (XbaI).

9, Single digest of pAAV 5'F SO-ERRγ samples (SmaI).

10, Single digest of pAAV 5'F SO-ERRγ samples (BsHII).

11, 14, Undigested samples of pAAV 3'F SO-ERRγ samples

12, 15, Single digest of pAAV 3'F SO-ERRγ samples (XbaI).

13, 16, Single digest of pAAV 3'F SO-ERRγ samples (BsHII).

(SO= Sequence optimized), (5'F= Flag at 5 end), (3'F= Flag at 3 end)

5.2.2. FLAG fusion protein was detected in pAAV 3'F SO-ERRγ but not pAAV SO 5'F-ERRγ:

To evaluate the protein level of ERRγ *in vitro*, Human embryonic kidney cells (HEK-293T) cells were co-transfected with either non-optimized pAAV-ERRγ or pAAV SO 5'F-ERRγ or pAAV 3'F SO-ERRγ and pCAGGβ-Galactosidase (β-gal) plasmid as a control to standardize amounts. A β-Gal ELISA was run on cell lysate to assess the transfection efficiency between all plasmids and showed no difference in transfection efficiency between them (figure 5.6 A). Then, in order to detect FLAG protein in the sequence optimized plasmids, we run western blot on the lysate of the transfected HEK-293T cells. Unexpectedly, we detected the band only on the 3'F optimized ERRγ and therefore we carried out the work on this plasmid only (figure 5.6 B).

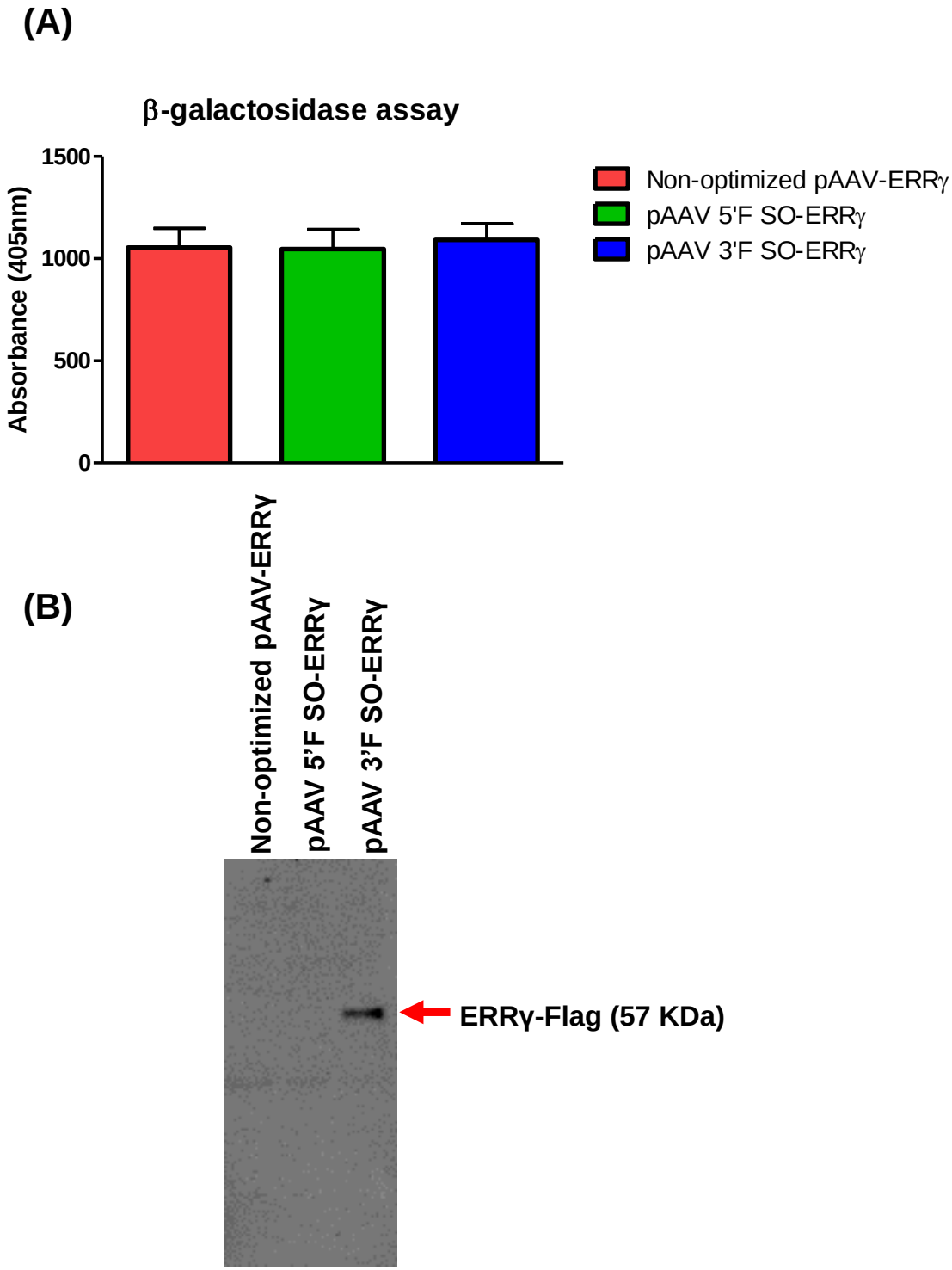

Figure 5.6. β-gal assay and western blot of FLAG antibody in HEK-293T cells transfected with non-optimized pAAV-ERRγ, pAAV 5'F SO-ERRγ and pAAV 3'F SO-ERRγ

A) β-gal assay showed no difference in the transfection efficiency between the HEK-293T cells co-transfected with non-optimized ERRγ or sequence optimized 5'F ERRγ and sequence optimized 3'F ERRγ and β-gal plasmid. B) The presence of ERRγ-Flag in HEK-293T cells transfected with either non-optimized pAAV-ERRγ, pAAV 5'F SO ERRγ

and pAAV 3'F SO ERRγ was determined by western blot analysis using 20 µg of the protein and Flag antibody. ERRγ-Flag band was detected at the expected size of ERRγ (57 KDa) in the lysate of HEK-293T cells transfected with pAAV 3'F SO ERRγ. (SO= Sequence optimized), (5'F= Flag at 5 end), (3'F= Flag at 3 end)

5.2.3. Sequence optimized pAAV 3'F SO ERRγ showed increased ERRγ protein level in transfected HEK-293T cells:

To find out the level of ERRγ protein following sequence optimization of ERRγ, western blot has been run on HEK-293T cells lysate transfected with either non-optimized pAAV-ERRγ or pAAV 3'F SO ERRγ. Densitometry analysis showed 20 fold increase in the level of ERRγ protein as a result of optimizing ERRγ sequence (p=0.0001). Cells transfected with native, non-optimized pAAV-ERRγ showed weak signal (figure 5.7).

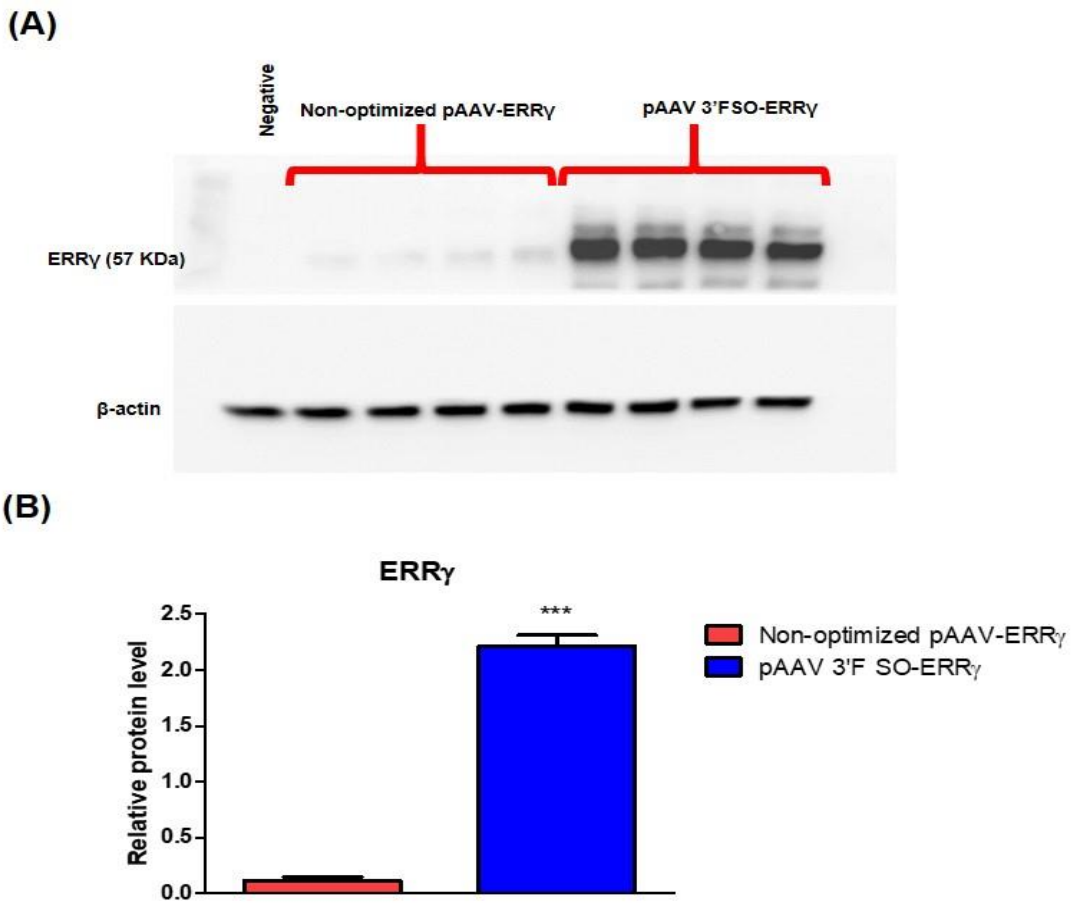

Figure 5.7. Western blot of ERRγ in HEK-293T cells transfected with non-optimized pAAV-ERRγ and pAAV 3'F SO-ERRγ

A) The levels of ERRγ in HEK-293T cells transfected with non-optimized ERRγ or sequence optimized 3'F ERRγ were determined by western blot analysis using 20 µg of protein. The total ERRγ was determined using ERRγ antibody. β-actin was used for normalization using β-actin antibody. The intensity of the bands was quantified using ImageJ software. B) Western blot analysis showed 20 fold increase (n=4, unpaired student's t-test, *p*=0.0001) in the ERRγ protein level in the HEK-293T cells transfected with sequence optimized 3'F ERRγ. (SO= Sequence optimized), (5'F= Flag at 5 end), (3'F= Flag at 3 end)

5.2.4. NADPH assay showed no difference between non-optimized and sequence optimized plasmids:

The CellTiter 96® AQueous One Solution Cell Proliferation Assay was used to evaluate the effect of sequence optimized ERRγ on cell metabolic activity and comparing that effect with the non-optimized sequence following transient transfection of C_2C_{12} cells with the three different plasmids. However, there was no difference in the metabolic activity of the cells transfected with either plasmids expressing sequence optimized of ERRγ and none of them showed metabolic difference compared to the plasmid expressing non-optimized sequence of ERRγ. However, there was an increase in the myoblast metabolic activity transfected with the sequence optimized plasmids compared to the control cells transfected with pAAV-eGFP plasmid and in the cells transfected with non-optimized sequence ERRγ plasmid compared to the control as well (figure 5.8).

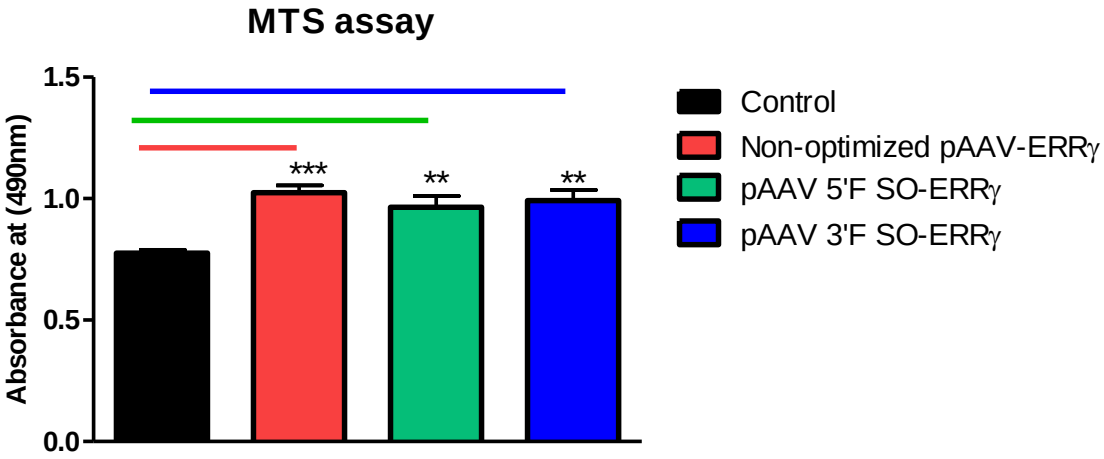

Figure 5.8. MTS assay of C2C12 cells transfected with non-optimized pAAV-ERRγ and pAAV 5'F SO-ERRγ and pAAV 3'F SO-ERRγ

C_2C_{12} cells transfected with either non-optimized pAAV-ERRγ (p=0.0001) or pAAV 5'F SO-ERRγ (p=0.001) and pAAV 3'F SO-ERRγ plasmids (p=0.001) showed significant difference in the proliferation activity of the cells when they are compared to the control (pAAV-eGFP plasmid). (SO= Sequence optimized), (5'F= Flag at 5 end), (3'F= Flag at 3 end).

5.2.5. Intraperitoneal administration of $2X10^{12}$ vg rAAV9 3'F SO-ERRγ into 3 week old *mdx* mice improves muscle function:

In order to assess if the over-expression of rAAV9 3'F SO-ERRγ improved muscle function in *mdx* mice, $2X10^{12}$ vg of a rAAV9 3'F SO-ERRγ under the control of spc5-12 promoter was administered via intraperitoneal route into 3 week-old *mdx*. Muscle samples were recovered 6 weeks post virus administration. EDL muscles were examined for muscle function. There was no difference between treated and control EDL muscle mass (p=0.808). The injection of rAAV9 3'F SO-ERRγ had no effect on maximal tetanic force compared to untreated *mdx* injected with saline. However, specific force was significantly improved by 14% (p=0.021) following treatment with rAAV9 expressing sequence optimized ERRγ compared to mice injected with saline. In addition, we tested the ability of sequence optimized ERRγ to protect *mdx* EDL muscle from eccentric

contraction by assessing force production following a series of 10 eccentric contractions. Injection of AAV9 3'F SO-ERRγ was unable to protect *mdx* muscles from force deficit induced by the contraction induced injury (figure 5.9).

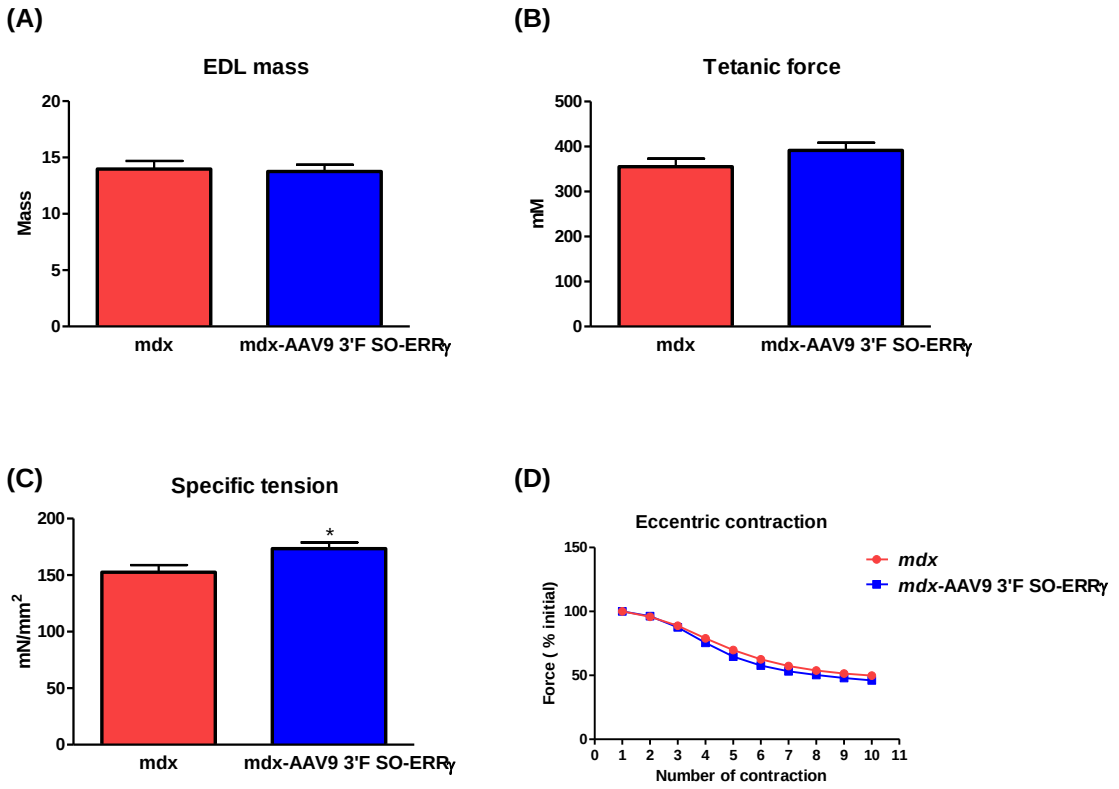

Figure 5.9. Gene transfer of rAAV9 3'F SO-ERRγ improves specific force in the EDL muscle of *mdx* mice.

A) ERRγ gene transfer of AAV9 3'F SO-ERRγ into 3 week-old *mdx* does not change muscle mass (p=0.808). Muscles were stimulated according to standard techniques in order to assess tetanic force and specific force. B) ERRγ gene transfer of AAV9 3'F SO-ERRγ into 3 week-old *mdx* has no effect on maximal tetanic force (p=0.154). C) Tetanic force normalized by muscle cross sectional area is specific force. Cross sectional area (mm^2) is calculated using the following equation; mass (mg)/ [(L_o mm)* (L/L_o)* (1.06 mg/mm^3)], where L/L_o is the ratio of fibre to muscle length (0.45 for EDL) and 1.06 is the density of muscle. ERRγ gene transfer of AAV9 3'F SO-ERRγ into 3 week-old *mdx* leads to 14% recovery of specific force in EDL muscles (p=0.021). D) EDL muscles were given a series of 10 lengthening contractions (150 Hz for 500 msec, followed by 200 msec at a 110% L_o) in order to evaluate sarcolemma stability. Force deficit induced by a series of eccentric contraction was not different between *mdx* control and *mdx* treated with AAV9 3'F SO-ERRγ (n=10 *mdx*, n=12 *mdx*-ERRγ, unpaired student's t-test). (SO= Sequence optimized), (3'F= Flag at 3 end).

5.2.6. ERRγ protein level is not increased in the EDL muscle following gene transfer of rAAV9 3'F SO-ERRγ:

To test the hypothesis that optimizing the sequence of ERRγ would result in an increase in ERRγ protein levels within the muscle, analysis of ERRγ protein in EDL muscles from mice injected with AAV9 3'F SO-ERRγ was assessed by western blot. No difference in ERRγ protein level was detectable between control and treated muscles (p=0.436) (figure 5.10).

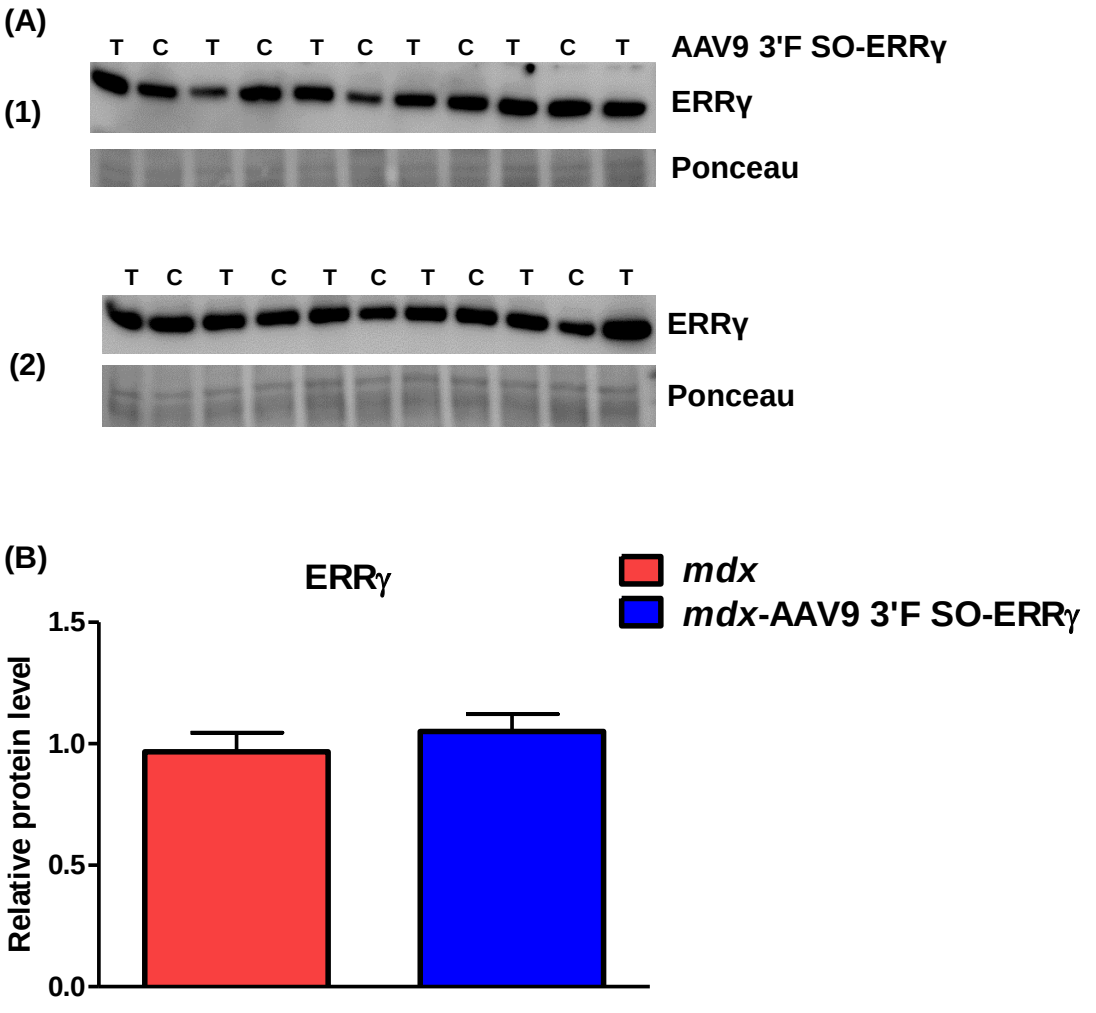

Figure 5.10. Western blot analysis of ERRγ in EDL muscles

The level of ERRγ in EDL muscles was determined by western blot analysis using 40 µg of protein and Ponceau stain was used for normalization. A) The total ERRγ was determined using ERRγ antibody. B) The intensity of the bands was quantified using ImageJ software. Analysis showed no difference in the protein level of ERRγ between

mdx control and *mdx* injected with AAV9 3'F SO-ERRγ (n=10 *mdx*, n=12 *mdx*-ERRγ, unpaired student's t-test, p=0.436).

5.3. Discussion:

The application of sequence optimization of a eukaryotic gene in an attempt to maximize transgene levels is a well trodden path. Here we seek to determine in the sequence optimization of ERRγ in muscle following rAAV gene transfer and to assess the impact on the muscle function of the *mdx* mouse.

Foster et al., demonstrated that systemic delivery of an rAAV expressing a sequence optimised microdystrophin into *mdx* mice significantly improved mRNA up to 30 fold and improved protein expression and the physiological assessment showed improvements in specific force (Foster et al., 2008). Recently, systemic delivery of rAAV mediated sequence optimized β-sarcoglycan into a model of limb-girdle muscular dystrophy type 2 (*sgcb*$^{-/-}$) improved diaphragm force, reduced the level of creatine kinase and increased protein expression of the transgene in all muscles which initially exhibited a complete loss of β-sarcoglycan protein (Pozsgai et al., 2017). Here the delivery of rAAV9 3'F SO-ERRγ into the *mdx* mouse has been assessed, to investigate its impact on ERRγ mRNA and protein levels in the muscle and its impact on dystrophic muscle function.

ERRγ sequence was optimized to include a consensus kozak sequence (GCCACC), which has been shown to induce translation efficiency. It plays a role in the initiation of translation by influencing the recognition of AUG start codon by eukaryotic ribosomes (Garmory et al., 2003). In addition, codon usage within the ERRγ gene was modified based on optimal transfer RNA (tRNA) frequencies.

Codon usage is defined as a degeneracy of the genetic code. All amino acids can be encoded by more than one codon, however, not all synonymous codons are used with equal frequency and certain codons are used more frequently to encode any given amino acids especially with highly expressed genes. These frequencies are correlated with the corresponding tRNA levels in the cells and they are species specific (Ikemura, 1981). In addition, G-C% content was increased in the optimized sequence of ERRγ by 9%. Previously it was shown that increasing GC content increased mRNA synthesis, enhanced mRNA stability, induce nuclear export of mRNA and protein translation (Kudla et al., 2006).

The first aim of this study was to assess the mRNA and protein level of ERRγ *in vitro* following transient transfection of sequence optimisation of the ERRγ gene. Although sequence optimization should increase transcript stability and hence enhancing protein level, we do not have a conclusion on how much optimizing sequence of ERRγ increased mRNA transcript. Although, the cDNA was synthesized from RNA that was extracted from C_2C_{12} cells transfected either with the plasmid of non-optimized or optimized sequence of ERRγ and specific primers were designed for the optimized sequence, however, we encountered a contamination on non-template control for a reason that could not be explained, and as a result it has not been possible to generate the data of relative RNA expression levels. Clearly, moving forward, it will be important to address this issue. Therefore, we carried out on assessing the protein level. Optimization of ERRγ gene resulted in a 20 fold increase in the protein level of ERRγ in the HEK-293T cells following transfection of the pAAV 3'F SO ERRγ compared to the non-

optimized sequence. We demonstrated here, that optimizing sequence of ERRγ gene induce significant protein level *in vitro*.

To further assess the impact of using optimized sequence of ERRγ *in vitro*, we asses MTS assay, which is a colorimetric method for determining the metabolic activity of the cells. We showed here that sequence optimization of ERRγ, like the non-optimized sequence, promotes the metabolic activity of myoblast C_2C_{12} cells. No significant differences in the metabolic activity were observed between the cells transfected with the optimized and non-optimized sequence of ERRγ and no difference was observed between the two plasmid expressing the sequence optimized ERRγ. This was unexpected as the sequence optimized ERRγ resulted in 20 fold increase in ERRγ protein level compared to the non-optimized, which suggested the effect of over-expression of ERRγ on metabolic activity should be more. As the metabolic activity appeared to be the same, therefore, it is not the sequence having the effect. The possible explanation is that, despite increasing protein level, the cells have limited capacity to respond to the increase in the protein level of ERRγ. Although, the two plasmids induced similar induction on metabolic activity of the myoblast cell. This highlighted the significant effect of ERRγ on improving muscle metabolism. As demonstrated previously by Rangwala et al., there was an increase in the mitochondrial function represented by the upregulation of fatty acid metabolism and citrate synthase activity genes following adeno virus mediated expression of ERRγ in primary mouse myotubes (Rangwala et al., 2010).

Histological and morphological changes in skeletal muscles of the *mdx* mouse are a result of dystrophin loss has detrimental effects on muscle function (Capote

et al., 2010). The second aim of this study was to deliver the optimized transgene efficiently to skeletal muscles in order to produce strong level of ERRγ expression and evaluate the impact of its expression on function of the muscle. Administration of rAAV9 3'F SO-ERRγ into 3 week-old *mdx* muscle improved specific force compared to untreated *mdx* muscles by 14%. Previously, using codon optimization approach has been investigated in spinal muscular atrophy (SMA) and the survival analysis showed increased life expectancy from 27 to over 340 days. Also, it showed correction of motor function (by monitoring spontaneous activity) and rescue the weight loss phenotype in mice (Dominguez et al., 2011). Furthermore, administration of AAV8 expressing codon optimized sequence of ornithine transcarbamylase (OTC) for ornithine transcarbamylase deficiency (OTCD), which is the common urea cycle disorder, has improved the protein expression and achieved sustained correction of OTCD biomarker and clinical protection against an ammonia challenge (Wang et al., 2012)

Using optimized sequences has been reported previously to induce protein level in skeletal muscle (Foster et al., 2008) and liver (Wang et al., 2012). Surprisingly, despite the increase in the protein level (20 fold) following HEK-293T cell transfection with the plasmid expressing optimized ERRγ, administration of rAAV9 3'F SO-ERRγ has no effect in the protein level of ERRγ in the treated EDL muscles compared to untreated, with reasons postulated herein.

For our results here and similar to the previous chapter, we showed an improvement in specific force by 14% following administration of rAAV8-ERRγ using the same titre and the same age of mice. In the previous study, we showed that the increase in specific force was correlated with an increase in the level of

ERRγ protein and an increase in the protein level of mitochondrial complexes; I, II and III, and an increase in the expression of angiogenic factors; VEGF-165, VEGF-189 and capillary number per fibre. However, in the absence of any data to support the increase of muscle force following systemic administration AAV9 mediated expression of optimized sequence of ERRγ, we speculatively refer the increase in specific force to the increased level of ATP production and may also indicate an increase in mitochondrial volume or number, which potentially reduce Ca^{+2} level per mitochondria that consequently help to maintain Ca^{+2} homeostasis and reduce mitochondrial dysfunction. Therefore, for future study, we may need to consider re–administration to make sustained change in the protein level. Further, based on the data from previous chapter in young *mdx* mice where we showed increased protein expression of mitochondrial complex, increased capillary number, increased RYR receptor, there is a potential decrease in the level of oxidative stress and ROS level, which is possibly another factor of improved force capacity. Alternatively, it is possible to suggest that the cargo makes adaptive response in terms of improving muscle function, before it is lost due to the cycles of degeneration/regeneration. For example; rAAV9 3'F SO-ERRγ may be there for sufficient time to improve muscle force, however, due to the regenerative process, this lead to loss of vector and hence, no detection of any increase in the protein level, however, some benefits maintained as shown by the increase in specific force. Previously, it was shown that dystrophin restoration was declined following 6 months of AAV mediated exon skipping therapy (Peccate et al., 2016). It is possible that AAV mediated expression of sequence optimized ERRγ is lost from the muscle earlier than that of AAV

mediated exon skipping of dystrophin. Therefore, we could not detect any change at the protein level, while the effect on muscle function is still preserved.

As all parameters are the same as the previous study, it is unclear why there is no increase in the protein level in the presence of increased specific force. It is possible that inability to detect any increase in the protein level is due to the antibody failure, which require investigating another antibodies. In conclusion, further evaluation of RNA and protein level is required to investigate this result. Moreover, as the sequence is Flag-tagged, it is possible to check the number of positive fibres in the muscle as a further evaluation of sequence optimized effect on protein level.

6. Chapter Six

General discussion

6.1. General discussion:

Dystrophic skeletal muscles undergo repeated bouts of myofibre necrosis, regeneration and growth, processes with a high metabolic cost. Moreover, the dystropathology is associated with inflammation, increased intracellular calcium, oxidative stress and metabolic abnormalities. Since muscle mass makes up such a high proportion, which is about 40% of total body mass, there must have been considerable selective pressure to minimize the cost of maintenance and to maximize the functionality of muscle tissue for all species.

The broad aim of this project research was to demonstrate the potential of gene therapy approach implying AAV mediated expression of ERRγ to improve oxidative capacity and angiogenesis in *mdx* mice, a model of DMD. The collective studies presented in this thesis have investigated the potential of ERRγ over-expression to improve force production and pathology associated with *mdx* mice, at different ages, with different doses. The main aim of this thesis was to assess the short-term effect of over-expression of ERRγ on function and pathology of *mdx* male mice. We hypothesized that over-expression of ERRγ on male *mdx* mice will improve the oxidative capacity and angiogenesis markers.

The main outcomes of the research presented in this thesis are summarized as:

1. Ontology data from IM of AAV8-ERRγ into TA muscles at 6 weeks of age showed that over-expression of ERRγ has changed gene expression pattern compared to the *mdx*. In addition, PCA analysis has demonstrated that treated samples are completely distinguishable from the untreated *mdx* phenotype. Principal component analysis (PCA) of transcriptomic data showed that following ERRγ over-expression, treated muscle could be distinguished from untreated

dystrophic muscle. Profiles of genes expressed in *mdx*-ERRγ versus *mdx* suggests that ERRγ may help in restoring the defective process known to be pathological drivers in dystrophic muscle. Although gene expression studies can be highly informative, their biological interpretation is limited. For example, most of transcriptomic studies employing RNA-seq methodology of microarrays presume that change in the abundance of mRNA are matched by corresponding alterations in protein expression; this is not always consistent (Zhang et al., 2010, Maier et al., 2009, Gygi et al., 1999). Therefore, multilevel analysis which investigate the transcriptome and proteome concomitantly will have greater potential for providing an understanding of gene regulation and cellular metabolism that might not be possible with any single analysis (Schwanhausser et al., 2011).

2. Cmap analyses generated a list of FDA approved pharmaceuticals that may act mimetics for the over-expression of ERRγ, providing alternative approaches to an AAV gene medicine approach.

3. The first study of local administration of AAV8-ERRγ into TA muscles at 6 weeks of age, active period of regeneration and degeneration, has no effect on oxidative capacity or vasculature of *mdx* mice. However, there was a reduction of pro-inflammatory cytokines (TNF-α and IL-1β).

4. Systemic administration of AAV8-ERRγ into 6 week-old *mdx* for short period of time (4 weeks) has no effect on muscle force, oxidative capacity and angiogenesis. However, there was a reduction in the centrally nucleated fibres.

5. Systemic administration of AAV8-ERRγ into 3 week-old *mdx* and recovered at 10 weeks of age, showed improvement in specific force, over-expression of mitochondrial proteins, angiogenesis markers and increases in capillary density.

6. Sequence optimized ERRγ plasmid showed 20 fold over-expression of ERRγ protein following *in-vitro* transfection of HEK-293T cells with plasmid mediated expression of sequence optimized ERRγ.

Limited outcomes of the 6-week cohort study:

Local administration of AAV8-ERRγ into TA muscles at 6 week-old *mdx* mice showed no difference in the genes of oxidative metabolism, mitochondrial biogenesis and angiogenesis, inconsistent with the results obtained from systemic administration at 6 week-old *mdx* but with a different dose. Although, the highest level of ERRγ from the systemic administration was detected in gastrocnemius muscle, this did not seem to have any effect in the genes associated with oxidative metabolism or angiogenesis. In addition, functional output in terms of specific force was unaffected with the over-expression of ERRγ in EDL muscles. Therefore, we have no evidence to support that ERRγ has any effect on oxidative metabolism or angiogenesis during active period of degeneration and regeneration following postnatal over-expression in *mdx* mice. These results were particularly surprising as it was an age/sex matched study consistent with the transcriptomic study in which the PCA and gene ontology data was particularly encouraging.

Although, the reduction in central nucleation was consistent in TA and gastrocnemius muscles from local and systemic administration, respectively,

however, this reduction was moderate. Considering the constant damage of the muscle, moderate improvement in the level of damage may dilute any change in other parameters such as, IgG and MYH-3, ending upp in non-significant difference. At the end, these results raise a question about how many fibres per muscle overexpress ERRγ. The answer for this question was not possible because none of the protocols we used were successful to detect the Ha-tag protein, as the AAV8-ERRγ fused with Ha-tag. This limitation represents one of the weaknesses in this thesis. Therefore, there is a need to develop a protocol to detect the positive fibres overexpressing ERRγ and then we will have a better idea whether the increase was per muscle or per fibre. In addition and more importantly, we should consider the validity of ERRγ antibody, which will be discussed later.

Subsequently, assessing the effect of ERRγ over-expression on younger, pre-crisis mice helped to rescue deficits in muscle function, with potentially coordinateted improvements in the oxidative capacity and angiogenic potential. Hence, the observed differences between the two studies should reflect the impact of the time of intervention and dosing strategies in DMD therapeutic regimens. Further assessment of the EDL histology from 6 weeks study will conclude the difference between the muscles of different ages.

Comparison between EDL from 6 weeks and 3 weeks studies:

This thesis has demonstrated that EDL muscles from the two systemic administration studies showed similar over-expression of ERRγ which resulted in improving specific force of 3 weeks treated *mdx* but not of 6 weeks, in the absence of dystrophin restoration. Several reasons may help to explain that difference.

1) *Prior to crisis vs ongoing crisis*. 3 weeks of age is considered a prior to onset pathology of *mdx* life compared to regenerative/degenerative period at 6 weeks. Therefore, it is acceptable to suggest that during active period of regeneration and degeneration, any transgene may eventually be lost following damage and repair. In preclinical trials of DMD using AAV mediated exon skipping therapy, dystrophin restoration was declined after six months. This reduction was correlated with loss of virus due to alteration of myofibre membrane (Peccate et al., 2016). According to the authors of that work, pre-treating mice with cell penetrating peptide conjugated to a phosphorodiamidate morpholino antisense oligonucleotides led to early dystrophin restoration, thus allowing more efficient maintenance of AAV cargo, leading to improved long term viral mediated restoration of dystrophin and improved muscle force. However, in our study of systemic administration of AAV-ERRγ, in the absence of dystrophin restoration, it is possible that virus cargo was lost due to active cycles of degeneration/regeneration and then the benefits from any therapeutic transgene will only establish a transient improvement. For the next future long term-study based on AAV-ERRγ, we are suggesting a combined approach to improve the transgene efficiency.

2) The length of the studies. 4 weeks post administration recovery vs 6 weeks post administration recovery, subsequent to AAV8-ERRγ gene transfer could affect the force production despite similar over-expression of ERRγ in the EDL muscles of the two ages, possibly of greater time for positive adaptive response.

3) Increasing the expression of mitochondrial proteins complex; I, II and III. The increase in the expression of mitochondrial protein complex, possibly, results in more ATP generation that can be match the demand at cross bridge level. As mentioned previously, *mdx* exhibited a deficit in mitochondrial ATP synthesis (Rybalka et al., 2014), which is one reason for impaired force production in *mdx* muscles. Furthermore, we could speculate that increased ATP production following over-expression of mitochondrial protein complex means increased volume or/and number of mitochondria and this increase will limit the contribution of free radicals and calpain into disease pathology. Further, as a consequence of increased mitochondrial volume, it was hypothesized that there is less Ca^{+2}/mitochondrial leading to less mitochondrial dysfunction throughout the cell which allow more ATP production (Selsby et al., 2012).

4) Increasing expression of angiogenesis factors; VEGF-165 *and* VEGF-189 *and improving the capillary number per fibre.* Angiogenic factors have been shown to promote regeneration and cell survival (Messina et al., 2007). Speculatively, angiokines promote activation of SC to activate and proliferate through its regenerative effects. It has been hypothesized that the vasculature is important for regulating cellular energy homeostasis, through delivering substances such as oxygen, carbohydrates and fatty acid oxygen, thus determining cellular metabolism (Fraisl et al., 2009). Therefore, improving pro-angiogenic potential in

skeletal muscle will probably improve the metabolic activity by providing oxygen and fuel to the surrounding tissue, hence improving oxidative metabolism may improve antioxidant status and improve oxidative stress. Under this condition, there will be less ROS and the available ATP will be sufficient to maintain muscle contraction.

In the current study, increasing number of capillary per fibre will increase the capacity of skeletal muscle to use oxygen supplied through increasing blood flow for regeneration of ATP. Given that we showed an increase in capillary density, we hypothesise that the muscle fibres will receive more oxygen in order to support more ATP production for its metabolic and contractile activities which provides further reasons for improved force production following AAV8-ERRγ administration. Given that following a yearlong treatment with antisense oligonucleotides in *mdx* mice to restore dystrophin to muscle by exon skipping, *mdx* mice have shown foci of dystrophin negative muscle that reflect the poor vascularisation of dystrophic muscle (Malerba et al., 2011). Based on the results shown in this thesis of increasing angiogenic markers and improving capillary density, we can speculate that ERRγ upregulation could be adjuvant therapy as a pre-treatment to allow better pharmacodynamics of subsequent treatments to enhance cargo delivery.

5) Increasing expression of RYR-1 *calcium marker.* Increasing expression of RYR-1 may be another reason that mediate an increase in specific force. In theory, reduced RYR-1 expression or function lead to reduced SR storage of Ca^{+2}, reduced Ca^{+2} binding capacity of troponin C, reduced ATP availability and could reduce contractility of skeletal muscle (Cong et al., 2016). During the early

stage of myofibre damage in DMD, the overall function of RYR-1 is reduced which lead to reduced Ca^{+2} release and hence the generated action potential (Lovering et al., 2009, Hernandez-Ochoa et al., 2015). As the level of myofibre contraction and subsequent force production are controlled in part by intracellular Ca^{+2} release (Chin, 2010), a gradual decrease of RYR-1 Ca^{+2} release in DMD contributes to the development of muscle weakness. Speculatively, the increase in RYR-1 expression facilitates the release of Ca^{+2} available for muscle contraction.

6) Increasing expression of inflammatory cytokines. Cruz-Guzmán et al., has reported a study that systemic inflammation is increased in patients with better muscle function and decreased in patients with poorer muscle function (Cruz-Guzmán et al., 2015). Therefore, increasing inflammatory cytokines is possibly involved in repair process. Speculatively, increased expression of pro-inflammatory markers in young *mdx* mice in this thesis could be another factor of improved function, as there is a relationship between inflammation and angiogenesis pathways. For example; studies have showed that IL-6 induce VEGF expression, leading to enhanced angiogenesis and vasculature in synovial fibroblast, which are specialized cells located inside joints and play crucial role in the chronic inflammatory diseases (Nakahara et al., 2003). We could hypothesize that increasing expression of IL-6 in young *mdx* muscle improves function through modulating angiogenesis. Future work should address quantity of different immune cells to understand the role of inflammation in muscle function.

As inflammatory cytokines were assessed using qRT-PCR, there are disadvantages encountered on using this technique. It does not directly measure

proteins levels as the secretion of some cytokines such as IL-10 is regulated at the translational level and IL-1β is regulated post-translationally. Moreover, classifying the source of cytokines required a separate isolation of different cell types (Amsen et al., 2009). However, the results reported in this thesis represented the secreted cytokines from whole muscles, which highlighted a question of which cells types are affected by ERRγ over-expression. Although, the implication of more advanced method such as; cytokine bead array allow for detection of a whole panel of cytokines using small volume of sample, the high cost and low sensitivity of such approach represent the main disadvantage, which may affect the interpretation. During the analysis of inflammatory cytokines, I have tried to optimize this approach on blood serum from 6 weeks study. The low sensitivity of the kit despite using the lowest possible concentration of the sample represent the main hurdle of using such approach. Another protocol based on in-situ hybridization on fresh tissue samples has been recommended in order to specify the localization and type of cytokines-producing cells, but, this method is not quantitative and does not reflect the protein levels (Amsen et al., 2009). Further fluorescence-activated cell sorting (FACS) analysis and histology analysis on damaged sections would be required to quantify the number of different immune cells within the tissue.

Interestingly, inflammatory cytokines showed different expression pattern following ERRγ over-expression between muscles of different ages. Specifically, expression of pro-inflammatory cytokines were reduced after 4 weeks of ERRγ over-expression in TA muscles obtained from IM of AAV8- ERRγ into 6 week-old *mdx*. On the contrary, EDL muscles from mice treated at the same age, with different dose but, for the same length of time showed no difference in pro-

inflammatory cytokines. However, EDL muscles from mice treated at 3 weeks of age showed reduced expression of the same cytokines. Therefore, the inconsistency in these results reflect how complex is the immune system in DMD pathology, suggesting that inflammatory cytokines may increase or decrease dependent on the level of damage of the cells and the time of the damage as well as the time of any therapeutic intervention in dystrophic muscle.

The status of the cells will determine the need to upregulate, down regulate or unchanged expression of inflammation pathway. Since the muscles are under ongoing asynchronous degeneration/regeneration cycles, the interpretation of these data is difficult taking into account that fibres are not going into damage at the same time. Moreover, the regeneration of the muscle depends on the balance between pro-inflammation and anti-inflammatory factors that determine whether the damage will be repaired with the muscle replacement and functional contractility or with scar tissue formation (Loell and Lundberg, 2011, Wynn and Vannella, 2016, Karin and Clevers, 2016). Therefore, even if the anti-inflammation cytokines increased at some points, once the other fibre starts damaging, the pro-inflammatory cytokines will increase, which ensures a failure of the transition from the M1 pro-inflammatory phenotype to the M2 repairs phenotype.

Another factor to consider for future work is the autophagy assessment. To assess autophagy, for future work, we should consider autophagy as a multistep pathway with each step characterized by a particular rate. Using approach of a single cell fluorescence live-cell imaging based approach that describes the autophagosome pool size, autophagosome flux and the transition time required

to continue the intracellular autophagosome pool. This method will provide quantitative measurement of autophagosome flux (Loos et al., 2014).

Generally, two main outcomes were highlighted from these two studies; the efficient therapy implemented at early time of intervention and the significance of using high dose. In one hand, Head et al., recommended that therapy need to be implemented in the early phase of disease as he suggested two stages of muscle damage in *mdx*. The absence of dystrophin, in young muscles, activates channels that elevate Ca^{+2} followed by damage caused by this increase. This damage later, causes splitting of fibres that leads to further damage and weaken muscle force. Due to imbalances of force generation around the split site, fibres from *mdx* exhibit branches sides, possibly due to abnormal or incomplete regeneration (Head, 2010, Chan and Head, 2011). The notion of age-dependent limitations in the effectiveness of any intervention has been reported in exon skipping as the effectiveness is limited in more damaged muscles (Wu et al., 2014).

Since the effectiveness of activating ERRγ approach was limited to younger mice, therefore, early time of intervention through AAV-ERRγ is one of the important factors that potentially results in the increase in specific force and improvements in pathology.

Noteworthy, therapeutic applications based on AAV gene therapy will require high viral titre loads *e.g.* potentially $1X10^{15}$ to $1X10^{16}$ vector particles/kg (Hinderer et al., 2018). Therefore, the highest dose in this thesis ($2X10^{12}$ vg of AAV8) was conducted in the youngest mice in an attempt to achieve greatest vector particles/kg. Recently, severe toxicity was reported following high dose of AAV.

Although, targeting liver via systemic administration of AAV vectors was successful in term of reaching therapeutic level of transduction efficiency using doses range between 10^{12}-10^{13} vg/kg. However, in poor capillary network organs such as skeletal muscle, targeting therapeutic level requires high dose, which is equal to 10^{14} or more of viral genome. As demonstrated recently, systemic administration of high dose of AAV9 variant (AAVhu68) expressing SMN gene targeting spinal muscular atrophy (SMA) showed unexpected toxicity in monkeys and piglets. The researchers reported sensory motor degeneration and elevated transaminases in both species whereas acute inflammation, coagulation defects and hepatic toxicity were observed in monkeys. This toxicity was due to reasons does not involve immune response to viral capsid or the transgene. Whether the toxicity was due to the high dose, or a contamination or a procedure of tittering the virus or human gene in non-human tissues, is a future work to address (Hinderer et al., 2018). Similar toxic events was observed using high dose of AAV-PHP.B ($7.5x10^{13}$ GC/kg), another AAV9 variant into nonhuman primates (Hordeaux et al., 2018). However, there are two possible explanation for the reported toxicity as suggested by the authors; 1) large numbers of vector genome lead to toxicity and contamination of the vector to hepatocytes through activation of DNA damage response or activation of endoplasmic reticulum (ER) stress pathways by transgene over-expression. However, since different labs use different methods to measure the dose, it would be more practical that key stakeholders in the gene therapy field work together to develop reference standards and standardized methods, as this would eliminate the variation of virus sources and production facilities and therefore, we will have more comparative studies. 2) Activation of adaptive immunity and destruction of

hepatocytes through antigen specific-T-cell responses to either the transgene product or vector capsid (Hordeaux et al., 2018). On the other hand, regarding the dose effect, the modest dose of $2X10^{12}$ vg/kg of AAV8 expressing factor IX in haemophiliaX clinical trials showed an increased level of transaminase, which associate with adaptive immune response but that does not meet the criteria of toxic effects (Manno et al., 2006). The peak of transaminase was different between these two studies, where in the former, the toxicity was reminiscent of that observed with acute acetominophen poisoning that result from diffuse hepatocellular injury caused by release of excessive ROS and decreased antioxidants molecules (Jaeschke et al., 2012).

In the absence of dystrophin restoration, vector copies will likely be lost due to muscle cell turnover, re-administration of virus will become an increasing translational bottleneck to overcome. However, AAV vectors at high does have the potential to elicit immune response against vector capsid and transgene. The fact that most people developed an immune response against a particular variants, resulting in pre-exciting of adaptive response. This can include the presence of neutralizing antibodies or T cells dependent B-cell response that will eliminate the cells that have been transduced or diminish the efficacy of re-administration approach with AAV (Naso et al., 2017). To date, this represent one of the biggest challenge to therapeutic AAV. Therefore, nowadays several transient immune modulatory regimens have been applied in gene therapy researches to prevent humoral and cellular immune response. For example, treatment with antibody against CD4 allows transgene expression (Chirmule et al., 2000). Combined immunosuppression drugs of anti-thymocyte globulin (ATG), cyclosporine (CSP) and mycophenolate mofetil (MMF) have been used

to suppress the immune response to vector and transgene in the muscle transduced with AAV mediated expression of µDys in canine X-linked muscular dystrophy (*cxmd*) dog (Wang et al., 2007). In addition, although, immune response to transgene product can be affected by the innate immune response to vector. However, immune response against the transgene were not detected in most of the clinical trials following IM gene transfer using AAV in muscular dystrophy, hemophilia B, lipoprotein lipase deficiency (Mingozzi and High, 2013). The work conducted in this thesis was based on a single administration of AAV. The future direction may consider re administration of AAV combined with immunosuppressant drugs to reduce the immune response.

Then, the next step to finalize the experiment of sequence optimized ERRγ gene transfer is to solve the problem encountered with qRT-PCR primers and to assess the histological outcomes in terms of SDH, MYH-3, IgG and H&E. Although, the western blot data in that chapter does not fully support the increase in ERRγ, however, we cannot draw a full conclusion from that results in the presence of an increase in the functional output. Moreover, other studies have been solely dependent on RNA data only with no demonstrable evidence of protein over-expression. For example, three studies of AAV6-PGC-1α did not showed any data of PGC-1α protein level and confirmed the increase of PGC-1α using qRT-PCR data only (Hollinger and Selsby, 2015, Hollinger et al., 2013, Selsby et al., 2012). Further, because sequence analysis reveals that ERRs share a high degree of homology within their DNA and ligand-binding domains (LBDs), (Dufour et al., 2007, Misawa and Inoue, 2015), there is high chance of amino-acid overlapping, hence, limit the efficiency of antibody detection. It should be noted for example that the antibody used to detect ERRβ binding sites in the mouse

embryonic stem cells study also recognized ERRγ (Chen et al., 2008). Further, to detect ERRα in tissues of cancer, an antibody was generated specific to a sequence in LBD to minimize the overlapping detection with other ERR receptors (Gaillard et al., 2007). For future work, we should consider trying another antibody for ERRγ.

Moreover, it is also possible that the method of preparing samples need further optimization. Therefore, using a different protocol to fractionate samples into nuclear and cytosolic fractions will give better indication of the level of change in the markers assessed in this thesis. (Figure 2, (A-B)) in (Wan et al., 2012), for example, showed different pattern of protein level of PGC-1α and ERRγ between the different fractions at different time points.

In conclusion, AAV-ERRγ approach could provide transient benefits when administration takes place at 3 weeks of age as shown in this thesis, however, we should consider assessing different time points. Moreover, due to loss of virus, minimal benefits and possible immune response to AAV, we should also consider the data from the cMap list. On the basis of cMap list, an emerging drugs could be a suitable target to mimic ERRγ over-expression as an alternative pharmaceuticals approach especially those with known established effect. The advantage of reconsidering established drugs is that they have already been approved and hence they can potentially be re-marketed in a faster and more efficient way by skipping Phase I clinical trials (Iorio et al., 2013).

Generally, for efficient gene transfer, critical parameters should be considered; vector design, capsid selection, desired target cells and tissue type and route of administration. The transgene to be delivered optimized for expression, the right

AAV variant with an appropriate capsid for target cell transduction and immunity profiles and the appropriate delivery approach to maximize target tissue exposure. Understanding the disease mechanism, the turnover rate of the target cell, the effect of the therapeutic transgene, all of these factors will allow better designing of the trials, optimization of vector construction and developing the right gene therapeutic. Toxicities will require to be monitored in the course of any AAV clinical development.

6.2. Future works:

- Assess the mtDNA to investigate the role of postnatal over-expression of ERRγ on mitochondrial biogenesis, as there is no direct evidence has been addressed here.
- Completion of assessing factors associated with oxidative capacity, angiogenesis, inflammation and pathology in muscles from 3 weeks old *mdx* of intraperitoneal administration of AAV9-ERRγ.
- Assess the long-term effect changes in pathology, function and biomarker profiling in dystrophic skeletal muscle following AAV mediated ERRγ expression.
- Assess the pathological and functional changes in dystrophic skeletal muscle following re-administration of AAV-ERRγ.
- Assess the pathological and functional changes in dystrophic skeletal muscle following dual administration of AAV-ERRγ and AAV-μdystrophin
- Assess the pathological and functional changes in dystrophic muscle following administration of AAV-ERRγ followed by administration of

antisense oligonucleotides to restore dystrophin to muscle by exon skipping, as over-expression of ERRγ reflect an increase in the capillary density which potentially will improve delivery of antisense oligonucleotides.

- Developing the mimetic drug approaches that achieve similar effects as AAV mediated over-expression of ERRγ

6.3. Limitations:

Study One:

The main limitation of this work is inability to count the number of positive fibres for ERRγ in sections as the ERRγ construct was fused with Ha-tag and no increase in the ERRγ protein level was detected. Part two of that study has no western blot for ERRγ, as the samples have been lost.

Study two:

Two glycolytic muscles only were assessed as gastrocnemius showed the highest over-expression of ERRγ and EDL was used for functional measurement. I think assessment of diaphragm as an example of sever pathophysiology resembles disease feature in humans would be a good comparison.

Study 3:

Assess the oxidative stress using oxyblot to measure carbonylated proteins as a measure of a reduction in oxidative stress as there is evidence of increased mitochondrial proteins and enhancement of vasculature, which potentially help on reducing mitochondrial stress.

7. APPENDIX

7.1. List of Equipment:

- Countess Cell Counter machine (Life Technology)
- Cryostat Bright OTF5000
- Image J software
- Image Quanta
- Nanodrop: Thermo Scientific NanoDrop 2000 spectrophotometer
- PCR machine T100 Thermal cycler B10-Rad
- Step one Plus Real time PCR system (Applied Biosystems)

7.2. List of materials:

- ABC kit (Vector laboratory, PK-6100)
- Agar (Sigma A1296)
- Agarose (Sigma A9539)
- Avidin-Biotin Blocking kit (Vector laboratory, SP2001)
- Benzonase (Sigma E8263 Ultrapure)
- Beta gal assay #11 539 426 001-Roche)
- β-mercaptoethanol (Sigma 63689)
- CK assay Randox Laboratory limited, CK522 (#1530).
- Clarity western ECL substrate (Bio-Rad 170-5060)
- Dako fluorescent (Dako S3023)
- DC assay (Bio-Rad DCTM Protein Assay)
- DMEM (Sigma D6429)
- DNA gel stain (Invitrogen S33102)
- DNase 1: 10 mg/ml in H20 or RQ1 DNase 1 (1 U/µl Promega)
- DPX (VWR 360294H)

- Fetal Calf Serum FCS (Sigma F2442)
- Gel extraction kit (QIAEX II Gel Extraction Kit, # 20051, QIAGEN).
- Gel loading buffer (Sigma G2526)
- Glucose (Sigma G 8270)
- Glycogen (invitrogen)
- Housekeeping genes (Primer design HK-SY-mo-600).
- Isopentane (VWR)
- KCN (Fisher 1059938)
- LB-agar
- LB-Broth (Sigma L7658)
- Linear polyethylenimine (PEI) (408727, Sigma)
- Mayers haematoxylin (MHS80-Sigma)
- Non-fat milk powder
- MOPS running buffer (Sigma PCG 3003)
- Nitroblue tetrazolium (Sigma 74032)
- Nitrocellulose membrane: (Hybond-C Extra; GE Healthcare Life Science, Pittsburgh, PA, USA)
- Novex sharp Pre-stained Protein standard (Invitrogen LC5800)
- NP-40
- NuPAGE LDS sample buffer (4X) (Novex, NP0008)
- OCT (Tissue Tek 4583)
- PBS tablet (Gibco, Life Technology 18912-014)
- Penicillin-Steptomycin (Sigma P4333)
- Perfecta SYBR Green FastMix (# 019358, Quantabio).
- Peroxidase substrate kit (DAB) kit (Vector Laboratory SK-4100)

- Phosphatase inhibitors (Sigma P5726)
- Ponceau (Sigma P7170)
- Proliferation assay (G3582, Promega)
- Protease inhibitors (Sigma S8820)
- Proteinase K: (10 mg/ml in water. Sigma P2038)
- QIAprep Spin Miniprep Kit (Quanta- 27106)
- QScript cDNA Synthesis Kit (Quanta-733-1174P)
- Quick-Seal ultra-clear: Beckman 361 625
- RNA extraction protocol (Sigma T9424)
- SDS (Sigma 05030)
- Sodium deschocloalte
- Succinate stock (Fisher 11418852)
- Transfer buffer (Sigma TruPAGETM Transfer PCG3011)
- TRI-reagent (Sigma 9424)
- Triton X100 (Sigma T9284)
- TruPAGE Precast Gel (4-12% SDS), (Sigma, PCG2003-10EA)
- Tween-20 (Sigma P7949)
- Trypsin/EDTA (sigma T4174)
- XL-10 gold (Agilent echnologies)
- Xylene (Fisher X/025/17)
- 25:24:1 phenol/chloroform/isoamyl alcohol (Sigma P2069)

7.3. Buffer formulation:

- 40% Polyethylene glycol (PEG) 8000:

40% [w/v] PEG 8000 with 2.5 M NaCl in water. (For 500 ml – 200 g PEG 8000, 73.05 g NaCl). Sterilise by passing through a 0.22 µm filter. Store at room temperature

- Lysis buffer (500 ml):

  4.38 g NaCl (0.15 M), 25 ml 1M Tris.Cl pH8.5 (50 mM). and autoclaved.

- 5X PBS-MK (100 ml):

  Take 5 Phosphate Buffered Saline Tablets and add to 90 ml of distilled water. Autoclave, cool, and add 0.5 ml 1M $MgCl_2$ (5 mM) and 1.25 ml of 1 M KCl (12.5 mM). Make up to 100 ml with sterile water. (It is important not to add the $MgCl_2$ and KCl before autoclaving as these salts will precipitate out of solution and will not go back in even when the solution is cooled.)

- 2x Proteinase K buffer:

  20 mM Tris.Cl (pH 8.0), 20 mM EDTA (pH8.0), 1% (w/v) SDS. Store at RT

- 20x SSC (1 litre):

  175 g NaCl (1.5 M), 88 g Na_3 citrate (0.3M)

- Hybridisation buffer:

  (Nonradioactive labelling of probe and detection (Amersham RPN3000) required volume of ECL gold hybridisation buffer to cover blot, 0.5 M NaCl, 5% (w/v) blocking agent (usually use 34 ml ECL hybridisation buffer, 1 g NaCl, 1.7 g blocking agent). Mix at RT until dissolved (0.5-1 hr) and heat to 42°C (0.5 hr).

- Primary wash buffer (1litre):

  360 g urea (6 M), 4 g SDS (0.4%), 25 ml 20x SSC (0.5x SSC). Store at 4°C.

- 3 M NaAc pH 5.2:

  81.66 g sodium acetate. $3H_2O$ in 150 ml water, Adjust to pH5.2 with glacial acetic acid. Adjust volume to 200 ml with H_2O. Sterilize by autoclaving

- Formol calcium:

  100 ml of 40% formaldehyde, 20g calcium chloride and with 900 ml of water

- Permeabilization buffer:

  (200 mM Hepes, 300 mM sucrose, 50 mM NaCl, 0.5%TX100, 3 mM $MgCl_2$ and 0.05% Na azide)

- Washing buffer:

  (5% fetal calf serum, 200 mg Na azide, 0.05% TritonX and 500 ml PBS)

- RIPA lysis buffer:

  (50 mM tris-HCl, 150 mM NaCl, 1 mM EDTA, 1% NP-40, 0.25% w/v sodium deoxycholate, protease inhibitors (1:10) and phosphatase inhibitors (1:100)

- Western blot blocking buffer:

  5% milk in Tris buffered saline, 0.1% Tween 20 (TBST)

7.4. Native pAAV-ERRγ

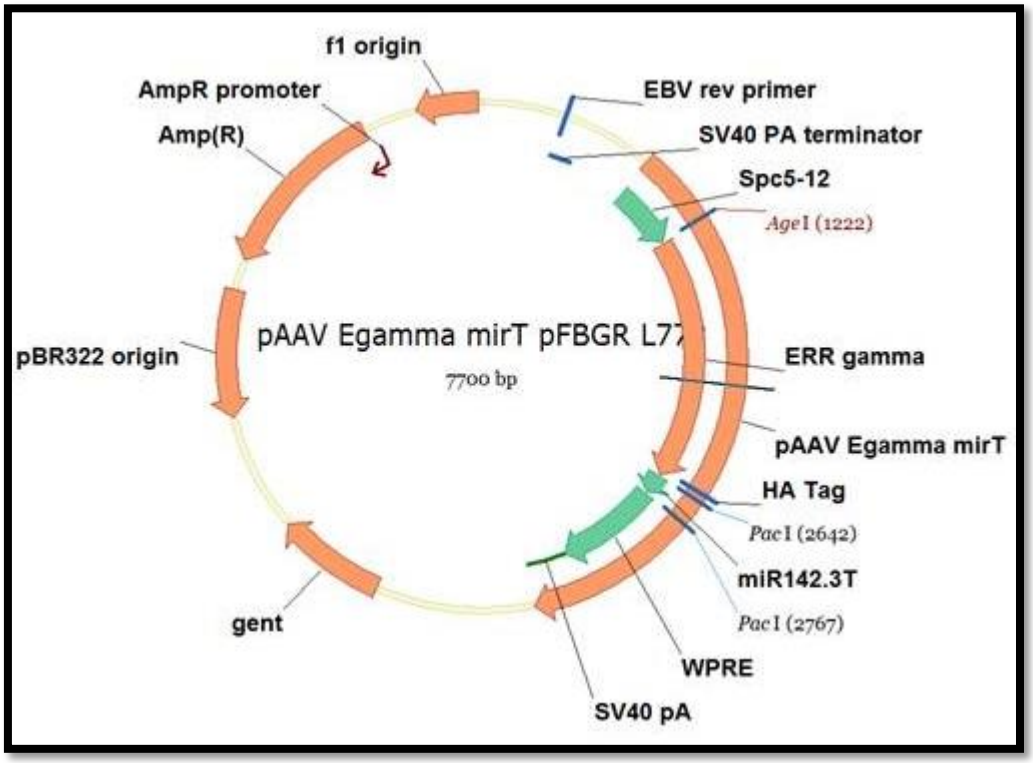

7.5. pAAV SO 3F' ERRγ

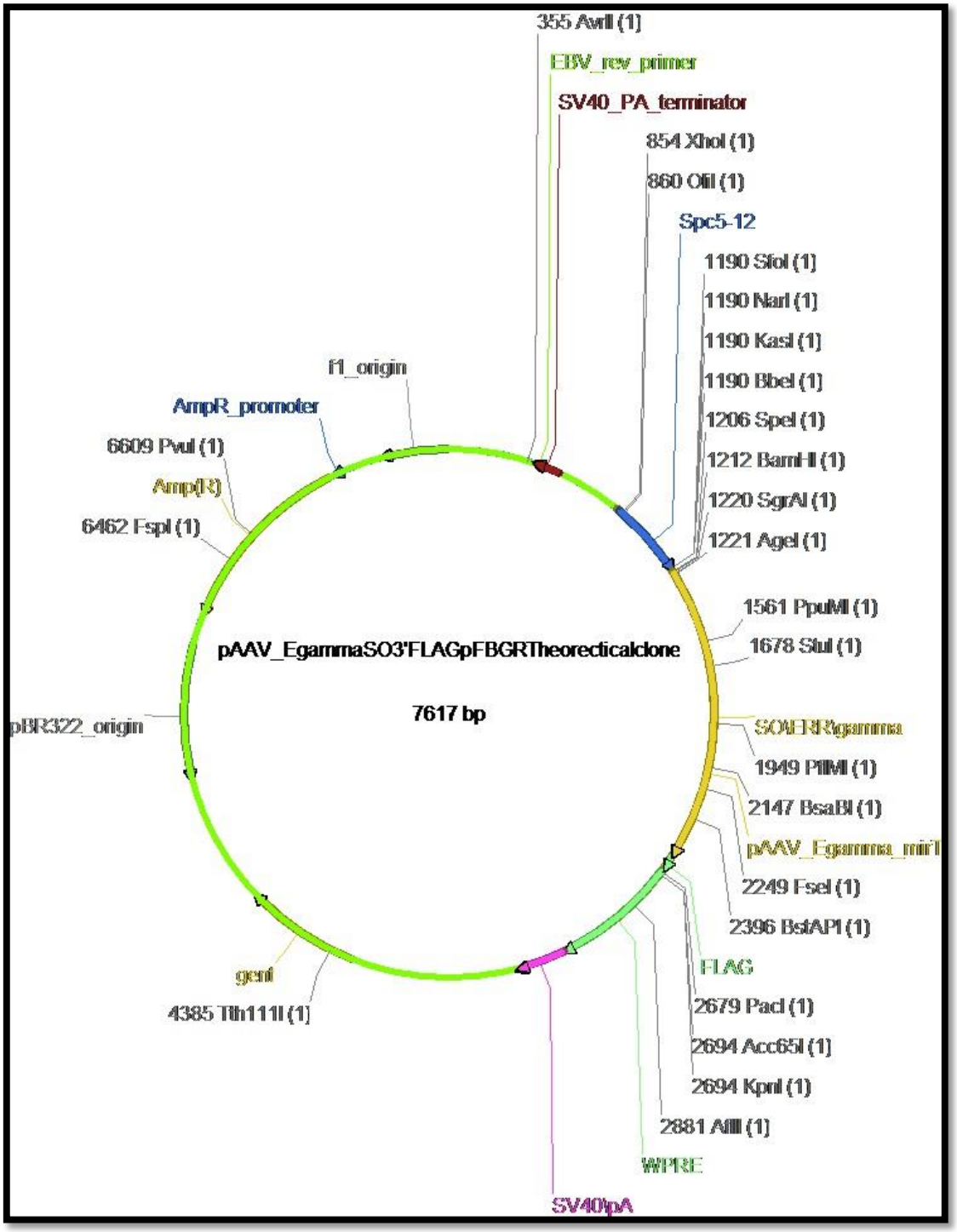

7.6. Sequence optimization:

5'F SO ERRγ:

Accggtgccacc ATG GACTACAAAGATCACGATGGGGACTATAAGGACCATGACATCG
ACTACAAAGACGATGACGACAAA ATG GATAGCGTCGAACTGTGTCTGCCAGAGAG
CTTCTCTTTGCATTACGAAGAGGAGCTGTTGTGCAGAATGAGCAATAAGGATAGG
CACATCGATTCCTCTTGTTCATCCTTCATCAAAACCGAACCCAGCTCACCAGCTTC
CCTGACTGACTCAGTGAACCACCATTCTCCTGGTGGCAGTTCAGACGCATCCGG
GTCATATAGCTCTACTATGAATGGGCATCAGAATGGCCTGGACAGTCCACCACTG
TATCCCTCTGCCCCTATACTGGGTGGTTCTGGACCTGTTCGCAAACTGTACGACG
ATTGCAGCAGTACTATCGTTGAGGATCCGCAGACAAAATGCGAGTACATGCTGAA
CAGTATGCCCAAACGTCTGTGCTTGGTGTGCGGAGATATCGCCAGTGGGTATCAC
TACGGAGTGGCTTCCTGTGAAGCCTGTAAGGCCTTCTTTAAGCGGACAATTCAGG
GGAACATCGAGTACTCCTGTCCGGCTACCAATGAGTGCGAGATCACCAAACGGA
GGCGGAAATCTTGCCAGGCATGTCGCTTCATGAAGTGCCTCAAAGTGGGGATGC
TGAAAGAGGGCGTTCGTTTGGACCGGGTGAGAGGAGGCAGGCAGAAGTACAAGA
GGAGAATTGACGCGGAAAACTCCCCATATCTGAATCCCCAGCTCGTTCAACCAGC
CAAGAAGCCCTACAACAAGATTGTGAGCCATCTGCTGGTAGCTGAACCTGAGAAG
ATATACGCAATGCCTGACCCTACAGTACCTGACAGCGACATCAAAGCGCTTACGA
CTCTGTGTGATCTCGCCGATAGGGAACTTGTGGTGATTATTGGCTGGGCCAAGCA
CATTCCCGGCTTTAGCACACTGTCTCTCGCTGATCAGATGTCCCTGCTTCAATCC
GCTTGGATGGAGATCCTGATTCTGGGAGTCGTGTATCGATCACTGTCTTTCGAGG
ATGAGCTCGTCTACGCCGATGACTATATCATGGATGAAGATCAGAGTAAACTTGC
GGGTTTGCTCGACCTGAACAACGCCATCCTGCAGCTGGTGAAGAAGTATAAGAG
CATGAAGCTCGAGAAAGAGGAATTTGTCACACTGAAGGCTATTGCCCTTGCCAAT
AGCGACAGCATGCACATAGAAGATGTTGAGGCTGTCCAGAAGTTGCAGGACGTG
CTGCATGAAGCTCTCCAGGATTATGAAGCAGGCCAACACATGGAGGACCCAAGA
CGCGCAGGAAAGATGCTCATGACCCTTCCGCTGTTGCGACAAACCAGTACGAAA
GCAGTACAGCACTTCTACAACATAAAGCTTGAAGGCAAGGTGCCCATGCACAAGC
TCTTTCTGGAGATGCTGGAGGCAAAGGTCTGA ttaattaa

3’F SO ERRγ:

Accggtgccacc ATGGATAGCGTCGAACTGTGTCTGCCAGAGAGCTTCTCTTTGCATT
ACGAAGAGGAGCTGTTGTGCAGAATGAGCAATAAGGATAGGCACATCGATTCCTC
TTGTTCATCCTTCATCAAAACCGAACCCAGCTCACCAGCTTCCCTGACTGACTCAG
TGAACCACCATTCTCCTGGTGGCAGTTCAGACGCATCCGGGTCATATAGCTCTAC
TATGAATGGGCATCAGAATGGCCTGGACAGTCCACCACTGTATCCCTCTGCCCCT
ATACTGGGTGGTTCTGGACCTGTTCGCAAACTGTACGACGATTGCAGCAGTACTA
TCGTTGAGGATCCGCAGACAAAATGCGAGTACATGCTGAACAGTATGCCCAAACG
TCTGTGCTTGGTGTGCGGAGATATCGCCAGTGGGTATCACTACGGAGTGGCTTC
CTGTGAAGCCTGTAAGGCCTTCTTTAAGCGGACAATTCAGGGGAACATCGAGTAC
TCCTGTCCGGCTACCAATGAGTGCGAGATCACCAAACGGAGGCGGAAATCTTGC
CAGGCATGTCGCTTCATGAAGTGCCTCAAAGTGGGGATGCTGAAAGAGGGCGTT
CGTTTGGACCGGGTGAGAGGAGGCAGGCAGAAGTACAAGAGGAGAATTGACGC
GGAAAACTCCCCATATCTGAATCCCCAGCTCGTTCAACCAGCCAAGAAGCCCTAC
AACAAGATTGTGAGCCATCTGCTGGTAGCTGAACCTGAGAAGATATACGCAATGC
CTGACCCTACAGTACCTGACAGCGACATCAAAGCGCTTACGACTCTGTGTGATCT
CGCCGATAGGGAACTTGTGGTGATTATTGGCTGGGCCAAGCACATTCCCGGCTTT
AGCACACTGTCTCTCGCTGATCAGATGTCCCTGCTTCAATCCGCTTGGATGGAGA
TCCTGATTCTGGGAGTCGTGTATCGATCACTGTCTTTCGAGGATGAGCTCGTCTA
CGCCGATGACTATATCATGGATGAAGATCAGAGTAAACTTGCGGGTTTGCTCGAC
CTGAACAACGCCATCCTGCAGCTGGTGAAGAAGTATAAGAGCATGAAGCTCGAGA
AAGAGGAATTTGTCACACTGAAGGCTATTGCCCTTGCCAATAGCGACAGCATGCA
CATAGAAGATGTTGAGGCTGTCCAGAAGTTGCAGGACGTGCTGCATGAAGCTCTC
CAGGATTATGAAGCAGGCCAACACATGGAGGACCCAAGACGCGCAGGAAAGATG
CTCATGACCCTTCCGCTGTTGCGACAAACCAGTACGAAAGCAGTACAGCACTTCT
ACAACATAAAGCTTGAAGGCAAGGTGCCCATGCACAAGCTCTTTCTGGAGATGCT
GGAGGCAAAGGTCATG GACTACAAAGATCACGATGGGGACTATAAGGACCATGA
CATCGACTACAAAGACGATGACGACAAA TGA ttaattaa

SO ERRγ=Gray

Flag sequence=Turquoise

Kozak=Red

AgeI=Green

PacI=Pink

7.7. List of primers:

Table 7.1. List of primers

Atp5b.F	GGTTCATCCTGCCAGAGACTA
Atp5b.R	AATCCCTCATCGAACTGGACG
Atrogin-1.F	GCAAACACTGCCACATTCTCTC
Atrogin-1.R	CTTGAGGGGAAAGTGAGACG
Beclin-1.F	TGAATGAGGATGACAGTGAGCA
Beclin-1.R	CACCTGGTTCTCCACACTCTTG
Bnip3.F	TTCCACTAGCACCTTCTGATGA
Bnip3.R	GAACACCGCATTTACAGAACAA
CathepsinL.F	GTGGACTGTTCTCACGCTCAAG
CathepsinL.R	TCCGTCCTTCGCTTCATAGG
Cat.F	GGATTATGGCCTCCGAGATCTT
Cat.R	TAAAACGTCCAGGACGGGTAA
Cox5b.F	AAGTGCATCTGCTTGTCTCG
Cox5b.R	GTCTTCCTTGGTGCCTGAAG
CPT1β.F	TCTTCTTCCGACAAACCCTGA
CPT1β.R	GAGACGGACACAGATAGCCC
CTP1α.F	CAC CAA CGG GCT CAT CTT CTA
CTP1α.R	CAA AAT GAC CTA GCC TTC TAT CGA A
ERRγ.F	ACT TGG CTG ACC GAG AGT TG
ERRγ.R	GCC AGG GAC AGT GTG GAG AA
FOXO1.F	GCTGGGTGTCAGGCTAAGAG
FOXO1.R	AGGGGTGAAGGGCATCT
Gadd34.F	AGAGAAGACCAAGGGACGTG
Gadd34.R	CAGCAAGGAATGGACTGTG
IL1-B. F	GGATGATGATGATAACCTGC
IL1-B. R	CATGGAGAATATCACTTGTTGG
IL6. F	GTCTATACCACTTCACAAGTC
IL6. R	TGCATCATCGTTGTTCATAC
IL10. F	CAGGACTTTAAGGGTTACTTG
IL10. R	ATTTTCACAGGGGAGAAATC
MuRF1.F	ACCTGCTGGTGGAAAACATC
MuRF1.R	CTTCGTGTTCCTTGCACATC
ND2-F	AGGGATCCCACTGCACATAG
ND2-R	CTCCTCATGCCCCTATGAAA
Ndufb5.F	CTTCGAACTTCCTGCTCCTT
Ndufb5.R	GGCCCTGAAAAGAACTACG
NF-κB. F	CATATGACGGCATCTCCCCA
NF-κB. R	TTCATAACAAAATTGCCCTGCTGA
NRF2 -F	CCTCTGTCACCAGCTCAAGG
NRF2 -R	TTGATGACCAGGACTCACGG
P62.F	CCCAGTGTCTTGGCATTCTT
P62.R	AGGGAAAGCAGAGGAAGCTC
PERM1.F	CCTGGTCGTAAGAAGAGGCG
PERM1.R	CTTGGGCCTGGTAAGCTGT
PGC1α.F	AAC CAC ACC CAC AGG ATC AGA
PGC1α.R	TCT TCG CTT TAT TGC TCC ATG A
PPARα.F	ACA AGG CCT CAG GGT ACC A
PPARα.R	GCC GAA AGA AGC CCT TAC AG
PPARδ.F	GCC TCG GGC TTC CAC TAC
PPARδ.R	AGA TCC GAT CGC ACT TCT CA
PPARγ.F	GACGCGGAAGAAGAGACCTG
PPARγ.R	GTGTGACTTCTCCTCAGCCC
RYR-1. F	GCACACAGTCGTATGTACCTG
RYR-1. R	CCTCCCCTGTTGCGTCTTC
Sdha.F	GGAACACTCCAAAAACAGACCT
Sdha.R	CCACCACTGGGTATTGAGTAGAA
Sdhc.F	GCTGCGTTCTTGCTGAGACA
Sdhc.R	ATCTCCTCCTTAGCTGTGGTT
SERCA-1.F	AGCCAGTGATGGAGAACTCG
SERCA-1. R	CACCACCAACCAGATGTCAG
SIRT1. F	GATGACAGAACGTCACACGC
SIRT1. R	ATTGTTCGAGGATCGGTGCC
SOD2. F	AGGAGAGTTGCTGGAGGCTA
SOD2. R	CTGTAAGCGACCTTGCTCCT
TFAM. F	CCTTCGATTTTCCACAGAACA
TFAM. R	GCTCACAGCTTCTTTGTATGCTT
TNF-alpha. F	CTATGTCTCAGCCTCTTCTC
TNF-alpha. R	CATTTGGGAACTTCTCATCC
UTRN. F	ATCCAGCCAGCCAACATTTC
UTRN. R	GTCTTGGGATTGGCATTTGC
VEGFA165.F	TGC AGG CTG CTG TAA CGA TG
VEGFA165.R	GAA CAA GGC TCA CAG TGA TTT TCT
VEGFA189.F	TGC AGG CTG CTG TAA CGA TG
VEGFA189.R	CTC CAG GAT TTA AAC CGG GAT T

7.8. CMap List:

Table 7.2. List of drugs from cMap

COMPOUND	correl	significance
eucatropine	0.32	4.07(149)
sitosterol	0.31	3.64(131)
mephenesin	0.42	3.50(64)
todralazine	0.47	3.45(49)
Prestwick-860	0.29	3.25(122)
promazine	0.31	3.18(100)
urapidil	0.4	3.16(60)
fluorocurarine	0.44	3.11(47)
tanespimycin	0.16	3.06(380)
epitiostanol	0.45	3.01(41)
tyloxapol	0.24	2.97(147)
alvespimycin	0.22	2.97(178)
pancuronium_bromide	0.31	2.93(89)
trioxysalen	0.25	2.90(133)
metamizole_sodium	0.24	2.88(145)
Prestwick-665	0.26	2.80(114)
noscapine	0.55	2.79(23)
GW-8510	0.16	2.79(305)
ebselen	0.25	2.78(120)
apigenin	0.18	2.73(236)
carbachol	0.22	2.72(146)
alpha-estradiol	0.19	2.72(198)
azlocillin	0.31	2.67(74)
deptropine	0.28	2.66(88)
metacycline	0.26	2.66(106)
ellipticine	0.21	2.65(159)
sulconazole	0.19	2.65(197)
torasemide	0.27	2.63(93)
oxymetazoline	0.36	2.60(51)
(-)-MK-801	0.33	2.57(59)
dimethadione	0.44	2.57(32)
glibenclamide	0.29	2.56(77)
sulfacetamide	0.37	2.56(47)
hesperetin	0.35	2.53(51)
felodipine	0.29	2.53(75)
levonorgestrel	0.18	2.51(188)

COMPOUND	correl	significance
cefalexin	0.25	2.51(100)
8-azaguanine	0.17	2.48(216)
thioridazine	0.2	2.48(158)
paracetamol	0.35	2.45(49)
tinidazole	0.42	2.44(33)
Prestwick-967	0.47	2.44(26)
trichlormethiazide	0.3	2.43(65)
chlorambucil	0.29	2.43(67)
azaperone	0.31	2.43(60)
0175029-0000	0.15	2.43(272)
geldanamycin	0.19	2.43(163)
aminophylline	0.27	2.41(79)
sulfamethizole	0.33	2.41(54)
benfotiamine	0.31	2.40(58)
cefalonium	0.36	2.40(44)
nordihydroguaiaretic_acid	0.27	2.35(73)
thioguanosine	0.16	2.34(210)
doxazosin	0.19	2.33(151)
mitoxantrone	0.2	2.30(134)
bisacodyl	0.17	2.30(180)
gibberellic_acid	0.36	2.29(39)
lanatoside_C	0.18	2.29(168)
triprolidine	0.38	2.26(35)
methylergometrine	0.24	2.25(88)
hexestrol	0.19	2.25(140)
halcinonide	0.24	2.24(84)
novobiocin	0.38	2.23(35)
nialamide	0.27	2.23(68)
monorden	0.2	2.23(129)
zomepirac	0.23	2.22(89)
delsoline	0.25	2.22(81)
nicergoline	0.33	2.21(45)
clomipramine	0.22	2.20(100)
imidurea	0.24	2.20(87)
artemisinin	0.22	2.19(95)
roxarsone	0.24	2.19(86)
mebendazole	0.17	2.17(159)
netilmicin	0.3	2.15(50)
flunarizine	0.22	2.15(95)
helveticoside	0.17	2.14(155)
diflorasone	0.3	2.13(49)
luteolin	0.14	2.12(239)
phthalylsulfathiazole	0.14	2.11(227)
hydroquinine	0.29	2.11(54)
seneciphylline	0.32	2.10(44)
kanamycin	0.27	2.10(60)
clioquinol	0.21	2.10(96)
cefuroxime	0.3	2.08(49)
molindone	0.33	2.07(39)
flunixin	0.2	2.07(107)
ergocalciferol	0.32	2.07(41)
ticarcillin	0.27	2.06(59)
monocrotaline	0.25	2.05(65)
hydrastine_hydrochloride	0.26	2.05(64)
benzonatate	0.33	2.03(39)
trifluoperazine	0.17	2.03(148)
ouabain	0.18	2.01(130)
salbutamol	0.25	2.01(64)

8.References

AARTSMA-RUS, A. & KRIEG, A. M. 2017. FDA Approves Eteplirsen for Duchenne Muscular Dystrophy: The Next Chapter in the Eteplirsen Saga. *Nucleic Acid Therapeutics,* 27**,** 1-3.

ABOU-KHALIL, R., MOUNIER, R. & CHAZAUD, B. 2010. Regulation of myogenic stem cell behavior by vessel cells: the "menage a trois" of satellite cells, periendothelial cells and endothelial cells. *Cell Cycle,* 9**,** 892-6.

ACHARYYA, S., BUTCHBACH, M. E. R., SAHENK, Z., WANG, H., SAJI, M., CARATHERS, M., RINGEL, M. D., SKIPWORTH, R. J. E., FEARON, K. C. H., HOLLINGSWORTH, M. A., MUSCARELLA, P., BURGHES, A. H. M., RAFAEL-FORTNEY, J. A. & GUTTRIDGE, D. C. 2005. Dystrophin glycoprotein complex dysfunction: A regulatory link between muscular dystrophy and cancer cachexia. *Cancer Cell,* 8**,** 421-432.

ACHARYYA, S., VILLALTA, S. A., BAKKAR, N., BUPHA-INTR, T., JANSSEN, P. M. L., CARATHERS, M., LI, Z.-W., BEG, A. A., GHOSH, S., SAHENK, Z., WEINSTEIN, M., GARDNER, K. L., RAFAEL-FORTNEY, J. A., KARIN, M., TIDBALL, J. G., BALDWIN, A. S. & GUTTRIDGE, D. C. 2007. Interplay of IKK/NF-κB signaling in macrophages and myofibers promotes muscle degeneration in Duchenne muscular dystrophy. *The Journal of Clinical Investigation,* 117**,** 889-901.

AIDLEY, D. J. & ASHLEY, D. 1998. *The physiology of excitable cells*, Cambridge University Press Cambridge.

AKIMOTO, T., POHNERT, S. C., LI, P., ZHANG, M., GUMBS, C., ROSENBERG, P. B., WILLIAMS, R. S. & YAN, Z. 2005. Exercise stimulates Pgc-1alpha transcription in skeletal muscle through activation of the p38 MAPK pathway. *J Biol Chem,* 280**,** 19587-93.

AKIMOTO, T., RIBAR, T. J., WILLIAMS, R. S. & YAN, Z. 2004. Skeletal muscle adaptation in response to voluntary running in Ca2+/calmodulin-dependent protein kinase IV-deficient mice. *Am J Physiol Cell Physiol,* 287**,** C1311-9.

AL HAJ ZEN, A., OIKAWA, A., BAZAN-PEREGRINO, M., MELONI, M., EMANUELI, C. & MADEDDU, P. 2010. Inhibition of delta-like-4-mediated signaling impairs reparative angiogenesis after ischemia. *Circ Res,* 107**,** 283-93.

ALAYNICK, W. A., KONDO, R. P., XIE, W., HE, W., DUFOUR, C. R., DOWNES, M., JONKER, J. W., GILES, W., NAVIAUX, R. K. & GIGUERE, V. 2007. ERRγ directs and maintains the transition to oxidative metabolism in the postnatal heart. *Cell metabolism,* 6**,** 13-24.

ALLEN, D. G. & WHITEHEAD, N. P. 2011. Duchenne muscular dystrophy–what causes the increased membrane permeability in skeletal muscle? *The international journal of biochemistry & cell biology,* 43**,** 290-294.

ALLEN, D. G., WHITEHEAD, N. P. & FROEHNER, S. C. 2016. Absence of Dystrophin Disrupts Skeletal Muscle Signaling: Roles of Ca2+, Reactive Oxygen Species, and Nitric Oxide in the Development of Muscular Dystrophy. *Physiol Rev,* 96**,** 253-305.

ALTAMIRANO, F., LOPEZ, J. R., HENRIQUEZ, C., MOLINSKI, T., ALLEN, P. D. & JAIMOVICH, E. 2012. Increased resting intracellular calcium modulates NF-kappaB-dependent inducible nitric-oxide synthase gene expression in dystrophic mdx skeletal myotubes. *J Biol Chem,* 287**,** 20876-87.

AMSEN, D., DE VISSER, K. E. & TOWN, T. 2009. Approaches to determine expression of inflammatory cytokines. *Inflammation and Cancer.* Springer.

AMTHOR, H., MACHARIA, R., NAVARRETE, R., SCHUELKE, M., BROWN, S. C., OTTO, A., VOIT, T., MUNTONI, F., VRBOVA, G., PARTRIDGE, T., ZAMMIT, P., BUNGER, L. & PATEL, K. 2007. Lack of myostatin results in excessive muscle growth but impaired force generation. *Proc Natl Acad Sci U S A,* 104**,** 1835-40.

ANDERSEN, P. & HENRIKSSON, J. 1977. Training induced changes in the subgroups of human type II skeletal muscle fibres. *Acta Physiol Scand,* 99**,** 123-5.

ANDO, J. & KAMIYA, A. 1993. Blood flow and vascular endothelial cell function. *Frontiers of medical and biological engineering: the international journal of the Japan Society of Medical Electronics and Biological Engineering,* 5**,** 245-264.

ANGELINI, C. & PETERLE, E. 2012. Old and new therapeutic developments in steroid treatment in Duchenne muscular dystrophy. *Acta Myologica,* 31**,** 9-15.

ANGIONE, A. R., JIANG, C., PAN, D., WANG, Y.-X. & KUANG, S. 2011. PPARδ regulates satellite cell proliferation and skeletal muscle regeneration. *Skeletal Muscle,* 1**,** 33.

ANGUS, L. M., CHAKKALAKAL, J. V., MEJAT, A., EIBL, J. K., BELANGER, G., MEGENEY, L. A., CHIN, E. R., SCHAEFFER, L., MICHEL, R. N. & JASMIN, B. J. 2005. Calcineurin-NFAT signaling, together with GABP and peroxisome PGC-1{alpha}, drives utrophin gene expression at the neuromuscular junction. *Am J Physiol Cell Physiol,* 289**,** C908-17.

AOKI, Y., YOKOTA, T., NAGATA, T., NAKAMURA, A., TANIHATA, J., SAITO, T., DUGUEZ, S. M., NAGARAJU, K., HOFFMAN, E. P., PARTRIDGE, T. & TAKEDA, S. 2012. Bodywide skipping of exons 45-55 in dystrophic mdx52 mice by systemic antisense delivery. *Proc Natl Acad Sci U S A,* 109**,** 13763-8.

ARANY, Z., FOO, S. Y., MA, Y., RUAS, J. L., BOMMI-REDDY, A., GIRNUN, G., COOPER, M., LAZNIK, D., CHINSOMBOON, J., RANGWALA, S. M., BAEK, K. H., ROSENZWEIG, A. & SPIEGELMAN, B. M. 2008. HIF-independent regulation of VEGF and angiogenesis by the transcriptional coactivator PGC-1alpha. *Nature,* 451**,** 1008-12.

ARANY, Z., LEBRASSEUR, N., MORRIS, C., SMITH, E., YANG, W., MA, Y., CHIN, S. & SPIEGELMAN, B. M. 2007. The transcriptional coactivator PGC-1β drives the formation of oxidative type IIX fibers in skeletal muscle. *Cell metabolism,* 5**,** 35-46.

ARMSTRONG, R. & PHELPS, R. 1984. Muscle fiber type composition of the rat hindlimb. *Developmental Dynamics,* 171**,** 259-272.

ARNOLD, L., HENRY, A., PORON, F., BABA-AMER, Y., VAN ROOIJEN, N., PLONQUET, A., GHERARDI, R. K. & CHAZAUD, B. 2007. Inflammatory monocytes recruited after skeletal muscle injury switch into antiinflammatory macrophages to support myogenesis. *Journal of Experimental Medicine,* 204**,** 1057-1069.

ARORA, S., LIDOR, A., ABULARRAGE, C. J., WEISWASSER, J. M., NYLEN, E., KELLICUT, D. & SIDAWY, A. N. 2006. Thiamine (vitamin B1) improves endothelium-dependent vasodilatation in the presence of hyperglycemia. *Annals of vascular surgery,* 20**,** 653-658.

ARSIC, N., ZACCHIGNA, S., ZENTILIN, L., RAMIREZ-CORREA, G., PATTARINI, L., SALVI, A., SINAGRA, G. & GIACCA, M. 2004. Vascular endothelial growth factor stimulates skeletal muscle regeneration in vivo. *Mol Ther,* 10**,** 844-54.

ASAI, A., SAHANI, N., KANEKI, M., OUCHI, Y., MARTYN, J. A. & YASUHARA, S. E. 2007. Primary role of functional ischemia, quantitative evidence for the two-hit mechanism, and phosphodiesterase-5 inhibitor therapy in mouse muscular dystrophy. *PLoS One,* 2**,** e806.

ASCAH, A., KHAIRALLAH, M., DAUSSIN, F., BOURCIER-LUCAS, C., GODIN, R., ALLEN, B. G., PETROF, B. J., DES ROSIERS, C. & BURELLE, Y. 2011. Stress-induced opening of the permeability transition pore in the dystrophin-deficient heart is attenuated by acute treatment with sildenafil. *Am J Physiol Heart Circ Physiol,* 300**,** H144-53.

AUSTIN, L., DE NIESE, M., MCGREGOR, A., ARTHUR, H., GURUSINGHE, A. & GOULD, M. K. 1992. Potential oxyradical damage and energy status in individual muscle fibres from degenerating muscle diseases. *Neuromuscul Disord,* 2**,** 27-33.

BAAR, K., WENDE, A. R., JONES, T. E., MARISON, M., NOLTE, L. A., CHEN, M., KELLY, D. P. & HOLLOSZY, J. O. 2002. Adaptations of skeletal muscle to exercise: rapid increase in the transcriptional coactivator PGC-1. *Faseb j,* 16**,** 1879-86.

BABINET, C. 2000. Transgenic mice: an irreplaceable tool for the study of mammalian development and biology. *J Am Soc Nephrol,* 11 Suppl 16**,** S88-94.

BAKER, M. J., FRAZIER, A. E., GULBIS, J. M. & RYAN, M. T. 2007. Mitochondrial protein-import machinery: correlating structure with function. *Trends Cell Biol,* 17**,** 456-64.

BARANY, M. 1967. ATPase activity of myosin correlated with speed of muscle shortening. *J Gen Physiol,* 50**,** Suppl:197-218.

BARBIERI, E. & SESTILI, P. 2012. Reactive oxygen species in skeletal muscle signaling. *J Signal Transduct,* 2012**,** 982794.

BARROS MARANHAO, J., DE OLIVEIRA MOREIRA, D., MAURICIO, A. F., DE CARVALHO, S. C., FERRETTI, R., PEREIRA, J. A., SANTO NETO, H. & MARQUES, M. J. 2015. Changes in calsequestrin, TNF-alpha, TGF-beta and MyoD levels during the progression of skeletal muscle dystrophy in mdx mice: a comparative analysis of the quadriceps, diaphragm and intrinsic laryngeal muscles. *Int J Exp Pathol,* 96**,** 285-93.

BARTON-DAVIS, E. R., SHOTURMA, D. I., MUSARO, A., ROSENTHAL, N. & SWEENEY, H. L. 1998. Viral mediated expression of IGF-I blocks the aging-related loss of skeletal muscle function. *Molecular Biology of the Cell,* 9**,** 182A-182A.

BASSEL-DUBY, R. & OLSON, E. N. 2006. Signaling pathways in skeletal muscle remodeling. *Annu. Rev. Biochem.,* 75**,** 19-37.

BAUM, O., DA SILVA-AZEVEDO, L., WILLERDING, G., WOCKEL, A., PLANITZER, G., GOSSRAU, R., PRIES, A. R. & ZAKRZEWICZ, A. 2004. Endothelial NOS is main mediator for shear stress-dependent angiogenesis in skeletal muscle after prazosin administration. *Am J Physiol Heart Circ Physiol,* 287**,** H2300-8.

BEDARD, K. & KRAUSE, K. H. 2007. The NOX family of ROS-generating NADPH oxidases: physiology and pathophysiology. *Physiol Rev,* 87**,** 245-313.

BELLINGER, A. M., REIKEN, S., CARLSON, C., MONGILLO, M., LIU, X., ROTHMAN, L., MATECKI, S., LACAMPAGNE, A. & MARKS, A. R. 2009. Hypernitrosylated ryanodine receptor calcium release channels are leaky in dystrophic muscle. *Nature medicine,* 15**,** 325-330.

BELLINGER, A. M., REIKEN, S., DURA, M., MURPHY, P. W., DENG, S. X., LANDRY, D. W., NIEMAN, D., LEHNART, S. E., SAMARU, M., LACAMPAGNE, A. & MARKS, A. R. 2008. Remodeling of ryanodine receptor complex causes "leaky" channels: a molecular mechanism for decreased exercise capacity. *Proc Natl Acad Sci U S A,* 105**,** 2198-202.

BENNY KLIMEK, M. E., SALI, A., RAYAVARAPU, S., VAN DER MEULEN, J. H. & NAGARAJU, K. 2016. Effect of the IL-1 Receptor Antagonist Kineret(R) on Disease Phenotype in mdx Mice. *PLoS One,* 11**,** e0155944.

BENTELE, K., SAFFERT, P., RAUSCHER, R., IGNATOVA, Z. & BLÜTHGEN, N. 2013. Efficient translation initiation dictates codon usage at gene start. *Molecular systems biology,* 9**,** 675.

BERCHTOLD, M. W., BRINKMEIER, H. & MÜNTENER, M. 2000. Calcium ion in skeletal muscle: its crucial role for muscle function, plasticity, and disease. *Physiological reviews,* 80**,** 1215-1265.

BERG, J. M., TYMOCZKO, J. L. & STRYER, L. 2002. Biochemistry, ; W. H. Freeman: New York.

BERGERON, R., REN, J. M., CADMAN, K. S., MOORE, I. K., PERRET, P., PYPAERT, M., YOUNG, L. H., SEMENKOVICH, C. F. & SHULMAN, G. I. 2001. Chronic activation of AMP kinase results in NRF-1 activation and mitochondrial biogenesis. *Am J Physiol Endocrinol Metab,* 281**,** E1340-6.

BERNASCONI, P., DI BLASI, C., MORA, M., MORANDI, L., GALBIATI, S., CONFALONIERI, P., CORNELIO, F. & MANTEGAZZA, R. 1999. Transforming growth factor-beta1 and fibrosis in congenital muscular dystrophies. *Neuromuscul Disord,* 9**,** 28-33.

BISH, L. T., MORINE, K., SLEEPER, M. M., SANMIGUEL, J., WU, D., GAO, G., WILSON, J. M. & SWEENEY, H. L. 2008. Adeno-associated virus (AAV) serotype 9 provides global cardiac gene transfer superior to AAV1, AAV6, AAV7, and AAV8 in the mouse and rat. *Hum Gene Ther,* 19**,** 1359-68.

BLOCH, R. J., REED, P., O'NEILL, A., STRONG, J., WILLIAMS, M., PORTER, N. & GONZALEZ-SERRATOS, H. 2004. Costameres mediate force transduction in healthy skeletal muscle and are altered in muscular dystrophies. *J Muscle Res Cell Motil,* 25**,** 590-2.

BODENSTEINER, J. B. & ENGEL, A. G. 1978. Intracellular calcium accumulation in Duchenne dystrophy and other myopathies: a study of 567,000 muscle fibers in 114 biopsies. *Neurology,* 28**,** 439-46.

BODOR, M. & MCDONALD, C. M. 2013. Why short stature is beneficial in Duchenne muscular dystrophy. *Muscle & nerve,* 48**,** 336-342.

BOOTH, F. W. & BALDWIN, K. M. 2010. Muscle Plasticity: Energy Demand and Supply Processes. *Comprehensive Physiology.* John Wiley & Sons, Inc.

BORSELLI, C., STORRIE, H., BENESCH-LEE, F., SHVARTSMAN, D., CEZAR, C., LICHTMAN, J. W., VANDENBURGH, H. H. & MOONEY, D. J. 2010. Functional muscle regeneration with combined delivery of angiogenesis

and myogenesis factors. *Proceedings of the National Academy of Sciences,* 107**,** 3287-3292.

BOYE, S. E., BOYE, S. L., LEWIN, A. S. & HAUSWIRTH, W. W. 2013. A comprehensive review of retinal gene therapy. *Mol Ther,* 21**,** 509-19.

BRENMAN, J. E., CHAO, D. S., XIA, H., ALDAPE, K. & BREDT, D. S. 1995. Nitric oxide synthase complexed with dystrophin and absent from skeletal muscle sarcolemma in Duchenne muscular dystrophy. *Cell,* 82**,** 743-52.

BROOKE, M. H. & KAISER, K. K. 1970. Muscle fiber types: how many and what kind? *Arch Neurol,* 23**,** 369-79.

BROOKES, P. S. & DARLEY-USMAR, V. M. 2004. Role of calcium and superoxide dismutase in sensitizing mitochondria to peroxynitrite-induced permeability transition. *American Journal of Physiology-Heart and Circulatory Physiology,* 286**,** H39-H46.

BROOKS, S. V. & FAULKNER, J. A. 1988. Contractile properties of skeletal muscles from young, adult and aged mice. *J Physiol,* 404**,** 71-82.

BROOKS, S. V. & FAULKNER, J. A. 1994. Skeletal muscle weakness in old age: underlying mechanisms. *Medicine and science in sports and exercise,* 26**,** 432-439.

BRUUSGAARD, J. C., LIESTØL, K., EKMARK, M., KOLLSTAD, K. & GUNDERSEN, K. 2003. Number and spatial distribution of nuclei in the muscle fibres of normal mice studied in vivo. *The Journal of Physiology,* 551**,** 467-478.

BULFIELD, G., SILLER, W. G., WIGHT, P. A. & MOORE, K. J. 1984. X chromosome-linked muscular dystrophy (mdx) in the mouse. *Proc Natl Acad Sci U S A,* 81**,** 1189-92.

BULLER, A. J., ECCLES, J. C. & ECCLES, R. M. 1960. Interactions between motoneurones and muscles in respect of the characteristic speeds of their responses. *J Physiol,* 150**,** 417-39.

BURDI, R., ROLLAND, J.-F., FRAYSSE, B., LITVINOVA, K., COZZOLI, A., GIANNUZZI, V., LIANTONIO, A., CAMERINO, G. M., SBLENDORIO, V. & CAPOGROSSO, R. F. 2009. Multiple pathological events in exercised dystrophic mdx mice are targeted by pentoxifylline: outcome of a large array of in vivo and ex vivo tests. *Journal of applied physiology,* 106**,** 1311-1324.

CAI, D., FRANTZ, J. D., TAWA, N. E., MELENDEZ, P. A., OH, B.-C., LIDOV, H. G. W., HASSELGREN, P.-O., FRONTERA, W. R., LEE, J., GLASS, D. J. & SHOELSON, S. E. 2004. IKKβ/NF-κB Activation Causes Severe Muscle Wasting in Mice. *Cell,* 119**,** 285-298.

CAI, Q., LIN, T., KAMARAJUGADDA, S. & LU, J. 2013. Regulation of glycolysis and the Warburg effect by estrogen-related receptors. *Oncogene,* 32**,** 2079.

CALCEDO, R. & WILSON, J. M. 2013. Humoral Immune Response to AAV. *Front Immunol,* 4**,** 341.

CANTÓ, C. & AUWERX, J. 2012. Targeting SIRT1 to improve metabolism: all you need is NAD(+)? *Pharmacological reviews,* 64**,** 166-187.

CAPOTE, J., DIFRANCO, M. & VERGARA, J. L. 2010. Excitation-contraction coupling alterations in mdx and utrophin/dystrophin double knockout mice: a comparative study. *Am J Physiol Cell Physiol,* 298**,** C1077-86.

CARLSON, C. G., SAMADI, A. & SIEGEL, A. 2005. Chronic treatment with agents that stabilize cytosolic IkappaB-alpha enhances survival and

improves resting membrane potential in MDX muscle fibers subjected to chronic passive stretch. *Neurobiology of disease,* 20**,** 719-730.

CARLSON, M. E., HSU, M. & CONBOY, I. M. 2008. Imbalance between pSmad3 and Notch induces CDK inhibitors in old muscle stem cells. *Nature,* 454**,** 528-32.

CEYLAN-ISIK, A. F., WU, S., LI, Q., LI, S.-Y. & REN, J. 2006. High-dose benfotiamine rescues cardiomyocyte contractile dysfunction in streptozotocin-induced diabetes mellitus. *Journal of applied physiology,* 100**,** 150-156.

CHAHAL, P. S., SCHULZE, E., TRAN, R., MONTES, J. & KAMEN, A. A. 2014. Production of adeno-associated virus (AAV) serotypes by transient transfection of HEK293 cell suspension cultures for gene delivery. *Journal of virological methods,* 196**,** 163-173.

CHAKKALAKAL, J. V., STOCKSLEY, M. A., HARRISON, M.-A., ANGUS, L. M., DESCHÊNES-FURRY, J., ST-PIERRE, S., MEGENEY, L. A., CHIN, E. R., MICHEL, R. N. & JASMIN, B. J. 2003. Expression of utrophin A mRNA correlates with the oxidative capacity of skeletal muscle fiber types and is regulated by calcineurin/NFAT signaling. *Proceedings of the National Academy of Sciences,* 100**,** 7791-7796.

CHAKKALAKAL, J. V., THOMPSON, J., PARKS, R. J. & JASMIN, B. J. 2005. Molecular, cellular, and pharmacological therapies for Duchenne/Becker muscular dystrophies. *The FASEB Journal,* 19**,** 880-891.

CHALKIADAKI, A., IGARASHI, M., NASAMU, A. S., KNEZEVIC, J. & GUARENTE, L. 2014. Muscle-specific SIRT1 gain-of-function increases slow-twitch fibers and ameliorates pathophysiology in a mouse model of duchenne muscular dystrophy. *PLoS Genet,* 10**,** e1004490.

CHAMBERLAIN, J. S., METZGER, J., REYES, M., TOWNSEND, D. & FAULKNER, J. A. 2007. Dystrophin-deficient mdx mice display a reduced life span and are susceptible to spontaneous rhabdomyosarcoma. *Faseb j,* 21**,** 2195-204.

CHAN, S. & HEAD, S. I. 2011. The role of branched fibres in the pathogenesis of Duchenne muscular dystrophy. *Exp Physiol,* 96**,** 564-71.

CHANDRASEKHARAN, K., YOON, J. H., XU, Y., CAMBONI, M., JANSSEN, P. M., VARKI, A. & MARTIN, P. T. 2010. A human-specific deletion in mouse Cmah increases disease severity in the mdx model of Duchenne muscular dystrophy. *Science translational medicine,* 2**,** 42ra54-42ra54.

CHATTERJEE, S., NAM, D., GUO, B., KIM, J. M., WINNIER, G. E., LEE, J., BERDEAUX, R., YECHOOR, V. K. & MA, K. 2013. Brain and muscle Arnt-like 1 is a key regulator of myogenesis. *J Cell Sci,* 126**,** 2213-24.

CHEN, S.-E., JIN, B. & LI, Y.-P. 2007. TNF-α regulates myogenesis and muscle regeneration by activating p38 MAPK. *American journal of physiology. Cell physiology,* 292**,** C1660-C1671.

CHEN, X., XU, H., YUAN, P., FANG, F., HUSS, M., VEGA, V. B., WONG, E., ORLOV, Y. L., ZHANG, W. & JIANG, J. 2008. Integration of external signaling pathways with the core transcriptional network in embryonic stem cells. *Cell,* 133**,** 1106-1117.

CHENG, X. W., KUZUYA, M., KIM, W., SONG, H., HU, L., INOUE, A., NAKAMURA, K., DI, Q., SASAKI, T., TSUZUKI, M., SHI, G.-P., OKUMURA, K. & MUROHARA, T. 2010. Exercise Training Stimulates Ischemia-Induced Neovascularization via Phosphatidylinositol 3-

Kinase/Akt-Dependent Hypoxia-Induced Factor-1α Reactivation in Mice of Advanced Age. *Circulation,* 122**,** 707-716.

CHI, M. M. Y., HINTZ, C. S., MCKEE, D., FELDER, S., GRANT, N., KAISER, K. K. & LOWRY, O. H. Effect of Duchenne muscular dystrophy on enzymes of energy metabolism in individual muscle fibers. *Metabolism - Clinical and Experimental,* 36**,** 761-767.

CHIN, E. R. 2010. Intracellular Ca2+ signaling in skeletal muscle: decoding a complex message. *Exerc Sport Sci Rev,* 38**,** 76-85.

CHIN, E. R., OLSON, E. N., RICHARDSON, J. A., YANG, Q., HUMPHRIES, C., SHELTON, J. M., WU, H., ZHU, W., BASSEL-DUBY, R. & WILLIAMS, R. S. 1998. A calcineurin-dependent transcriptional pathway controls skeletal muscle fiber type. *Genes Dev,* 12**,** 2499-509.

CHINSOMBOON, J., RUAS, J., GUPTA, R. K., THOM, R., SHOAG, J., ROWE, G. C., SAWADA, N., RAGHURAM, S. & ARANY, Z. 2009. The transcriptional coactivator PGC-1alpha mediates exercise-induced angiogenesis in skeletal muscle. *Proc Natl Acad Sci U S A,* 106**,** 21401-6.

CHIRMULE, N., XIAO, W., TRUNEH, A., SCHNELL, M. A., HUGHES, J. V., ZOLTICK, P. & WILSON, J. M. 2000. Humoral immunity to adeno-associated virus type 2 vectors following administration to murine and nonhuman primate muscle. *J Virol,* 74**,** 2420-5.

CHO, Y., HAZEN, B. C., GANDRA, P. G., WARD, S. R., SCHENK, S., RUSSELL, A. P. & KRALLI, A. 2016. Perm1 enhances mitochondrial biogenesis, oxidative capacity, and fatigue resistance in adult skeletal muscle. *The FASEB Journal,* 30**,** 674-687.

CHO, Y., HAZEN, B. C., RUSSELL, A. P. & KRALLI, A. 2013. Peroxisome proliferator-activated receptor gamma coactivator 1 (PGC-1)- and estrogen-related receptor (ERR)-induced regulator in muscle 1 (Perm1) is a tissue-specific regulator of oxidative capacity in skeletal muscle cells. *J Biol Chem,* 288**,** 25207-18.

CIRAK, S., ARECHAVALA-GOMEZA, V., GUGLIERI, M., FENG, L., TORELLI, S., ANTHONY, K., ABBS, S., GARRALDA, M. E., BOURKE, J., WELLS, D. J., DICKSON, G., WOOD, M. J. A., WILTON, S. D., STRAUB, V., KOLE, R., SHREWSBURY, S. B., SEWRY, C., MORGAN, J. E., BUSHBY, K. & MUNTONI, F. 2011. Exon skipping and dystrophin restoration in patients with Duchenne muscular dystrophy after systemic phosphorodiamidate morpholino oligomer treatment: an open-label, phase 2, dose-escalation study. *Lancet,* 378**,** 595-605.

CLÉMENT, N. & GRIEGER, J. C. 2016. Manufacturing of recombinant adeno-associated viral vectors for clinical trials. *Molecular Therapy. Methods & Clinical Development,* 3**,** 16002.

CLERK, A., MORRIS, G. E., DUBOWITZ, V., DAVIES, K. E. & SEWRY, C. A. 1993. Dystrophin-related protein, utrophin, in normal and dystrophic human fetal skeletal muscle. *Histochem J,* 25**,** 554-61.

CLOP, A., MARCQ, F., TAKEDA, H., PIROTTIN, D., TORDOIR, X., BIBÉ, B., BOUIX, J., CAIMENT, F., ELSEN, J.-M. & EYCHENNE, F. 2006. A mutation creating a potential illegitimate microRNA target site in the myostatin gene affects muscularity in sheep. *Nature genetics,* 38**,** 813-818.

COHEN, T., NAHARI, D., CEREM, L. W., NEUFELD, G. & LEVI, B.-Z. 1996. Interleukin 6 induces the expression of vascular endothelial growth factor. *Journal of Biological Chemistry,* 271**,** 736-741.

COLEY, W. D., BOGDANIK, L., VILA, M. C., YU, Q., VAN DER MEULEN, J. H., RAYAVARAPU, S., NOVAK, J. S., NEARING, M., QUINN, J. L., SAUNDERS, A., DOLAN, C., ANDREWS, W., LAMMERT, C., AUSTIN, A., PARTRIDGE, T. A., COX, G. A., LUTZ, C. & NAGARAJU, K. 2016. Effect of genetic background on the dystrophic phenotype in mdx mice. *Hum Mol Genet,* 25**,** 130-45.

COLLIN, R. W., KALAY, E., TARIQ, M., PETERS, T., VAN DER ZWAAG, B., VENSELAAR, H., OOSTRIK, J., LEE, K., AHMED, Z. M., CAYLAN, R., LI, Y., SPIERENBURG, H. A., EYUPOGLU, E., HEISTER, A., RIAZUDDIN, S., BAHAT, E., ANSAR, M., ARSLAN, S., WOLLNIK, B., BRUNNER, H. G., CREMERS, C. W., KARAGUZEL, A., AHMAD, W., CREMERS, F. P., VRIEND, G., FRIEDMAN, T. B., RIAZUDDIN, S., LEAL, S. M. & KREMER, H. 2008. Mutations of ESRRB encoding estrogen-related receptor beta cause autosomal-recessive nonsyndromic hearing impairment DFNB35. *Am J Hum Genet,* 82**,** 125-38.

COMIM, C. M., HOEPERS, A., VENTURA, L., FREIBERGER, V., DOMINGUINI, D., MINA, F., MENDONCA, B. P., SCAINI, G., VAINZOF, M., STRECK, E. L. & QUEVEDO, J. 2016. Activity of Krebs cycle enzymes in mdx mice. *Muscle Nerve,* 53**,** 91-5.

CONG, X., DOERING, J., GRANGE, R. W. & JIANG, H. 2016. Defective excitation-contraction coupling is partially responsible for impaired contractility in hindlimb muscles of Stac3 knockout mice. *Scientific reports,* 6**,** 26194.

COOKE, R. 1997. Actomyosin interaction in striated muscle. *Physiol Rev,* 77**,** 671-97.

CORNACHIONE, A. S., BENEDINI-ELIAS, P. C. O., POLIZELLO, J. C., CARVALHO, L. C. & MATTIELLO-SVERZUT, A. C. 2011. Characterization of Fiber Types in Different Muscles of the Hindlimb in Female Weanling and Adult Wistar Rats. *Acta Histochemica et Cytochemica,* 44**,** 43-50.

COYLE, E. F., MARTIN, W. H., 3RD, SINACORE, D. R., JOYNER, M. J., HAGBERG, J. M. & HOLLOSZY, J. O. 1984. Time course of loss of adaptations after stopping prolonged intense endurance training. *J Appl Physiol Respir Environ Exerc Physiol,* 57**,** 1857-64.

CRESCENZO, R., BIANCO, F., MAZZOLI, A., GIACCO, A., LIVERINI, G. & IOSSA, S. 2015. Skeletal muscle mitochondrial energetic efficiency and aging. *Int J Mol Sci,* 16**,** 10674-85.

CRUZ-GUZMÁN, O. D. R., RODRÍGUEZ-CRUZ, M. & ESCOBAR CEDILLO, R. E. 2015. Systemic inflammation in Duchenne muscular dystrophy: association with muscle function and nutritional status. *BioMed research international,* 2015.

CULLIGAN, K., BANVILLE, N., DOWLING, P. & OHLENDIECK, K. 2002. Drastic reduction of calsequestrin-like proteins and impaired calcium binding in dystrophic mdx muscle. *J Appl Physiol (1985),* 92**,** 435-45.

CULLIGAN, K. & OHLENDIECK, K. 2002. Abnormal calcium handling in muscular dystrophy. *BAM-PADOVA-,* 12**,** 151-162.

DANGAIN, J. & VRBOVA, G. 1984. Muscle development in mdx mutant mice. *Muscle Nerve,* 7**,** 700-4.

DAS, A. M. & HARRIS, D. A. 1990. Control of mitochondrial ATP synthase in heart cells: inactive to active transitions caused by beating or positive inotropic agents. *Cardiovascular research,* 24**,** 411-417.

DAVIES, K. E. & NOWAK, K. J. 2006. Molecular mechanisms of muscular dystrophies: old and new players. *Nat Rev Mol Cell Biol,* 7**,** 762-73.

DAYA, S. & BERNS, K. I. 2008. Gene therapy using adeno-associated virus vectors. *Clinical microbiology reviews,* 21**,** 583-593.

DE LANGE, P., FARINA, P., MORENO, M., RAGNI, M., LOMBARDI, A., SILVESTRI, E., BURRONE, L., LANNI, A. & GOGLIA, F. 2006. Sequential changes in the signal transduction responses of skeletal muscle following food deprivation. *Faseb j,* 20**,** 2579-81.

DE PAEPE, B. & DE BLEECKER, J. L. 2013. Cytokines and Chemokines as Regulators of Skeletal Muscle Inflammation: Presenting the Case of Duchenne Muscular Dystrophy. *Mediators of Inflammation,* 2013**,** 10.

DE PALMA, C., MORISI, F., CHELI, S., PAMBIANCO, S., CAPPELLO, V., VEZZOLI, M., ROVERE-QUERINI, P., MOGGIO, M., RIPOLONE, M. & FRANCOLINI, M. 2012. Autophagy as a new therapeutic target in Duchenne muscular dystrophy. *Cell death & disease,* 3**,** e418.

DEASY, B. M., FEDUSKA, J. M., PAYNE, T. R., LI, Y., AMBROSIO, F. & HUARD, J. 2009. Effect of VEGF on the regenerative capacity of muscle stem cells in dystrophic skeletal muscle. *Molecular Therapy,* 17**,** 1788-1798.

DEBLOIS, G. & GIGUERE, V. 2013. Oestrogen-related receptors in breast cancer: control of cellular metabolism and beyond. *Nat Rev Cancer,* 13**,** 27-36.

DEBLOIS, G. & GIGUÈRE, V. 2011. Functional and physiological genomics of estrogen-related receptors (ERRs) in health and disease. *Biochimica et Biophysica Acta (BBA) - Molecular Basis of Disease,* 1812**,** 1032-1040.

DELLORUSSO, C., CRAWFORD, R. W., CHAMBERLAIN, J. S. & BROOKS, S. V. 2001. Tibialis anterior muscles in mdx mice are highly susceptible to contraction-induced injury. *Journal of muscle research and cell motility,* 22**,** 467-475.

DEMBITSKY, V. M., GLORIOZOVA, T. A. & POROIKOV, V. V. 2017. Pharmacological activities of epithio steroids. *J. Pharm. Res. Int,* 18**,** 1-19.

DI MAURO, S., ANGELINI, C. & CATANI, C. 1967. Enzymes of the glycogen cycle and glycolysis in various human neuromuscular disorders. *Journal of Neurology, Neurosurgery, and Psychiatry,* 30**,** 411-415.

DIMAURO, S. 2006. Mitochondrial myopathies. *Curr Opin Rheumatol,* 18**,** 636-41.

DING, Y. H., LUAN, X. D., LI, J., RAFOLS, J. A., GUTHINKONDA, M., DIAZ, F. G. & DING, Y. 2004. Exercise-induced overexpression of angiogenic factors and reduction of ischemia/reperfusion injury in stroke. *Curr Neurovasc Res,* 1**,** 411-20.

DIVET, A. & HUCHET-CADIOU, C. 2002. Sarcoplasmic reticulum function in slow- and fast-twitch skeletal muscles from mdx mice. *Pflugers Arch,* 444**,** 634-43.

DOGRA, C., CHANGOTRA, H., WERGEDAL, J. E. & KUMAR, A. 2006. Regulation of phosphatidylinositol 3-kinase (PI3K)/Akt and nuclear factor-

kappa B signaling pathways in dystrophin-deficient skeletal muscle in response to mechanical stretch. *J Cell Physiol,* 208**,** 575-85.

DOMINGUEZ, E., MARAIS, T., CHATAURET, N., BENKHELIFA-ZIYYAT, S., DUQUE, S., RAVASSARD, P., CARCENAC, R., ASTORD, S., PEREIRA DE MOURA, A., VOIT, T. & BARKATS, M. 2011. Intravenous scAAV9 delivery of a codon-optimized SMN1 sequence rescues SMA mice. *Hum Mol Genet,* 20**,** 681-93.

DUDLEY, R. W., KHAIRALLAH, M., MOHAMMED, S., LANDS, L., DES ROSIERS, C. & PETROF, B. J. 2006. Dynamic responses of the glutathione system to acute oxidative stress in dystrophic mouse (mdx) muscles. *Am J Physiol Regul Integr Comp Physiol,* 291**,** R704-10.

DUFOUR, C. R., WILSON, B. J., HUSS, J. M., KELLY, D. P., ALAYNICK, W. A., DOWNES, M., EVANS, R. M., BLANCHETTE, M. & GIGUERE, V. 2007. Genome-wide orchestration of cardiac functions by the orphan nuclear receptors ERRalpha and gamma. *Cell Metab,* 5**,** 345-56.

DUPONT-VERSTEEGDEN, E. E., BALDWIN, R. A., MCCARTER, R. J. & VONLANTHEN, M. G. 1994. Does muscular dystrophy affect metabolic rate?: A study in mdx mice. *Journal of the neurological sciences,* 121**,** 203-207.

EICHNER, L. J., PERRY, M.-C., DUFOUR, C. R., BERTOS, N., PARK, M., ST-PIERRE, J. & GIGUÈRE, V. 2010. miR-378∗ mediates metabolic shift in breast cancer cells via the PGC-1β/ERRγ transcriptional pathway. *Cell metabolism,* 12**,** 352-361.

EMERY, A. E. 2002. The muscular dystrophies. *Lancet,* 359**,** 687-95.

ENDO, T. 2015. Molecular mechanisms of skeletal muscle development, regeneration, and osteogenic conversion. *Bone,* 80**,** 2-13.

ENNEN, J. P., VERMA, M. & ASAKURA, A. 2013. Vascular-targeted therapies for Duchenne muscular dystrophy. *Skeletal Muscle,* 3**,** 9-9.

EVANS, N. P., MISYAK, S. A., ROBERTSON, J. L., BASSAGANYA-RIERA, J. & GRANGE, R. W. 2009a. Dysregulated intracellular signaling and inflammatory gene expression during initial disease onset in Duchenne muscular dystrophy. *Am J Phys Med Rehabil,* 88**,** 502-22.

EVANS, N. P., MISYAK, S. A., ROBERTSON, J. L., BASSAGANYA-RIERA, J. & GRANGE, R. W. 2009b. Immune-mediated mechanisms potentially regulate the disease time-course of duchenne muscular dystrophy and provide targets for therapeutic intervention. *Pm r,* 1**,** 755-68.

EVANS, W. J. 2010. Skeletal muscle loss: cachexia, sarcopenia, and inactivity–. *The American journal of clinical nutrition,* 91**,** 1123S-1127S.

EVEN, P. C., DECROUY, A. & CHINET, A. 1994. Defective regulation of energy metabolism in mdx-mouse skeletal muscles. *Biochem J,* 304 (Pt 2)**,** 649-54.

FAIRCLOUGH, R. J., BAREJA, A. & DAVIES, K. E. 2011. Progress in therapy for Duchenne muscular dystrophy. *Exp Physiol,* 96**,** 1101-13.

FERRARI, G., CUSELLA-DE ANGELIS, G., COLETTA, M., PAOLUCCI, E., STORNAIUOLO, A., COSSU, G. & MAVILIO, F. 1998. Muscle regeneration by bone marrow-derived myogenic progenitors. *Science,* 279**,** 1528-30.

FIGARI, I. S., MORI, N. A. & PALLADINO, M. A., JR. 1987. Regulation of neutrophil migration and superoxide production by recombinant tumor

necrosis factors-alpha and -beta: comparison to recombinant interferon-gamma and interleukin-1 alpha. *Blood,* 70**,** 979-84.

FINCK, B. N. & KELLY, D. P. 2006. PGC-1 coactivators: inducible regulators of energy metabolism in health and disease. *Journal of Clinical Investigation,* 116**,** 615.

FITTS, R. H. 1994. Cellular mechanisms of muscle fatigue. *Physiological reviews,* 74**,** 49-94.

FLOETER, M. K. 2010. Structure and function of muscle fibers and motor units. *Disorders of Voluntary Muscle., 8th ed. Cambridge University Press, Cambridge***,** 1-10.

FONG, P., TURNER, P. R., DENETCLAW, W. F. & STEINHARDT, R. A. 1990. Increased activity of calcium leak channels in myotubes of Duchenne human and mdx mouse origin. *Science,* 250**,** 673-676.

FOO, S. S., TURNER, C. J., ADAMS, S., COMPAGNI, A., AUBYN, D., KOGATA, N., LINDBLOM, P., SHANI, M., ZICHA, D. & ADAMS, R. H. 2006. Ephrin-B2 controls cell motility and adhesion during blood-vessel-wall assembly. *Cell,* 124**,** 161-73.

FOROUGH, R., WEYLIE, B., COLLINS, C., PARKER, J. L., ZHU, J., BARHOUMI, R. & WATSON, D. K. 2006. Transcription factor Ets-1 regulates fibroblast growth factor-1-mediated angiogenesis in vivo: role of Ets-1 in the regulation of the PI3K/AKT/MMP-1 pathway. *J Vasc Res,* 43**,** 327-37.

FORSYTHE, J. A., JIANG, B. H., IYER, N. V., AGANI, F., LEUNG, S. W., KOOS, R. D. & SEMENZA, G. L. 1996. Activation of vascular endothelial growth factor gene transcription by hypoxia-inducible factor 1. *Mol Cell Biol,* 16**,** 4604-13.

FOSTER, H., SHARP, P. S., ATHANASOPOULOS, T., TROLLET, C., GRAHAM, I. R., FOSTER, K., WELLS, D. J. & DICKSON, G. 2008. Codon and mRNA sequence optimization of microdystrophin transgenes improves expression and physiological outcome in dystrophic mdx mice following AAV2/8 gene transfer. *Molecular therapy,* 16**,** 1825-1832.

FRAISL, P., MAZZONE, M., SCHMIDT, T. & CARMELIET, P. 2009. Regulation of Angiogenesis by Oxygen and Metabolism. *Developmental Cell,* 16**,** 167-179.

FRANCIS, S. H., BUSCH, J. L. & CORBIN, J. D. 2010. cGMP-dependent protein kinases and cGMP phosphodiesterases in nitric oxide and cGMP action. *Pharmacological reviews,* 62**,** 525-563.

FROEHNER, S. C., REED, S. M., ANDERSON, K. N., HUANG, P. L. & PERCIVAL, J. M. 2014. Loss of nNOS inhibits compensatory muscle hypertrophy and exacerbates inflammation and eccentric contraction-induced damage in mdx mice. *Human molecular genetics,* 24**,** 492-505.

FUJIMORI, K., ITOH, Y., YAMAMOTO, K., MIYAGOE-SUZUKI, Y., YUASA, K., YOSHIZAKI, K., YAMAMOTO, H. & TAKEDA, S. I. 2002. Interleukin 6 induces overexpression of the sarcolemmal utrophin in neonatal mdx skeletal muscle. *Human gene therapy,* 13**,** 509-518.

FUKADA, S., MORIKAWA, D., YAMAMOTO, Y., YOSHIDA, T., SUMIE, N., YAMAGUCHI, M., ITO, T., MIYAGOE-SUZUKI, Y., TAKEDA, S., TSUJIKAWA, K. & YAMAMOTO, H. 2010. Genetic background affects properties of satellite cells and mdx phenotypes. *Am J Pathol,* 176**,** 2414-24.

GAILLARD, S., DWYER, M. A. & MCDONNELL, D. P. 2007. Definition of the molecular basis for estrogen receptor-related receptor-alpha-cofactor interactions. *Mol Endocrinol,* 21**,** 62-76.

GAN, Z., RUMSEY, J., HAZEN, B. C., LAI, L., LEONE, T. C., VEGA, R. B., XIE, H., CONLEY, K. E., AUWERX, J. & SMITH, S. R. 2013. Nuclear receptor/microRNA circuitry links muscle fiber type to energy metabolism. *The Journal of clinical investigation,* 123**,** 2564-2575.

GAO, Q. & MCNALLY, E. M. 2015. The Dystrophin Complex: structure, function and implications for therapy. *Comprehensive Physiology,* 5**,** 1223-1239.

GARIKIPATI, D. K. & RODGERS, B. D. 2012. Myostatin inhibits myosatellite cell proliferation and consequently activates differentiation: evidence for endocrine-regulated transcript processing. *Journal of Endocrinology,* 215**,** 177-187.

GARMORY, H. S., BROWN, K. A. & TITBALL, R. W. 2003. DNA vaccines: improving expression of antigens. *Genetic vaccines and therapy,* 1**,** 2.

GAUDET, D., DE WAL, J., TREMBLAY, K., DÉRY, S., VAN DEVENTER, S., FREIDIG, A., BRISSON, D. & MÉTHOT, J. 2010. Review of the clinical development of alipogene tiparvovec gene therapy for lipoprotein lipase deficiency. *Atherosclerosis Supplements,* 11**,** 55-60.

GEHRIG, S. M., VAN DER POEL, C., SAYER, T. A., SCHERTZER, J. D., HENSTRIDGE, D. C., CHURCH, J. E., LAMON, S., RUSSELL, A. P., DAVIES, K. E. & FEBBRAIO, M. A. 2012. Hsp72 preserves muscle function and slows progression of severe muscular dystrophy. *Nature,* 484**,** 394.

GENG, T., LI, P., OKUTSU, M., YIN, X., KWEK, J., ZHANG, M. & YAN, Z. 2010. PGC-1alpha plays a functional role in exercise-induced mitochondrial biogenesis and angiogenesis but not fiber-type transformation in mouse skeletal muscle. *Am J Physiol Cell Physiol,* 298**,** C572-9.

GERHART-HINES, Z., RODGERS, J. T., BARE, O., LERIN, C., KIM, S. H., MOSTOSLAVSKY, R., ALT, F. W., WU, Z. & PUIGSERVER, P. 2007. Metabolic control of muscle mitochondrial function and fatty acid oxidation through SIRT1/PGC-1alpha. *Embo j,* 26**,** 1913-23.

GERMANI, A., DI CARLO, A., MANGONI, A., STRAINO, S., GIACINTI, C., TURRINI, P., BIGLIOLI, P. & CAPOGROSSI, M. C. 2003. Vascular Endothelial Growth Factor Modulates Skeletal Myoblast Function. *The American Journal of Pathology,* 163**,** 1417-1428.

GERVÁSIO, O. L., WHITEHEAD, N. P., YEUNG, E. W., PHILLIPS, W. D. & ALLEN, D. G. 2008. TRPC1 binds to caveolin-3 and is regulated by Src kinase–role in Duchenne muscular dystrophy. *Journal of cell science,* 121**,** 2246-2255.

GIGUERE, V. 2008. Transcriptional control of energy homeostasis by the estrogen-related receptors. *Endocr Rev,* 29**,** 677-96.

GIGUÈRE, V. 1999. Orphan nuclear receptors: from gene to function 1. *Endocrine reviews,* 20**,** 689-725.

GILLIS, J. M. 1999. Understanding dystrophinopathies: an inventory of the structural and functional consequences of the absence of dystrophin in muscles of the mdx mouse. *J Muscle Res Cell Motil,* 20**,** 605-25.

GINGRAS, A.-C., KENNEDY, S. G., O'LEARY, M. A., SONENBERG, N. & HAY, N. 1998. 4E-BP1, a repressor of mRNA translation, is phosphorylated and

inactivated by the Akt (PKB) signaling pathway. *Genes & development,* 12**,** 502-513.

GINZLER, E. M., WAX, S., RAJESWARAN, A., COPT, S., HILLSON, J., RAMOS, E. & SINGER, N. G. 2012. Atacicept in combination with MMF and corticosteroids in lupus nephritis: results of a prematurely terminated trial. *Arthritis Res Ther,* 14**,** R33.

GIOSTRA, E., MAGISTRIS, M. R., PIZZOLATO, G., COX, J. & CHEVROLET, J. C. 1994. Neuromuscular disorder in intensive care unit patients treated with pancuronium bromide. Occurrence in a cluster group of seven patients and two sporadic cases, with electrophysiologic and histologic examination. *Chest,* 106**,** 210-20.

GODFREY, C., MUSES, S., MCCLOREY, G., WELLS, K. E., COURSINDEL, T., TERRY, R. L., BETTS, C., HAMMOND, S., O'DONOVAN, L., HILDYARD, J., EL ANDALOUSSI, S., GAIT, M. J., WOOD, M. J. & WELLS, D. J. 2015. How much dystrophin is enough: the physiological consequences of different levels of dystrophin in the mdx mouse. *Human Molecular Genetics,* 24**,** 4225-4237.

GODIN, R., DAUSSIN, F., MATECKI, S., LI, T., PETROF, B. J. & BURELLE, Y. 2012. Peroxisome proliferator-activated receptor γ coactivator 1-α gene transfer restores mitochondrial biomass and improves mitochondrial calcium handling in post-necrotic mdx mouse skeletal muscle. *The Journal of Physiology,* 590**,** 5487-5502.

GOEMANS, N., MERCURI, E., BELOUSOVA, E., KOMAKI, H., DUBROVSKY, A., MCDONALD, C. M., KRAUS, J. E., LOURBAKOS, A., LIN, Z., CAMPION, G., WANG, S. X. & CAMPBELL, C. 2018. A randomized placebo-controlled phase 3 trial of an antisense oligonucleotide, drisapersen, in Duchenne muscular dystrophy. *Neuromuscul Disord,* 28**,** 4-15.

GOEMANS, N. M., TULINIUS, M., VAN DEN AKKER, J. T., BURM, B. E., EKHART, P. F., HEUVELMANS, N., HOLLING, T., JANSON, A. A., PLATENBURG, G. J., SIPKENS, J. A., SITSEN, J. M., AARTSMA-RUS, A., VAN OMMEN, G. J., BUYSE, G., DARIN, N., VERSCHUUREN, J. J., CAMPION, G. V., DE KIMPE, S. J. & VAN DEUTEKOM, J. C. 2011. Systemic administration of PRO051 in Duchenne's muscular dystrophy. *N Engl J Med,* 364**,** 1513-22.

GOLDSTEIN, J. A. & MCNALLY, E. M. 2010. Mechanisms of muscle weakness in muscular dystrophy. *The Journal of general physiology,* 136**,** 29-34.

GOLL, D. E., THOMPSON, V. F., LI, H., WEI, W. & CONG, J. 2003. The calpain system. *Physiological reviews,* 83**,** 731-801.

GOLLNICK, P. D., SJÖDIN, B., KARLSSON, J., JANSSON, E. & SALTIN, B. 1974. Human soleus muscle: a comparison of fiber composition and enzyme activities with other leg muscles. *Pflügers Archiv,* 348**,** 247-255.

GOONASEKERA, S. A., LAM, C. K., MILLAY, D. P., SARGENT, M. A., HAJJAR, R. J., KRANIAS, E. G. & MOLKENTIN, J. D. 2011. Mitigation of muscular dystrophy in mice by SERCA overexpression in skeletal muscle. *J Clin Invest,* 121**,** 1044-52.

GORDON, B. S., DELGADO DIAZ, D. C. & KOSTEK, M. C. 2013. Resveratrol decreases inflammation and increases utrophin gene expression in the mdx mouse model of Duchenne muscular dystrophy. *Clin Nutr,* 32**,** 104-11.

GOYENVALLE, A., SETO, J. T., DAVIES, K. E. & CHAMBERLAIN, J. 2011. Therapeutic approaches to muscular dystrophy. *Human molecular genetics,* 20**,** R69-R78.

GREEN, H. J., THOMSON, J. A., DAUB, W. D., HOUSTON, M. E. & RANNEY, D. A. 1979. Fiber composition, fiber size and enzyme activities in vastus lateralis of elite athletes involved in high intensity exercise. *Eur J Appl Physiol Occup Physiol,* 41**,** 109-17.

GREGOREVIC, P., ALLEN, J. M., MINAMI, E., BLANKINSHIP, M. J., HARAGUCHI, M., MEUSE, L., FINN, E., ADAMS, M. E., FROEHNER, S. C., MURRY, C. E. & CHAMBERLAIN, J. S. 2006. rAAV6-microdystrophin preserves muscle function and extends lifespan in severely dystrophic mice. *Nat Med,* 12**,** 787-9.

GREGOREVIC, P., BLANKINSHIP, M. J., ALLEN, J. M., CRAWFORD, R. W., MEUSE, L., MILLER, D. G., RUSSELL, D. W. & CHAMBERLAIN, J. S. 2004. Systemic delivery of genes to striated muscles using adeno-associated viral vectors. *Nat Med,* 10**,** 828-34.

GREISING, S. M., GRANSEE, H. M., MANTILLA, C. B. & SIECK, G. C. 2012. Systems Biology of Skeletal Muscle: Fiber Type as an Organizing Principle. *Wiley interdisciplinary reviews. Systems biology and medicine,* 4**,** 10.1002/wsbm.1184.

GROSSO, S., PERRONE, S., LONGINI, M., BRUNO, C., MINETTI, C., GAZZOLO, D., BALESTRI, P. & BUONOCORE, G. 2008. Isoprostanes in dystrophinopathy: evidence of increased oxidative stress. *Brain and Development,* 30**,** 391-395.

GROUNDS, M. D., RADLEY, H. G., LYNCH, G. S., NAGARAJU, K. & DE LUCA, A. 2008. Towards developing standard operating procedures for pre-clinical testing in the mdx mouse model of Duchenne muscular dystrophy. *Neurobiol Dis,* 31**,** 1-19.

GROUNDS, M. D. & TORRISI, J. 2004. Anti-TNFalpha (Remicade) therapy protects dystrophic skeletal muscle from necrosis. *Faseb j,* 18**,** 676-82.

GRUMATI, P., COLETTO, L., SABATELLI, P., CESCON, M., ANGELIN, A., BERTAGGIA, E., BLAAUW, B., URCIUOLO, A., TIEPOLO, T., MERLINI, L., MARALDI, N. M., BERNARDI, P., SANDRI, M. & BONALDO, P. 2010. Autophagy is defective in collagen VI muscular dystrophies, and its reactivation rescues myofiber degeneration. *Nat Med,* 16**,** 1313-20.

GYGI, S. P., ROCHON, Y., FRANZA, B. R. & AEBERSOLD, R. 1999. Correlation between protein and mRNA abundance in yeast. *Mol Cell Biol,* 19**,** 1720-30.

HADDAD, F. & ADAMS, G. R. 2006. Aging-sensitive cellular and molecular mechanisms associated with skeletal muscle hypertrophy. *J Appl Physiol (1985),* 100**,** 1188-203.

HAFNER, P., BONATI, U., ERNE, B., SCHMID, M., RUBINO, D., POHLMAN, U., PETERS, T., RUTZ, E., FRANK, S., NEUHAUS, C., DEUSTER, S., GLOOR, M., BIERI, O., FISCHMANN, A., SINNREICH, M., GUEVEN, N. & FISCHER, D. 2016. Improved Muscle Function in Duchenne Muscular Dystrophy through L-Arginine and Metformin: An Investigator-Initiated, Open-Label, Single-Center, Proof-Of-Concept-Study. *PLoS ONE,* 11**,** e0147634.

HAIHAN, L. & TANG, Q. 2018. GW27-e0432 Efficient AAV9-mediated gene delivery to the heart. *Journal of the American College of Cardiology,* 68**,** C18.

HAKIM, C. H. & DUAN, D. 2012. Gender differences in contractile and passive properties of mdx extensor digitorum longus muscle. *Muscle Nerve,* 45**,** 250-6.

HAKIM, C. H., WASALA, N. B., PAN, X., KODIPPILI, K., YUE, Y., ZHANG, K., YAO, G., HAFFNER, B., DUAN, S. X., RAMOS, J., SCHNEIDER, J. S., YANG, N. N., CHAMBERLAIN, J. S. & DUAN, D. 2017. A Five-Repeat Micro-Dystrophin Gene Ameliorated Dystrophic Phenotype in the Severe DBA/2J-mdx Model of Duchenne Muscular Dystrophy. *Molecular Therapy. Methods & Clinical Development,* 6**,** 216-230.

HANDSCHIN, C., KOBAYASHI, Y. M., CHIN, S., SEALE, P., CAMPBELL, K. P. & SPIEGELMAN, B. M. 2007. PGC-1α regulates the neuromuscular junction program and ameliorates Duchenne muscular dystrophy. *Genes & development,* 21**,** 770-783.

HANDSCHIN, C., RHEE, J., LIN, J., TARR, P. T. & SPIEGELMAN, B. M. 2003. An autoregulatory loop controls peroxisome proliferator-activated receptor γ coactivator 1α expression in muscle. *Proceedings of the National Academy of Sciences,* 100**,** 7111-7116.

HANDSCHIN, C. & SPIEGELMAN, B. M. 2006. Peroxisome proliferator-activated receptor gamma coactivator 1 coactivators, energy homeostasis, and metabolism. *Endocr Rev,* 27**,** 728-35.

HAREENDRAN, S., BALAKRISHNAN, B., SEN, D., KUMAR, S., SRIVASTAVA, A. & JAYANDHARAN, G. R. 2013. Adeno-associated virus (AAV) vectors in gene therapy: immune challenges and strategies to circumvent them. *Reviews in medical virology,* 23**,** 399-413.

HARPER, S. Q., HAUSER, M. A., DELLORUSSO, C., DUAN, D., CRAWFORD, R. W., PHELPS, S. F., HARPER, H. A., ROBINSON, A. S., ENGELHARDT, J. F. & BROOKS, S. V. 2002. Modular flexibility of dystrophin: implications for gene therapy of Duchenne muscular dystrophy. *Nature medicine,* 8**,** 253.

HASLETT, J. N., SANOUDOU, D., KHO, A. T., BENNETT, R. R., GREENBERG, S. A., KOHANE, I. S., BEGGS, A. H. & KUNKEL, L. M. 2002. Gene expression comparison of biopsies from Duchenne muscular dystrophy (DMD) and normal skeletal muscle. *Proceedings of the National Academy of Sciences,* 99**,** 15000-15005.

HASSON, S. S. A. A., AL-BUSAIDI, J. K. Z. & SALLAM, T. A. 2015. The past, current and future trends in DNA vaccine immunisations. *Asian Pacific Journal of Tropical Biomedicine,* 5**,** 344-353.

HASTIE, E. & SAMULSKI, R. J. 2015. Adeno-associated virus at 50: a golden anniversary of discovery, research, and gene therapy success--a personal perspective. *Hum Gene Ther,* 26**,** 257-65.

HAUSER, E., HOGER, H., BITTNER, R., WIDHALM, K., HERKNER, K. & LUBEC, G. 1995. Oxyradical damage and mitochondrial enzyme activities in the mdx mouse. *Neuropediatrics,* 26**,** 260-262.

HAY, N. & SONENBERG, N. 2004. Upstream and downstream of mTOR. *Genes Dev,* 18**,** 1926-45.

HAYCOCK, J. W., MAC NEIL, S., JONES, P., HARRIS, J. B. & MANTLE, D. 1996. Oxidative damage to muscle protein in Duchenne muscular dystrophy. *Neuroreport,* 8**,** 357-361.

HE, W. A., BERARDI, E., CARDILLO, V. M., ACHARYYA, S., AULINO, P., THOMAS-AHNER, J., WANG, J., BLOOMSTON, M., MUSCARELLA, P. & NAU, P. 2013. NF-κB–mediated Pax7 dysregulation in the muscle microenvironment promotes cancer cachexia. *The Journal of clinical investigation,* 123**,** 4821-4835.

HEAD, S. I. 2010. Branched fibres in old dystrophic mdx muscle are associated with mechanical weakening of the sarcolemma, abnormal Ca2+ transients and a breakdown of Ca2+ homeostasis during fatigue. *Exp Physiol,* 95**,** 641-56.

HEAD, S. I., WILLIAMS, D. A. & STEPHENSON, D. G. 1992. Abnormalities in structure and function of limb skeletal muscle fibres of dystrophic mdx mice. *Proc Biol Sci,* 248**,** 163-9.

HEIER, C. R., GUERRON, A. D., KOROTCOV, A., LIN, S., GORDISH-DRESSMAN, H., FRICKE, S., SZE, R. W., HOFFMAN, E. P., WANG, P. & NAGARAJU, K. 2014. Non-invasive MRI and spectroscopy of mdx mice reveal temporal changes in dystrophic muscle imaging and in energy deficits. *PLoS One,* 9**,** e112477.

HERMONAT, P. L. & MUZYCZKA, N. 1984. Use of adeno-associated virus as a mammalian DNA cloning vector: transduction of neomycin resistance into mammalian tissue culture cells. *Proceedings of the National Academy of Sciences,* 81**,** 6466-6470.

HERNANDEZ-OCHOA, E. O., PRATT, S. J., GARCIA-PELAGIO, K. P., SCHNEIDER, M. F. & LOVERING, R. M. 2015. Disruption of action potential and calcium signaling properties in malformed myofibers from dystrophin-deficient mice. *Physiol Rep,* 3**,** e12366.

HINDERER, C., KATZ, N., BUZA, E. L., DYER, C., GOODE, T., BELL, P., RICHMAN, L. & WILSON, J. M. 2018. Severe toxicity in nonhuman primates and piglets following high-dose intravenous administration of an AAV vector expressing human SMN. *Human Gene Therapy,* 29**,** 285-298.

HIRST, R., MCCULLAGH, K. & DAVIES, K. 2005. Utrophin upregulation in Duchenne muscular dystrophy. *Acta myologica: myopathies and cardiomyopathies: official journal of the Mediterranean Society of Myology,* 24**,** 209-216.

HLAVATY, J., SCHITTMAYER, M., STRACKE, A., JANDL, G., KNAPP, E., FELBER, B. K., SALMONS, B., GÜNZBURG, W. H. & RENNER, M. 2005. Effect of posttranscriptional regulatory elements on transgene expression and virus production in the context of retrovirus vectors. *Virology,* 341**,** 1-11.

HOCK, M. B. & KRALLI, A. 2009. Transcriptional control of mitochondrial biogenesis and function. *Annual review of physiology,* 71**,** 177-203.

HODGETTS, S., RADLEY, H., DAVIES, M. & GROUNDS, M. D. 2006. Reduced necrosis of dystrophic muscle by depletion of host neutrophils, or blocking TNFalpha function with Etanercept in mdx mice. *Neuromuscul Disord,* 16**,** 591-602.

HOFFMAN, E. P., BRONSON, A., LEVIN, A. A., TAKEDA, S. I., YOKOTA, T., BAUDY, A. R. & CONNOR, E. M. 2011. Restoring dystrophin expression

in duchenne muscular dystrophy muscle: progress in exon skipping and stop codon read through. *The American journal of pathology,* 179**,** 12-22.

HOFFMAN, E. P., BROWN, R. H., JR. & KUNKEL, L. M. 1987. Dystrophin: the protein product of the Duchenne muscular dystrophy locus. *Cell,* 51**,** 919-28.

HOFFMAN, E. P. & MCNALLY, E. M. 2014. Exon-skipping Therapy for Muscular Dystrophy: A Roadblock, Detour, or Bump in the Road? *Science translational medicine,* 6**,** 230fs14-230fs14.

HOLLINGER, K., GARDAN-SALMON, D., SANTANA, C., RICE, D., SNELLA, E. & SELSBY, J. T. 2013. Rescue of dystrophic skeletal muscle by PGC-1α involves restored expression of dystrophin-associated protein complex components and satellite cell signaling. *American Journal of Physiology-Regulatory, Integrative and Comparative Physiology,* 305**,** R13-R23.

HOLLINGER, K. & SELSBY, J. T. 2015. PGC-1α gene transfer improves muscle function in dystrophic muscle following prolonged disease progress. *Experimental physiology,* 100**,** 1145-1158.

HOLLINGER, K., SHANELY, R. A., QUINDRY, J. C. & SELSBY, J. T. 2015. Long-term quercetin dietary enrichment decreases muscle injury in mdx mice. *Clin Nutr,* 34**,** 515-22.

HONG, H., YANG, L. & STALLCUP, M. R. 1999. Hormone-independent transcriptional activation and coactivator binding by novel orphan nuclear receptor ERR3. *Journal of Biological Chemistry,* 274**,** 22618-22626.

HONG, Y. H., BETIK, A. C. & MCCONELL, G. K. 2014. Role of nitric oxide in skeletal muscle glucose uptake during exercise. *Experimental physiology,* 99**,** 1569-1573.

HOPPELER, H. & FLUECK, M. 2003. Plasticity of skeletal muscle mitochondria: structure and function. *Medicine & Science in Sports & Exercise,* 35**,** 95-104.

HORDEAUX, J., WANG, Q., KATZ, N., BUZA, E. L., BELL, P. & WILSON, J. M. 2018. The Neurotropic Properties of AAV-PHP.B Are Limited to C57BL/6J Mice. *Mol Ther,* 26**,** 664-668.

HORI, Y. S., KUNO, A., HOSODA, R., TANNO, M., MIURA, T., SHIMAMOTO, K. & HORIO, Y. 2011. Resveratrol ameliorates muscular pathology in the dystrophic mdx mouse, a model for Duchenne muscular dystrophy. *J Pharmacol Exp Ther,* 338**,** 784-94.

HORIO, Y., HAYASHI, T., KUNO, A. & KUNIMOTO, R. 2011. Cellular and molecular effects of sirtuins in health and disease. *Clin Sci (Lond),* 121**,** 191-203.

HORMAN, S., BROWNE, G. J., KRAUSE, U., PATEL, J. V., VERTOMMEN, D., BERTRAND, L., LAVOINNE, A., HUE, L., PROUD, C. G. & RIDER, M. H. 2002. Activation of AMP-Activated Protein Kinase Leads to the Phosphorylation of Elongation Factor 2 and an Inhibition of Protein Synthesis. *Current Biology,* 12**,** 1419-1423.

HOROWITZ, E. D., RAHMAN, K. S., BOWER, B. D., DISMUKE, D. J., FALVO, M. R., GRIFFITH, J. D., HARVEY, S. C. & ASOKAN, A. 2013. Biophysical and Ultrastructural Characterization of Adeno-Associated Virus Capsid Uncoating and Genome Release. *Journal of Virology,* 87**,** 2994-3002.

HUANG, H., NGUYEN, T., IBRAHIM, S., SHANTHARAM, S., YUE, Z. & CHEN, J. Y. 2015. DMAP: a connectivity map database to enable identification of novel drug repositioning candidates. *BMC Bioinformatics,* 16**,** S4-S4.

HUSS, J. M., GARBACZ, W. G. & XIE, W. 2015. Constitutive activities of estrogen-related receptors: transcriptional regulation of metabolism by the ERR pathways in health and disease. *Biochimica et Biophysica Acta (BBA)-Molecular Basis of Disease,* 1852**,** 1912-1927.

HUSS, J. M., KOPP, R. P. & KELLY, D. P. 2002. Peroxisome Proliferator-activated Receptor Coactivator-1α (PGC-1α) Coactivates the Cardiac-enriched Nuclear Receptors Estrogen-related Receptor-α and-γ IDENTIFICATION OF NOVEL LEUCINE-RICH INTERACTION MOTIF WITHIN PGC-1α. *Journal of Biological Chemistry,* 277**,** 40265-40274.

HUSS, J. M., TORRA, I. P., STAELS, B., GIGUERE, V. & KELLY, D. P. 2004. Estrogen-related receptor α directs peroxisome proliferator-activated receptor α signaling in the transcriptional control of energy metabolism in cardiac and skeletal muscle. *Molecular and cellular biology,* 24**,** 9079-9091.

IKEMURA, T. 1981. Correlation between the abundance of Escherichia coli transfer RNAs and the occurrence of the respective codons in its protein genes: a proposal for a synonymous codon choice that is optimal for the E. coli translational system. *Journal of molecular biology,* 151**,** 389-409.

IMAI, S., ARMSTRONG, C. M., KAEBERLEIN, M. & GUARENTE, L. 2000. Transcriptional silencing and longevity protein Sir2 is an NAD-dependent histone deacetylase. *Nature,* 403**,** 795-800.

INAGAKI, K., FUESS, S., STORM, T. A., GIBSON, G. A., MCTIERNAN, C. F., KAY, M. A. & NAKAI, H. 2006. Robust systemic transduction with AAV9 vectors in mice: efficient global cardiac gene transfer superior to that of AAV8. *Molecular Therapy,* 14**,** 45-53.

IORIO, F., RITTMAN, T., GE, H., MENDEN, M. & SAEZ-RODRIGUEZ, J. 2013. Transcriptional data: a new gateway to drug repositioning? *Drug Discovery Today,* 18**,** 350-357.

ITO, K., KIMURA, S., OZASA, S., MATSUKURA, M., IKEZAWA, M., YOSHIOKA, K., UENO, H., SUZUKI, M., ARAKI, K. & YAMAMURA, K.-I. 2006. Smooth muscle-specific dystrophin expression improves aberrant vasoregulation in mdx mice. *Human molecular genetics,* 15**,** 2266-2275.

JAESCHKE, H., MCGILL, M. R. & RAMACHANDRAN, A. 2012. Oxidant stress, mitochondria, and cell death mechanisms in drug-induced liver injury: lessons learned from acetaminophen hepatotoxicity. *Drug metabolism reviews,* 44**,** 88-106.

JÄGER, S., HANDSCHIN, C., ST.-PIERRE, J. & SPIEGELMAN, B. M. 2007. AMP-activated protein kinase (AMPK) action in skeletal muscle via direct phosphorylation of PGC-1α. *Proceedings of the National Academy of Sciences of the United States of America,* 104**,** 12017-12022.

JAHNKE, V. E., VAN DER MEULEN, J. H., JOHNSTON, H. K., GHIMBOVSCHI, S., PARTRIDGE, T., HOFFMAN, E. P. & NAGARAJU, K. 2012. Metabolic remodeling agents show beneficial effects in the dystrophin-deficient mdx mouse model. *Skelet Muscle,* 2**,** 16.

JENSEN, J., RUSTAD, P. I., KOLNES, A. J. & LAI, Y.-C. 2011. The Role of Skeletal Muscle Glycogen Breakdown for Regulation of Insulin Sensitivity by Exercise. *Frontiers in Physiology,* 2**,** 112.

JIANG, H., COUTO, L. B., PATARROYO-WHITE, S., LIU, T., NAGY, D., VARGAS, J. A., ZHOU, S., SCALLAN, C. D., SOMMER, J., VIJAY, S., MINGOZZI, F., HIGH, K. A. & PIERCE, G. F. 2006. Effects of transient

immunosuppression on adenoassociated, virus-mediated, liver-directed gene transfer in rhesus macaques and implications for human gene therapy. *Blood,* 108**,** 3321-3328.

JIANG, J. X., CHOI, R. C., SIOW, N. L., LEE, H. H., WAN, D. C. & TSIM, K. W. 2003. Muscle induces neuronal expression of acetylcholinesterase in neuron-muscle co-culture: transcriptional regulation mediated by cAMP-dependent signaling. *J Biol Chem,* 278**,** 45435-44.

JOHNSON, K., LIU, L., MAJDZADEH, N., CHAVEZ, C., CHIN, P. C., MORRISON, B., WANG, L., PARK, J., CHUGH, P. & CHEN, H. M. 2005. Inhibition of neuronal apoptosis by the cyclin-dependent kinase inhibitor GW8510: Identification of 3′ substituted indolones as a scaffold for the development of neuroprotective drugs. *Journal of neurochemistry,* 93**,** 538-548.

JOHNSTONE, C. N., CHAND, A., PUTOCZKI, T. L. & ERNST, M. 2015. Emerging roles for IL-11 signaling in cancer development and progression: Focus on breast cancer. *Cytokine & Growth Factor Reviews,* 26**,** 489-498.

JONES, D., ROUND, J. & DE HAAN, A. 2004. *Skeletal muscle from molecules to movement. A textbook of muscle physiology for sport, exercise, physiotherapy and medicine*, Churchill Livingstone, Elsevier Science Limited, London, UK. .

JONES, D. A., TURNER, D. L., MCINTYRE, D. B. & NEWHAM, D. J. 2009. Energy turnover in relation to slowing of contractile properties during fatiguing contractions of the human anterior tibialis muscle. *J Physiol,* 587**,** 4329-38.

JUNG, Y. S., LEE, J.-M., KIM, D.-K., LEE, Y.-S., KIM, K.-S., KIM, Y.-H., KIM, J., LEE, M.-S., LEE, I.-K. & KIM, S. H. 2016. The orphan nuclear receptor ERRγ regulates hepatic CB1 receptor-mediated fibroblast growth factor 21 gene expression. *PloS one,* 11**,** e0159425.

KAMEI, Y., MIURA, S., SUZUKI, M., KAI, Y., MIZUKAMI, J., TANIGUCHI, T., MOCHIDA, K., HATA, T., MATSUDA, J., ABURATANI, H., NISHINO, I. & EZAKI, O. 2004. Skeletal muscle FOXO1 (FKHR) transgenic mice have less skeletal muscle mass, down-regulated Type I (slow twitch/red muscle) fiber genes, and impaired glycemic control. *J Biol Chem,* 279**,** 41114-23.

KAMMOUN, M., CASSAR-MALEK, I., MEUNIER, B. & PICARD, B. 2014. A Simplified Immunohistochemical Classification of Skeletal Muscle Fibres in Mouse. *European Journal of Histochemistry : EJH,* 58**,** 2254.

KARGACIN, M. E. & KARGACIN, G. J. 1996. The sarcoplasmic reticulum calcium pump is functionally altered in dystrophic muscle. *Biochim Biophys Acta,* 1290**,** 4-8.

KARIN, M. & CLEVERS, H. 2016. Reparative inflammation takes charge of tissue regeneration. *Nature,* 529**,** 307.

KATTENHORN, L. M., TIPPER, C. H., STOICA, L., GERAGHTY, D. S., WRIGHT, T. L., CLARK, K. R. & WADSWORTH, S. C. 2016. Adeno-Associated Virus Gene Therapy for Liver Disease. *Hum Gene Ther,* 27**,** 947-961.

KAY, M. A. 2011. State-of-the-art gene-based therapies: the road ahead. *Nature Reviews Genetics,* 12**,** 316-328.

KHAIRALLAH, R. J., SHI, G., SBRANA, F., PROSSER, B. L., BORROTO, C., MAZAITIS, M. J., HOFFMAN, E. P., MAHURKAR, A., SACHS, F. & SUN, Y. 2012. Microtubules underlie dysfunction in duchenne muscular dystrophy. *Sci. Signal.,* 5**,** ra56-ra56.

KIL, J., PIERCE, C., TRAN, H., GU, R. & LYNCH, E. D. 2007. Ebselen treatment reduces noise induced hearing loss via the mimicry and induction of glutathione peroxidase. *Hear Res,* 226**,** 44-51.

KIM-HAN, J. S., ANTENOR-DORSEY, J. A. & O'MALLEY, K. L. 2011. The parkinsonian mimetic, MPP+, specifically impairs mitochondrial transport in dopamine axons. *Journal of Neuroscience,* 31**,** 7212-7221.

KIM, D.-K., KIM, J. R., KOH, M., KIM, Y. D., LEE, J.-M., CHANDA, D., PARK, S. B., MIN, J.-J., LEE, C.-H., PARK, T.-S. & CHOI, H.-S. 2011. Estrogen-related Receptor γ (ERRγ) Is a Novel Transcriptional Regulator of Phosphatidic Acid Phosphatase, LIPIN1, and Inhibits Hepatic Insulin Signaling. *The Journal of Biological Chemistry,* 286**,** 38035-38042.

KIM, H.-J., PARK, K.-G., YOO, E.-K., KIM, Y.-H., KIM, Y.-N., KIM, H.-S., KIM, H. T., PARK, J.-Y., LEE, K.-U. & JANG, W. G. 2007. Effects of PGC-1α on TNF-α–Induced MCP-1 and VCAM-1 Expression and NF-κB Activation in Human Aortic Smooth Muscle and Endothelial Cells. *Antioxidants & redox signaling,* 9**,** 301-307.

KIM, K., KIM, Y. H., LEE, S. H., JEON, M. J., PARK, S. Y. & DOH, K. O. 2014. Effect of exercise intensity on unfolded protein response in skeletal muscle of rat. *Korean J Physiol Pharmacol,* 18**,** 211-6.

KLEIJN, M., SCHEPER, G. C., VOORMA, H. O. & THOMAS, A. A. 1998. Regulation of translation initiation factors by signal transduction. *Eur J Biochem,* 253**,** 531-44.

KOBZIK, L., REID, M. B., BREDT, D. S. & STAMLER, J. S. 1994. Nitric oxide in skeletal muscle. *Nature,* 372**,** 546-8.

KOLEDOVA, V. V. & KHALIL, R. A. 2006. Ca(2+), Calmodulin, and Cyclins in Vascular Smooth Muscle Cell Cycle. *Circulation research,* 98**,** 1240-1243.

KOMEN, J. & THORBURN, D. 2014. Turn up the power–pharmacological activation of mitochondrial biogenesis in mouse models. *British journal of pharmacology,* 171**,** 1818-1836.

KONIECZNY, P., SWIDERSKI, K. & CHAMBERLAIN, J. S. 2013. Gene and cell-mediated therapies for muscular dystrophy. *Muscle & nerve,* 47**,** 649-663.

KOPPANATI, B. M., LI, J., XIAO, X. & CLEMENS, P. R. 2009. Systemic delivery of AAV8 in utero results in gene expression in diaphragm and limb muscle: Treatment implications for muscle disorders. *Gene therapy,* 16**,** 1130.

KORNEGAY, J. N., LI, J., BOGAN, J. R., BOGAN, D. J., CHEN, C., ZHENG, H., WANG, B., QIAO, C., HOWARD, J. F. & XIAO, X. 2010. Widespread Muscle Expression of an AAV9 Human Mini-dystrophin Vector After Intravenous Injection in Neonatal Dystrophin-deficient Dogs. *Molecular Therapy,* 18**,** 1501-1508.

KOSTEK, M. C., NAGARAJU, K., PISTILLI, E., SALI, A., LAI, S.-H., GORDON, B. & CHEN, Y.-W. 2012. IL-6 signaling blockade increases inflammation but does not affect muscle function in the mdx mouse. *BMC musculoskeletal disorders,* 13**,** 106.

KOTTERMAN, M. A. & SCHAFFER, D. V. 2014. Engineering adeno-associated viruses for clinical gene therapy. *Nat Rev Genet,* 15**,** 445-51.

KOZAK, M. 1999. Initiation of translation in prokaryotes and eukaryotes. *Gene,* 234**,** 187-208.

KOZAK, M. 2005. Regulation of translation via mRNA structure in prokaryotes and eukaryotes. *Gene,* 361**,** 13-37.

KRESS, M., HUXLEY, H. E., FARUQI, A. R. & HENDRIX, J. 1986. Structural changes during activation of frog muscle studied by time-resolved X-ray diffraction. *Journal of Molecular Biology,* 188**,** 325-342.

KUDLA, G., LIPINSKI, L., CAFFIN, F., HELWAK, A. & ZYLICZ, M. 2006. High guanine and cytosine content increases mRNA levels in mammalian cells. *PLoS Biol,* 4**,** e180.

KUMAR, A. & BORIEK, A. M. 2003. Mechanical stress activates the nuclear factor-kappaB pathway in skeletal muscle fibers: a possible role in Duchenne muscular dystrophy. *Faseb j,* 17**,** 386-96.

KUNKEL, L. M. 2005. Cloning of the DMD Gene. *American journal of human genetics,* 76**,** 205.

KUWABARA, M., KAKINUMA, Y., ANDO, M., KATARE, R. G., YAMASAKI, F., DOI, Y. & SATO, T. 2006. Nitric oxide stimulates vascular endothelial growth factor production in cardiomyocytes involved in angiogenesis. *J Physiol Sci,* 56**,** 95-101.

KUZNETSOV, A. V., WINKLER, K., WIEDEMANN, F., VON BOSSANYI, P., DIETZMANN, K. & KUNZ, W. S. 1998. Impaired mitochondrial oxidative phosphorylation in skeletal muscle of the dystrophin-deficient mdx mouse. *Molecular and cellular biochemistry,* 183**,** 87-96.

LABARGE, S., MCDONALD, M., SMITH-POWELL, L., AUWERX, J. & HUSS, J. M. 2014. Estrogen-related receptor-α (ERRα) deficiency in skeletal muscle impairs regeneration in response to injury. *The FASEB Journal,* 28**,** 1082-1097.

LAI, Y., THOMAS, G. D., YUE, Y., YANG, H. T., LI, D., LONG, C., JUDGE, L., BOSTICK, B., CHAMBERLAIN, J. S., TERJUNG, R. L. & DUAN, D. 2009. Dystrophins carrying spectrin-like repeats 16 and 17 anchor nNOS to the sarcolemma and enhance exercise performance in a mouse model of muscular dystrophy. *J Clin Invest,* 119**,** 624-35.

LAMB, G. 2000. Excitation–contraction coupling in skeletal muscle: comparisons with cardiac muscle. *Clinical and Experimental Pharmacology and Physiology,* 27**,** 216-224.

LAMB, G. D. & STEPHENSON, D. G. 1996. Effects of FK506 and rapamycin on excitation-contraction coupling in skeletal muscle fibres of the rat. *J Physiol,* 494 (Pt 2)**,** 569-76.

LAMB, J., CRAWFORD, E. D., PECK, D., MODELL, J. W., BLAT, I. C., WROBEL, M. J., LERNER, J., BRUNET, J. P., SUBRAMANIAN, A., ROSS, K. N., REICH, M., HIERONYMUS, H., WEI, G., ARMSTRONG, S. A., HAGGARTY, S. J., CLEMONS, P. A., WEI, R., CARR, S. A., LANDER, E. S. & GOLUB, T. R. 2006. The Connectivity Map: using gene-expression signatures to connect small molecules, genes, and disease. *Science,* 313**,** 1929-35.

LANCET, J., GOJO, I., BURTON, M., QUINN, M., TIGHE, S., KERSEY, K., ZHONG, Z., ALBITAR, M., BHALLA, K. & HANNAH, A. 2010. Phase I study of the heat shock protein 90 inhibitor alvespimycin (KOS-1022, 17-DMAG) administered intravenously twice weekly to patients with acute myeloid leukemia. *Leukemia,* 24**,** 699.

LATROCHE, C., WEISS-GAYET, M., MULLER, L., GITIAUX, C., LEBLANC, P., LIOT, S., BEN-LARBI, S., ABOU-KHALIL, R., VERGER, N., BARDOT, P., MAGNAN, M., CHRETIEN, F., MOUNIER, R., GERMAIN, S. & CHAZAUD, B. 2017. Coupling between Myogenesis and Angiogenesis during Skeletal Muscle Regeneration Is Stimulated by Restorative Macrophages. *Stem Cell Reports,* 9**,** 2018-2033.

LAVU, S., BOSS, O., ELLIOTT, P. J. & LAMBERT, P. D. 2008. Sirtuins--novel therapeutic targets to treat age-associated diseases. *Nat Rev Drug Discov,* 7**,** 841-53.

LAWLER, J. M. 2011. Exacerbation of pathology by oxidative stress in respiratory and locomotor muscles with Duchenne muscular dystrophy. *The Journal of physiology,* 589**,** 2161-2170.

LE GUINER, C., SERVAIS, L., MONTUS, M., LARCHER, T., FRAYSSE, B., MOULLEC, S., ALLAIS, M., FRANÇOIS, V., DUTILLEUL, M. & MALERBA, A. 2017. Long-term microdystrophin gene therapy is effective in a canine model of Duchenne muscular dystrophy. *Nature communications,* 8**,** 16105.

LE HIR, M., GOYENVALLE, A., PECCATE, C., PRÉCIGOUT, G., DAVIES, K. E., VOIT, T., GARCIA, L. & LORAIN, S. 2013. AAV Genome Loss From Dystrophic Mouse Muscles During AAV-U7 snRNA-mediated Exon-skipping Therapy. *Molecular Therapy,* 21**,** 1551-1558.

LEBRASSEUR, N. K., SCHELHORN, T. M., BERNARDO, B. L., COSGROVE, P. G., LORIA, P. M. & BROWN, T. A. 2009. Myostatin inhibition enhances the effects of exercise on performance and metabolic outcomes in aged mice. *The Journals of Gerontology Series A: Biological Sciences and Medical Sciences,* 64**,** 940-948.

LEGER, B., DERAVE, W., DE BOCK, K., HESPEL, P. & RUSSELL, A. P. 2008. Human sarcopenia reveals an increase in SOCS-3 and myostatin and a reduced efficiency of Akt phosphorylation. *Rejuvenation Res,* 11**,** 163-175b.

LEONE, T. C., LEHMAN, J. J., FINCK, B. N., SCHAEFFER, P. J., WENDE, A. R., BOUDINA, S., COURTOIS, M., WOZNIAK, D. F., SAMBANDAM, N. & BERNAL-MIZRACHI, C. 2005. PGC-1α deficiency causes multi-system energy metabolic derangements: muscle dysfunction, abnormal weight control and hepatic steatosis. *PLoS biology,* 3**,** e101.

LI, D., YUE, Y., LAI, Y., HAKIM, C. H. & DUAN, D. 2011. Nitrosative stress elicited by nNOSmicro delocalization inhibits muscle force in dystrophin-null mice. *J Pathol,* 223**,** 88-98.

LI, H., MALHOTRA, S. & KUMAR, A. 2008. Nuclear factor-kappa B signaling in skeletal muscle atrophy. *Journal of molecular medicine,* 86**,** 1113-1126.

LI, W. W., TALCOTT, K. E., ZHAI, A. W., KRUGER, E. A. & LI, V. W. 2005. The role of therapeutic angiogenesis in tissue repair and regeneration. *Advances in skin & wound care,* 18**,** 491-500.

LIANG, H. & WARD, W. F. 2006. PGC-1α: a key regulator of energy metabolism. *Advances in physiology education,* 30**,** 145-151.

LIANG, J., HAN, F. & CHEN, Y. 2013. Transcriptional regulation of VEGF expression by estrogen-related receptor γ. *Acta Pharmaceutica Sinica B,* 3**,** 373-380.

LIEBER, R. L. 2009. *Skeletal muscle structure, function, and plasticity*, Lippincott Williams & Wilkins Baltimore, MD:.

LIEBER, R. L. & WARD, S. R. 2013. Cellular mechanisms of tissue fibrosis. 4. Structural and functional consequences of skeletal muscle fibrosis. *Am J Physiol Cell Physiol,* 305**,** C241-52.

LIN, C. H., HUDSON, A. J. & STRICKLAND, K. P. 1972. Fatty acid oxidation by skeletal muscle mithochondria in duchenne dystrophy. *Life Sciences,* 11**,** 355-362.

LIN, J., WU, H., TARR, P. T., ZHANG, C. Y., WU, Z., BOSS, O., MICHAEL, L. F., PUIGSERVER, P., ISOTANI, E., OLSON, E. N., LOWELL, B. B., BASSEL-DUBY, R. & SPIEGELMAN, B. M. 2002. Transcriptional co-activator PGC-1 alpha drives the formation of slow-twitch muscle fibres. *Nature,* 418**,** 797-801.

LIN, J., WU, P. H., TARR, P. T., LINDENBERG, K. S., ST-PIERRE, J., ZHANG, C. Y., MOOTHA, V. K., JAGER, S., VIANNA, C. R., REZNICK, R. M., CUI, L., MANIERI, M., DONOVAN, M. X., WU, Z., COOPER, M. P., FAN, M. C., ROHAS, L. M., ZAVACKI, A. M., CINTI, S., SHULMAN, G. I., LOWELL, B. B., KRAINC, D. & SPIEGELMAN, B. M. 2004. Defects in adaptive energy metabolism with CNS-linked hyperactivity in PGC-1alpha null mice. *Cell,* 119**,** 121-35.

LIN, J. H. 2008. Applications and limitations of genetically modified mouse models in drug discovery and development. *Curr Drug Metab,* 9**,** 419-38.

LISOWSKI, L., DANE, A. P., CHU, K., ZHANG, Y., CUNNINGHAM, S. C., WILSON, E. M., NYGAARD, S., GROMPE, M., ALEXANDER, I. E. & KAY, M. A. 2014. Selection and evaluation of clinically relevant AAV variants in a xenograft liver model. *Nature,* 506**,** 382-386.

LISOWSKI, L., TAY, S. S. & ALEXANDER, I. E. 2015. Adeno-associated virus serotypes for gene therapeutics. *Current opinion in pharmacology,* 24**,** 59-67.

LIU, W., JENSEN, D., LEE, E., GILLS, J. & HOLZBEIERLEIN, J. M. 2018. New HSP90 selective inhibitors as therapeutic agents for prostate and bladder cancer. *Journal of Clinical Oncology,* 36**,** 285-285.

LJUBICIC, V., BURT, M., LUNDE, J. A. & JASMIN, B. J. 2014. Resveratrol induces expression of the slow, oxidative phenotype in mdx mouse muscle together with enhanced activity of the SIRT1-PGC-1alpha axis. *Am J Physiol Cell Physiol,* 307**,** C66-82.

LJUBICIC, V., MIURA, P., BURT, M., BOUDREAULT, L., KHOGALI, S., LUNDE, J. A., RENAUD, J. M. & JASMIN, B. J. 2011. Chronic AMPK activation evokes the slow, oxidative myogenic program and triggers beneficial adaptations in mdx mouse skeletal muscle. *Hum Mol Genet,* 20**,** 3478-93.

LLOYD, P. G., PRIOR, B. M., LI, H., YANG, H. T. & TERJUNG, R. L. 2005. VEGF receptor antagonism blocks arteriogenesis, but only partially inhibits angiogenesis, in skeletal muscle of exercise-trained rats. *Am J Physiol Heart Circ Physiol,* 288**,** H759-68.

LOELL, I. & LUNDBERG, I. 2011. Can muscle regeneration fail in chronic inflammation: a weakness in inflammatory myopathies? *Journal of internal medicine,* 269**,** 243-257.

LOOS, B., DU TOIT, A. & HOFMEYR, J.-H. S. 2014. Defining and measuring autophagosome flux—concept and reality. *Autophagy,* 10**,** 2087-2096.

LORAIN, S., GROSS, D.-A., GOYENVALLE, A., DANOS, O., DAVOUST, J. & GARCIA, L. 2008. Transient Immunomodulation Allows Repeated

Injections of AAV1 and Correction of Muscular Dystrophy in Multiple Muscles. *Molecular Therapy,* 16**,** 541-547.

LOUFRANI, L., DUBROCA, C., YOU, D., LI, Z., LEVY, B., PAULIN, D. & HENRION, D. 2004. Absence of dystrophin in mice reduces NO-dependent vascular function and vascular density: total recovery after a treatment with the aminoglycoside gentamicin. *Arteriosclerosis, thrombosis, and vascular biology,* 24**,** 671-676.

LOUFRANI, L., MATROUGUI, K., GORNY, D., DURIEZ, M., BLANC, I., LÉVY, B. I. & HENRION, D. 2001. Flow (shear stress)-induced endothelium-dependent dilation is altered in mice lacking the gene encoding for dystrophin. *Circulation,* 103**,** 864-870.

LOVERING, R. M., MICHAELSON, L. & WARD, C. W. 2009. Malformed mdx myofibers have normal cytoskeletal architecture yet altered EC coupling and stress-induced Ca2+ signaling. *Am J Physiol Cell Physiol,* 297**,** C571-80.

LU, Q., BOU-GHARIOS, G. & PARTRIDGE, T. 2003a. Non-viral gene delivery in skeletal muscle: A protein factory. *Gene Therapy,* 10**,** 131-42.

LU, Q. L., LIANG, H. D., PARTRIDGE, T. & BLOMLEY, M. J. 2003b. Microbubble ultrasound improves the efficiency of gene transduction in skeletal muscle in vivo with reduced tissue damage. *Gene Ther,* 10**,** 396-405.

LU, Q. L., RABINOWITZ, A., CHEN, Y. C., YOKOTA, T., YIN, H., ALTER, J., JADOON, A., BOU-GHARIOS, G. & PARTRIDGE, T. 2005. Systemic delivery of antisense oligoribonucleotide restores dystrophin expression in body-wide skeletal muscles. *Proceedings of the National Academy of Sciences of the United States of America,* 102**,** 198-203.

LU, S. C. 2013. Glutathione synthesis. *Biochimica et Biophysica Acta (BBA)-General Subjects,* 1830**,** 3143-3153.

LUO, G., HERSHKO, D. D., ROBB, B. W., WRAY, C. J. & HASSELGREN, P. O. 2003a. IL-1beta stimulates IL-6 production in cultured skeletal muscle cells through activation of MAP kinase signaling pathway and NF-kappa B. *Am J Physiol Regul Integr Comp Physiol,* 284**,** R1249-54.

LUO, J., SLADEK, R., BADER, J.-A., MATTHYSSEN, A., ROSSANT, J. & GIGUÈRE, V. 1997. Placental abnormalities in mouse embryos lacking the orphan nuclear receptor ERR-β. *Nature,* 388**,** 778.

LUO, J., SLADEK, R., CARRIER, J., BADER, J.-A., RICHARD, D. & GIGUÈRE, V. 2003b. Reduced fat mass in mice lacking orphan nuclear receptor estrogen-related receptor α. *Molecular and cellular biology,* 23**,** 7947-7956.

LUO, Y., KUMAR, P. & MENDELSON, C. R. 2013. Estrogen-Related Receptor γ (ERRγ) Regulates Oxygen-Dependent Expression of Voltage-gated Potassium (K(+)) Channels and Tissue Kallikrein during Human Trophoblast Differentiation. *Molecular Endocrinology,* 27**,** 940-952.

LUQUET, S., LOPEZ-SORIANO, J., HOLST, D., FREDENRICH, A., MELKI, J., RASSOULZADEGAN, M. & GRIMALDI, P. A. 2003. Peroxisome proliferator-activated receptor δ controls muscle development and oxidative capability. *The FASEB Journal,* 17**,** 2299-2301.

MACINTOSH, B. R., GARDINER, P. F. & MCCOMAS, A. J. 2006. *Skeletal muscle: form and function*, Human Kinetics.

MACLENNAN, D. H., RICE, W. J. & GREEN, N. M. 1997. The mechanism of Ca2+ transport by sarco(endo)plasmic reticulum Ca2+-ATPases. *J Biol Chem,* 272**,** 28815-8.

MAH, J. K., KORNGUT, L., FIEST, K. M., DYKEMAN, J., DAY, L. J., PRINGSHEIM, T. & JETTE, N. 2016. A Systematic Review and Meta-analysis on the Epidemiology of the Muscular Dystrophies. *Can J Neurol Sci,* 43**,** 163-77.

MAIER, T., GUELL, M. & SERRANO, L. 2009. Correlation of mRNA and protein in complex biological samples. *FEBS Lett,* 583**,** 3966-73.

MAJOWICZ, A., SALAS, D., ZABALETA, N., RODRIGUEZ-GARCIA, E., GONZALEZ-ASEGUINOLAZA, G., PETRY, H. & FERREIRA, V. 2017. Successful Repeated Hepatic Gene Delivery in Mice and Non-human Primates Achieved by Sequential Administration of AAV5(ch) and AAV1. *Mol Ther,* 25**,** 1831-1842.

MAK, R. H., IKIZLER, A. T., KOVESDY, C. P., RAJ, D. S., STENVINKEL, P. & KALANTAR-ZADEH, K. 2011. Wasting in chronic kidney disease. *Journal of cachexia, sarcopenia and muscle,* 2**,** 9-25.

MAKOFF, A., OXER, M., ROMANOS, M., FAIRWEATHER, N. & BALLANTINE, S. 1989. Expression of tetanus toxin fragment C in E. coli: high level expression by removing rare codons. *Nucleic acids research,* 17**,** 10191-10202.

MALERBA, A., BOLDRIN, L. & DICKSON, G. 2011. Long-term systemic administration of unconjugated morpholino oligomers for therapeutic expression of dystrophin by exon skipping in skeletal muscle: implications for cardiac muscle integrity. *Nucleic Acid Ther,* 21**,** 293-8.

MALI, S. 2013. Delivery systems for gene therapy. *Indian Journal of Human Genetics,* 19**,** 3-8.

MAMMUCARI, C., SCHIAFFINO, S. & SANDRI, M. 2008. Downstream of Akt: FoxO3 and mTOR in the regulation of autophagy in skeletal muscle. *Autophagy,* 4**,** 524-6.

MANN, C. J., HONEYMAN, K., CHENG, A. J., LY, T., LLOYD, F., FLETCHER, S., MORGAN, J. E., PARTRIDGE, T. A. & WILTON, S. D. 2001. Antisense-induced exon skipping and synthesis of dystrophin in the mdx mouse. *Proceedings of the National Academy of Sciences,* 98**,** 42-47.

MANN, C. J., PERDIGUERO, E., KHARRAZ, Y., AGUILAR, S., PESSINA, P., SERRANO, A. L. & MUÑOZ-CÁNOVES, P. 2011. Aberrant repair and fibrosis development in skeletal muscle. *Skeletal muscle,* 1**,** 21.

MANNO, C. S., PIERCE, G. F., ARRUDA, V. R., GLADER, B., RAGNI, M., RASKO, J. J., OZELO, M. C., HOOTS, K., BLATT, P. & KONKLE, B. 2006. Successful transduction of liver in hemophilia by AAV-Factor IX and limitations imposed by the host immune response. *Nature medicine,* 12**,** 342.

MARTINI, F. 2007. *Anatomy and Physiology'2007 Ed*, Rex Bookstore, Inc.

MASAT, E., PAVANI, G. & MINGOZZI, F. 2013. Humoral immunity to AAV vectors in gene therapy: challenges and potential solutions. *Discov Med,* 15**,** 379-89.

MASON, S. D., RUNDQVIST, H., PAPANDREOU, I., DUH, R., MCNULTY, W. J., HOWLETT, R. A., OLFERT, I. M., SUNDBERG, C. J., DENKO, N. C., POELLINGER, L. & JOHNSON, R. S. 2007. HIF-1alpha in endurance

training: suppression of oxidative metabolism. *Am J Physiol Regul Integr Comp Physiol,* 293**,** R2059-69.

MATSAKAS, A., OTTO, A., ELASHRY, M. I., BROWN, S. C. & PATEL, K. 2010. Altered primary and secondary myogenesis in the myostatin-null mouse. *Rejuvenation Res,* 13**,** 717-27.

MATSAKAS, A. & PATEL, K. 2009. Skeletal muscle fibre plasticity in response to selected environmental and physiological stimuli. *Histol Histopathol,* 24**,** 611-29.

MATSAKAS, A., YADAV, V., LORCA, S., EVANS, R. M. & NARKAR, V. A. 2012. Revascularization of ischemic skeletal muscle by estrogen-related receptor-γ. *Circulation research,* 110**,** 1087-1096.

MATSAKAS, A., YADAV, V., LORCA, S. & NARKAR, V. 2013. Muscle ERRγ mitigates Duchenne muscular dystrophy via metabolic and angiogenic reprogramming. *The FASEB Journal,* 27**,** 4004-4016.

MAURO, V. P. & CHAPPELL, S. A. 2014. A critical analysis of codon optimization in human therapeutics. *Trends in molecular medicine,* 20**,** 604-613.

MAXWELL, L. C., WHITE, T. P. & FAULKNER, J. A. 1980. Oxidative capacity, blood flow, and capillarity of skeletal muscles. *J Appl Physiol Respir Environ Exerc Physiol,* 49**,** 627-33.

MCGEACHIE, J. K., GROUNDS, M. D., PARTRIDGE, T. A. & MORGAN, J. E. 1993. Age-related changes in replication of myogenic cells in mdx mice: quantitative autoradiographic studies. *J Neurol Sci,* 119**,** 169-79.

MCGREEVY, J. W., HAKIM, C. H., MCINTOSH, M. A. & DUAN, D. 2015. Animal models of Duchenne muscular dystrophy: from basic mechanisms to gene therapy. *Dis Model Mech,* 8**,** 195-213.

MCINTOSH, J., COCHRANE, M., COBBOLD, S., WALDMANN, H., NATHWANI, S., DAVIDOFF, A. & NATHWANI, A. C. 2012. Successful attenuation of humoral immunity to viral capsid and transgenic protein following AAV-mediated gene transfer with a non-depleting CD4 antibody and cyclosporine. *Gene therapy,* 19**,** 78.

MCMAHON, J., SIGNORI, E., WELLS, K., FAZIO, V. & WELLS, D. 2001. Optimisation of electrotransfer of plasmid into skeletal muscle by pretreatment with hyaluronidase--increased expression with reduced muscle damage. *Gene therapy,* 8**,** 1264-1270.

MCPHERRON, A. C., LAWLER, A. M. & LEE, S. J. 1997. Regulation of skeletal muscle mass in mice by a new TGF-beta superfamily member. *Nature,* 387**,** 83-90.

MENDELL, J. R., RODINO-KLAPAC, L., SAHENK, Z., MALIK, V., KASPAR, B. K., WALKER, C. M. & CLARK, K. R. 2012. Gene therapy for muscular dystrophy: lessons learned and path forward. *Neuroscience letters,* 527**,** 90-99.

MENDELL, J. R., RODINO-KLAPAC, L. R., SAHENK, Z., ROUSH, K., BIRD, L., LOWES, L. P., ALFANO, L., GOMEZ, A. M., LEWIS, S., KOTA, J., MALIK, V., SHONTZ, K., WALKER, C. M., FLANIGAN, K. M., CORRIDORE, M., KEAN, J. R., ALLEN, H. D., SHILLING, C., MELIA, K. R., SAZANI, P., SAOUD, J. B. & KAYE, E. M. 2013. Eteplirsen for the treatment of Duchenne muscular dystrophy. *Ann Neurol,* 74**,** 637-47.

MERTEN, O., GENY-FIAMMA, C. & DOUAR, A. 2005. Current issues in adeno-associated viral vector production. *Gene therapy,* 12**,** S51-S61.

MESSINA, S., ALTAVILLA, D., AGUENNOUZ, M. H., SEMINARA, P., MINUTOLI, L., MONICI, M. C., BITTO, A., MAZZEO, A., MARINI, H. & SQUADRITO, F. 2006. Lipid peroxidation inhibition blunts nuclear factor-κB activation, reduces skeletal muscle degeneration, and enhances muscle function in mdx mice. *The American journal of pathology,* 168**,** 918-926.

MESSINA, S., MAZZEO, A., BITTO, A., AGUENNOUZ, M. H., MIGLIORATO, A., DE PASQUALE, M. G., MINUTOLI, L., ALTAVILLA, D., ZENTILIN, L. & GIACCA, M. 2007. VEGF overexpression via adeno-associated virus gene transfer promotes skeletal muscle regeneration and enhances muscle function in mdx mice. *The FASEB journal,* 21**,** 3737-3746.

MINGOZZI, F. & HIGH, K. A. 2013. Immune responses to AAV vectors: overcoming barriers to successful gene therapy. *Blood,* 122**,** 23-36.

MISAWA, A. & INOUE, S. 2015. Estrogen-Related Receptors in Breast Cancer and Prostate Cancer. *Frontiers in Endocrinology,* 6**,** 83.

MISRA, J., KIM, D.-K. & CHOI, H.-S. 2017. ERRγ: a Junior Orphan with a Senior Role in Metabolism. *Trends in Endocrinology & Metabolism,* 28**,** 261-272.

MOKHTARIAN, A., DECROUY, A., CHINET, A. & EVEN, P. 1996. Components of energy expenditure in themdx mouse model of Duchenne muscular dystrophy. *Pflügers Archiv,* 431**,** 527-532.

MOKHTARIAN, A., LEFAUCHEUR, J. P., EVEN, P. C. & SEBILLE, A. 1995. Effects of treadmill exercise and high-fat feeding on muscle degeneration in mdx mice at the time of weaning. *Clinical Science,* 89**,** 447-452.

MORGAN, J. E. & ZAMMIT, P. S. 2010. Direct effects of the pathogenic mutation on satellite cell function in muscular dystrophy. *Experimental Cell Research,* 316**,** 3100-3108.

MORGAN, M. J. & LIU, Z. G. 2011. Crosstalk of reactive oxygen species and NF-kappaB signaling. *Cell Res,* 21**,** 103-15.

MORRISON, J., LU, Q. L., PASTORET, C., PARTRIDGE, T. & BOU-GHARIOS, G. 2000. T-cell-dependent fibrosis in the mdx dystrophic mouse. *Lab Invest,* 80**,** 881-91.

MOSHER, D. S., QUIGNON, P., BUSTAMANTE, C. D., SUTTER, N. B., MELLERSH, C. S., PARKER, H. G. & OSTRANDER, E. A. 2007. A mutation in the myostatin gene increases muscle mass and enhances racing performance in heterozygote dogs. *PLoS genetics,* 3**,** e79.

MOULAY, G., OHTANI, T., OGUT, O., GUENZEL, A., BEHFAR, A., ZAKERI, R., HAINES, P., STORLIE, J., BOWEN, L. & PHAM, L. 2015. Cardiac AAV9 gene delivery strategies in adult canines: assessment by long-term serial SPECT imaging of sodium iodide symporter expression. *Molecular Therapy,* 23**,** 1211-1221.

MULLER, A., CADENAS, E., GRAF, P. & SIES, H. 1984. A novel biologically active seleno-organic compound--I. Glutathione peroxidase-like activity in vitro and antioxidant capacity of PZ 51 (Ebselen). *Biochem Pharmacol,* 33**,** 3235-9.

MUNTONI, F., MATEDDU, A., MARCHEI, F., CLERK, A. & SERRA, G. 1993. Muscular weakness in the mdx mouse. *J Neurol Sci,* 120**,** 71-7.

MURRAY, J., AUWERX, J. & HUSS, J. M. 2013. Impaired myogenesis in estrogen-related receptor γ (ERRγ)-deficient skeletal myocytes due to oxidative stress. *The FASEB Journal,* 27**,** 135-150.

NAGATA, D., MOGI, M. & WALSH, K. 2003. AMP-activated protein kinase (AMPK) signaling in endothelial cells is essential for angiogenesis in response to hypoxic stress. *Journal of Biological Chemistry,* 278**,** 31000-31006.

NAGATA, T., UCHIJIMA, M., YOSHIDA, A., KAWASHIMA, M. & KOIDE, Y. 1999. Codon optimization effect on translational efficiency of DNA vaccine in mammalian cells: analysis of plasmid DNA encoding a CTL epitope derived from microorganisms. *Biochemical and biophysical research communications,* 261**,** 445-451.

NAKAHARA, H., SONG, J., SUGIMOTO, M., HAGIHARA, K., KISHIMOTO, T., YOSHIZAKI, K. & NISHIMOTO, N. 2003. Anti-interleukin-6 receptor antibody therapy reduces vascular endothelial growth factor production in rheumatoid arthritis. *Arthritis Rheum,* 48**,** 1521-9.

NAKAI, H., FUESS, S., STORM, T. A., MURAMATSU, S.-I., NARA, Y. & KAY, M. A. 2005. Unrestricted Hepatocyte Transduction with Adeno-Associated Virus Serotype 8 Vectors in Mice. *Journal of Virology,* 79**,** 214-224.

NAKAMURA, A. 2015. X-Linked Dilated Cardiomyopathy: A Cardiospecific Phenotype of Dystrophinopathy. *Pharmaceuticals (Basel),* 8**,** 303-20.

NAKAMURA, A. 2017. Moving towards successful exon-skipping therapy for Duchenne muscular dystrophy. *J Hum Genet,* 62**,** 871-876.

NARKAR, V. A., FAN, W., DOWNES, M., RUTH, T. Y., JONKER, J. W., ALAYNICK, W. A., BANAYO, E., KARUNASIRI, M. S., LORCA, S. & EVANS, R. M. 2011. Exercise and PGC-1α-independent synchronization of type l muscle metabolism and vasculature by ERRγ. *Cell metabolism,* 13**,** 283-293.

NASO, M. F., TOMKOWICZ, B., PERRY, W. L. & STROHL, W. R. 2017. Adeno-Associated Virus (AAV) as a Vector for Gene Therapy. *Biodrugs,* 31**,** 317-334.

NATHWANI, A. C., REISS, U. M., TUDDENHAM, E. G., ROSALES, C., CHOWDARY, P., MCINTOSH, J., DELLA PERUTA, M., LHERITEAU, E., PATEL, N. & RAJ, D. 2014. Long-term safety and efficacy of factor IX gene therapy in hemophilia B. *New England Journal of Medicine,* 371**,** 1994-2004.

NATHWANI, A. C., TUDDENHAM, E. G., RANGARAJAN, S., ROSALES, C., MCINTOSH, J., LINCH, D. C., CHOWDARY, P., RIDDELL, A., PIE, A. J. & HARRINGTON, C. 2011. Adenovirus-associated virus vector–mediated gene transfer in hemophilia B. *New England Journal of Medicine,* 365**,** 2357-2365.

NAYAK, S. & HERZOG, R. W. 2010. Progress and prospects: immune responses to viral vectors. *Gene therapy,* 17**,** 295.

NGUYEN, K.-L., LLANO, M., AKARI, H., MIYAGI, E., POESCHLA, E. M., STREBEL, K. & BOUR, S. 2004. Codon optimization of the HIV-1 vpu and vif genes stabilizes their mRNA and allows for highly efficient Rev-independent expression. *Virology,* 319**,** 163-175.

NIETUPSKI, J. B., HURLBUT, G. D., ZIEGLER, R. J., CHU, Q., HODGES, B. L., ASHE, K. M., BREE, M., CHENG, S. H., GREGORY, R. J., MARSHALL, J. & SCHEULE, R. K. 2011. Systemic administration of AAV8-alpha-galactosidase A induces humoral tolerance in nonhuman primates despite low hepatic expression. *Mol Ther,* 19**,** 1999-2011.

NOVOA, E. M. & DE POUPLANA, L. R. 2012. Speeding with control: codon usage, tRNAs, and ribosomes. *Trends in Genetics,* 28**,** 574-581.

NOVOA, I., ZENG, H., HARDING, H. P. & RON, D. 2001. Feedback inhibition of the unfolded protein response by GADD34-mediated dephosphorylation of eIF2alpha. *J Cell Biol,* 153**,** 1011-22.

OJUKA, E. O., JONES, T. E., HAN, D. H., CHEN, M. & HOLLOSZY, J. O. 2003. Raising Ca2+ in L6 myotubes mimics effects of exercise on mitochondrial biogenesis in muscle. *Faseb j,* 17**,** 675-81.

OLESEN, J., LARSSON, S., IVERSEN, N., YOUSAFZAI, S., HELLSTEN, Y. & PILEGAARD, H. 2012. Skeletal muscle PGC-1α is required for maintaining an acute LPS-induced TNFα response. *PloS one,* 7**,** e32222.

OLFERT, I. M., HOWLETT, R. A., TANG, K., DALTON, N. D., GU, Y., PETERSON, K. L., WAGNER, P. D. & BREEN, E. C. 2009. Muscle-specific VEGF deficiency greatly reduces exercise endurance in mice. *J Physiol,* 587**,** 1755-67.

OLICHON-BERTHE, C., GAUTIER, N., VAN OBBERGHEN, E. & LE MARCHAND-BRUSTEL, Y. 1993. Expression of the glucose transporter GLUT4 in the muscular dystrophic mdx mouse. *Biochemical Journal,* 291**,** 257-261.

ONISHI, A., PENG, G. H., POTH, E. M., LEE, D. A., CHEN, J., ALEXIS, U., DE MELO, J., CHEN, S. & BLACKSHAW, S. 2010. The orphan nuclear hormone receptor ERRbeta controls rod photoreceptor survival. *Proc Natl Acad Sci U S A,* 107**,** 11579-84.

ONOPIUK, M., BRUTKOWSKI, W., WIERZBICKA, K., WOJCIECHOWSKA, S., SZCZEPANOWSKA, J., FRONK, J., LOCHMÜLLER, H., GÓRECKI, D. C. & ZABŁOCKI, K. 2009. Mutation in dystrophin-encoding gene affects energy metabolism in mouse myoblasts. *Biochemical and biophysical research communications,* 386**,** 463-466.

ONWUAMAEGBU, M., HENEIN, M. & COATS, A. 2004. Cachexia in malaria and heart failure: therapeutic considerations in clinical practice. *Postgraduate medical journal,* 80**,** 642-649.

OUCHI, N., SHIBATA, R. & WALSH, K. 2005. AMP-activated protein kinase signaling stimulates VEGF expression and angiogenesis in skeletal muscle. *Circ Res,* 96**,** 838-46.

PAEPE, B. D., CREUS, K. K., WEIS, J. & BLEECKER, J. L. 2012. Heat shock protein families 70 and 90 in Duchenne muscular dystrophy and inflammatory myopathy: balancing muscle protection and destruction. *Neuromuscul Disord,* 22**,** 26-33.

PALLADINO, M., GATTO, I., NERI, V., STRAINO, S., SMITH, R. C., SILVER, M., GAETANI, E., MARCANTONI, M., GIARRETTA, I., STIGLIANO, E., CAPOGROSSI, M., HLATKY, L., LANDOLFI, R. & POLA, R. 2013. Angiogenic impairment of the vascular endothelium: a novel mechanism and potential therapeutic target in muscular dystrophy. *Arterioscler Thromb Vasc Biol,* 33**,** 2867-76.

PALMER, R. M., FERRIGE, A. G. & MONCADA, S. 1987. Nitric oxide release accounts for the biological activity of endothelium-derived relaxing factor. *Nature,* 327**,** 524-6.

PARDO, J. V., SILICIANO, J. D. & CRAIG, S. W. 1983. A vinculin-containing cortical lattice in skeletal muscle: transverse lattice elements

("costameres") mark sites of attachment between myofibrils and sarcolemma. *Proc Natl Acad Sci U S A,* 80**,** 1008-12.

PARK, D., JEONG, H., LEE, M. N., KOH, A., KWON, O., YANG, Y. R., NOH, J., SUH, P. G., PARK, H. & RYU, S. H. 2016. Resveratrol induces autophagy by directly inhibiting mTOR through ATP competition. *Sci Rep,* 6**,** 21772.

PASIAKOS, S. M., MCCLUNG, H. L., MCCLUNG, J. P., URSO, M. L., PIKOSKY, M. A., CLOUTIER, G. J., FIELDING, R. A. & YOUNG, A. J. 2010. Molecular responses to moderate endurance exercise in skeletal muscle. *Int J Sport Nutr Exerc Metab,* 20**,** 282-90.

PAULY, M., DAUSSIN, F., BURELLE, Y., LI, T., GODIN, R., FAUCONNIER, J., KOECHLIN-RAMONATXO, C., HUGON, G., LACAMPAGNE, A., COISY-QUIVY, M., LIANG, F., HUSSAIN, S., MATECKI, S. & PETROF, B. J. 2012. AMPK activation stimulates autophagy and ameliorates muscular dystrophy in the mdx mouse diaphragm. *Am J Pathol,* 181**,** 583-92.

PEAREN, M. A. & MUSCAT, G. E. 2012. Orphan nuclear receptors and the regulation of nutrient metabolism: understanding obesity. *Physiology (Bethesda),* 27**,** 156-66.

PECCATE, C., MOLLARD, A., LE HIR, M., JULIEN, L., MCCLOREY, G., JARMIN, S., LE HERON, A., DICKSON, G., BENKHELIFA-ZIYYAT, S., PIETRI-ROUXEL, F., WOOD, M. J., VOIT, T. & LORAIN, S. 2016. Antisense pre-treatment increases gene therapy efficacy in dystrophic muscles. *Hum Mol Genet,* 25**,** 3555-3563.

PEDEMONTE, M., SANDRI, C., SCHIAFFINO, S. & MINETTI, C. 1999. Early decrease of IIx myosin heavy chain transcripts in Duchenne muscular dystrophy. *Biochemical and biophysical research communications,* 255**,** 466-469.

PEDERSEN, B. K. 2007. IL-6 signalling in exercise and disease. *Biochemical Society Transactions,* 35**,** 1295-1297.

PELOSI, L., BERARDINELLI, M. G., FORCINA, L., SPELTA, E., RIZZUTO, E., NICOLETTI, C., CAMILLI, C., TESTA, E., CATIZONE, A., DE BENEDETTI, F. & MUSARO, A. 2015. Increased levels of interleukin-6 exacerbate the dystrophic phenotype in mdx mice. *Hum Mol Genet,* 24**,** 6041-53.

PENDRAK, K., SELSBY, J. T., MORINE, K. J., BARTON, E. R. & SWEENEY, H. 2012. Rescue of Dystrophic Skeletal Muscle by PGC-1a Involves a Fast to Slow Fiber Type Shift in the mdx Mouse. *Figshare,* 1.

PERCIVAL, J. M., ANDERSON, K. N., HUANG, P., ADAMS, M. E. & FROEHNER, S. C. 2010. Golgi and sarcolemmal neuronal NOS differentially regulate contraction-induced fatigue and vasoconstriction in exercising mouse skeletal muscle. *The Journal of clinical investigation,* 120**,** 816-826.

PERCIVAL, J. M., SIEGEL, M. P., KNOWELS, G. & MARCINEK, D. J. 2013. Defects in mitochondrial localization and ATP synthesis in the mdx mouse model of Duchenne muscular dystrophy are not alleviated by PDE5 inhibition. *Human Molecular Genetics,* 22**,** 153-167.

PERCIVAL, J. M., WHITEHEAD, N. P., ADAMS, M. E., ADAMO, C. M., BEAVO, J. A. & FROEHNER, S. C. 2012. Sildenafil reduces respiratory muscle weakness and fibrosis in the mdx mouse model of Duchenne muscular dystrophy. *J Pathol,* 228**,** 77-87.

PEREZ-ZOGHBI, J. F., KARNER, C., ITO, S., SHEPHERD, M., ALRASHDAN, Y. A. & SANDERSON, M. J. 2009. Ion channel regulation of intracellular calcium and airway smooth muscle function. *Pulmonary pharmacology & therapeutics,* 22**,** 388-397.

PETER, A. K. & CROSBIE, R. H. 2006. Hypertrophic response of Duchenne and limb-girdle muscular dystrophies is associated with activation of Akt pathway. *Exp Cell Res,* 312**,** 2580-91.

PETRILLO, S., PELOSI, L., PIEMONTE, F., TRAVAGLINI, L., FORCINA, L., CATTERUCCIA, M., PETRINI, S., VERARDO, M., D'AMICO, A., MUSARO, A. & BERTINI, E. 2017. Oxidative stress in Duchenne muscular dystrophy: focus on the NRF2 redox pathway. *Hum Mol Genet,* 26**,** 2781-2790.

PETROF, B. J., SHRAGER, J. B., STEDMAN, H. H., KELLY, A. M. & SWEENEY, H. L. 1993a. Dystrophin protects the sarcolemma from stresses developed during muscle contraction. *Proceedings of the National Academy of Sciences,* 90**,** 3710-3714.

PETROF, B. J., STEDMAN, H. H., SHRAGER, J. B., EBY, J., SWEENEY, H. L. & KELLY, A. M. 1993b. Adaptations in myosin heavy chain expression and contractile function in dystrophic mouse diaphragm. *Am J Physiol,* 265**,** C834-41.

PETTE, D. & STARON, R. S. 1997. Mammalian skeletal muscle fiber type transitions. *International review of cytology,* 170**,** 143-223.

PETTE, D. & STARON, R. S. 2000. Myosin isoforms, muscle fiber types, and transitions. *Microscopy research and technique,* 50**,** 500-509.

PETTE, D. & STARON, R. S. 2001. Transitions of muscle fiber phenotypic profiles. *Histochemistry and cell biology,* 115**,** 359-372.

PHELPS, S. F., HAUSER, M. A., COLE, N. M., RAFAEL, J. A., HINKLE, R. T., FAULKNER, J. A. & CHAMBERLAIN, J. S. 1995. Expression of full-length and truncated dystrophin mini-genes in transgenic mdx mice. *Human molecular genetics,* 4**,** 1251-1258.

PHIELIX, E. & MENSINK, M. 2008. Type 2 diabetes mellitus and skeletal muscle metabolic function. *Physiol Behav,* 94**,** 252-8.

PICHAVANT, C., AARTSMA-RUS, A., CLEMENS, P. R., DAVIES, K. E., DICKSON, G., TAKEDA, S. I., WILTON, S. D., WOLFF, J. A., WOODDELL, C. I. & XIAO, X. 2011. Current status of pharmaceutical and genetic therapeutic approaches to treat DMD. *Molecular Therapy,* 19**,** 830-840.

POTTHOFF, M. J., WU, H., ARNOLD, M. A., SHELTON, J. M., BACKS, J., MCANALLY, J., RICHARDSON, J. A., BASSEL-DUBY, R. & OLSON, E. N. 2007. Histone deacetylase degradation and MEF2 activation promote the formation of slow-twitch myofibers. *J Clin Invest,* 117**,** 2459-67.

POWELL-BRAXTON, L., HOLLINGSHEAD, P., WARBURTON, C., DOWD, M., PITTS-MEEK, S., DALTON, D., GILLETT, N. & STEWART, T. A. 1993. IGF-I is required for normal embryonic growth in mice. *Genes Dev,* 7**,** 2609-17.

POZSGAI, E. R., GRIFFIN, D. A., HELLER, K. N., MENDELL, J. R. & RODINO-KLAPAC, L. R. 2017. Systemic AAV-Mediated beta-Sarcoglycan Delivery Targeting Cardiac and Skeletal Muscle Ameliorates Histological and Functional Deficits in LGMD2E Mice. *Mol Ther,* 25**,** 855-869.

PRIOR, B. M., YANG, H. T. & TERJUNG, R. L. 2004. What makes vessels grow with exercise training? *J Appl Physiol (1985),* 97**,** 1119-28.

PUIGSERVER, P. & SPIEGELMAN, B. M. 2003. Peroxisome proliferator-activated receptor-γ coactivator 1α (PGC-1α): transcriptional coactivator and metabolic regulator. *Endocrine reviews,* 24**,** 78-90.

PUIGSERVER, P., WU, Z., PARK, C. W., GRAVES, R., WRIGHT, M. & SPIEGELMAN, B. M. 1998. A cold-inducible coactivator of nuclear receptors linked to adaptive thermogenesis. *Cell,* 92**,** 829-839.

QIAO, C., YUAN, Z., LI, J., HE, B., ZHENG, H., MAYER, C., LI, J. & XIAO, X. 2011. Liver-specific microRNA-122 target sequences incorporated in AAV vectors efficiently inhibits transgene expression in the liver. *Gene Ther,* 18**,** 403-10.

QUINLAN, J. G., HAHN, H. S., WONG, B. L., LORENZ, J. N., WENISCH, A. S. & LEVIN, L. S. 2004. Evolution of the mdx mouse cardiomyopathy: physiological and morphological findings. *Neuromuscular Disorders,* 14**,** 491-496.

QUINLAN, J. G., JOHNSON, S. R., MCKEE, M. K. & LYDEN, S. P. 1992. Twitch and tetanus in mdx mouse muscle. *Muscle Nerve,* 15**,** 837-42.

RADCLIFFE, P. A., SION, C. J., WILKES, F. J., CUSTARD, E. J., BEARD, G. L., KINGSMAN, S. M. & MITROPHANOUS, K. A. 2008. Analysis of factor VIII mediated suppression of lentiviral vector titres. *Gene Ther,* 15**,** 289-97.

RADLEY, H. G., DAVIES, M. J. & GROUNDS, M. D. 2008. Reduced muscle necrosis and long-term benefits in dystrophic mdx mice after cV1q (blockade of TNF) treatment. *Neuromuscul Disord,* 18**,** 227-38.

RADLEY, H. G. & GROUNDS, M. D. 2006. Cromolyn administration (to block mast cell degranulation) reduces necrosis of dystrophic muscle in mdx mice. *Neurobiol Dis,* 23**,** 387-97.

RAFAEL, J. A., SUNADA, Y., COLE, N. M., CAMPBELL, K. P., FAULKNER, J. A. & CHAMBERLAIN, J. S. 1994. Prevention of dystrophic pathology in mdx mice by a truncated dystrophin isoform. *Hum Mol Genet,* 3**,** 1725-33.

RAFAEL, J. A., TINSLEY, J. M., POTTER, A. C., DECONINCK, A. E. & DAVIES, K. E. 1998. Skeletal muscle-specific expression of a utrophin transgene rescues utrophin-dystrophin deficient mice. *Nature genetics,* 19**,** 79-82.

RAMASWAMY, K. S., PALMER, M. L., VAN DER MEULEN, J. H., RENOUX, A., KOSTROMINOVA, T. Y., MICHELE, D. E. & FAULKNER, J. A. 2011. Lateral transmission of force is impaired in skeletal muscles of dystrophic mice and very old rats. *The Journal of Physiology,* 589**,** 1195-1208.

RANDO, T. A. 2007. Non-viral gene therapy for Duchenne muscular dystrophy: progress and challenges. *Biochimica et Biophysica Acta (BBA)-Molecular Basis of Disease,* 1772**,** 263-271.

RANGWALA, S. M., WANG, X., CALVO, J. A., LINDSLEY, L., ZHANG, Y., DEYNEKO, G., BEAULIEU, V., GAO, J., TURNER, G. & MARKOVITS, J. 2010. Estrogen-related receptor γ is a key regulator of muscle mitochondrial activity and oxidative capacity. *Journal of Biological Chemistry,* 285**,** 22619-22629.

REBOLLEDO, D. L., KIM, M. J., WHITEHEAD, N. P., ADAMS, M. E. & FROEHNER, S. C. 2016. Sarcolemmal targeting of nNOSmu improves contractile function of mdx muscle. *Hum Mol Genet,* 25**,** 158-66.

REILLY, S. M. & LEE, C.-H. 2008. PPARδ as a therapeutic target in metabolic disease. *FEBS Letters,* 582**,** 26-31.

REMELS, A. H., GOSKER, H. R., BAKKER, J., GUTTRIDGE, D. C., SCHOLS, A. M. & LANGEN, R. C. 2013. Regulation of skeletal muscle oxidative phenotype by classical NF-kappaB signalling. *Biochim Biophys Acta,* 1832**,** 1313-25.

REMELS, A. H., GOSKER, H. R., SCHRAUWEN, P., HOMMELBERG, P. P., SLIWINSKI, P., POLKEY, M., GALDIZ, J., WOUTERS, E. F., LANGEN, R. C. & SCHOLS, A. M. 2010. TNF-alpha impairs regulation of muscle oxidative phenotype: implications for cachexia? *Faseb j,* 24**,** 5052-62.

RENJINI, R., GAYATHRI, N., NALINI, A. & SRINIVAS BHARATH, M. M. 2012. Oxidative damage in muscular dystrophy correlates with the severity of the pathology: role of glutathione metabolism. *Neurochem Res,* 37**,** 885-98.

REZVANI, M., CAFARELLI, E. & HOOD, D. A. 1995. Performance and excitability of mdx mouse muscle at 2, 5, and 13 wk of age. *J Appl Physiol (1985),* 78**,** 961-7.

RHOADS, R. P., FLANN, K. L., CARDINAL, T. R., RATHBONE, C. R., LIU, X. & ALLEN, R. E. 2013. Satellite cells isolated from aged or dystrophic muscle exhibit a reduced capacity to promote angiogenesis in vitro. *Biochem Biophys Res Commun,* 440**,** 399-404.

ROBERTS, T. C., JOHANSSON, H. J., MCCLOREY, G., GODFREY, C., BLOMBERG, K. E. M., COURSINDEL, T., GAIT, M. J., SMITH, C. E., LEHTIÖ, J. & EL ANDALOUSSI, S. 2015. Multi-level omics analysis in a murine model of dystrophin loss and therapeutic restoration. *Human molecular genetics,* 24**,** 6756-6768.

ROBIN, G., BERTHIER, C. & ALLARD, B. 2012. Sarcoplasmic reticulum Ca(2+) permeation explored from the lumen side in mdx muscle fibers under voltage control. *The Journal of General Physiology,* 139**,** 209-218.

ROCKL, K. S., HIRSHMAN, M. F., BRANDAUER, J., FUJII, N., WITTERS, L. A. & GOODYEAR, L. J. 2007. Skeletal muscle adaptation to exercise training: AMP-activated protein kinase mediates muscle fiber type shift. *Diabetes,* 56**,** 2062-9.

RODINO-KLAPAC, L. R., CHICOINE, L. G., KASPAR, B. K. & MENDELL, J. R. 2007. Gene therapy for duchenne muscular dystrophy: expectations and challenges. *Archives of neurology,* 64**,** 1236-1241.

RODINO-KLAPAC, L. R., MENDELL, J. R. & SAHENK, Z. 2013. Update on the treatment of Duchenne muscular dystrophy. *Current neurology and neuroscience reports,* 13**,** 332.

ROMANICK, M., THOMPSON, L. V. & BROWN-BORG, H. M. 2013. Murine models of atrophy, cachexia, and sarcopenia in skeletal muscle. *Biochim Biophys Acta,* 1832**,** 1410-20.

ROMERO, N. B., BRAUN, S., BENVENISTE, O., LETURCQ, F., HOGREL, J.-Y., MORRIS, G. E., BAROIS, A., EYMARD, B., PAYAN, C. & ORTEGA, V. 2004. Phase I study of dystrophin plasmid-based gene therapy in Duchenne/Becker muscular dystrophy. *Human gene therapy,* 15**,** 1065-1076.

ROSE, J. A., HOGGAN, M. D. & SHATKIN, A. J. 1966. Nucleic acid from an adeno-associated virus: chemical and physical studies. *Proc Natl Acad Sci U S A,* 56**,** 86-92.

ROUSLIN, W. 1983. Mitochondrial complexes I, II, III, IV, and V in myocardial ischemia and autolysis. *American Journal of Physiology-Heart and Circulatory Physiology,* 244**,** H743-H748.

RUSSELL, B., MOTLAGH, D. & ASHLEY, W. W. 2000. Form follows function: how muscle shape is regulated by work. *Journal of applied physiology,* 88**,** 1127-1132.

RYBAKOVA, I. N., PATEL, J. R. & ERVASTI, J. M. 2000. The dystrophin complex forms a mechanically strong link between the sarcolemma and costameric actin. *J Cell Biol,* 150**,** 1209-14.

RYBALKA, E., TIMPANI, C. A., COOKE, M. B., WILLIAMS, A. D. & HAYES, A. 2014. Defects in mitochondrial ATP synthesis in dystrophin-deficient mdx skeletal muscles may be caused by complex I insufficiency. *PloS one,* 9**,** e115763.

RYBALKA, E., TIMPANI, C. A., STATHIS, C. G., HAYES, A. & COOKE, M. B. 2015. Metabogenic and Nutriceutical Approaches to Address Energy Dysregulation and Skeletal Muscle Wasting in Duchenne Muscular Dystrophy. *Nutrients,* 7**,** 9734-9767.

RYU, D., ZHANG, H., ROPELLE, E. R., SORRENTINO, V., MÁZALA, D. A., MOUCHIROUD, L., MARSHALL, P. L., CAMPBELL, M. D., ALI, A. S. & KNOWELS, G. M. 2016. NAD+ repletion improves muscle function in muscular dystrophy and counters global PARylation. *Science translational medicine,* 8**,** 361ra139-361ra139.

SAKOWSKI, S. A., SCHUYLER, A. D. & FELDMAN, E. L. 2009. Insulin-like growth factor-I for the treatment of amyotrophic lateral sclerosis. *Amyotrophic lateral sclerosis : official publication of the World Federation of Neurology Research Group on Motor Neuron Diseases,* 10**,** 63-73.

SAKUMA, K. & YAMAGUCHI, A. 2012. Sarcopenia and cachexia: the adaptations of negative regulators of skeletal muscle mass. *Journal of cachexia, sarcopenia and muscle,* 3**,** 77-94.

SALADIN, K. S. & MILLER, L. 1998. *Anatomy & physiology*, WCB/McGraw-Hill New York (NY).

SALIMENA, M. C., LAGROTA-CANDIDO, J. & QUIRICO-SANTOS, T. 2004. Gender dimorphism influences extracellular matrix expression and regeneration of muscular tissue in mdx dystrophic mice. *Histochem Cell Biol,* 122**,** 435-44.

SANDER, M., CHAVOSHAN, B., HARRIS, S. A., IANNACCONE, S. T., STULL, J. T., THOMAS, G. D. & VICTOR, R. G. 2000. Functional muscle ischemia in neuronal nitric oxide synthase-deficient skeletal muscle of children with Duchenne muscular dystrophy. *Proc Natl Acad Sci U S A,* 97**,** 13818-23.

SANDRI, M., COLETTO, L., GRUMATI, P. & BONALDO, P. 2013. Misregulation of autophagy and protein degradation systems in myopathies and muscular dystrophies. *J Cell Sci,* 126**,** 5325-33.

SANDRI, M., SANDRI, C., GILBERT, A., SKURK, C., CALABRIA, E., PICARD, A., WALSH, K., SCHIAFFINO, S., LECKER, S. H. & GOLDBERG, A. L. 2004. Foxo Transcription Factors Induce the Atrophy-Related Ubiquitin Ligase Atrogin-1 and Cause Skeletal Muscle Atrophy. *Cell,* 117**,** 399-412.

SCARPULLA, R. C. 2008. Transcriptional paradigms in mammalian mitochondrial biogenesis and function. *Physiol Rev,* 88**,** 611-38.

SCARPULLA, R. C., VEGA, R. B. & KELLY, D. P. 2012. Transcriptional integration of mitochondrial biogenesis. *Trends Endocrinol Metab,* 23**,** 459-66.

SCHELLER, J., CHALARIS, A., SCHMIDT-ARRAS, D. & ROSE-JOHN, S. 2011. The pro- and anti-inflammatory properties of the cytokine interleukin-6. *Biochim Biophys Acta,* 1813**,** 878-88.

SCHIAFFINO, S. & REGGIANI, C. 2011. Fiber types in mammalian skeletal muscles. *Physiol Rev,* 91**,** 1447-531.

SCHNEIDER, S. M., SRIDHAR, V., BETTIS, A. K., HEATH-BARNETT, H., BALOG-ALVAREZ, C. J., GUO, L. J., JOHNSON, R., JAQUES, S., VITHA, S., GLOWCWSKI, A. C., KORNEGAY, J. N. & NGHIEM, P. P. 2018. Glucose Metabolism as a Pre-clinical Biomarker for the Golden Retriever Model of Duchenne Muscular Dystrophy. *Mol Imaging Biol,* 20**,** 780-788.

SCHOLTE, H. R. & BUSCH, H. F. 1980. Early changes of muscle mitochondria in Duchenne dystrophy. Partition and activity of mitochondrial enzymes in fractionated muscle of unaffected boys and adults and patients. *J Neurol Sci,* 45**,** 217-34.

SCHULER, M., ALI, F., CHAMBON, C., DUTEIL, D., BORNERT, J.-M., TARDIVEL, A., DESVERGNE, B., WAHLI, W., CHAMBON, P. & METZGER, D. 2006. PGC1α expression is controlled in skeletal muscles by PPARβ, whose ablation results in fiber-type switching, obesity, and type 2 diabetes. *Cell metabolism,* 4**,** 407-414.

SCHWANHAUSSER, B., BUSSE, D., LI, N., DITTMAR, G., SCHUCHHARDT, J., WOLF, J., CHEN, W. & SELBACH, M. 2011. Global quantification of mammalian gene expression control. *Nature,* 473**,** 337-42.

SCOTT, W., STEVENS, J. & BINDER–MACLEOD, S. A. 2001. Human skeletal muscle fiber type classifications. *Physical therapy,* 81**,** 1810-1816.

SCULLY, M. A., PANDYA, S. & MOXLEY, R. T. 2013. Review of Phase II and Phase III clinical trials for Duchenne muscular dystrophy. *Expert Opinion on Orphan Drugs,* 1**,** 33-46.

SELSBY, J. T., BALLMANN, C. G., SPAULDING, H. R., ROSS, J. W. & QUINDRY, J. C. 2016. Oral quercetin administration transiently protects respiratory function in dystrophin-deficient mice. *The Journal of Physiology,* 594**,** 6037-6053.

SELSBY, J. T., MORINE, K. J., PENDRAK, K., BARTON, E. R. & SWEENEY, H. L. 2012. Rescue of dystrophic skeletal muscle by PGC-1α involves a fast to slow fiber type shift in the mdx mouse. *PloS one,* 7**,** e30063.

SERRANO, A. L., BAEZA-RAJA, B., PERDIGUERO, E., JARDI, M. & MUNOZ-CANOVES, P. 2008. Interleukin-6 is an essential regulator of satellite cell-mediated skeletal muscle hypertrophy. *Cell Metab,* 7**,** 33-44.

SERRANO, A. L., MANN, C. J., VIDAL, B., ARDITE, E., PERDIGUERO, E. & MUNOZ-CANOVES, P. 2011. Cellular and molecular mechanisms regulating fibrosis in skeletal muscle repair and disease. *Curr Top Dev Biol,* 96**,** 167-201.

SEVER, R. & GLASS, C. K. 2013. Signaling by nuclear receptors. *Cold Spring Harbor perspectives in biology,* 5**,** a016709.

SHIN, J., TAJRISHI, M. M., OGURA, Y. & KUMAR, A. 2013. Wasting mechanisms in muscular dystrophy. *The international journal of biochemistry & cell biology,* 45**,** 2266-2279.

SHKRYL, V. M., MARTINS, A. S., ULLRICH, N. D., NOWYCKY, M. C., NIGGLI, E. & SHIROKOVA, N. 2009. Reciprocal amplification of ROS and Ca2+ signals in stressed mdx dystrophic skeletal muscle fibers. *Pflügers Archiv-European Journal of Physiology,* 458**,** 915-928.

SHWEIKI, D., ITIN, A., SOFFER, D. & KESHET, E. 1992. Vascular endothelial growth factor induced by hypoxia may mediate hypoxia-initiated angiogenesis. *Nature,* 359**,** 843.

SICINSKI, P., GENG, Y., RYDER-COOK, A. S., BARNARD, E. A., DARLISON, M. G. & BARNARD, P. J. 1989. The molecular basis of muscular dystrophy in the mdx mouse: a point mutation. *Science,* 244**,** 1578-1580.

SILVESTRE, J. S., MALLAT, Z., DURIEZ, M., TAMARAT, R., BUREAU, M. F., SCHERMAN, D., DUVERGER, N., BRANELLEC, D., TEDGUI, A. & LEVY, B. I. 2000. Antiangiogenic effect of interleukin-10 in ischemia-induced angiogenesis in mice hindlimb. *Circ Res,* 87**,** 448-52.

SMALLEY, E. 2017. First AAV gene therapy poised for landmark approval. Nat Biotechnol.

SPENCER, M. J., MARINO, M. W. & WINCKLER, W. M. 2000. Altered pathological progression of diaphragm and quadriceps muscle in TNF-deficient, dystrophin-deficient mice. *Neuromuscul Disord,* 10**,** 612-9.

SPENCER, M. J. & MELLGREN, R. L. 2002. Overexpression of a calpastatin transgene in mdx muscle reduces dystrophic pathology. *Hum Mol Genet,* 11**,** 2645-55.

SPERL, W., SKLADAL, D., GNAIGER, E., WYSS, M., MAYR, U., HAGER, J. & GELLERICH, F. N. 1997. High resolution respirometry of permeabilized skeletal muscle fibers in the diagnosis of neuromuscular disorders. *Mol Cell Biochem,* 174**,** 71-8.

SPITALI, P., GRUMATI, P., HILLER, M., CHRISAM, M., AARTSMA-RUS, A. & BONALDO, P. 2013. Autophagy is impaired in the tibialis anterior of dystrophin null mice. *PLoS currents,* 5.

SUHR, F., GEHLERT, S., GRAU, M. & BLOCH, W. 2013. Skeletal muscle function during exercise-fine-tuning of diverse subsystems by nitric oxide. *Int J Mol Sci,* 14**,** 7109-39.

SUMMERMATTER, S., THURNHEER, R., SANTOS, G., MOSCA, B., BAUM, O., TREVES, S., HOPPELER, H., ZORZATO, F. & HANDSCHIN, C. 2012. Remodeling of calcium handling in skeletal muscle through PGC-1α: impact on force, fatigability, and fiber type. *American journal of physiology-cell physiology,* 302**,** C88-C99.

TAKAGI, A., KOJIMA, S., IDA, M. & ARAKI, M. 1992. Increased leakage of calcium ion from the sarcoplasmic reticulum of the mdx mouse. *Journal of the Neurological Sciences,* 110**,** 160-164.

TAMMELA, T., ENHOLM, B., ALITALO, K. & PAAVONEN, K. 2005a. The biology of vascular endothelial growth factors. *Cardiovascular Research,* 65**,** 550-563.

TAMMELA, T., ENHOLM, B., ALITALO, K. & PAAVONEN, K. 2005b. The biology of vascular endothelial growth factors. *Cardiovasc Res,* 65**,** 550-63.

TANAKA, T., YAMAMOTO, J., IWASAKI, S., ASABA, H., HAMURA, H., IKEDA, Y., WATANABE, M., MAGOORI, K., IOKA, R. X., TACHIBANA, K., WATANABE, Y., UCHIYAMA, Y., SUMI, K., IGUCHI, H., ITO, S., DOI, T., HAMAKUBO, T., NAITO, M., AUWERX, J., YANAGISAWA, M., KODAMA, T. & SAKAI, J. 2003. Activation of peroxisome proliferator-activated

receptor delta induces fatty acid beta-oxidation in skeletal muscle and attenuates metabolic syndrome. *Proc Natl Acad Sci U S A,* 100**,** 15924-9.

TANG, W., INGALLS, C. P., DURHAM, W. J., SNIDER, J., REID, M. B., WU, G., MATZUK, M. M. & HAMILTON, S. L. 2004. Altered excitation-contraction coupling with skeletal muscle specific FKBP12 deficiency. *Faseb j,* 18**,** 1597-9.

TANG, Y., REAY, D. P., SALAY, M. N., MI, M. Y., CLEMENS, P. R., GUTTRIDGE, D. C., ROBBINS, P. D., HUARD, J. & WANG, B. 2010. Inhibition of the IKK/NF-κB Pathway by AAV Gene Transfer Improves Muscle Regeneration in Older mdx Mice. *Gene therapy,* 17**,** 1476-1483.

TENGAN, C. H., RODRIGUES, G. S. & GODINHO, R. O. 2012. Nitric Oxide in Skeletal Muscle: Role on Mitochondrial Biogenesis and Function. *International Journal of Molecular Sciences,* 13**,** 17160-17184.

THOMAS, G. D., SANDER, M., LAU, K. S., HUANG, P. L., STULL, J. T. & VICTOR, R. G. 1998. Impaired metabolic modulation of α-adrenergic vasoconstriction in dystrophin-deficient skeletal muscle. *Proceedings of the National Academy of Sciences of the United States of America,* 95**,** 15090-15095.

THOMAS, G. D., SHAUL, P. W., YUHANNA, I. S., FROEHNER, S. C. & ADAMS, M. E. 2003. Vasomodulation by skeletal muscle–derived nitric oxide requires α-syntrophin–mediated sarcolemmal localization of neuronal nitric oxide synthase. *Circulation research,* 92**,** 554-560.

TIDBALL, J. G. 2005. Inflammatory processes in muscle injury and repair. *American Journal of Physiology-Regulatory, Integrative and Comparative Physiology,* 288**,** R345-R353.

TIDBALL, J. G. & WEHLING-HENRICKS, M. 2004. Evolving therapeutic strategies for Duchenne muscular dystrophy: targeting downstream events. *Pediatr Res,* 56**,** 831-41.

TIDBALL, J. G. & WEHLING-HENRICKS, M. 2014. Nitric oxide synthase deficiency and the pathophysiology of muscular dystrophy. *The Journal of Physiology,* 592**,** 4627-4638.

TILEMANN, L., ISHIKAWA, K., WEBER, T. & HAJJAR, R. J. 2012. Gene therapy for heart failure. *Circulation research,* 110**,** 777-793.

TIMPANI, C. A., HAYES, A. & RYBALKA, E. 2015. Revisiting the dystrophin-ATP connection: How half a century of research still implicates mitochondrial dysfunction in Duchenne Muscular Dystrophy aetiology. *Medical hypotheses,* 85**,** 1021-1033.

TINSLEY, J., DECONINCK, N., FISHER, R., KAHN, D., PHELPS, S., GILLIS, J.-M. & DAVIES, K. 1998. Expression of full-length utrophin prevents muscular dystrophy in mdx mice. *Nature medicine,* 4**,** 1441-1444.

TONKIN, J., VILLARROYA, F., PURI, P. L. & VINCIGUERRA, M. 2012. SIRT1 signaling as potential modulator of skeletal muscle diseases. *Curr Opin Pharmacol,* 12**,** 372-6.

TOTHOVA, Z., KOLLIPARA, R., HUNTLY, B. J., LEE, B. H., CASTRILLON, D. H., CULLEN, D. E., MCDOWELL, E. P., LAZO-KALLANIAN, S., WILLIAMS, I. R., SEARS, C., ARMSTRONG, S. A., PASSEGUE, E., DEPINHO, R. A. & GILLILAND, D. G. 2007. FoxOs are critical mediators of hematopoietic stem cell resistance to physiologic oxidative stress. *Cell,* 128**,** 325-39.

TSAI, E. J. & KASS, D. A. 2009. Cyclic GMP signaling in cardiovascular pathophysiology and therapeutics. *Pharmacology & therapeutics,* 122**,** 216-238.

TSAI, S., SITZMANN, J. M., DASTIDAR, S. G., RODRIGUEZ, A. A., VU, S. L., MCDONALD, C. E., ACADEMIA, E. C., O'LEARY, M. N., ASHE, T. D., LA SPADA, A. R. & KENNEDY, B. K. 2015. Muscle-specific 4E-BP1 signaling activation improves metabolic parameters during aging and obesity. *J Clin Invest,* 125**,** 2952-64.

TURNER, P. R., FONG, P., DENETCLAW, W. F. & STEINHARDT, R. A. 1991. Increased calcium influx in dystrophic muscle. *The Journal of cell biology,* 115**,** 1701-1712.

VAN BENNEKOM, C. A., OERLEMANS, F. T., KULAKOWSKI, S. & DE BRUYN, C. H. 1984. Enzymes of purine metabolism in muscle specimens from patients with Duchenne-type muscular dystrophy. *Adv Exp Med Biol,* 165 Pt B**,** 447-50.

VERDIJK, L. B., GLEESON, B. G., JONKERS, R. A. M., MEIJER, K., SAVELBERG, H. H. C. M., DENDALE, P. & VAN LOON, L. J. C. 2009. Skeletal Muscle Hypertrophy Following Resistance Training Is Accompanied by a Fiber Type–Specific Increase in Satellite Cell Content in Elderly Men. *The Journals of Gerontology Series A: Biological Sciences and Medical Sciences,* 64A**,** 332-339.

VERTHELYI, D. 2006. Female's heightened immune status: estrogen, T cells, and inducible nitric oxide synthase in the balance. *Endocrinology,* 147**,** 659-661.

VILLALTA, S. A., RINALDI, C., DENG, B., LIU, G., FEDOR, B. & TIDBALL, J. G. 2010. Interleukin-10 reduces the pathology of mdx muscular dystrophy by deactivating M1 macrophages and modulating macrophage phenotype. *Human molecular genetics,* 20**,** 790-805.

VINCIGUERRA, M., FULCO, M., LADURNER, A., SARTORELLI, V. & ROSENTHAL, N. 2010. SirT1 in muscle physiology and disease: lessons from mouse models. *Dis Model Mech,* 3**,** 298-303.

VOISIN, V., SEBRIE, C., MATECKI, S., YU, H., GILLET, B., RAMONATXO, M., ISRAEL, M. & DE LA PORTE, S. 2005. L-arginine improves dystrophic phenotype in mdx mice. *Neurobiol Dis,* 20**,** 123-30.

VON HAEHLING, S., LAINSCAK, M., SPRINGER, J. & ANKER, S. D. 2009. Cardiac cachexia: a systematic overview. *Pharmacology & therapeutics,* 121**,** 227-252.

WAN, X., GUPTA, S., ZAGO, M. P., DAVIDSON, M. M., DOUSSET, P., AMOROSO, A. & GARG, N. J. 2012. Defects of mtDNA Replication Impaired Mitochondrial Biogenesis During Trypanosoma cruzi Infection in Human Cardiomyocytes and Chagasic Patients: The Role of Nrf1/2 and Antioxidant Response. *Journal of the American Heart Association: Cardiovascular and Cerebrovascular Disease,* 1**,** e003855.

WANG, B. 2010. Gene Therapy and Muscles: The Use of Adeno-associated Virus—Where are We Today? *Operative Techniques in Orthopaedics,* 20**,** 136-143.

WANG, B., LI, J., FU, F. H. & XIAO, X. 2009. Systemic human minidystrophin gene transfer improves functions and life span of dystrophin and dystrophin/utrophin-deficient mice. *J Orthop Res,* 27**,** 421-6.

WANG, L., LIU, J., SAHA, P., HUANG, J., CHAN, L., SPIEGELMAN, B. & MOORE, D. D. 2005. The orphan nuclear receptor SHP regulates PGC-1α expression and energy production in brown adipocytes. *Cell Metabolism,* 2**,** 227-238.

WANG, L., MORIZONO, H., LIN, J., BELL, P., JONES, D., MCMENAMIN, D., YU, H., BATSHAW, M. L. & WILSON, J. M. 2012. Preclinical Evaluation of a Clinical Candidate AAV8 Vector for Ornithine Transcarbamylase (OTC) Deficiency Reveals Functional Enzyme from Each Persisting Vector Genome. *Molecular Genetics and Metabolism,* 105**,** 203-211.

WANG, T., MCDONALD, C., PETRENKO, N. B., LEBLANC, M., WANG, T., GIGUERE, V., EVANS, R. M., PATEL, V. V. & PEI, L. 2015. Estrogen-related receptor α (ERRα) and ERRγ are essential coordinators of cardiac metabolism and function. *Molecular and cellular biology,* 35**,** 1281-1298.

WANG, Y. X., ZHANG, C. L., YU, R. T., CHO, H. K., NELSON, M. C., BAYUGA-OCAMPO, C. R., HAM, J., KANG, H. & EVANS, R. M. 2004. Regulation of muscle fiber type and running endurance by PPARdelta. *PLoS Biol,* 2**,** e294.

WANG, Z., KUHR, C. S., ALLEN, J. M., BLANKINSHIP, M., GREGOREVIC, P., CHAMBERLAIN, J. S., TAPSCOTT, S. J. & STORB, R. 2007. Sustained AAV-mediated dystrophin expression in a canine model of Duchenne muscular dystrophy with a brief course of immunosuppression. *Mol Ther,* 15**,** 1160-6.

WARD, N. J., BUCKLEY, S. M., WADDINGTON, S. N., VANDENDRIESSCHE, T., CHUAH, M. K., NATHWANI, A. C., MCINTOSH, J., TUDDENHAM, E. G., KINNON, C. & THRASHER, A. J. 2011. Codon optimization of human factor VIII cDNAs leads to high-level expression. *Blood,* 117**,** 798-807.

WEBSTER, C., SILBERSTEIN, L., HAYS, A. P. & BLAU, H. M. 1988. Fast muscle fibers are preferentially affected in Duchenne muscular dystrophy. *Cell,* 52**,** 503-13.

WEHLING-HENRICKS, M., JORDAN, M. C., GOTOH, T., GRODY, W. W., ROOS, K. P. & TIDBALL, J. G. 2010. Arginine metabolism by macrophages promotes cardiac and muscle fibrosis in mdx muscular dystrophy. *PLoS One,* 5**,** e10763.

WEHLING, M., SPENCER, M. J. & TIDBALL, J. G. 2001. A nitric oxide synthase transgene ameliorates muscular dystrophy in mdx mice. *J Cell Biol,* 155**,** 123-31.

WELLS, D. J. & WELLS, K. E. 2002. Gene transfer studies in animals: what do they really tell us about the prospects for gene therapy in DMD? *Neuromuscular Disorders,* 12**,** S11-S22.

WHITEHEAD, N. P., KIM, M. J., BIBLE, K. L., ADAMS, M. E. & FROEHNER, S. C. 2015. A new therapeutic effect of simvastatin revealed by functional improvement in muscular dystrophy. *Proc Natl Acad Sci U S A,* 112**,** 12864-9.

WHITEHEAD, N. P., PHAM, C., GERVASIO, O. L. & ALLEN, D. G. 2008. N-Acetylcysteine ameliorates skeletal muscle pathophysiology in mdx mice. *The Journal of physiology,* 586**,** 2003-2014.

WHITEHEAD, N. P., YEUNG, E. W. & ALLEN, D. G. 2006. Muscle damage in mdx (dystrophic) mice: role of calcium and reactive oxygen species. *Clinical and experimental pharmacology and physiology,* 33**,** 657-662.

WHITEHEAD, N. P., YEUNG, E. W., FROEHNER, S. C. & ALLEN, D. G. 2010. Skeletal muscle NADPH oxidase is increased and triggers stretch-induced damage in the mdx mouse. *PloS one,* 5**,** e15354.

WIMALASENA, N. K., LE, V. Q., WIMALASENA, K., SCHREIBER, S. L. & KARMACHARYA, R. 2016. Gene Expression-Based Screen for Parkinson's Disease Identifies GW8510 as a Neuroprotective Agent. *ACS Chem Neurosci,* 7**,** 857-63.

WRAGG, J. W., DURANT, S., MCGETTRICK, H. M., SAMPLE, K. M., EGGINTON, S. & BICKNELL, R. 2014. Shear stress regulated gene expression and angiogenesis in vascular endothelium. *Microcirculation,* 21**,** 290-300.

WU, B., CLOER, C., LU, P., MILAZI, S., SHABAN, M., SHAH, S. N., MARSTON-POE, L., MOULTON, H. M. & LU, Q. L. 2014. Exon skipping restores dystrophin expression, but fails to prevent disease progression in later stage dystrophic dko mice. *Gene Ther,* 21**,** 785-93.

WU, B., LU, P., BENRASHID, E., MALIK, S., ASHAR, J., DORAN, T. J. & LU, Q. L. 2010. Dose-dependent restoration of dystrophin expression in cardiac muscle of dystrophic mice by systemically delivered morpholino. *Gene Ther,* 17**,** 132-40.

WU, B., XIAO, B., CLOER, C., SHABAN, M., SALI, A., LU, P., LI, J., NAGARAJU, K., XIAO, X. & LU, Q. L. 2011. One-year treatment of morpholino antisense oligomer improves skeletal and cardiac muscle functions in dystrophic mdx mice. *Mol Ther,* 19**,** 576-83.

WU, H., KANATOUS, S. B., THURMOND, F. A., GALLARDO, T., ISOTANI, E., BASSEL-DUBY, R. & WILLIAMS, R. S. 2002. Regulation of mitochondrial biogenesis in skeletal muscle by CaMK. *Science,* 296**,** 349-52.

WU, H., NAYA, F. J., MCKINSEY, T. A., MERCER, B., SHELTON, J. M., CHIN, E. R., SIMARD, A. R., MICHEL, R. N., BASSEL-DUBY, R., OLSON, E. N. & WILLIAMS, R. S. 2000. MEF2 responds to multiple calcium-regulated signals in the control of skeletal muscle fiber type. *Embo j,* 19**,** 1963-73.

WU, Z., PUIGSERVER, P., ANDERSSON, U., ZHANG, C., ADELMANT, G., MOOTHA, V., TROY, A., CINTI, S., LOWELL, B. & SCARPULLA, R. C. 1999. Mechanisms controlling mitochondrial biogenesis and respiration through the thermogenic coactivator PGC-1. *Cell,* 98**,** 115-124.

WYNN, T. A. & VANNELLA, K. M. 2016. Macrophages in tissue repair, regeneration, and fibrosis. *Immunity,* 44**,** 450-462.

XIAO, W., LIU, Y., LUO, B., ZHAO, L., LIU, X., ZENG, Z. & CHEN, P. 2016. Time-dependent gene expression analysis after mouse skeletal muscle contusion. *Journal of Sport and Health Science,* 5**,** 101-108.

XIAO, X., XIAO, W., LI, J. & SAMULSKI, R. J. 1997. A novel 165-base-pair terminal repeat sequence is the sole cis requirement for the adeno-associated virus life cycle. *Journal of virology,* 71**,** 941-948.

YAFFE, D. & SAXEL, O. 1977. Serial passaging and differentiation of myogenic cells isolated from dystrophic mouse muscle. *Nature,* 270**,** 725-7.

YAN, Z., OKUTSU, M., AKHTAR, Y. N. & LIRA, V. A. 2011. Regulation of exercise-induced fiber type transformation, mitochondrial biogenesis, and angiogenesis in skeletal muscle. *Journal of Applied Physiology,* 110**,** 264-274.

YAP, Y. L., ZHANG, X. W., SMITH, D., SOONG, R. & HILL, J. 2007. Molecular gene expression signature patterns for gastric cancer diagnosis. *Computational biology and chemistry,* 31**,** 275-287.

YEUNG, E. W., WHITEHEAD, N. P., SUCHYNA, T. M., GOTTLIEB, P. A., SACHS, F. & ALLEN, D. G. 2005. Effects of stretch-activated channel blockers on [Ca(2+)](i) and muscle damage in the mdx mouse. *The Journal of Physiology,* 562**,** 367-380.

YIN, H., PRICE, F. & RUDNICKI, M. A. 2013. Satellite cells and the muscle stem cell niche. *Physiol Rev,* 93**,** 23-67.

YOON, M. J., LEE, G. Y., CHUNG, J.-J., AHN, Y. H., HONG, S. H. & KIM, J. B. 2006. Adiponectin increases fatty acid oxidation in skeletal muscle cells by sequential activation of AMP-activated protein kinase, p38 mitogen-activated protein kinase, and peroxisome proliferator–activated receptor α. *Diabetes,* 55**,** 2562-2570.

YOSHIDA, M., YONETANI, A., SHIRASAKI, T. & WADA, K. 2006. Dietary NaCl supplementation prevents muscle necrosis in a mouse model of Duchenne muscular dystrophy. *Am J Physiol Regul Integr Comp Physiol,* 290**,** R449-55.

ZHANG, G., LUDTKE, J. J., THIOUDELLET, C., KLEINPETER, P., ANTONIOU, M., HERWEIJER, H., BRAUN, S. & WOLFF, J. A. 2004. Intraarterial delivery of naked plasmid DNA expressing full-length mouse dystrophin in the mdx mouse model of duchenne muscular dystrophy. *Hum Gene Ther,* 15**,** 770-82.

ZHANG, H., DAVIES, K. J. & FORMAN, H. J. 2015. Oxidative stress response and Nrf2 signaling in aging. *Free Radical Biology and Medicine,* 88**,** 314-336.

ZHANG, L., RAJAN, V., LIN, E., HU, Z., HAN, H., ZHOU, X., SONG, Y., MIN, H., WANG, X. & DU, J. 2011. Pharmacological inhibition of myostatin suppresses systemic inflammation and muscle atrophy in mice with chronic kidney disease. *The FASEB Journal,* 25**,** 1653-1663.

ZHANG, W., LI, F. & NIE, L. 2010. Integrating multiple 'omics' analysis for microbial biology: application and methodologies. *Microbiology,* 156**,** 287-301.

ZHANG, Y. & DUAN, D. 2012. Novel mini-dystrophin gene dual adeno-associated virus vectors restore neuronal nitric oxide synthase expression at the sarcolemma. *Hum Gene Ther,* 23**,** 98-103.

ZHANG, Y., MA, K., SADANA, P., CHOWDHURY, F., GAILLARD, S., WANG, F., MCDONNELL, D. P., UNTERMAN, T. G., ELAM, M. B. & PARK, E. A. 2006. Estrogen-related receptors stimulate pyruvate dehydrogenase kinase isoform 4 gene expression. *Journal of Biological Chemistry,* 281**,** 39897-39906.

ZHAO, Y., YANG, J., LIAO, W., LIU, X., ZHANG, H., WANG, S., WANG, D., FENG, J., YU, L. & ZHU, W. G. 2010. Cytosolic FoxO1 is essential for the induction of autophagy and tumour suppressor activity. *Nat Cell Biol,* 12**,** 665-75.

ZHOU, L. & LU, H. 2010. Targeting fibrosis in Duchenne muscular dystrophy. *Journal of neuropathology and experimental neurology,* 69**,** 771.

ZINCARELLI, C., SOLTYS, S., RENGO, G. & RABINOWITZ, J. E. 2008. Analysis of AAV serotypes 1–9 mediated gene expression and tropism in mice after systemic injection. *Molecular Therapy,* 16**,** 1073-1080.

ZWETSLOOT, K. A., WESTERKAMP, L. M., HOLMES, B. F. & GAVIN, T. P. 2008. AMPK regulates basal skeletal muscle capillarization and VEGF expression, but is not necessary for the angiogenic response to exercise. *The Journal of Physiology,* 586**,** 6021-6035.